

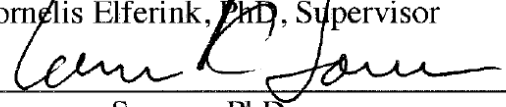
**The Dissertation Committee for Daniel P. Jackson Certifies that this is the approved
version of the following Dissertation:**

**A RHAPSODY ON THE ARYL HYDROCARBON RECEPTOR:
MOLECULAR AND ENVIRONMENTAL HEALTH INSIGHTS
THROUGH NOVEL AND CANONICAL SIGNALING PATHWAYS**

Committee:



Cornelis Elferink, PhD, Supervisor



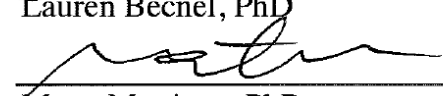
Lawrence Sowers, PhD



Lisa Elferink, PhD



Lauren Becnel, PhD



Muge Martinez, PhD

Dean, Graduate School of Biomedical Sciences

**A Rhapsody on the Aryl Hydrocarbon Receptor: Molecular and
Environmental Health Insights Through Novel and Canonical Signaling
Pathways**

by

Daniel Patrick Jackson, BA

Dissertation

Presented to the Faculty of the Graduate School of
The University of Texas Medical Branch
in Partial Fulfillment
of the Requirements
for the Degree of

Doctor of Philosophy

**The University of Texas Medical Branch
November, Two-Thousand and Fifteen**

Dedication

To my parents, for inspiring me to fulfill my childhood dream of being a scientist. To Peach, *mi dolce amore, bella luce del core*; you have made the personal and professional trials I've experienced in graduate school survivable.

Acknowledgements

As can be expected for a doctoral dissertation, there are many, many people to acknowledge and thank. First, I would like to thank all my friends and family who have supported me in my endeavours; your support has been instrumental to my success. Next, I would like to thank my mentor Dr. Cornelis Elferink, for challenging me to be a better scientist in every way, week after week, and for believing I would make it, even when I, myself, did not. I would also like to thank Dr. Bill Ameredes for involving me with the NIEHS T-32, which has given me inestimable mentoring, teaching, and manuscript writing skills. I would like to thank Tracy Albritton and others in the office of sponsored programs for helping me submit my NIEHS NRSA F31 application. I would also like to thank current and past members of the Elferink lab for helping make my research work- Aditya Joshi, Kristin Mitchell, Li Chen, Tod Harper, Dwayne Carter, and Shelly Wilson. Finally, I would like to thank my dissertation committee members- Lisa Elferink, Lauren Becnel, Lawrence Sowers, and Muge Martinez- for their advice, support, and constant guidance as I navigated my way through graduate school, and for their extraordinary letters of recommendation when I applied for post-doctoral fellowships. I owe a special thanks to Dr. Lisa Elferink for all the extra advice on how to navigate the social and political aspects of science, and for taking many hours to help turn a dismal oral presentation into a polished product; without all of your help I wouldn't have had the success I did in presenting my seminar for postdoc interviews.

A Rhapsody on the Aryl Hydrocarbon Receptor: Molecular and Environmental Health Insights Through Novel and Canonical Signaling Pathways

Publication No. _____

Daniel P. Jackson, PhD

The University of Texas Medical Branch, 20152

Supervisor: Cornelis J. Elferink

Abstract: The Aryl Hydrocarbon Receptor is a ubiquitously expressed, cytosolic transcription factor, which is activated by myriad structurally-diverse xenobiotic compounds, most notably 2,3,7,8-teterechlorodibenzo-*p*-dioxin. In this role, the AhR is known to play a fundamental role in several physiological process, for example cell division. Pathologically, the AhR has been identified as a fundamental driver of the toxic effects of numerous persistent, potent, and commonly encountered environmental contaminants. As such, we have investigated the specific role of the AhR in cellular replication during liver regeneration. Based on our findings, we then set out to assess transcriptional targets of the AhR in the mouse liver following exposure to 2,3,7,8-teterechlorodibenzo-*p*-dioxin. Finally, given the toxicities with which the AhR is associated, we undertook studies to quantify PAH contamination in Gulf of Mexico seafood as a result of two recent oil spills in an effort to assess safe seafood consumption levels, given the well-known link between the AhR and its toxic xenobiotic PAH ligands.

Table of Contents

A Rhapsody on the Aryl Hydrocarbon Receptor: Molecular and Environmental Health Insights Through Novel and Canonical Signaling Pathways	i
--	----------

Table of Contents	ii
--------------------------------	-----------

List of Tables.....	ix
---------------------	----

List of Figures	x
-----------------------	---

List of Abbreviations	xii
-----------------------------	-----

Chapter 1: Introduction	1
--------------------------------------	----------

THE ARYL HYDROCARBON RECEPTOR.....	2
------------------------------------	---

The History of the Aryl Hydrocarbon Receptor	2
--	---

THE CANONICAL (XRE) PATHWAY	6
-----------------------------------	---

XRE target genes for the AhR	8
------------------------------------	---

The AhR in the Cell Cycle	12
---------------------------------	----

Cofactors for the AhR in the XRE Pathway	15
--	----

Identification of the Non-Consensus (NC-XRE) Pathway	18
--	----

A Novel Protein Partner: Kruppel-like Factor 6	19
--	----

Hypothesis.....	21
-----------------	----

Chapter 2: Ah Receptor Mediated Suppression of Liver Regeneration Occurs Through NC-XRE Driven Expression of p21Waf1/Cip1	23
--	-----------

INTRODUCTION	23
--------------------	----

MATERIALS AND METHODS	25
-----------------------------	----

Animals	25
---------------	----

Chemicals.....	25
----------------	----

Partial Hepatectomy.....	26
--------------------------	----

BrdU Incorporation Studies	26
----------------------------------	----

Immunoprecipitation/Western Blotting.....	27
Kinase Assay.....	28
Semi-quantitative PCR.....	28
Quantitative PCR.....	28
Chromatin Immunoprecipitation.....	29
Statistical Analysis.....	31
RESULTS	32
TCDD Induced Suppression of Liver Regeneration is Abrogated in p21Waf1/Cip1 Knock-out Animals.....	32
TCDD Induced Transactivation of p21 Gene Expression Requires the AhR	34
The AhR and KLF6 Regulate p21Cip1 Expression Through Direct Binding of the p21Cip1 Transcript 2 Promoter.....	36
DISCUSSION	38
Chapter 3: Transcriptomic Analysis of TCDD Inducible AhR-Mediated Gene Expression Changes in the Mouse Liver.....	43
INTRODUCTION	43
Background.....	43
Need For Transcriptomic Studies of AhR Targets In Vivo	45
MATERIALS AND METHODS.....	47
Animals.....	47
Chemicals.....	48
In Vitro TnT Reticulocyte Lysate Generated Proteins	48
Immunoprecipitation/Western Blotting.....	48
Electrophoretic Mobility Shift Assay Experiments	49
RNA-Sequencing Library Generation and Sequencing.....	50

Chromatin Immunoprecipitation for Next-generation Sequencing (ChIP-seq)	50
Differential Expression Analysis	52
Primary Hepatocyte Isolation	52
Semi-Quantitative PCR.....	52
Quantitative PCR	53
Primers	53
RESULTS.....	53
AhR Interaction With KLF6 Involves C-terminus Protein-Protein Interaction and N-terminal DNA-binding.....	53
The AhR Directly Regulates Expression of Myriad Genes Following Activation by TCDD.....	55
Murine KLF6 Knock-out Models are Not Viable for RNA-sequencing Studies.....	69
DISCUSSION.....	73
The AhR/KLF6 Protein Interaction	73
RNA-sequencing Identification of Potentially Novel AhR Target Genes	74
Common Elements Between AhR CKO and WT RNA-sequencing Datasets May be Misleading.....	79
Correlations Between RNA-sequencing and ChIP-Sequencing.....	81
ChIP-sequencing Can Be Used to Anchor the RNA-sequencing Results to Functional AhR DNA-binding Events.....	83
CONCLUSIONS	92
Chapter 4: A CALUX Based Assessment of Petrogenic PAH Contamination in Gulf Seafood Following the Deepwater Horizon Oil Disaster	94
INTRODUCTION	94
Background.....	94

PAHs in Crude Oil	95
Toxic Equivalency Factors in Quantifying PAH Contamination	97
MATERIALS AND METHODS	98
Sample Collection	98
Method of extraction	99
Chemicals	99
Cell Culture	100
Luciferase Assays	100
Protein Assays	101
Experimental Design	101
Statistical Analysis	102
Results	102
Seafood Sample Collection	102
CALUX Assessment of PAH Contamination	104
DISCUSSION	108
The CALUX Bioassay for Measuring PAH Contamination	111
Seafood Consumption Guidelines Based on CALUX Results	114
CONCLUSIONS	115
Chapter 5: Galveston Texas Seafood Before and After the 2014 Houston Ship Channel Bunker Oil Spill: An Assessment of Petrogenic PAH Contamination and Associated Toxicology	116
INTRODUCTION	116
Background	116
Bunker Oil Composition	116
Pre-spill Baseline Data for PAH Levels in Galveston Seafood	117

MATERIALS AND METHODS	119
Sample Collection	119
Seafood PAH Extracts	119
Chemicals and Reagents	119
Cell Culture and CALUX assays	120
BaPTEQ calculations	121
Statistical Analysis	122
RESULTS	123
PAH Extract CALUX Activity Was Elevated During and After HSC Oil Spill	123
PAH Levels Increase After HSC spill, Trend Toward Decreases Over Time Thereafter	124
PAH Extract Color Correlates With CALUX Activity	127
DISCUSSION	132
PAHs and Methods of Quantification	132
Activity of Parent PAHs in the CALUX Assay	133
Elevated PAH Levels in Seafood After the HSC Spill.....	136
Persistence of Elevated PAH Levels in Galveston Seafood After the HSC Spill	136
The Value of Pre-spill Data Describing PAH Levels Before a Spill.....	138
Chapter 6: Dissertation Conclusion	140
INTRODUCTION	140
Cross-talk between the XRE and NC-XRE pathways	142
Environmental PAH contamination in Gulf of Mexico seafood.....	145
RNA-sequencing identification of AhR target genes.....	146

CONCLUSIONS.....	147
FUTURE DIRECTIONS	148
Appendices.....	149
Appendix I: Primers.....	149
Appendix I (continued).....	150
Appendix II: KLF6 and AhR Vector maps	151
Appendix II (continued).....	152
Appendix II (continued).....	153
Appendix II (continued).....	154
Appendix II (continued).....	155
Appendix II (continued).....	156
Appendix II (continued).....	157
Appendix II (continued).....	158
Appendix III: Significant Gene Expression Changes in Wild-type Mice at 2 Hours.....	159
Appendix III (continued)	160
Appendix III (continued)	161
Appendix III (continued)	162
Appendix III (continued)	163
Appendix IV: IPA Analysis of 2 hour WT RNA-Sequencing.....	164
Appendix IV (continued):	165
Appendix IV (continued):	166
Appendix V: IPA Analysis of 8 hour WT RNA-Sequencing	167
Appendix V (continued):	168
Appendix V (continued):	169

Appendix V (continued):	170
Appendix VI: 2 hour RNA-sequencing compared to lo et al.....	171
Appendix VII 8 hour RNA-sequencing compared to lo et al.	172
Appendix VII (continued).....	173
Appendix VII (continued).....	174
Appendix VIII: GCHARMS Supplemental Methods	175
Appendix VIII (continued)	176
Appendix VIII (continued)	177
Appendix VIII (continued)	178
Appendix IX: GCHARMS Seafood Sample Information	179
Appendix X: Heat map of Significant WT Expression Changes, 8 hour Comparison	183
Appendix XI: TCDD Structure	184
Appendix XII: Signaling Pathways from 2 hour IPA Analysis.....	185
Appendix XII: Signaling Pathways from 2 hour IPA Analysis (continued) .. 186	
Appendix XII: Signaling Pathways from 2 hour IPA Analysis (continued) .. 187	
Appendix XIII: Canonical Pathways from 2 hour IPA Analysis	188
Appendix XIV: Functional Pathways from 2 hour IPA Analysis.....	189
Permission to Publish	190
References	191
Vita	243

List of Tables

Table 1.....	87
Table 2.....	89
Table 3.....	91
Table 4.....	91
Table 5.....	125
Table 6.....	126
Table 7.....	127

List of Figures

Figure 1.....	6
Figure 2.....	7
Figure 3.....	10
Figure 4.....	21
Figure 5.....	21
Figure 6.....	32
Figure 7.....	33
Figure 8.....	34
Figure 9.....	35
Figure 10.....	36
Figure 11.....	37
Figure 12.....	37
Figure 13.....	41
Figure 14.....	53
Figure 15.....	53
Figure 16.....	54
Figure 17.....	54
Figure 18.....	54
Figure 19.....	55
Figure 20.....	56
Figure 21.....	56
Figure 22.....	57
Figure 23.....	57
Figure 24.....	58
Figure 25.....	58
Figure 26.....	60
Figure 27.....	61
Figure 28.....	62
Figure 29.....	63
Figure 30.....	63

Figure 31.....	64
Figure 32.....	64
Figure 33.....	65
Figure 34.....	66
Figure 35.....	70
Figure 36.....	72
Figure 37.....	79
Figure 38.....	80
Figure 39.....	84
Figure 40.....	86
Figure 41.....	103
Figure 42.....	104
Figure 43.....	105
Figure 44.....	106
Figure 45.....	107
Figure 46.....	108
Figure 47.....	109
Figure 48.....	122
Figure 49.....	123
Figure 50.....	124
Figure 51.....	128
Figure 52.....	129
Figure 53.....	130
Figure 54.....	131
Figure 55.....	142

List of Abbreviations

AhR	Aryl Hydrocarbon Receptor
Arnt	Ahr nuclear translocator
Pai-1	Serpine1, plasminogen activator inhibitor 1
PAS	Per/Arnt/Sim family of proteins
CKO	Conditional Knockout
TCDD	2,3,7,8-tetrachlorodibenzo- <i>p</i> -dioxin
BaP	Benzo[a]Pyrene
BaPE	Benzo[a]Pyrene Equivalence
TEQ	Toxic Equivalency
H/PAH	Halogenated and Polycyclic Aromatic Hydrocarbons
XRE	Canonical Xenobiotic Response Element 5'-GCGTG-3'
Cyp1a1	Cytochrome P450 family 1A1
AhRR	AhR Repressor protein
NC-XRE	Nonconsensus Xenobiotic Response Element 5'-GGGAGGGA-3'
KLF6	Kruppel-like Factor 6
pRb	Retinoblastoma tumor suppressor protein
ChIP	Chromatin Immunoprecipitation
IPA	Ingenuity Pathways Analysis
CALUX	Chemically Activated Luciferase Expression bioassay
TBST	Tris-buffered saline + 0.1% Tween20

PCR	Polymerase Chain Reaction
qRT-PCR	Quantitative real-time PCR
WT	wild-type
TSS	transcription start site
TnT	<i>in vitro</i> coupled transcription and translation system
NGS	Next-generation sequencing
kb	kilobases
Flox (Fx)	flanking loxP sites in a gene allele
RT	room-temperature
EMSA	Electrophoretic Mobility Shift Assay
ER	Estrogen Receptor
PH	Partial Hepatectomy

Chapter 1: Introduction¹

The Aryl Hydrocarbon Receptor (AhR) is the focus of a classic environmental toxicology research field, which began with the hypothesis for the AhR in 1976 (Poland et al., 1976; Denison et al., 2011). While the genesis of AhR research is indeed firmly rooted in environmental toxicology, the AhR has been studied in relation to a diversity of diseases, disorders, and pathophysiologies. This includes immunology (Stevens et al., 2009; Veldhoen and Duarte, 2010), nuclear hormone signaling (Abdelrahim et al., 2006; Denison et al., 2011), metabolic homeostasis and disorders (Lindén et al., 2010), cell growth and death (Marlowe and Puga, 2005; Chopra and Schrenk, 2011), developmental biology (Wells et al., 2010), carcinogenesis (Dietrich and Kaina, 2010), dioxin toxicity (White and Birnbaum, 2009), cardiotoxicity (Korashy and El-Kadi, 2006), and hepatotoxicity (Bock and Köhle, 2006). While these are all important manifestations of AhR biology, the tremendous body of evidence encompassed within the AhR research area precludes an exhaustive review of the field. With this in mind, the focus of this first chapter is four-fold: 1) to briefly chronicle the AhR field as it relates to the elucidation of the Xenobiotic Response Element (XRE) mediated canonical pathway, 2) to review some classical AhR roles and downstream target genes, 3) to consider AhR function in the context of the newly described non-canonical pathway involving the interaction between the AhR and the tumor suppressor Kruppel-Like Factor 6 (KLF6) at the Non-Consensus Xenobiotic Response Element (NC-XRE) (Wilson et al., 2013), and 4) to speculate on the implications for NC-XRE-driven gene expression, including future research directions. The reader is referred to the excellent reviews cited above, which cover areas not addressed in detail here. For a review of the structurally diverse AhR ligands we refer readers to Denison and Nagy 2003 (Denison and Nagy, 2003) and Nguyen and Bradfield, 2008 (Nguyen and Bradfield, 2008).

¹ Pages 1-21 reprinted with permission from *Toxicology Research* according to license to publish agreement

THE ARYL HYDROCARBON RECEPTOR

The History of the Aryl Hydrocarbon Receptor

The earliest work in the Ah Receptor field stemmed from the observation that exposure to various halogenated and polycyclic aromatic hydrocarbon (H/PAHs) compounds (i.e. benzo[a]pyrene, 3-methylcholanthrene) led to the induction of aryl hydrocarbon hydroxylase enzyme activity (AhH, Cyp1a1) (Alfred and Gelboin, 1967; Nebert and Gelboin, 1968a; b). This knowledge came from carcinogen studies which showed that coal tar applied to the skin of rabbit ears led to the formation of cancerous lesions (Yamagiwa and Ichikawa, 1918; Yamagiwa and Murayama, 1924; Narat, 1925). Identification of BaP as the causative agent of those cancerous lesions (Cook *et al.*, 1933; Barry *et al.*, 1935) and the subsequent induction of Cyp1a1 following BaP treatment (Conney *et al.*, 1956; 1957; 1959) gave way to broader studies of the PAH family (White and White, 1939; Friedewald and Rous, 1944) and their ability to affect gene expression. Later work identified the much more striking induction of Cyp1a1 by the HAH 2,3,7,8-tetrachlorodibenzo-p-dioxin (TCDD, dioxin) (see **appendix 11**) (Poland and Glover, 1973a; b). Although numerous well-documented accidental toxic exposures to TCDD exist (Kimbrough *et al.*, 1977; Baccarelli *et al.*, 2004; Sorg *et al.*, 2009; White and Birnbaum, 2009), TCDD was first identified as the etiological agent of chloracne in a 1957 study of factory workers producing a synthetic auxin (Kimmig and Schulz, 1957). Subsequent studies of TCDD estimated it to be about 30,000 times as potent as 3-methylcholanthrene in Cyp1a1 induction (Poland and Glover, 1973b). This led the field to characterize the perimortem pathology associated with oral acute exposure to TCDD in various species (Gupta *et al.*, 1973; Gasiewicz *et al.*, 1980).

While characterizing the pathophysiology of dioxin toxicity and the induction of Cyp1a1 by TCDD, laboratories reported significant differences between species, as well as between different strains of the same species, in both the oral acute LD₅₀ of TCDD and the extent of Cyp1a1 enzyme induction by TCDD (Thomas *et al.*, 1972; Schwetz *et al.*,

1973; McConnell *et al.*, 1978; Henck *et al.*, 1981). For example, the oral acute LD₅₀ for TCDD in guinea pigs is ~1-2 µg/kg, while in the remarkably resistant golden syrian hamster it is ~5 mg/kg (Henck *et al.*, 1981). Interestingly, the dramatically reduced TCDD susceptibility in the golden syrian hamster is not reflected in the relatively modest differences in agonist binding affinities observed amongst species. Nevertheless, the studies of differences in TCDD sensitivity ultimately identified two strains of mice that varied in sensitivity to TCDD exposure, termed the responsive and non-responsive strains, C57BL/6J mice and DBA/2 mice respectively (Gielen *et al.*, 1972; Thomas *et al.*, 1972). It was determined that induction of Cyp1a1 by these H/PAHs was dose-dependent rather than an altogether non-responsive phenotype, such that the ED₅₀ for Cyp1a1 induction in the C57BL/6J strain was approximately 1 nmol/kg while the ED₅₀ for the DBA/2 strain was >10 nmol/kg (Poland *et al.*, 1974). This finding led to the hypothesis that Cyp1a1 induction was mediated by a receptor (Poland *et al.*, 1976). Indeed, in acquiring the first evidence for such a receptor, the data supported the hypothesis for a proteinic receptor present in the cytosol, whose agonist binding varied between the B6 (AhR^{b/b}) and D2 (AhR^{d/d}) strains, thus accounting for the large difference in resultant enzyme induction (Poland *et al.*, 1976; Guenthner and Nebert, 1977; Okey *et al.*, 1979). It is noteworthy that later work in studying these two alleles found the difference in sensitivity to TCDD was attributable to 5 amino acids differing between the two variants (Chang *et al.*, 1993). Following the seminal work by Poland, Nebert, and Glover the actual term 'Ah Receptor' was first used in a 1980 report by Okey *et al.*, wherein they describe the non-liganded AhR present in the cytoplasm and its' translocation from the cytosol to the nucleus following dioxin exposure in cell culture (Okey *et al.*, 1980; Hannah *et al.*, 1981).

AhR nuclear translocation follows ligand binding (Okey *et al.*, 1979; Greenlee and Poland, 1979; Tierney *et al.*, 1980) and is a critical step in the induction of Cyp1a1 (Tukey *et al.*, 1982; Israel and Whitlock, 1984). Furthermore, it was demonstrated that

induction of Cyp1a1 by TCDD was regulated by cis-DNA elements in the target gene promoter (Israel and Whitlock, 1984; Jones *et al.*, 1985; Jones, *et al.*, 1986). These motifs were rigorously studied to elucidate the core recognition motif 5'-GCGTG-3', which was dubbed the Xenobiotic Response Element (XRE) (Denison, Fisher, and Whitlock, 1988a; b; Shen and Whitlock, 1992; Watson and Hankinson, 1992; Lusska *et al.*, 1993). While characterizing the induction of Cyp1a1 by the AhR, many labs identified proteins associated with the cytosolic receptor which were not associated with the nuclear form of the receptor (Prokipcak and Okey, 1988; Perdew, 1992). It was ultimately shown that several proteins were necessary for proper translocation and transcriptional activation by the AhR (Miller *et al.*, 1983; Hankinson, 1983; Hankinson *et al.*, 1985). In the case of the AhR protein partner Aryl hydrocarbon receptor nuclear translocator (Arnt), this discovery began with mutagen studies (Hankinson, 1979) identifying BaP resistant Hepa-1 cell clones with decreased Cyp1a1 induction following exposure to a number of different mutagens. The frequency with which these mutagenic clones developed increased with higher doses of the mutagen and the BaP resistant phenotype persisted in successive cell generations. These observations suggested a genetic aberration rather than an acquired resistance to explain the BaP resistant phenotype (Hankinson, 1981). Subsequent studies of several of these clones found that AhR expression as well as AhR nuclear translocation dynamics following TCDD exposure were similar to that of the parent Hepa1 line (Legraverend *et al.*, 1982). This was followed by studies assessing the biochemical characteristics of the AhR which hypothesized a smaller form of the receptor to exist following ligand binding, as assayed by sucrose density gradient and gel filtration analyses (Henry *et al.*, 1989), and a larger form of the receptor to be present in the nuclear fraction (Prokipcak and Okey, 1988).

The suggestion that the nuclear receptor might interact with other protein partners led several labs to the hypothesis that the additional proteins facilitated DNA-binding and more specifically that the DNA-bound form of nuclear AhR was heteromeric in structure

(Elferink *et al.*, 1990; Gasiewicz *et al.*, 1991). Ultimately, this heteromer was shown to include the protein identified as the now well known Arnt, through studies of the Hepa1 mutants discussed previously (Hoffman *et al.*, 1991). The Arnt cDNA was cloned and the protein was found to contain a basic helix-loop-helix region and 2 domains with homology to the drosophila proteins PERiod and SIngle-Minded (Per and Sim) (Hoffman *et al.*, 1991; Reyes *et al.*, 1992), a structural feature that unites all three in a protein family together with the AhR—the PAS family of bHLH proteins. The AhR protein was first purified in 1991 by Bradfield and coworkers (Bradfield *et al.*, 1991); the mouse and human AhR ORFs were subsequently cloned shortly thereafter (Burbach *et al.*, 1992; Dolwick *et al.*, 1993). Based on studies of the glucocorticoid receptor (Denis *et al.*, 1987), another group identified the HSP90 protein in an interaction with the AhR (Perdew, 1988). The HSP90/AhR interaction was later shown to have a functional role in maintaining the cytosolic form of the Ah receptor in a conformation capable of binding to TCDD (Pongratz *et al.*, 1992).

The Arnt protein was so named as it was thought to aid in translocation of the AhR from the cytoplasm to the nucleus upon ligand binding (Hoffman *et al.*, 1991; McGuire *et al.*, 1994). While not immediately clear at the time, later studies by the Poland lab and the Hankinson lab tenably cemented the framework for what we know as the canonical AhR signaling pathway (AhR/Arnt pathway, XRE pathway) with data showing: 1) the unliganded AhR is cytosolic, 2) upon ligand binding the AhR translocates to the nucleus, 3) Arnt is constitutively located in the nucleus—a finding not anticipated by the genetic studies, 4) the nuclear form of the AhR complex does not include HSP90, but does include Arnt and 5) AhR-DNA binding requires Arnt (Probst *et al.*, 1993; Pollenz *et al.*, 1994).

Following the discovery that the unliganded AhR and Arnt are found in the cytosol and nucleus respectively, data from the Hankinson lab functionally characterized the domains of the AhR and Arnt proteins. Extensive mutagenesis experiments have

ultimately characterized the regions necessary for AhR ligand binding, HSP90 interaction, dimerization, DNA-binding, and transcriptional activation (Reisz-Porszasz *et al.*, 1994; Fukunaga *et al.*, 1995; Ikuta *et al.*, 1998; Kewley *et al.*, 2004; Evans *et al.*, 2009; Rezvani *et al.*, 2011) (**Figure 1**). Previous work had reported the unliganded cytosolic AhR to interact with HSP90 and other as yet unidentified protein partners (Perdew, 1988; Chen and Perdew, 1994; Perdew and Bradfield, 1996). These proteins were subsequently identified as 1) a protein previously shown to interact with a hepatitis B virus protein known as X-associated protein 2 (XAP2) (Meyer *et al.*, 1998), and independently identified as the AhR interacting protein AIP (Ma and Whitlock, 1997) or ARA9 (Carver and Bradfield, 1997)—and 2) p23 (Nair *et al.*, 1996; Kazlauskas *et al.*, 1999).

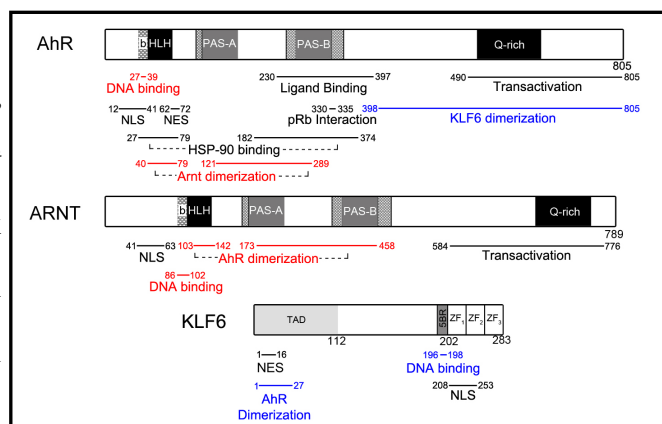


Figure 1. Location of the functional domains within the AhR, Arnt, and KLF6 proteins. Blue text refers to AhR/KLF6 NC-XRE pathway regions, red text to the AhR/Arnt XRE pathway, and black is non-specific, based on previous studies (Jackson *et al.*, 2015).

This body of research in the AhR field (including many other important studies not cited here) led to a functional characterization of the molecular events that constitute what is collectively dubbed the canonical AhR signaling pathway. While it took many years to delineate the cell signaling events precedent to Cyp1a1 enzyme induction following TCDD exposure, the advent of microarray and next-generation sequencing technologies has identified multifarious AhR target genes that are regulated via the classic XRE. Indeed, this new research has also identified novel protein partners and cis DNA motifs for the AhR. The protein partners and DNA-binding motifs are discussed below.

THE CANONICAL (XRE) PATHWAY

As depicted in **Figure 2**, in the canonical pathway the unliganded AhR resides in the cytosol, bound by chaperone proteins HSP90, p23, and ARA9 (XAP/AIP). Upon

ligand binding, the AhR is presumed to undergo a conformational change in the PAS A domain, which facilitates nuclear translocation and AhR/Arnt dimerization through the PAS A region, concomitant with dissociation from HSP90 (Soshilov and Denison, 2008). This change in structure following ligand binding presumably allows the conserved nuclear localization sequence in the N-terminal 42 amino acids to stimulate nuclear translocation (Henry, 2003), which is facilitated by importins (Ikuta *et al.*, 1998; Denison *et al.*, 2011). Once in the nucleus,

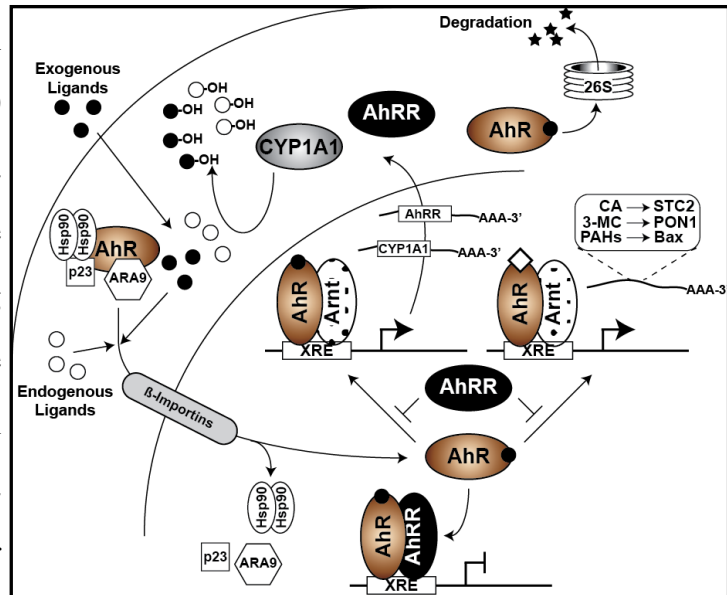


Figure 2: In the canonical pathway, AhR activation is induced by exogenous or endogenous ligand binding, nuclear translocation, and recruitment to XREs in partnership with the Arnt protein. AhR signaling is silenced by one of several mechanisms, including 1) induction of CYP1A1 and subsequent metabolic depletion of ligands, 2) expression of the AhR repressor (AhRR), and 3) AhR degradation through the 26S proteasome. AhR activity is also influenced by distinct properties of bound agonists (depicted by the open diamond) which can alter the signaling repertoire toward ligand specific target genes.

the AhR dissociates from chaperone proteins and heterodimerizes with Arnt. AhR/Arnt dimerization is thought to be facilitated by the ligand-induced conformational change in the PAS A region (Soshilov and Denison, 2008). As shown in **Figure 2**, the HLH domain of the AhR, and to a lesser extent the PAS A and B domains, are necessary for AhR/Arnt dimerization, while the basic region located in the N-terminus of the protein is necessary for XRE DNA-binding (Fukunaga *et al.*, 1995). Similar to the AhR, the basic region of Arnt is required for XRE DNA-binding, and the HLH and PAS A domain of Arnt mediate protein binding with the AhR (Reisz-Porszasz *et al.*, 1994; Evans *et al.*, 2009). Both of these proteins contain a nuclear localization signal in the N-terminus of the protein, while the nuclear export signal of the AhR is located between amino acids 62-72 (Ikuta *et al.*, 1998; Ikuta *et al.*, 2000). Although the precise mechanisms remain unclear (Backlund and Ingelman-Sundberg, 2005), it has been suggested that phosphorylation of the AhR and

Arnt may be necessary for DNA binding by the heterodimer, possibly through a mechanism involving protein kinase c (Pongratz *et al.*, 1991; Carrier *et al.*, 1992; Mahon and Gasiewicz, 1995).

The ligand bound AhR/Arnt heterodimer then binds to XRE DNA motifs within target gene promoters, a process that alters DNA topology (Elferink and Whitlock, 1990) as well as stability of the protein-DNA complex. The classic and most well characterized DNA-binding motif for the AhR/Arnt heterodimer is the XRE. It was first defined through experiments analyzing Cyp1a1 induction by the AhR (Jones, *et al.*, 1986), which identified a number of dioxin responsive domains bound by protein in an AhR-dependent manner, without the requirement of nascent protein synthesis (Denison, Fisher, and Whitlock, 1988a; b). An assessment of the critical nucleotides in the XRE needed to facilitate AhR binding revealed a core consensus motif of 5'-GCGTG-3' (Shen and Whitlock, 1992). In the case of transcriptional activation, flanking residues in the XRE (5'-T/GnGCGTGA/C-3') confer the greatest AhR transactivation capability (Shen and Whitlock, 1992; Lusska *et al.*, 1993), such that nucleotide substitutions within 4 bp 5' and/or 3' of the core motif decrease transactivation potential for the AhR (Lusska *et al.*, 1993; Swanson *et al.*, 1995).

XRE target genes for the AhR

The cytochrome p450 enzyme Cyp1a1 is the archetypal XRE-mediated target gene for the AhR. The Ah receptor Repressor (AhRR) gene is another XRE-mediated AhR target gene up-regulated following AhR activation with a number of xenobiotic ligands (Karchner *et al.*, 2002; BR Evans *et al.*, 2005). The AhRR functions as a dominant negative protein, competitively inhibiting AhR transactivation, possibly by binding to and sequestering Arnt to form a transcriptionally inactive heterodimer. However, Evans et al. (2005) recently presented evidence favoring a mechanism of AhRR action involving "transrepression" of AhR signaling that does not depend on competitively inhibiting the formation of an AhR/Arnt complex or its DNA binding

(Evans *et al.*, 2008). The discrepancies notwithstanding, the AhRR confers a type of negative feedback inhibition on the AhR signaling pathway (Mimura *et al.*, 1999; Karchner *et al.*, 2002; Evans *et al.*, 2005) (**Figure 2**). Following transcriptional activation, the AhR releases from DNA and is rapidly exported from the nucleus and degraded via the ubiquitin-mediated 26S proteasome pathway (Ma and Baldwin, 2000). The half-life of the cytosolic AhR is 28 hours, while the half-life of the AhR following TCDD exposure is 3 hours. Not surprisingly, inhibiting proteosomal degradation of the AhR significantly increases the amount of nuclear AhR, which “superinduces” Cyp1a1 gene expression (Ma and Baldwin, 2000). This suggests that rapid AhR turnover following its activation and DNA binding serves as a key regulatory step in the AhR signaling pathway. In fact, it was recently suggested that the TCDD-inducible poly-(ADP-ribose) polymerase (TiPARP), an established AhR target gene, suppresses ongoing AhR activity by TiPARP directly interacting with the AhR to disrupt receptor activity, and by promoting AhR turnover via proteosomal degradation (MacPherson *et al.*, 2012; MacPherson *et al.*, 2014).

In addition to Cyp1a1 and the AhRR gene, other XRE mediated AhR target genes include additional phase I heme monooxygenases in the cytochrome p450 family such as Cyp1a2 (Reiners *et al.*, 1997), Cyp2a5 (Arpiainen *et al.*, 2005), and Cyp1b1 (Sutter *et al.*, 1994) as well as the phase II enzymes Gsta1 (Friling *et al.*, 1990) and Aldh3 (Dunn *et al.*, 1988). Likewise, the AhR and Arnt transactivate NAD(P)H dehydrogenase quinone 1 (Nqo1) expression (Ma *et al.*, 2004) through a mechanism involving the erythroid 2-related nuclear factor protein (Nrf2) following exposure to either the classic AhR ligands or any of a number of different Nrf2 activators (Wang *et al.*, 2013) (**Figure 3**). The increased expression of these enzymes (including Cyp1a1) serves as a negative feedback loop for Ah receptor signaling whereby the enzymes attenuate AhR activation through metabolic depletion of the ligand pool (Weiss *et al.*, 1996) (**Figure 2**).

It has been suggested that the induction of metabolic enzymes by the AhR is a critical component of its role as a high fidelity biosensor, which prevents prolonged receptor activation (Gu *et al.*, 2000; Tsuji *et al.*, 2012). With respect to the endogenous ligands, their rapid turn-over protects against prolonged AhR activation which can lead to transcriptional changes that perturb the physiological equilibrium normally maintained by the AhR. Evidence of such perturbations under conditions of prolonged AhR

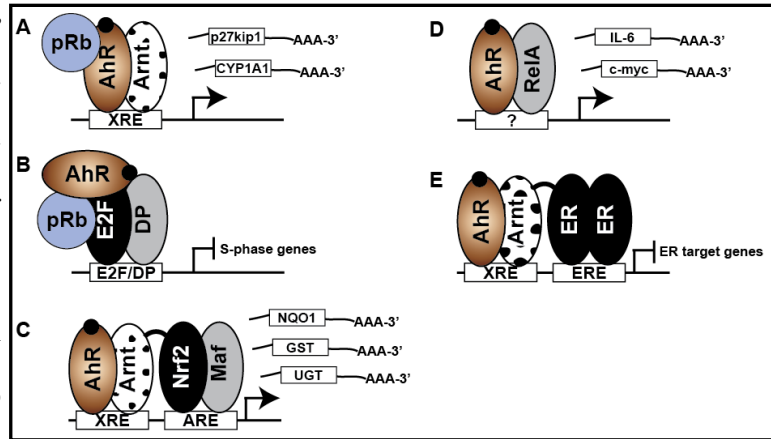


Figure 3 A) The canonical pathway involves AhR/Arnt heterodimer binding to XREs flanking target gene promoters, functioning as a scaffold for various cofactors (including pRb) necessary for maximal transcriptional activation. B) The AhR forms a co-repressor complex with pRb to suppress E2F/DP expression of S-phase genes. C) XRE binding by the AhR/Arnt heterodimer, close to antioxidant response elements, in phase II metabolic gene promoters facilitates an interaction with the Nrf2/Maf heterodimer to induce expression. The prototypical target gene for this interaction is NQO1. D) Via an interaction with RelA, the AhR binds to NFκB target gene promoters (i.e c-Myc and IL-6), to induce expression. The precise nature of the DNA motif remains unresolved— a RelA driven interaction at a NFκB response element, or binding to a novel AhR/RelA response element. E) Modulation of estrogen receptor (ER) signaling by direct AhR/Arnt heterodimer interactions, suppressing ER mediated gene expression, or by steric hindrance of ER DNA binding due to overlapping XRE and ERE sites.

activation affecting cell cycle control have been reported (Mitchell *et al.*, 2006; Mitchell and Elferink, 2009). While it may be a property associated with endogenous ligands, the resistance of certain exogenous agonists such as TCDD to metabolic degradation undermines the benefits of this negative feedback mechanism resulting in deleterious consequences. Agonist induced AhR signaling is highly conserved across the vertebrate lineage (McMillan and Bradfield, 2007b) suggesting that the clearance of agonists provides a general mechanism for controlling AhR biology. Although AhR and Arnt orthologs are present in several invertebrates (Hahn, 2002), the inability to demonstrate ligand binding by the invertebrate forms (Powell-Coffman *et al.*, 1998) imputes that AhR agonist binding and the metabolic clearance of agonists are more recent evolutionary events. Given that many of the exogenous AhR ligands are toxic (through a mechanism

requiring the AhR), it is not immediately clear what evolutionary benefit the AhR might confer as a sensor of exogenous ligands. This is especially true since many exogenous ligands that activate the AhR are 1) only relatively recently present in the environment in large quantities, and 2) some such as TCDD are poorly metabolized by AhR-induced biotransformation enzymes. This would suggest that activation of the receptor by exogenous ligands constitutes AhR ‘hijacking’ diverting it away from its innate physiological role. Paradoxically, Cyp1a1 knockout mice are more sensitive to toxicity from oral BaP exposure, compared with wild-type mice (Uno *et al.*, 2004), suggesting that the receptor’s response to certain exogenous agonists is beneficial. However, the lack of BaP genotoxicity in AhR knock out mice suggests that the protective role of Cyp1a1 is contingent on the presence of a functional receptor. These observations serve to illustrate that the variability in AhR signaling following exposure to endogenous and exogenous cues presents real difficulties in distinguishing toxic responses from the adaptive physiological responses.

The most toxic H/PAH AhR ligands (most notably TCDD), exhibit high affinity for the AhR and are poor substrates for the biotransformation enzymes up-regulated following receptor activation (Shimada and Fujii-Kuriyama, 2004; Ma and Lu, 2007). This endows them with the ability to persistently activate the AhR (Mitchell *et al.*, 2006; Ma and Lu, 2007). This fact bolsters the rationale for the hypothesis that the endogenous AhR ligand(s) are readily metabolized. Indeed, given the numerous well-known cell-type specific functions of the AhR and the myriad AhR ligands (endogenous and exogenous) (McMillan and Bradfield, 2007a; b; Hao *et al.*, 2012), it is tempting to speculate that there may be multiple endogenous ligands for the AhR, perhaps specific to cell or tissue type. This notion is supported by data showing AhR target gene responses vary with different agonists (Pansoy *et al.*, 2010). For example, the induction of Pon1 and Bax gene expression by PAHs (e.g. 3-MC) and not TCDD highlights the agonist specific responses (Matikainen *et al.*, 2001; Gouédard *et al.*, 2004). We recently identified a receptor target

gene, stanniocalcin 2 (Stc2) (Harper *et al.*, 2013), that is readily induced by the novel endogenous AhR ligand, cinnabarinnic acid (Lowe *et al.*, 2014), yet is not induced by TCDD or BaP (Joshi *et al.* submitted)(**Figure 2**).

It is clear that there are numerous mechanisms (AhRR, Cyp1a1-mediated ligand depletion, proteolytic degradation, and TiPARP) in place to tightly regulate receptor activity (**Figure 2**). The presence of myriad regulatory pathways suggests that aberrant receptor signaling is deleterious. In fact, there is plenty evidence to support this notion, including the plethora of toxic effects observed with persistent receptor activation (Mitchell and Elferink, 2009; Budinsky *et al.*, 2014) and the developmental defects seen with receptor loss (Fernandez-Salguero *et al.*, 1995; Schmidt *et al.*, 1996; Lund *et al.*, 2003; Vasquez *et al.*, 2003) or aberrant activation (Fenton *et al.*, 2002; Vasquez *et al.*, 2003; Burns *et al.*, 2013). The advent of such tight coordination is consistent with the existence of AhR functions beyond the transcriptional control of a few phase I and II enzymes. While the precise nature of the AhR-regulated events that warrant such tight control remain largely unexplored, some indications have come to light in studies examining the AhR in cell cycle control and cell proliferation.

The AhR in the Cell Cycle

As previously discussed, the early work in the receptor field focused on Cyp1a1 induction by exogenous AhR agonists (Gupta *et al.*, 1973). This research gave way to studies with TCDD responsive and non-responsive mice (Gielen *et al.*, 1972) and cell lines (Miller *et al.*, 1983). While studying these cell lines, Wiebel *et al.* reported that TCDD treatment of 5L rat hepatoma cells slowed their cell division concomitant with decreased DNA synthesis, suggesting cell cycle arrest at the G₁/S phase checkpoint (Gottlicher and Wiebel, 1991) in an AhR-dependent manner (Wiebel *et al.*, 1991; Ma and Whitlock, 1996). A similar TCDD-induced cell cycle arrest was also observed in AhR-null cells upon re-expression of the full length AhR (Weiss *et al.*, 1996). Intriguingly, it was found that loss of AhR expression in various cell lines also resulted in a prolonged

cell doubling time (Ma and Whitlock, 1996). The prolonged doubling time associated with loss of AhR expression appears to be a general phenomenon, having been observed in several cell types including hepa1 cells (Ma and Whitlock, 1996), epithelial cells (Shimba *et al.*, 2002), and breast cancer cell lines (Barhoover *et al.*, 2010). Therefore, paradoxically both TCDD-induced AhR activation and loss of the receptor, delay cell cycle progression through G₁-phase. In AhR null embryonic fibroblasts (Elizondo *et al.*, 2000) this was attributed to a mechanism thought to involve retinoblastoma tumor suppressor protein (pRb) and the transcriptional cofactor p300 (Tohkin *et al.*, 2000). Restoration of AhR expression in AhR-null cells restored the normal doubling time (Tohkin *et al.*, 2000), while over-expression of the AhR is known to accelerate cell cycle progression and decrease doubling time (Ma and Whitlock, 1996; Shimba *et al.*, 2002). This suggests that AhR signaling in response to endogenous cues hastens cell cycle progression. The implication is that the AhR plays a central role in the G₁-phase program where perturbations affecting normal receptor function—due to sustained AhR activation by TCDD or loss of the protein—delay cell cycle progression by blocking entry into S phase.

With respect to the aforementioned studies, it is important to bear in mind that many of the *in vitro* systems that have been used to study the role of the AhR in cell cycle progression are in fact cancer cell lines, which by their very nature have circumvented the normal checkpoint machinery in place to regulate cell division. Consequently, it is possible these studies have inadvertently overlooked important pieces to the puzzle. It is also possible that there are differences in the AhR signaling pathway between these cell lines. Taken together, while the TCDD induced AhR-mediated G₁-phase cell cycle arrest phenomenon has been well-characterized, it remains altogether unclear why loss of the AhR prolongs doubling time. Presumably, the AhR is necessary to activate a gene(s) necessary for proper G₁-phase progression, the absence of which prolongs the G₁-phase.

Nevertheless, it is clear that the AhR has an important role in the G₁/S checkpoint (Ge and Elferink, 1998; Tohkin *et al.*, 2000).

We have previously reported a direct interaction between the AhR and the hypophosphorylated “active” form of pRb (Ge and Elferink, 1998). We have also demonstrated that this interaction is critical for maximal AhR-mediated G₁-phase cell cycle arrest (Elferink *et al.*, 2001). Additionally, hyperphosphorylated pRb (ppRb) is predominant in dividing cells while hypophosphorylated pRb (pRb) is restricted to the G₀ and G₁ phases, imputing a cell cycle dependency to the functional consequences of the AhR/pRb interaction (Elferink *et al.*, 2001). pRb inhibits cell proliferation either by binding to E2F or other transcription factors to indirectly block gene transactivation (Helin *et al.*, 1993), or by binding with E2F at target gene promoters to actively repress gene expression (Weintraub *et al.*, 1992; 1995; Chang *et al.*, 2014). Puga *et al.* (2000) expanded on the interaction between the AhR and pRb, reporting that the proteins interacted in the absence of Arnt and suggesting a co-repressor mechanism by which the AhR/pRb complex might inhibit cell cycle progression through suppression of E2F activity (Puga, *et al.*, 2000; Elferink, 2003; Marlowe *et al.*, 2004) (see **Figure 3**). This suppression of E2F activity depends on an intact LXCXE (pRb binding) motif in the AhR (Elferink *et al.*, 2001). Although the AhR/pRb interaction was also documented to involve a region in the receptor’s transactivation domain, it has been reported that E2F transcriptional suppression occurs in the absence of functional AhR transactivation and DNA-binding domains (Puga, *et al.*, 2000; Marlowe *et al.*, 2004). In contrast, we have shown the AhR/pRb interaction to be necessary for maximal G₁-phase cell cycle arrest and maximal AhR-mediated induction of Cyp1a1 following TCDD treatment (Elferink *et al.*, 2001). Indeed, in this scenario the two proteins interact, with pRb functioning as a transcriptional co-activator to induce expression of Cyp1a1 and the cyclin-dependent kinase inhibitor p27^{kip1}, to promote cell cycle arrest (Kolluri *et al.*, 1999; Elferink *et al.*, 2001; Faust *et al.*, 2013) (see **Figure 3**). It is noteworthy that studies in rat hepatoma 5L

cells and mouse oval cells have shown the AhR to induce p27^{kip1} gene expression following TCDD treatment (Kolluri *et al.*, 1999; Faust *et al.*, 2013). However, *in vivo* studies in mice indicated that the cyclin-dependent kinase inhibitor, p21^{cip1}, rather than p27^{kip1} is TCDD responsive (Jackson *et al.*, 2014).

It is noteworthy that in characterizing the importance of the LXCXE motif in G₁-arrest, studies revealed that a mutant form of the AhR unable to interact with pRb still induced a modest, albeit significantly reduced G₁ arrest following TCDD exposure (Elferink *et al.*, 2001). This is consistent with a role for the cyclin-dependent kinase inhibitor p27^{kip1} (or p21^{cip1}, further discussed below) in the process. Since the pRb interaction with the AhR is limited to the active hypophosphorylated form, the interaction is restricted to the G₀ and G₁ phases of the cell cycle. However, the AhR/Arnt complex can interact with several cofactors (Ge and Elferink, 1998; Puga, *et al.*, 2000; Tohkin *et al.*, 2000), thus AhR activity can conceivably be modified throughout the cell cycle reflecting the nature of the cofactor interactions. Specifically, the AhR/Arnt complex has been shown to recruit the cofactors p300, CREB binding protein (CBP), and steroid receptor coactivator (SRC) 1 and 2 (Tohkin *et al.*, 2000). The involvement of these cofactors attests to the complexity of AhR mediated transcriptional control. Indeed, cofactors involved in AhR signaling via the XRE can vary depending on, among other things, the presence or absence of ligand, type of ligand, amount of ligand, species of organism, and cell type (**Figure 3**). The involvement of these cofactors suggests that both co-activation and co-repression contribute to AhR mediated cell cycle arrest in G₁-phase (Huang and Elferink, 2005; Marlowe and Puga, 2005). For a more in-depth review of AhR DNA-binding specifically to the Cyp1a1 promoter the readers are referred to Hankinson 2005 and Solaimani *et al.*, 2013 (Hankinson, 2005; Solaimani *et al.*, 2013).

Cofactors for the AhR in the XRE Pathway

Apart from the canonical signaling pathway involving the AhR/Arnt heterodimer, it has also been reported that the AhR interacts with the NF- κ B subunits RelA (Kim *et al.*,

2000) and RelB (Tian *et al.*, 1999; Vogel, Sciallo, and Matsumura, 2007). In 2007, Vogel *et al.* observed that following TCDD treatment, the AhR directly interacts with RelB and binds to the IL-8 promoter. Computational analysis failed to locate an XRE motif in the IL-8 promoter sequence (Vogel, Sciallo, and Matsumura, 2007). Further study revealed the presence of an eight nucleotide DNA-binding site on the IL-8 promoter, through which the AhR is capable of inducing IL-8 gene expression following dioxin exposure (Vogel, Sciallo, and Matsumura, 2007). These and other reports of the AhR interacting with new protein partners to transactivate genes through novel DNA motifs highlight a shift of focus in the field toward characterizing AhR target genes regulated by non-XRE receptor-mediated mechanisms.

For a number of the aforementioned phase II enzymes induced by the AhR, it is now known (see **Figure 3**) that there is an AhR interaction with Nrf2 (Auyeung *et al.*, 2003; Ma *et al.*, 2004), where the XRE-bound AhR/Arnt complex cooperates with the NRF2/Maf complex bound to proximal antioxidant response elements (AREs) located in the target gene promoter (Wang *et al.*, 2013). The prototypical target for this complex is Nqo1. Additionally, a number of other UGT and GST enzymes have also been suggested as AhR targets (Auyeung *et al.*, 2003; Yeager *et al.*, 2009). These enzymes are responsible for the biotransformation of several carcinogenic PAHs (Bock, 2012) including, the ultimate genotoxin benzo[a]pyrene (BaP)-7,8-dihydrodiol epoxide, formed during Cyp1a1 mediated hydroxylation of the parent compound, BaP (Eaton and Bammler, 1999). For a more in-depth review of the phase II targets for the AhR/Nrf2 interaction see Bock 2012 (Bock, 2012).

The AhR up-regulates certain targets via an interaction with the NF- κ B protein partners RelA (Tian *et al.*, 1999; Kim *et al.*, 2000) or RelB (Vogel, Sciallo, and Matsumura, 2007; Vogel, *et al.*, 2007). Two such targets for the AhR/RelA interaction are c-myc (Kim *et al.*, 2000) and the inflammatory cytokine interleukin 6 (IL-6) (Hollingshead *et al.*, 2008). Although the precise mechanism remains unclear, the data

suggest the AhR binds through either 'XRE-like' sites in the IL-6 promoter (DiNatale, *et al.*, 2010) or via interactions with NF- κ B elements through its RelA interaction (Chen *et al.*, 2012). AhR-mediated induction of IL-6 has been linked to a number of different physiologically relevant processes including inflammation (Hollingshead *et al.*, 2008), exogenous ligand-independent AhR activity (DiNatale, *et al.*, 2010), and tumorigenesis (DiNatale, *et al.*, 2010). In the case of the AhR/RelB interaction, the two proteins form a complex at a 'XRE-like' motif (5'-GGGTGCAT-3') dubbed the RelBAhRE in the IL-8 promoter (Vogel, Sciallo, and Matsumura, 2007), following exposure to either the diterpene plant derivative, forskolin, or TCDD (Vogel, *et al.*, 2007). While additional work is needed to fully understand the functional role of the interaction with the Rel proteins, these observations highlight the intricacies of AhR biology, which are far richer and more complex than suggested by the classic AhR/Arnt signaling pathway.

A number of studies have reported on the anti-estrogenic effects of numerous exogenous AhR ligands (Zacharewski *et al.*, 1994; Safe *et al.*, 2000). This anti-estrogenic activity is primarily attributed to AhR-mediated transactivation of Cyp1a1 and Cyp1b1, which metabolize the estrogen receptor (ER) ligand 17 β -estradiol (Safe *et al.*, 1998), and AhR/Arnt DNA-binding of so-called inhibitory XREs juxtaposing ER elements in ER target genes (Gillesby *et al.*, 1997; Wang *et al.*, 1998; Ohtake *et al.*, 2003). One other example of the AhR signaling via the XRE with novel protein partners is the interaction between the AhR/Arnt complex and the estrogen receptor (ER) (Wang *et al.*, 1998) (**Figure 3**). AhR binding attenuates ER transactivation (Safe *et al.*, 2000; Safe and Wormke, 2003) of a number of different ER target genes, including several cell cycle regulatory proteins (Wang *et al.*, 1998; Duan *et al.*, 1999; Porter *et al.*, 2001). In addition to the 'classical' AhR functions in inhibiting ER activity through agonist metabolism, the AhR has been shown to decrease ER activity by acting as an E3 ubiquitin ligase targeting nuclear ER degradation through the 26S proteasome pathway (Ohtake *et al.*, 2009).

Identification of the Non-Consensus (NC-XRE) Pathway

Mitchell *et al.* previously reported that TCDD exposure suppresses liver regeneration (Mitchell *et al.*, 2006), in part by increasing expression of the serine protease plasminogen activator inhibitor-1 (serpine 1, Pai-1) to inhibit urokinase plasminogen activator activity necessary for HGF activation. Huang and Elferink were specifically interested in Pai-1 because it is known to form a complex with urokinase plasminogen activator to inhibit liver regeneration by hampering activation of Hepatocyte Growth Factor (HGF), an important liver regeneration protein (Michalopoulos and DeFrances, 1997; Irigoyen *et al.*, 1999; Tanaka *et al.*, 2001; Shimizu *et al.*, 2001). The Elferink lab further investigated Pai-1 expression using a luciferase reporter assay, containing a 116 bp region of the Pai-1 promoter, in hepatoma cells and observed an AhR-dependent induction of Pai-1 expression following TCDD treatment (Huang and Elferink, 2012). Electrophoretic mobility shift assays (EMSA) performed using mouse liver nuclear extracts identified a region spanning nucleotides -116 to -76 of the Pai-1 promoter that supported TCDD inducible protein-DNA binding by the AhR (Huang and Elferink, 2012). The term Non-Consensus Xenobiotic Response Element (NC-XRE) was coined to distinguish this motif from the canonical XRE (Huang and Elferink, 2012). The hallmark of this sequence is the 5'-GGGA-3' tetranucleotide quadruple repeat. Ensuing sequential mutation analysis 40 bp of this region revealed that the second 5'-GGGA-3' motif substantially contributes to protein-DNA binding (AhR-NC-XRE interaction) (Huang and Elferink, 2012). It is worth noting that the four GGGA repeats characteristic to the NC-XRE, may form of a G-quadruplex DNA structure, potentially serving as an additional element to regulate Pai-1 gene expression at the transcriptional level. Indeed, a QGRS analysis (using the online QGRS mapping algorithm) of the murine Pai-1 gene identified a total of 71 non-overlapping quadruplex-forming G-rich sequences, one of which had a G-score of 84 (data not shown). However, while this phenomenon is worth further study to understand it's potential relation to AhR-mediated regulation of NC-XRE

gene expression, it's difficult, at this point, to say for sure how these structures in the Pai-1 gene may contribute to AhR regulation of expression. Another striking feature associated with the AhR interaction at the Pai-1 NC-XRE was the lack of Arnt binding. EMSA experiments showed that AhR binding to the NC-XRE sequence could not be competed for with a 10-fold molar excess of cold XRE oligonucleotide (Huang and Elferink, 2012). The hypothesis that the AhR/NC-XRE interaction was Arnt-independent was tested by ChIP experiments, which confirmed direct binding of the AhR to the Pai-1 promoter NC-XRE following TCDD treatment. In contrast, ChIP experiments targeting the Arnt protein failed to yield a product, suggesting that AhR binding to the NC-XRE was not dependent on Arnt. Subsequent functional studies confirmed that AhR-mediated Pai-1 transcriptional activation through the NC-XRE is in fact Arnt independent (Huang and Elferink, 2012).

A Novel Protein Partner: Kruppel-like Factor 6

A subsequent study of AhR binding to the NC-XRE identified a novel AhR DNA-binding partner (Wilson *et al.*, 2013). Wilson *et al.* focused on the Kruppel-like factor (KLF) protein family due to sequence homology between the NC-XRE and the KLF family DNA-binding motif, as well as a previous study showing KLF4 to regulate Cyp1a1 gene expression (Zhang *et al.*, 1998). The KLF family of transcription factors is related to the specificity protein factor family due to similarities in the C-terminal DNA binding domains (Suske *et al.*, 2005). Due to high C-terminal sequence homology shared by KLF family members, most KLF transcription factors bind to a similar DNA-motif known as a 'GC box' on a number of functionally diverse target genes (Philipsen and Suske, 1999; Bieker, 2001). Apart from the homology in the zinc-finger C-terminal regions, the KLF family proteins have significantly less sequence homology in the N-terminal portions, which disposes them to unique individual regulatory pathways (Andreoli *et al.*, 2010). Structural and functional studies showed that the C-terminus of the AhR and N-terminus of KLF6 are necessary for both the mouse and human proteins

to interact (Wilson *et al.*, 2013). Interestingly, KLF6 binding to the NC-XRE requires three arginine residues juxtaposing the KLF6 zinc-finger DNA binding domain, rather than the zinc-finger domain itself. In fact, the entire zinc-finger region is expendable for NC-XRE binding by KLF6. It should be noted that while loss of the zinc-finger domain did not preclude NC-XRE binding in the EMSA experiments (Wilson *et al.*, 2013), this region contains the NLS (**Figure 1**) required for KLF6 nuclear localization and thus the zinc-finger domain is likely necessary for the AhR KLF6 interaction in cells and *in vivo*. Furthermore, these experiments also showed that key AhR residues critical for XRE DNA-binding, specifically in the basic Helix-Loop-Helix domain of the AhR, were not required for NC-XRE DNA-binding (Wilson *et al.*, 2013).

KLF6 target genes regulate a number of different processes including cellular differentiation, proliferation, and apoptosis (Philipsen and Suske, 1999; Andreoli *et al.*, 2010). KLF6 loss of heterozygosity, protein mutations, and over-expression are linked to a number of cancers, including hepatocellular carcinoma (Narla *et al.*, 2007), gastric cancer (Sangodkar *et al.*, 2009), pancreatic cancer (Hartel *et al.*, 2008), colorectal cancer (HL Reeves *et al.*, 2004), prostate cancer (Narla *et al.*, 2001; 2005), and astrocytic glioma (Jeng, 2003). In this light, KLF6 is considered to be a tumor suppressor according to Knudson's two hit model (Knudson, 1971). It has been demonstrated to up-regulate E-cadherin (DiFeo *et al.*, 2006), transforming growth factor β 1 (Botella *et al.*, 2009), and insulin-like growth factor 1 receptor (Rubinstein *et al.*, 2004). KLF6 is known to activate expression of p21^{cip1} in a p53-independent manner (Andreoli *et al.*, 2010), which leads to the inhibition of cell cycle progression and decreased hepatocyte proliferation (Narla *et al.*, 2001; Benzeno *et al.*, 2004; Narla *et al.*, 2007; Lang *et al.*, 2013). A recent study has shown that p21^{cip1} knockdown in dividing cells impairs this KLF6 induced G₁-phase cell cycle arrest (Trucco *et al.*, 2014). Certainly, in the case of E-cadherin, we obtained evidence that the promoter harbors a NC-XRE and recruits the AhR/KLF6 complex in a

TCDD-dependent manner (**Figure 4**), suggesting that the AhR and KLF6 are partners in anti-tumor signaling pathways.

Collectively, the studies by Huang et al., and Wilson et al., have contributed to a characterization of what we have dubbed the non-canonical pathway, which parallels AhR/Arnt

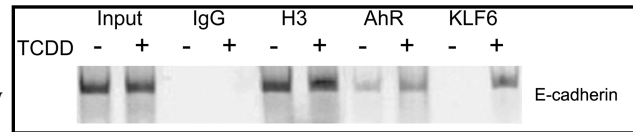


Figure 4: Mice were treated by oral gavage with vehicle (-) or 20 μ g/kg TCDD (+) for 2 hours. Chromatin immunoprecipitations (ChIP) were performed on livers using antibodies against the indicated proteins and the E-cadherin promoter (-220 to +37) encompassing a NC-XRE, amplified by PCR. The data show TCDD-dependent recruitment of the AhR and KLF6 to the E-cadherin promoter. This sequence was independently shown to harbor a KLF6 binding site in 3 separate human cancer cell lines (Calderon et al. 2012)

signaling (**Figure 5**). Nuclear localization of the AhR, stimulated by an exogenous or endogenous ligand drives the KLF6/AhR interaction, NC-XRE binding, and subsequent transcriptional events. In this context, the AhR is expected to modulate expression of both XRE- and NC-XRE-driven target genes (Huang and Elferink, 2012; Wilson *et al.*, 2013). Indeed, we envision that both pathways are activated concomitantly, and we hypothesize the two pathways function to alter the expression of distinct subsets

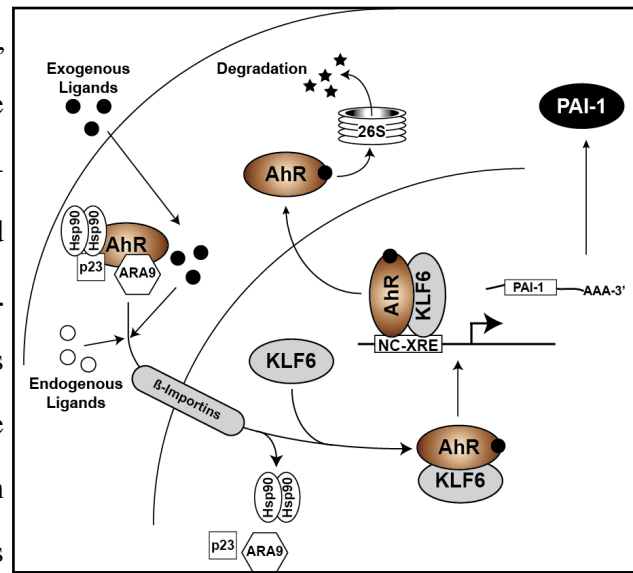


Figure 5: In the NC-XRE pathway, as in the canonical pathway, the AhR is activated by endogenous or exogenous ligands, to stimulate nuclear translocation. Unlike the canonical pathway, the NC-XRE pathway relies on an AhR association with KLF6 and recruitment to NC-XRE binding sites flanking target genes, including PAI-1

of target genes, specific to the Arnt or KLF6 protein partner and XRE or NC-XRE DNA motif, respectively.

Hypothesis

Given the research discussed above, and the recent finding that the AhR interacts with a novel protein partner to bind a novel DNA-motif in novel AhR target gene promoters, we hypothesize the XRE and NC-XRE pathways represent functionally distinct signaling pathways for the AhR. We hypothesize these two pathways have specific target genes for the AhR/Arnt heterodimer and the AhR/KLF6 heterodimer,

respectively. Given the documented evidence showing KLF6 to regulate p21 expression, and the historical observations showing the AhR to regulate G₁/S phase cell cycle progression, we further hypothesize the NC-XRE branch of AhR signaling is involved in regulating the expression of cell-cycle regulatory proteins (namely p21 and/or p27) to control cell division in the liver. To test this hypothesis we resolved to use a partial hepatectomy liver regeneration model to assess the role of p21 and p27, possibly transactivated by the AhR/KLF6 heterodimer, in proper liver regeneration.

Chapter 2: Ah Receptor Mediated Suppression of Liver Regeneration Occurs Through NC-XRE Driven Expression of p21^{Waf1/Cip1}

INTRODUCTION

The liver is the only solid organ known to regenerate organ mass in response to damage (Huang and Elferink, 2005). This is important given the role of the liver in metabolism of both endogenous and exogenous compounds. One such example is the metabolism of exogenous aromatic hydrocarbon compounds by enzymes of the cytochrome p450 system (Denison and Nagy, 2003). Central to both the regenerative and metabolic functions of the liver is the ligand-activated basic helix-loop-helix transcription factor of the Per-Arnt-Sim (PAS) family, known as the Aryl Hydrocarbon Receptor (AhR) (Fukunaga *et al.*, 1995). The AhR is activated by numerous polycyclic and halogenated aromatic hydrocarbons, including the prototypical ligand 2,3,7,8-tetrachlorodibenzo-*p*-dioxin (TCDD) (Denison and Nagy, 2003). In humans TCDD is known to cause a number of deleterious health effects, including liver toxicity, immunotoxicity, dermal toxicity, tumor promotion, and developmental abnormalities (Safe, 1986). These effects of TCDD are all mediated by the AhR (Poland and Knutson, 1982; Nebert *et al.*, 1993; Fernandez-Salguero *et al.*, 1996).

In the absence of a ligand, the AhR exists in the cytosol bound by chaperones, including heat-shock proteins (Hankinson, 1995) and an immunophilin-like protein (Whitlock, 1999). Upon ligand binding, the AhR translocates to the nucleus, dissociates from chaperones, and interacts with DNA-binding partners to regulate target gene expression. Canonically, the nuclear AhR heterodimerizes with the Aryl hydrocarbon receptor nuclear translocator (Arnt) (Probst *et al.*, 1993; Reisz-Porszasz *et al.*, 1994) and binds to a core recognition motif (5'-GCGTG-3') termed the Xenobiotic Response Element (XRE) (Watson and Hankinson, 1992; Swanson *et al.*, 1995). Cyp1a1 represents the prototypical XRE-regulated AhR target gene (for review, see Denison *et al.*, 2011).

² Pages 22-41 reprinted with permission of the American Society for Pharmacology and Experimental Therapeutics. All rights reserved

Recent work in the Elferink lab, has revealed that the TCDD activated AhR also forms a transcriptionally active heterodimeric complex with the Kruppel-like factor 6 (KLF6) protein. This heretofore unknown transcription factor complex regulates gene expression of novel AhR target genes via binding of the recently discovered non-consensus XRE (NC-XRE) (Huang and Elferink, 2012; Wilson *et al.*, 2013).

It is now well accepted that the AhR plays an important role in cell cycle progression (Ma and Whitlock, 1996; Kolluri *et al.*, 1999; Abdelrahim *et al.*, 2003; Denison *et al.*, 2011). Indeed, studies have shown that TCDD exposure leads to G₁ cell-cycle arrest in cell lines that express a functional AhR, but not in cell lines lacking AhR expression (Gottlicher and Wiebel, 1991; Weiss *et al.*, 1996). Previous work has also shown that the cell cycle effects depend on a direct interaction between the AhR and the active (hypophosphorylated) form of the retinoblastoma tumor suppressor protein (Rb) (Ge and Elferink, 1998; Puga, *et al.*, 2000; Elferink *et al.*, 2001; Marlowe *et al.*, 2004). One way the AhR-Rb interaction regulates cell-cycle progression is by repressing E2F-dependent gene expression thus preventing entry into S-phase (Marlowe *et al.*, 2004). Separate from its role as a repressor complex, the AhR-Rb interaction also promotes gene expression consistent with Rb functioning as a transcriptional co-activator, where sustained receptor activity in 5L rat hepatoma cells leads to induction of the G₁-phase cyclin-dependent kinase inhibitor p27^{Kip1} (Kolluri *et al.*, 1999; Levine-Fridman *et al.*, 2004; Huang and Elferink, 2005).

p27^{Kip1}, as well as p21^{Cip1} and the less well studied p57^{Kip2}, are members of the Cip/Kip family of cyclin-dependent kinase inhibitors targeting CDK2 activity (Sherr and Roberts, 2004). We have previously shown that AhR activation by TCDD suppresses cell proliferation during partial hepatectomy-induced liver regeneration (Mitchell *et al.*, 2006). The *in vivo* studies showed that CDK2 activity was diminished in the regenerating liver in mice pretreated with TCDD. It is noteworthy that the decrease in CDK2 activity was associated with increased binding of the p21^{Cip1} and p27^{Kip1} inhibitors to the CDK2-

cyclin E complex. The receptor's role in hepatic cell cycle control is more complicated however. Abdelrahim and coworkers (Abdelrahim *et al.*, 2003) showed that the AhR can both inhibit (MCF7 cells) and promote (HepG2 cells) cell growth, which was underscored by significant changes in the expression of several G₁-phase regulatory proteins in HepG2 cells. Likewise, while TCDD suppresses liver growth in hepatectomized mice, it promotes cell proliferation in animals treated with a hepatomitogen (Mitchell *et al.*, 2010), despite suppression of CDK2 activity.

Given the role for p21^{Cip1} and p27^{Kip1} in G₁-phase cell cycle control, we set out to determine if these proteins are functionally required for the TCDD-induced inhibition of liver regeneration in hepatectomized animals. The present study examined the regenerative response following 70% partial hepatectomy in mice lacking either p21^{Cip1} or p27^{Kip1}. The data reveal that p21^{Cip1}, rather than p27^{Kip1}, is essential for the TCDD-induced growth arrest, and that p21^{Cip1} induction by TCDD involves the recently described novel AhR-KLF6 complex binding to a NC-XRE in the p21^{Cip1} promoter.

MATERIALS AND METHODS

Animals

C57Bl/6 (WT), p21^{Cip1} KO, and p27^{Kip1} KO mice were purchased from Jackson Laboratories. These animals were maintained on a 12 hour light/dark cycle, in a temperature controlled facility in the UTMB animal resource center, with food and water *ad libitum*. Female mice 8-10 weeks old were used for our experiments. Animals were euthanized via isoflurane overdose followed by cervical dislocation. All experiments were conducted in accordance with approved IACUC procedures.

Chemicals

As reported previously (Mitchell *et al.*, 2010), TCDD was purchased from Cerilliant (Round Rock, TX) and dissolved in anisole, followed by dilution in peanut oil to 2 mg/ml. TCDD was administered via oral gavage at 20 μ g TCDD/kg body weight. Control animals received similar amounts of anisole dissolved in peanut oil.

Partial Hepatectomy

Partial hepatectomy (PH) or sham surgery was performed as previously described (Mitchell *et al.*, 2006). Briefly, mice were anesthetized via isoflurane inhalation and PH performed, resecting ~70% of the liver (as previously described by (Higgins and Anderson, 1931)). Sham surgery involved anesthetization followed by opening the abdominal cavity and gentle manipulation of the liver tissue without resection. Mice were allowed to recover and were then euthanized at indicated times by isoflurane inhalation followed by cervical dislocation. All animal handling and surgical procedures were performed in strict compliance with an approved UTMB IACUC protocol.

BrdU Incorporation Studies

In order to measure cell proliferation following partial hepatectomy, we performed 5-bromo-2'-deoxyuridine (BrdU) incorporation studies as previously described (Mitchell *et al.*, 2006). Briefly, 50 mg/kg BrdU (Sigma-Aldrich, St. Louis, MO) was administered i.p. 2 hours before euthanization. Tissues were then resected and fixed in 10% buffered formalin for 18 hours. For continuous labeling studies mice were provided with drinking water containing 0.8 mg/ml BrdU (bottles shielded from UV light) immediately following surgery until mice were sacrificed, at which time tissue was removed and fixed in 10% buffered formalin for 18 hours. Fixed tissues were sectioned, processed, and stained by the UTMB Histopathology Core Facility. Sections were stained for BrdU incorporation using a biotinylated anti-BrdU antibody (Invitrogen, Carlsbad, CA). These sections were then incubated with avidin-conjugated HRP and 3,3'-diaminobenzidine. Multiple sections from similar locations in each liver were used for BrdU counting. Results represent the number of brown stained nuclei in six (6) low-power fields per animal, expressed as a percent (number BrdU positive/total nuclei in field).

Immunoprecipitation/Western Blotting

Western Blots were conducted as previously described (Mitchell *et al.*, 2006; Wilson *et al.*, 2013). Briefly, fresh frozen liver tissue was homogenized using a polytron in TGH buffer (50 mM HEPES pH7.4, 150 mM NaCl, 1.5 mM MgCl₂, 1mM EGTA pH 8.0, 1%Triton X-100, 10% Glycerol) supplemented with 1 mM PMSF, 10 mM NaF, 1 mM Na₃VO₄, and 5 µg/ml protease inhibitors (Sigma p8340). Protein concentrations were determined using the DC protein assay kit (Bio-Rad Laboratories, Inc., Hercules, CA). For immunoprecipitation experiments, 50 µg of total protein from whole cell lysates was incubated with 2 µg anti-CDK2 antibody (sc-163 or sc-163g; Santa Cruz Biotechnology) for 4 hours at 4°C. Protein A or Protein G beads were then added and incubated 1 hour at 4°C. Beads were washed 5 times in NETN buffer (20 mM Tris-HCl, PH 8.0, 100 mM NaCl, 0.5% Nonidet P-40, 1 mM EDTA) and resuspended in 2x SDS loading buffer then boiled for 10 minutes at 100°C and fractionated on SDS gel as detailed below. For western blots, proteins were resolved on SDS-polyacrylamide (10%) gel and transferred to PVDF membranes (Amersham Hybond-LFP, GE Healthcare Life Sciences). Membranes were blocked for 1 hour at RT in 5% dry milk in Tris-buffered saline, 0.1% Tween 20 (v/v) (TBST), and incubated overnight at 4°C with primary antibody in 5% milk in TBST. Membranes were washed 3x with TBST, 10 minutes each, and incubated at RT for 1 hour with secondary antibody in 5% milk in TBST. Finally, membranes were washed 1x with TBST for 15 minutes and visualized on the Typhoon Trio Variable Mode Imager (GE Healthcare Life Sciences). Primary antibodies used include CDK2 (sc-163), p21^{Cip1} (sc-6246), p27^{Kip1} (sc-776), cyclin A (sc-751), and cyclin E (sc-247) (Santa Cruz Biotechnology). Secondary antibodies were Cy3/Cy5 anti-mouse or anti-rabbit (GE Healthcare Life Sciences). Blot analysis and densitometry were performed using ImageQuant software (GE Healthcare Life Sciences).

Kinase Assay

Kinase assays were conducted as previously described (Mitchell *et al.*, 2006). Briefly, 500 μg total protein was subjected to CDK2 immunoprecipitation as described above, except washed for 4 times in NETN (rather than 5), 1x in kinase assay buffer (see Mitchell *et al.*, 2006), resuspended in 15 μl kinase assay buffer supplemented with 10 μg of histone H1 and 5 μCi (^{32}P)-ATP (3000 Ci/mmol) and incubated for 40 minutes at RT. The reaction was stopped with 15 μl of 2x SDS loading buffer and reaction products were resolved on 15% SDS-polyacrylamide gel and analyzed by autoradiography.

Semi-quantitative PCR

RNA was isolated from total liver tissue using TRIzol (Life Technologies corp.) according to the manufacturers recommendations. SuperScript II (Invitrogen) was used for first strand cDNA synthesis using 1 μg total RNA according to the manufacturers recommendations. 2 μl of this cDNA was used as template for the PCR reactions. 10X PCR buffer (Fischer) was diluted to 1x with dH₂O, forward and reverse primers (table 1) were added at 0.2 μM final concentration, and 10 U/per reaction of *Taq* DNA polymerase was added to make a master mix. cDNA was warmed to 95°C before adding the master mix (hot-start). Cycling parameters were 95°C for 45 seconds, 68°C for 30 seconds, and 72°C for 90 seconds. This sequence was used to amplify the target sequence for the indicated number of cycles and a final extension at 72°C for 6 minutes was used. Reaction products were resolved on a 0.8% agarose EtBr gel. Gels were visualized on a Typhoon Trio variable mode imager (GE Healthcare Life Sciences) and densitometry was analyzed with ImageQuant software (GE Healthcare Life Sciences).

Quantitative PCR

Total RNA was isolated from fresh liver tissue using TRIzol (Life Technologies) according to the manufacturer's recommendations. Quantitative real-time PCR (qRT-PCR) was performed by the Real-Time PCR core facility at the University of Texas Medical Branch as previously described (Wilson *et al.*, 2013; Harper *et al.*, 2013).

Briefly, RT-PCR was performed using 20ng of total RNA for target gene detection. Target gene expression (2-CT) was calculated, following normalization of the triplicate CT value to 18S rRNA.

Chromatin Immunoprecipitation

ChIP experiments were performed as previously described (Huang and Elferink, 2012; Wilson *et al.*, 2013). Briefly, C57Bl/6 mice were treated *in vivo* with 20 μ g TCDD per kg body weight, or an equivalent amount of vehicle via oral gavage. Mice were then euthanized by isoflurane inhalation and cervical dislocation. Whole livers were resected and the gall bladder removed, then rinsed in 1x PBS. Livers were diced into fine pieces and cross linked in 1% formaldehyde for 10 minutes at RT. Cross-linking was stopped by addition of 500 mM glycine and incubation at room-temperature for 5 minutes. Tissue was pelleted via centrifugation at 3,200xg for 5 minutes at 4°C. Pellet was resuspended in 6 mL cold 1x PBS and homogenized using a dounce homogenizer on ice with **7 strokes** using a tight pestle (Wheaton, Millville, New Jersey). The homogenate was pelleted at 3,200xg for 5 minutes at 4°C and resuspended in 5mL cell lysis buffer (150 mM NaCl, 25 mM Tris pH 7.5, 5 mM EDTA, 1% Triton X-100, 0.1% SDS, 0.5% deoxycholate) supplemented with protease inhibitor cocktail (Sigma p8340), and homogenized in a dounce homogenizer on ice with **4 strokes** using a tight pestle. Homogenates were incubated on ice for 15 minutes and centrifuged at 3,200 xg for 5 minutes at 4°C. The samples were processed for ChIP using the Active Motif ChIP-IT Express Enzymatic Kit (Active Motif, Carlsbad, CA). This is the midpoint of the ChIP workflow and the following portion differs depending on whether the ChIP material is to be used for ChIP-seq or ChIP PCR. The following section is for ChIP PCR (and not ChIP-seq) In detail, the pelleted material was resuspended in 1ml of ice cold 1x lysis buffer supplemented with protease inhibitor cocktail (PIC) and phenylmethanesulfonylfluoride (PMSF), and incubated on ice for 30 minutes. During which time, a working stock enzymatic shearing cocktail was generated by adding 2 μ L of shearing cocktail to 198 μ L of 50% glycerol.

Pellet/cell lysis buffer mixture was transfer to a duncce homogenizer on ice and dounced **40 strokes** with a tight pestle. The solution was then transferred to eppindorf tubes and spun at 3,200 xg for 10 minutes at 4°C. The supernatant was aspirated and the pellet resuspended in 350 μ L of digestion buffer, supplemented with 1.75 μ L each PIC and PMSF, and incubated for 15 minutes at 37°C. Next, 17 μ L of the working shearing cocktail in glycerol was added the mixture incubated for 15 minutes at 37°C. The shearing reaction was halted by adding 7 μ L of ice cold 0.5M EDTA and incubating on ice for 10 minutes. The mixture was pelleted via spin at 6,400 xg for 10 minutes at 4°C, and the protein-DNA complex supernatant was transferred to new tubes. Protein DNA complexes were immunoprecipitated with the following antibodies: mouse monoclonal anti-AhR (ab2769 Abcam, Cambridge MA), goat polyclonal anti-KLF6 (SC-20885 Santa Cruz Biotechnology), mouse monoclonal anti-histone H3 (ab10799 Abcam, Cambridge MA), or rabbit monoclonal IgG Isotype control (#3900, Cell Signaling Technologies, Danvers, MA). This was accomplished using PIC, PMSF, ChIP buffer 1, antibody, magnetic beads, and chromatin according to the manufacturers recommendations (using 5 μ g of each respective antibody. IP was allied to proceed overnight (~12 hours). Following the IP, tubes were placed in a magnetic stand to pellet magnetic beads at the bottom. Tubes were removed from the stand and 500 μ L of wash buffer 1 was added and gently pipetted to resuspend. This was repeated for the next 2 washes according to the manufacturers recommendations. After the final wash, the solution was aspirated while the beads were on the magnet, and the beads were resuspended in 50 μ L of Elution Buffer AM2 and incubated for 45 minutes at RT. Tubes were spun to pellet solution and beads in table top galaxy micro centrifuge (for 10 seconds) and 50 μ L of reverse cross-linking buffer was added. Tubes were placed in magnetic stand to retain beads and supernatant was moved to a new tube. To process input DNA, 12 μ L of chromatin (which was added to the IP step for the immunoprecipitation) was diluted in ChIP buffer 2, along with 4 μ L of 5M NaCl, to have the same volume as other samples. All samples were then incubated

for 15 minutes at 95°C to reverse cross-links. Tubes were then returned to RT and 1μL RNase A was added and tube incubated for 30 minutes at 37°C. Again tubes were returned to RT and 2μL of proteinase k was added and incubated for 1 hour at 37°C. Following proteinase k treatment, reaction was stopped by addition of 2μL of stop solution at RT. To purify DNA, 100μL each of chloroform and phenol saturated buffer (pH 7.9) was added, tubes were vortexed to mix then centrifuged for 15 min at 12,000RPM at 4°C. The top layer was transferred to a new tube and 100μL chloroform was added vortexed and spun again. Supernatant was transferred to a new tube and 30μL NaO-Ac and 700μL of 100% EtOH was added and incubated at -20°C overnight. Tubes were then spun at maximum speed for 45 minutes, supernatant was aspirated and pellet was **carefully** washed with 700μL of 70% EtOH. Tubes were spun again at max speed for 45 minutes, supernatant was aspirated, tubes were allowed to air dry for 3 minutes and all samples were resuspended in 30μL DEPC treated dH₂O. Cyp1a1 and p21_{cip1} promoter sequences were amplified by PCR using primers flanking the XRE and NC-XRE sequences, respectively (Table 1). PCR products were resolved on a 5% polyacrylamide TBE gel and stained with 1x SYBR green for 30 minutes in the dark. Gels were rinsed with dH₂O and imaged on a Typhoon Trio Variable Mode Imager (GE Healthcare Life Sciences). Band intensity was measured using ImageQuant software (GE Healthcare Life Sciences).

Statistical Analysis

Data were analyzed using Prism 6 Graphpad software. Animal numbers for surgery experiments were based on a preliminary power analysis. Statistical significance of $p < 0.05$ was used for all experiments. Unless otherwise indicated, significance was determined by Holm-Sidak t-test.

RESULTS

TCDD Induced Suppression of Liver Regeneration is Abrogated in p21^{Waf1/Cip1}

Knock-out Animals

We have previously shown that persistent AhR activation by TCDD suppresses

liver regeneration in wild-type (WT) mice following 70% PH, concomitant with a decrease in CDK2 activity (Mitchell *et al.*, 2006). In order to test the hypothesis that this anti-proliferative response was due

to the p21^{Cip1} and/or p27^{Kip1} CDK inhibitors, we monitored hepatocyte proliferation in regenerating livers in WT,

p21^{Cip1} and p27^{Kip1} knockout mice following TCDD treatment (**Figure 6**). Commitment to DNA synthesis (S phase) was measured using 5-bromo-2'-deoxyuridine (BrdU) incorporation at various times after the PH. Substantial BrdU incorporation was first detected in WT mice at 36 hours post PH in keeping with a precisely regulated temporal program (Weglarz and Sandgren, 2000).

Consistent with our previous findings (Mitchell *et al.*, 2006), a significant decrease in BrdU positive nuclei is detected in livers from TCDD pretreated WT mice. Extensive BrdU incorporation occurred 12 hours sooner in the hepatectomized p21^{Cip1} KO mice, and significantly, the anti-proliferative property associated with TCDD treatment was absent in the p21^{Cip1} null background, suggesting that p21^{Cip1} plays a critical role in regulating normal liver regeneration. In contrast, BrdU incorporation in p27^{Kip1} KO mice was modest in both vehicle and TCDD-treated WT mice although peak

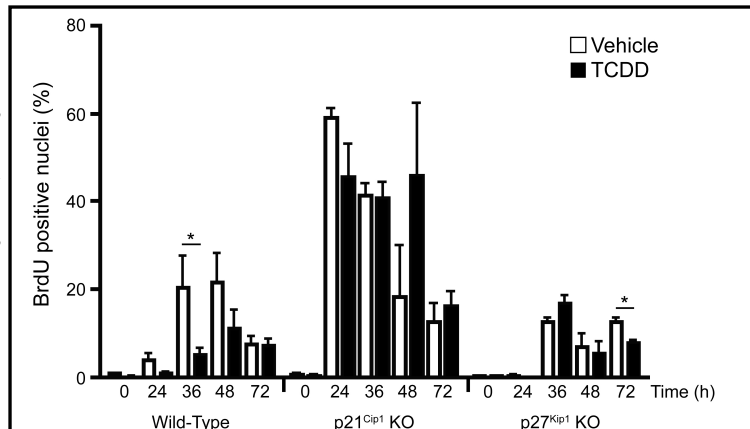


Figure 6: Analysis of hepatocyte proliferation during liver regeneration in vehicle or TCDD treated wild-type, p27^{Kip1} KO mice, or p21^{Cip1} KO mice. Mice were treated for 24 hours with vehicle or TCDD prior to PH or sham surgery, then pulsed with BrdU 2 hours before euthanization at indicated time points. Counts represent the number of BrdU positive nuclei as a percent of total nuclei from 6 random fields. Data represent the average percent positive nuclei from 3 animals per treatment group and are representative of 3 separate experiments. Data are plotted as mean \pm S.E.M. An asterisk indicates a significant difference between the vehicle and TCDD treated groups ($p < 0.05$).

DNA synthesis matched the temporal process observed in WT mice. TCDD-induced inhibition of DNA synthesis was reproducibly detected in the p27^{Kip1} KO mouse livers, but only 72 h post surgery. These findings suggest that p21^{Cip1} rather than p27^{Kip1} plays a critical role in regulating passage through G₁-phase during liver regeneration, and that loss of p21^{Cip1} function both hastens entry into S-phase and abrogates the AhR-mediated TCDD induced growth arrest. Indeed, Albrecht and coworkers have previously demonstrated that loss of p21^{Cip1} accelerated hepatocyte progression through the G₁-phase after PH (Albrecht *et al.*, 1998). BrdU incorporation was minimal (<4%) in sham-operated mice that were pretreated with either vehicle or TCDD (data not shown).

To examine the cumulative effect of p21^{Cip1} or p27^{Kip1} loss on liver regeneration, we performed a continuous BrdU labeling study over

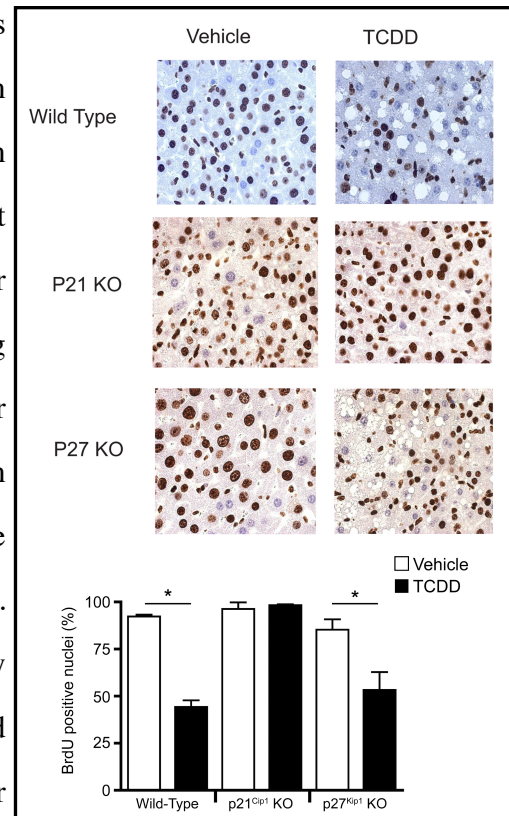


Figure 7: TCDD induced suppression of liver regeneration is abrogated in p21^{Cip1} KO mice but not in p27^{Kip1} KO mice. **A**, Representative sections of cumulative BrdU incorporation during liver regeneration in wild-type, p21^{Cip1} KO, or p27^{Kip1} KO mice. Mice were treated for 24 hours with vehicle or TCDD prior to PH surgery, then provided BrdU through their drinking water (0.8 mg BrdU/ml, shielded from light) immediately following PH for a period of 5 days post PH. **B**, Counts represent the number of BrdU positive nuclei as a percent of total nuclei from 6 random fields. Data represent the average percent positive nuclei from 3 animals per treatment group and are representative of 3 separate experiments. Data are plotted as mean \pm S.E.M. An asterisk indicates significant difference between the vehicle and TCDD treated groups ($p < 0.05$)

a 120 hour period following partial liver resection in WT, p21^{Cip1} KO, and p27^{Kip1} KO mice (**Figure 7**). The immunohistochemical data show that over the course of 5 days, DNA synthesis occurred in 85-100% of the hepatic nuclei in vehicle-treated mice irrespective of the genotype. In contrast, TCDD pretreatment suppressed liver cell proliferation in the WT and p27^{Kip1} KO mice by about 50-60%, while the p21^{Cip1} KO mouse livers were completely resistant to the TCDD effect. These data support the BrdU pulse labeling results (**Figure 6**). We also observed hydropic degeneration in the

hepatectomized livers from TCDD treated WT and p27^{Kip1} KO mice that was undetectable in the p21^{Cip1} KO mouse livers. The precise molecular basis for this difference is unknown, but is suggestive of a link between p21^{Cip1} activity and the TCDD induced pathology detected in the liver sections.

Given the finding that p21^{Cip1} KO mouse livers entered S-phase prematurely and were refractory to the TCDD effects, we examined CDK2 expression and function in these livers. CDK2 protein levels transiently increased during the first 24 h post PH, but remained largely unaltered during the subsequent 48 h of

liver regeneration and showed no TCDD dependency (**Figure 8A**). Consistent with observations made in WT mice (Albrecht *et al.*, 1998), co-immunoprecipitation of the p27^{Kip1} protein in the p21^{Cip1} null background

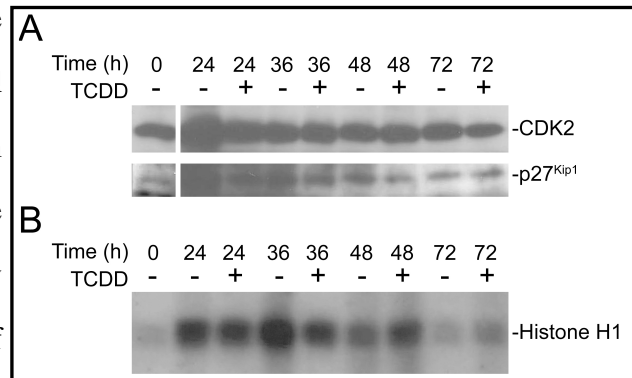


Figure 8: Loss of p21^{Cip1} alters CDK2/p27^{Kip1} association and CDK2 kinase activity. **A**, p21^{Cip1} KO mice were treated with vehicle or TCDD for 24 hours prior to PH then were euthanized at the indicated times post surgery. Livers were resected and homogenized then subjected to immunoprecipitation with anti-CDK2 antibody. These immunoprecipitates were probed for CDK2 and p27 via Western blot. Blots are representative of at least three separate experiments. **B**, CDK2 kinase assays were performed on liver homogenates from mice treated as in (A). Homogenates were subjected to immunoprecipitation with anti-CDK2 antibody. Resultant immunoprecipitates were incubated with histone H1 to measure phosphorylation. Blot is representative of three separate experiments.

revealed that CDK2 binding increased marginally following PH. Moreover, formation of the p27^{Kip1}/CDK2 complex did not display a TCDD dependency. Assessment of CDK2 activity in p21^{Cip1} KO mice readily detected enhanced kinase activity by 24 h post-PH (**Figure 8B**), without the pronounced TCDD induced inhibition seen in WT mice (Mitchell *et al.*, 2006).

TCDD Induced Transactivation of p21 Gene Expression Requires the AhR

Whereas CDK2 activity is first evident at 36 h post PH in WT mice (Albrecht *et al.*, 1998; Mitchell *et al.*, 2006), detecting CDK2 activity by 24 h in the p21^{Cip1} KO mice underscores the accelerated commitment to DNA synthesis. Therefore, despite the presence of p27^{Kip1}, the lack of p21^{Cip1} resulted in premature up-regulation of CDK2

activity, and loss of TCDD induced growth arrest. Under normal physiological conditions, p21^{Cip1} expression is largely undetectable in the quiescent liver, although PH triggers p21^{Cip1} gene expression (Albrecht *et al.*, 1998). In contrast, p21^{Cip1} expression is inducible in quiescent mouse livers following TCDD treatment for 24 hours (**Figure 9A**). In fact, significant hepatic p21^{Cip1} mRNA induction was evident within 2 hours of TCDD treatment in WT mice but not in AhR conditional KO (CKO) mice devoid of receptor protein in the liver parenchyma (**Figure 9B**), suggesting that p21^{Cip1} is indeed an AhR target gene. A similar observation was made for the prototypical AhR target gene, Cyp1a1, exhibiting robust induction in WT livers that was markedly attenuated in the CKO mouse liver (**Figure 9B**). Because these RNA isolations were performed using whole liver, the residual induction of Cyp1a1 in the CKO animals is attributed to AhR activity in the non-parenchymal cells of the liver, not subject to the Cre recombinase activity necessary to disrupt the AhR gene, which therefore express a functional AhR signaling cascade. In contrast, p27^{Kip1} mRNA levels did not change following TCDD exposure indicating that this is not a TCDD responsive murine gene *in vivo*, despite being TCDD responsive in the 5L rat hepatoma cell line (Kolluri *et al.*, 1999).

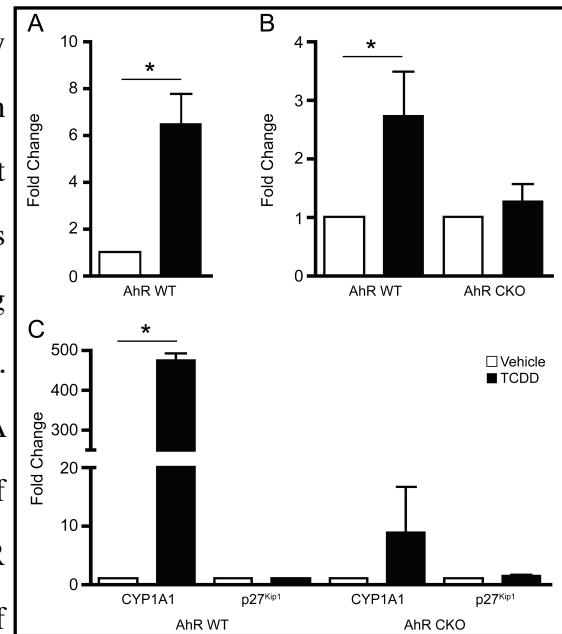


Figure 9: A, WT mice treated with vehicle or TCDD for 24 hours and euthanized at indicated times following PH. p21^{Cip1} mRNA levels quantified via qRT-PCR. Data represent the mean (\pm S.E.M) of five mice per treatment each assayed in triplicate. * indicates significance at $p < 0.01$ between vehicle and TCDD treatment B, WT mice treated with vehicle or TCDD for 2 hours. p21^{Cip1} mRNA levels measured via qRT-PCR. Data represent the mean (\pm S.E.M) of six WT mice or four AHR CKO mice per treatment, assayed in triplicate. * indicates significance $p < 0.05$ between vehicle and TCDD treatment C, as in B assessing CYP1A1 and p27^{Kip1} mRNA

The AhR and KLF6 Regulate p21^{Cip1} Expression Through Direct Binding of the p21^{Cip1} Transcript 2 Promoter

In order to verify that p21^{Cip1} is an AhR target gene, we performed chromatin immunoprecipitation (ChIP) assays. However, prior to assaying for AhR binding to the p21^{Cip1} promoter *in vivo*, it was first necessary to ascertain which of two alternate promoters (Gartel *et al.*, 2004) conferred TCDD inducible p21^{Cip1} expression in the liver. A third alternate p21^{Cip1} transcript has been described previously (Huppi *et al.*, 1994), but is not expressed in the liver (Gartel *et al.*, 2004). The genomic context for the two transcripts expressed in the liver are shown in **Figure 10A**. Transcription is under the control of two distinct promoters, where transcripts 1 and 2 differ in their 5' untranslated region, but encode the same p21^{Cip1} protein. RT-PCR on total RNA using variant-specific primers revealed that the downstream promoter is by far the dominant promoter during liver regeneration as well as in response to TCDD treatment (**Figure 10B**).

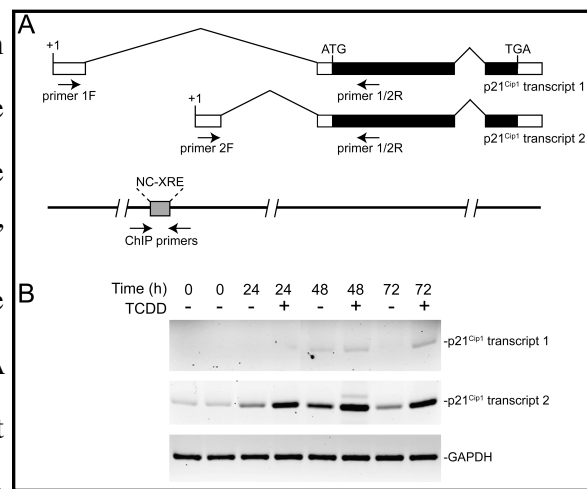


Figure 10: A, p21^{Cip1} variants and variant-specific primers used for RT-PCR analysis. **B**, Mice were treated with vehicle or TCDD 24 hours before PH, then euthanized at indicated times after surgery. mRNA levels were measured via RT-PCR (30 cycles for p21, 28 cycles for GAPDH). n=3 experiments

Our lab recently documented that the NC-XRE is a functional target site for a novel interaction involving the tumor suppressor KLF6 and the AhR (Wilson *et al.*, 2013). It is noteworthy that the downstream promoter of p21^{Cip1} contains a NC-XRE. Given the previous finding that p21^{Cip1} is a KLF6 target gene (Narla *et al.*, 2001; Narla *et al.*, 2007), ChIP assays concentrated on the NC-XRE containing promoter region. ChIP experiments were performed on mouse liver tissue obtained from animals treated with vehicle or TCDD via oral gavage. PCR amplification of the genomic region encompassing the NC-XRE revealed that both the AhR and KLF6 proteins were recruited

to the promoter within 2 hours following TCDD exposure (**Figure 11A**). Analysis on quantitated replicate experiments confirmed that AhR and KLF6 DNA binding is significantly increased by TCDD treatment, consistent with the rapid increase in p21^{Cip1} mRNA (**Figure 9B**). DNA binding by the AhR-KLF6 complex to the p21^{Cip1} promoter persists for at least 24 hours following TCDD exposure (**Figure 11B**, sham surgery). Significantly, PH—in the absence of TCDD—also induced recruitment of the AhR and KLF6 to the p21^{Cip1} promoter within 2 h (**Figure 11B**, partial hepatectomy), consistent with the transient increase of transcript 2 following PH (**Figure 10B**). TCDD pretreatment potentiated AhR-KLF6 binding to the p21^{Cip1} promoter in hepatectomized livers in keeping with the enhanced mRNA expression.

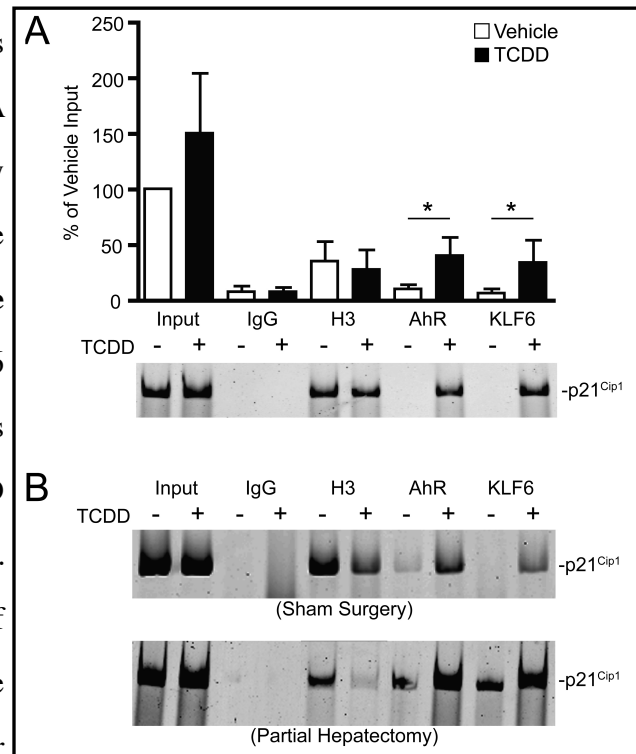


Figure 11: **A**, Mice were treated with vehicle or TCDD for 2 hours. Livers were resected and used for ChIP. Results are densitometry of four experiments, as percent input signal. Data are plotted as mean \pm S.E.M. (* $p < 0.05$). **B**, Mice were pretreated 24 hours with vehicle or TCDD prior to sham (top) or PH surgery (bottom). 24 hours after surgery livers were resected and used for ChIP. Gels are representative of three separate experiments.

These data indicate that PH triggers AhR activation in the absence of an exogenous agonist such as TCDD. The evidence for spontaneous AhR activation following PH resulting in p21^{Cip1} expression (**Figure 11**) is further supported by an increase in P450A1 (Cyp1a1) protein expression observed during the first 48 hours following PH (**Figure 12**). This represents a transient induction of the Cyp1a1 gene attributed to an

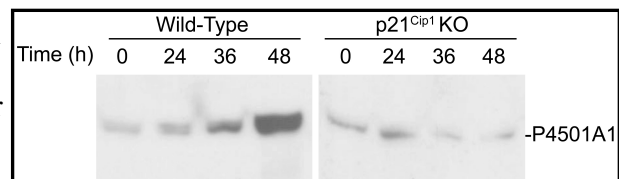


Figure 12: WT or p21^{Cip1} KO mice were subjected to sham (0 hr) or PH surgery and euthanized at the indicated times after PH. Livers were resected and processed for Western blot analysis to detect Cyp1a1 protein levels. Blot is representative of three experiments.

endogenous signaling mechanism activating the AhR that was previously observed during liver regeneration (Mitchell *et al.*, 2006). The surprising observation that this Cyp1a1 induction is attenuated in the p21^{Cip1} KO mice following PH implies that AhR functionality is dependent on a p21^{Cip1}-regulated process absent in the null mice.

DISCUSSION

The current understanding of the signaling events that regulate liver regeneration after two-thirds PH is incomplete. While 70% PH induces most of the remaining hepatocytes to replicate at least once before exiting the cell cycle, we have shown that TCDD treatment can disrupt the normal regenerative process following PH, with fully half of the hepatocytes in the liver remnant failing to proliferate (Mitchell *et al.*, 2006). The study also demonstrated that CDK2 activity, rather than CDK4 activity, was inhibited by TCDD treatment. Hence, the work reported here focused on the CDK2 inhibitors, p21^{Cip1} and p27^{Kip1}, rather than the INK4 inhibitors known to suppress CDK4 activity (Sherr and Roberts, 2004). Moreover, TCDD induced growth arrest in the 5L rat hepatoma cell line was attributed to p27^{Kip1} function (Kolluri *et al.*, 1999; Levine-Fridman *et al.*, 2004). However, the present finding using KO mice demonstrated that in mice *in vivo*, p21^{Cip1} rather than p27^{Kip1} conferred the TCDD induced inhibition in liver regeneration.

BrdU incorporation studies revealed that loss of p27^{Kip1} did not substantially alter the TCDD induced inhibition in hepatocyte proliferation observed in wild-type mice (**Figure 7**). In contrast, the absence of p21^{Cip1} expression completely abrogated the TCDD effect seen in WT mice. Accordingly, CDK2 activity in the p21^{Cip1} KO mouse liver was unaffected by TCDD treatment (**Figure 8B**), juxtaposing the earlier findings in WT mice where TCDD treatment inhibited CDK2 activity (Mitchell *et al.*, 2006). In keeping with other studies (Albrecht *et al.*, 1998), PH increased CDK2 activity in p21^{Cip1} KO mice at 24 hours, substantially earlier than the peak of CDK2 activity normally observed at 36 hours post PH (Mitchell *et al.*, 2006). This is congruent with the

accelerated commitment to S-phase measured by BrdU incorporation (**Figure 11**). Collectively, the results indicate that TCDD induced growth arrest in the regenerating liver is absolutely dependent on p21^{Cip1} activity, and that p27^{Kip1} does not confer functional redundancy. The finding that p21^{Cip1} rather than p27^{Kip1} is required for the TCDD effect *in vivo*, also bolsters the recognition that studies examining cell cycle control in tissue culture systems cannot automatically be extrapolated to liver regeneration *in vivo* (Loyer *et al.*, 1994; Kren and Steer, 1996).

p21^{Cip1} is the founding member of the Cip/Kip family of cyclin-dependent kinase inhibitors (Gartel *et al.*, 1996). Expression of p21^{Cip1} is controlled mostly at the transcriptional level by both p53-dependent and p53-independent mechanisms (Gartel and Tyner, 1999). Although the p21^{Cip1} genomic locus is organized differently in mice and humans, both produce multiple transcripts utilizing different promoters (Nozell and Chen, 2002; Gartel *et al.*, 2004). In mice, expression of the classical transcript (transcript 2) is p53-independent (Gartel *et al.*, 2004). This transcript appears to be the dominant transcript up-regulated following PH and exposure to TCDD (**Figure 10B**). It is noteworthy that the promoter regulating transcript 2 contains a NC-XRE. We recently showed that the NC-XRE is an AhR DNA-binding site. AhR mediated regulation of gene expression via the NC-XRE occurs through a mechanism involving the novel binding partner, KLF6 (Huang and Elferink, 2012; Wilson *et al.*, 2013). The basis for the modest increase in transcript 1 detected after PH and TCDD treatment is uncertain (**Figure 10B**). As such, further studies are required to explore whether this increased expression is due to direct transcriptional regulation of the upstream promoter or a secondary consequence of transcriptional activation at the downstream promoter.

Albrecht and coworkers demonstrated that in contrast to p27^{Kip1} expression, which changed little during liver regeneration, p21^{Cip1} expression, although undetectable in the quiescent liver, was dramatically induced within 3 hours following PH (Albrecht *et al.*, 1997; Albrecht *et al.*, 1998). Our data show that p21^{Cip1} transcript levels transiently

peaked at 48 hour post PH declining thereafter. Induction of p21^{Cip1} by TCDD is detectable at the mRNA level within 2 hours (**Figure 9B**), rapidly reaching a sustained level exceeding the increase observed following PH alone (**Figure 10B**). The lack of induction in the AhR CKO mouse liver suggests that p21^{Cip1} is an AhR target gene. Accordingly, p21^{Cip1} induction is concomitant with recruitment of the AhR and KLF6 to the transcript 2 promoter region harboring the NC-XRE (**Figure 11**). KLF6 was first implicated in regulating p53-independent p21^{Cip1} expression in human prostate cancer (Narla *et al.*, 2001). More recently, studies in transgenic mice over-expressing KLF6 in the liver showed marked p21^{Cip1} expression and diminished hepatocyte proliferation (Narla *et al.*, 2007). These authors concluded that KLF6 was a critical regulator of hepatocyte proliferation and liver size *in vivo*, through a mechanism dependent in large part on p21^{Cip1} expression.

Remarkably, the phenotype in the transgenic KLF6 mice closely resembled that observed in p21^{Cip1} transgenic mice over-expressing the kinase inhibitor in hepatocytes (Wu *et al.*, 1996). Moreover, liver regeneration in the p21^{Cip1} transgenic mice was markedly attenuated following PH (0.5%-14.5% of normal). Collectively, these data suggest that the increase in p21^{Cip1} expression during hepatocyte proliferation following PH contributes to the normal temporal process associated with liver regeneration; prolonged and elevated p21^{Cip1} expression in the transgenic mice, however impedes hepatocyte proliferation. We conclude that TCDD treated, hepatectomized mice similarly show enhanced induction of p21^{Cip1} expression through an AhR-KLF6 dependent transcriptional response resulting in growth arrest.

Hyperphosphorylation and concomitant inactivation of the Rb protein is considered to be the major function of the G₁ and S phase CDKs (Sherr and Roberts, 2004). Rb protein inactivation triggers its release from E2F, allowing for the transcriptional activation of S phase genes, thus resulting in cell cycle progression. Therefore, circumstances that interfere with CDK activation inhibit cell proliferation.

Albrecht and coworkers (Albrecht *et al.*, 1998) showed that Rb protein hyperphosphorylation and loss of E2F binding occurred sooner (36 hours versus 48 hours) in partially hepatectomized p21^{Cip1} KO mice as compared to wild-type mice, consistent with the shortened G₁ interval. Given our previous observation that the active (hypophosphorylated) Rb protein also binds to the AhR and contributes to AhR transcriptional activity (Ge and Elferink, 1998; Levine-Fridman *et al.*, 2004), it is reasonable to speculate that processes, which facilitate Rb protein inactivation may also disrupt AhR activity. This prediction is borne out by the failure of PH to increase P4501A1 expression in the p21^{Cip1} KO mouse liver, a response normally observed in the

regenerating liver of wild-type mice (Figure 12).

Based on the data we have collected and the findings presented elsewhere, we propose the following model (Figure 13).

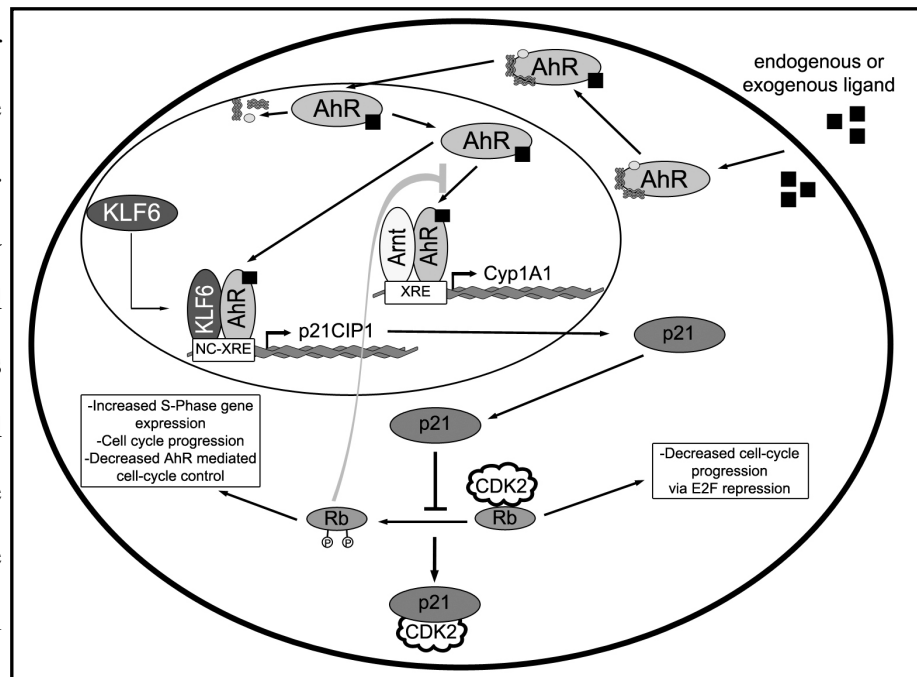


Figure 13 Proposed signaling for the AhR in the regenerating liver. Activation of the AhR stimulates nuclear translocation and chaperone dissociation. The naked AhR protein then interacts with various proteins to transcriptionally regulate target gene expression. For example, the AhR forms a complex with KLF6 to up-regulate p21 expression through binding of the NC-XRE in the p21 promoter. Conversely, the AhR interacts with Arnt to regulate canonical target gene expression via the XRE. Increased p21 expression leads to inhibition of CDK2-mediated hyper-phosphorylation of Rb. This inhibition drives G₁-phase arrest through decreased CDK2/cyclin E complex formation and pRb-AhR mediated repression of E2F dependent genes. In mice lacking p21 expression, rapid induction of cell-cycle progression by proliferative signaling in the regenerating liver leads to rapid CDK2 activity thus contributes to Rb hyper-phosphorylation. The hyper-phosphorylated form of Rb has not been shown to interact with the AhR, thus we propose that physiological AhR signaling in p21^{Cip1} KO mice is disrupted, explaining the data in Figure 12.

evidenced by AhR recruitment to the p21^{Cip1} promoter and P4501A1 induction, which involves AhR binding to the NC-XRE and XRE, respectively. Receptor binding to the

XRE is in concert with the Arnt protein while NC-XRE binding depends on partnering with KLF6. Under normal physiological conditions p21^{Cip1} expression is increased to temporally regulate G₁ phase CDK activity and Rb protein inactivation. The absence of p21^{Cip1} hastens passage through G₁ phase of the cell cycle by inactivating the Rb protein prematurely. Conversely, prolonged over-expression of p21^{Cip1} due to TCDD treatment inhibits G₁ phase kinase activity and delays Rb protein inactivation. Under normal physiological conditions the consequent increase in P4501A1 activity is presumed to facilitate the metabolic clearance of endogenous AhR agonists (Chang and Puga, 1998) resulting in attenuated AhR transcriptional activity, thus restoring balance to the signaling processes. However, because TCDD is refractory to metabolic clearance of the aforementioned endogenous agonists by Cyp1a1, AhR activity persists, thereby resulting in prolonged p21^{Cip1} expression and cell cycle arrest. Conversely, since the Rb protein functions as an AhR co-activator in Cyp1a1 gene expression (Ge and Elferink, 1998; Elferink *et al.*, 2001; Levine-Fridman *et al.*, 2004), the absence of p21^{Cip1} is expected to hasten Rb protein inactivation to promote cell cycle progression and thus impair Cyp1a1 induction.

In conclusion, we have shown that TCDD induced suppression of liver regeneration depends on induction of the p21^{Cip1} gene involving recruitment of the AhR-KLF6 complex to the NC-XRE present in the downstream promoter. Moreover, p21^{Cip1} rather than p27^{Kip1} confers the AhR-mediated attenuation of liver regeneration, and absence of p21^{Cip1} abrogates the TCDD induced effect on liver regeneration. The data also attest to integrated signaling of multiple AhR target genes regulated by distinct DNA recognition sites, and further support the notion that the NC-XRE and XRE singling pathways of the AhR represent functionally distinct processes regulating target genes specific to the AhR/KLF6 and AhR/Arnt interactions, respectively.

Chapter 3: Transcriptomic Analysis of TCDD Inducible AhR-Mediated Gene Expression Changes in the Mouse Liver

INTRODUCTION

Background

In an effort to better understand differential expression of TCDD dependent and independent, as well as AhR-mediated gene batteries, several groups performed microarray analyses on RNA from tissues or cells treated with TCDD or other AhR ligands. The Pohjanvirta laboratory extensively studied transcriptomic changes in wild type (AhR^{+/+}) and AhR null (AhR^{-/-}) mouse livers following TCDD treatment (Tijet *et al.*, 2006; Boutros *et al.*, 2009). They noted significant differences in the expression of 456 ProbeSets in wild-type mice (AhR-dependent) following TCDD treatment. The changes included a number of proteinase inhibitors, including the plasminogen activator inhibitor-1 (serpine1, Pai-1) (Tijet *et al.*, 2006). To evaluate physiological target genes for the AhR (in the absence of exogenous ligand), Tijet *et al.* assessed the transcriptome in both the presence and absence of the AhR. In the absence of an exogenous ligand, AhR status alone accounted for changes in the expression of 392 ProbeSets (Tijet *et al.*, 2006). This finding is consistent with a normal physiological function for the AhR, distinct from the xenobiotic response. In another study, compared to the 456 ProbeSets altered in wild-type mice treated with TCDD, only 32 ProbeSets showed significantly different expression in AhR^{-/-} mice at 19 hours post TCDD treatment (Tijet *et al.*, 2006). These results underscore the essential role of the AhR in nearly all dioxin mediated transcriptional changes. The striking difference in gene induction between the wild-type and the AhR^{-/-} mice is not surprising given the many reports documenting the complete lack of TCDD toxicity in AhR^{-/-} mice (Fernandez-Salguero *et al.*, 1996; Mimura *et al.*, 1997; Peters *et al.*, 1999).

Boverhof *et al.* (2005) studied temporal and TCDD dose-dependent changes in gene expression patterns in the mouse liver (Boverhof *et al.*, 2005). In these experiments, custom cDNA microarrays found 349 significant ($p < 0.05$) gene changes at one or more

doses and 255 significant gene changes at one or more time points following TCDD treatment (Boverhof *et al.*, 2005). Microarray analyses to determine TCDD induced changes in the human liver have been performed using the human HepG2 hepatoma cell line as well (Puga, *et al.*, 2000; Frueh *et al.*, 2001). After 10 nM TCDD treatment for 18 hr, a total of 112 significant genes were identified with at least two-fold change (Frueh *et al.*, 2001). Quantitative RT-PCR confirmed significant changes in human enhancer of filamentation 1 (HEF1), Cot, XMP (involved in cellular proliferation and met), HM74, and Pai-1, among others (Frueh *et al.*, 2001). Puga *et al.* (2000) treated HepG cells for 8 hours with 10 nM TCDD and performed microarray analyses; among the 202 genes significantly different in expression between the treatments, they reported that Pai-1 is significantly up-regulated following dioxin exposure (Puga, *et al.*, 2000). Furthermore, they showed this up-regulation persisted in the presence of pretreatment with 20 μ M cyclohexamide, which blocks nascent protein synthesis, suggesting Pai-1 is a direct AhR target gene up-regulated following TCDD treatment, in the liver (Puga, *et al.*, 2000).

Complementary chromatin immunoprecipitation (ChIP) DNA microarray (ChIP-chip) studies examining AhR bound genomic sequences revealed that 57.8% and 48.5% of AhR enriched regions, at 2 hours and 24 hours post-TCDD treatment respectively, did not contain an XRE core DNA sequence (5'-GCGTG-3') (Dere *et al.*, 2011) or any other known AhR DNA-binding motifs. This is consistent with several other reports using high throughput analyses (Kinehara *et al.*, 2008), DNA microarray (Pansoy *et al.*, 2010), ChIP-chip (Lo *et al.*, 2011), and ChIP next-generation sequencing (ChIP-Seq) (Lo and Matthews, 2012). It has been suggested that genes up-regulated following TCDD treatment that lack the known AhR DNA-binding motifs, may represent secondary transcriptional changes, activated downstream of one or more of the genes the AhR directly up-regulates. Several studies have suggested that while indirect events likely account for some portion of the expression changes in genes lacking an AhR motif, there are in fact a large number of TCDD responsive genes controlled in an AhR-dependent

manner that lack a classical AhR XRE DNA motif. This includes the microarray studies by Puga et al. (2000) involving cyclohexamide to assess transcriptomic changes without nascent protein synthesis, the ChIP-chip report by Dere et al. (2011) assessing multiple treatment time points, and the ChIP-sequencing studies by Lo and Matthews in MCF-7 cells to assess direct DNA-binding by the AhR (Puga, *et al.*, 2000; Dere *et al.*, 2011; Lo and Matthews, 2012). Given that the AhR functions as a transcription factor, and given the numerous (previously discussed) examples of the AhR interacting with multifarious protein partners to bind DNA motifs other than the XRE, it stands to reason that the AhR regulates a subset of target genes through a mechanism independent of the XRE. Pai-1 was identified as one such gene in several of the aforementioned studies (Puga, *et al.*, 2000; Frueh *et al.*, 2001; Son and Rozman, 2002; Tijet *et al.*, 2006). Pai-1 is a member of the serine protease inhibitor (serpine) family. It functions as an inhibitor of urokinase plasminogen activator and tissue plasminogen activator (Binder *et al.*, 2002; Durand *et al.*, 2004), which convert plasminogen to plasmin to facilitate fibrinolysis. Pai-1 is ubiquitously expressed, but most highly so in endothelial cells, adipocytes, and hepatocytes.

Need For Transcriptomic Studies of AhR Targets *In Vivo*

Indeed, we have shown that Pai-1 is TCDD inducible in an AhR-dependent manner via a novel DNA motif for the AhR, which we have dubbed the non-consensus XRE (NC-XRE) motif (Huang and Elferink, 2012). As discussed above, further study of AhR binding to the NC-XRE DNA-motif characterized the involvement of the novel AhR protein partner KLF6 (Wilson *et al.*, 2013). We have further shown that the AhR/KLF6 interaction involves the N-terminal 27 amino acids of KLF6, and the C-terminal portion of the AhR protein. Given the recent identification of the NC-XRE DNA-motif, the AhR/KLF6 protein-protein interaction in the NC-XRE pathway, and the newly discovered p21 and Pai-1 target genes for the AhR in the NC-XRE pathway (Jackson *et al.*, 2014; Jackson *et al.*, 2015), we questioned the potential existence of hitherto undiscovered

target genes regulated by the AhR *in vivo* in the liver. Tangential to this query, several important points should be considered. First, it is noteworthy that to date, most studies assessing AhR-mediated transcriptional changes, in several experimental paradigms, have centered around *in vitro* experiments in dividing cells. Some such studies have involved the use of human and mouse derived liver cancer cell lines (Puga, *et al.*, 2000; Swedenborg *et al.*, 2012), which by their very nature have pathological alterations to the basic physiological processes regulating cell division, and by extension, gene expression (Hanahan and Weinberg, 2011). Second, studies assessing links between KLF6 and cancer growth and metastasis have shown that the KLF6 can be found *in vivo* in four distinct isoforms, three of which are splice variants of a single coding sequence for the WT protein (Narla *et al.*, 2005; Andreoli *et al.*, 2010). Interestingly, at least two of these splice variants lack the nuclear localization sequence needed to target the protein to the nucleus. Further, one of those two isoforms lacks the protein region required for NC-XRE binding with the AhR altogether; however, both variants retain the N-terminal region of KLF6 required for the interaction with the AhR. Given that the expression of various KLF6 isoforms has been shown to vary between cancers (Hartel *et al.*, 2008; Andreoli *et al.*, 2010), it is entirely possible that studies assessing AhR-mediated transcriptional changes in the aforementioned liver cancer cell lines may have overlooked entire subsets of NC-XRE regulated AhR targets as a result of alterations to KLF6 protein expression. Thus, while these studies lend insight on some aspects of the transcriptional changes mediated by the AhR, further studies *in vivo*, or at least in cell lines with ‘normal’ KLF6 expression, will provide a more full understanding of the transcriptional targets of the AhR.

It is also worth noting that many studies assessing AhR-mediated transcriptional changes (both *ex vivo* and *in vitro*) to date have been accomplished through the use of microarray (Puga, *et al.*, 2000; Frueh *et al.*, 2001; Tijet *et al.*, 2006; Boutros *et al.*, 2009; Forgacs *et al.*, 2013; Jackson *et al.*, 2015) analysis. While microarray is a valuable tool in

transcriptomic studies, recent advances in next-generation sequencing technologies have led to the advent of whole transcriptome shotgun sequencing (RNA-sequencing). RNA-sequencing has significant advantages over microarray-based methodologies because it does not depend on probesets hybridized to chips to accurately quantify gene expression levels. As a result, it is possible to identify (and thus quantify) a much wider range of mRNA sequences with RNA-seq, than has traditionally been possible with array based methods. It is also worth noting that few of those studies (discussed above, assessing transcriptomics of the AhR) have involved the use of AhR null or AhR conditional knock-out mice (Puga, *et al.*, 2000; Boutros *et al.*, 2009). Given recent findings (Wilson *et al.*, 2013; Jackson *et al.*, 2014; Jackson *et al.*, 2015) regarding the role of KLF6 in AhR-mediated transcriptional changes and the aforementioned limitations of previous transcriptomic analyses of the AhR, we resolved to 1) assess gene expression changes in livers of wild-type and AhR CKO mice treated with vehicle or TCDD *in vivo* for 2 or 8 hours, and 2) to further characterize the C-terminal region of the AhR necessary for the interaction with KLF6.

MATERIALS AND METHODS

Animals

C57Bl/6J (WT) and AhR^{Fx/FxCre^{Alb}} conditional knock-out (AhR CKO, C57Bl/6J background) mice were purchased from Jackson Laboratories. Animals were maintained on a 12 hour light/dark cycle, in a temperature controlled facility at the University of Texas Medical Branch animal resource center. Food and water were provided *ad libitum*. Female mice 8-10 weeks old were used for all experiments involving mice. For vehicle/TCDD treatments, mice were gavaged with vehicle (anisole dissolved in peanut oil) or TCDD (dissolved in anisole and diluted in peanut oil) for 2 or 8 hours. Animals were euthanized via isoflurane overdose followed by cervical dislocation and removal of a vital organ. The livers were resected and snap frozen in liquid nitrogen then either stored at -80°C for future experiments, or thawed and placed in TRIzol for immediate RNA

isolation. All experiments described herein were conducted in accordance with approved institutional animal care and use committee protocols.

Chemicals

As previously described (Jackson *et al.*, 2014), TCDD was purchased from Cerilliant (Round Rock, TX) and dissolved in anisole, then diluted in peanut oil to give a concentration of 2 mg/ml. Unless otherwise indicated, for *in vivo* studies TCDD was administered via oral gavage at a dose of 20 µg TCDD/kg body weight. Control animals received a vehicle treatment consisting of similar amounts of anisole dissolved in peanut oil.

***In Vitro* TnT Reticulocyte Lysate Generated Proteins**

For recombinant protein generation 1 µg of cDNA construct (vector maps in **Appendix 2**) for each protein was used according to the manufacturers recommendations for the TnT coupled reticulocyte lysate system (Promega, Madison, Wisconsin): 25µL of Reticulocyte lysate, 2µL buffer, 1µL each of amino acid cocktail minus methionine and amino acid cocktail minus leucine, 1µL of ribonuclease inhibitor, and 1 µL of SP6 or T7 polymerase. This mixtures was incubated for 90 minutes at 27°C for protein synthesis.

Immunoprecipitation/Western Blotting

For immunoprecipitations using TnT proteins (see above), 15µL of each recombinant protein (AhR and KLF6) were added together with 7µL of vehicle (DMSO) or 7µL of TCDD and 33µL of HEDG buffer (25mM HEPES, 1mM EDTA, 1mM (added fresh) DTT and 10% glycerol) and incubated at 30°C for 60 minutes. Next, 450µL of TGH buffer (50mM HEPES (pH 7.4), 150mM NaCl, 1.5mM MgCl₂, 1mM EGTA, 1% Triton X-100, 10% glycerol) supplemented with 1mM PMSF, 10mM NaF, 1mM Na₃VO₄ and 5µL/ml protease inhibitors was added along with 5µg antibody and BSA to a final concentration of 1µg/ml. This mixture was incubated overnight on a rotating mixer at 4°C. The next day, 50µL agarose protein A/G beads (sc-2003, Santa Cruz Biotech, Dallas, TX) was added and incubated for 4 hours on a rotating mixer at 4°C. Following

incubation, tubes were spun at 4°C at 14,000 RPM, supernatant was removed and beads were washed with 500µL ice cold TGH buffer and spun again at 4°C at 14,000 RPM, this sequence was repeated for a total of 5 washes. After the final spin, supernatant was removed and beads were resuspended in 40µL 2x SDS loading buffer with 10% β-mercaptoethanol, boiled for 5 minutes at 100°C and spun for 2 minutes at 4°C at 9,000 RPM. Denatured proteins were resolved on 10% SDS-PAGE gels, transferred for 1 hour onto PVDF membranes, and blocked for 1 hour in TBS- containing 0.1% Tween 20 (TBS-T) with 5% dry milk. Blots were probed overnight with antibodies against the AhR (Biomol Rabbit 1:1000), or KLF6 (Santa Cruz sc-7158 rabbit anti-KLF6 1:200, or Santa Cruz sc-365633 mouse anti-KLF6 1:200). The next day, blots were washed three times, 15 minutes each with TBS-T at room-temperature then probed with secondary antibody (Cy5 donkey anti-rabbit 1:1000, GE Healthcare Life Sciences, Pittsburgh, PA or Clean-blot 1:1000, Thermo Scientific, Waltham, MA) and detected with Typhoon Variable mode Imager (GE Healthcare Life Sciences, Pittsburgh, PA) or HRP chemiluminescence detection.

Electrophoretic Mobility Shift Assay Experiments

Electrophoretic Mobility Shift Assays (EMSAs) were performed as previously described (Wilson *et al.*, 2013). Using TnT generated proteins (see above) 5µL of each protein were incubated together in 20µL HEDG buffer with 100ng poly(deoxyinosinic-deoxy-cytidylic) acid (PolydI-dC) and 100mM KCl for 10 minutes at room-temperature. 300ng of ³²P ATP end-labeled NC-XRE dsDNA probe (3000mCi/mmol) (Huang and Elferink, 2012) was added and incubated for 15 minutes at room-temperature. Mixture was resolved on 5% non-denaturing poly-acrylamide gels with TAE (40mM Tris, 20mM acetic acid, 1mM EDTA pH 8) running buffer; gels were dried onto blotting paper under vacuum at 37°C for 90 minutes and exposed to phosphor screens overnight at room-temperature. Screens were imaged the next day via Typhoon Variable mode Imager (GE Healthcare Life Sciences, Pittsburgh, PA).

RNA-Sequencing Library Generation and Sequencing

Total RNA was isolated from livers of WT or AhR CKO mice (female mice, 8-10 weeks old) treated with vehicle or TCDD (all treated at ~0700 hours to minimize differences due to circadian rhythm) using TRIzol (Life Technologies, Carlsbad, California) according to the manufacturers recommendations. RNA concentrations were quantified using a nanospectrophotometer (Nanodrop ND-100, Thermo Scientific) and RNA quality was assessed using Agilent Bioanalyzer. Following the quality control steps, RNA was used to generate libraries which were amplified, evaluated for quality, size selected, and sequenced on the Illumina Genome Analyzer Hi-seq 1000 by the UTMB Next-Generation Sequencing Core, with a sequencing depth of coverage at ~40 million reads per sample (n=3 per treatment per genotype). Reads were called and aligned using CASAVA-1.8.2.

Chromatin Immunoprecipitation for Next-generation Sequencing (ChIP-seq)

The first portion of the chromatin immunoprecipitation experiments were performed as described in materials and methods **Chapter 2**. At the midpoint of the experiment the protocol differs depending on the final output, ChIP-Sequencing or ChIP PCR. The following second half of the protocol described here is for ChIP-sequencing. In detail, the pelleted material was resuspended in 1ml of ice cold 1x lysis buffer supplemented with protease inhibitor cocktail (PIC) and phenylmethanesulfonylfluoride (PMSF), and incubated on ice for 30 minutes. During which time, a working stock enzymatic shearing cocktail was generated by adding 2 μ L of shearing cocktail to 198 μ L of 50% glycerol. Pellet/cell lysis buffer mixture was transferred to a dounce homogenizer on ice and dounced **40 strokes** with a tight pestle. The solution was then transferred to eppendorf tubes and spun at 3,200 xg for 10 minutes at 4°C. The supernatant was aspirated and the pellet resuspended in 350 μ L of digestion buffer, supplemented with 1.75 μ L each PIC and PMSF, and incubated for 15 minutes at 37°C. The chromatin was sheared using Covaris acoustic sonication in 120 μ L aliquots using 175 peak power, 5%

duty factor, for 7 minutes. The mixture was pelleted via spin at 6,400 xg for 10 minutes at 4°C, and the protein-DNA complex supernatant was transferred to new tubes. Protein DNA complexes were immunoprecipitated with the following antibodies: mouse monoclonal anti-AhR (ab2769 Abcam, Cambridge MA), goat polyclonal anti-KLF6 (SC-20885 Santa Cruz Biotechnology), mouse monoclonal anti-histone H3 (ab10799 Abcam, Cambridge MA), or rabbit monoclonal IgG Isotype control (#3900, Cell Signaling Technologies, Danvers, MA). This was accomplished using PIC, PMSF, ChIP buffer 1, antibody, magnetic beads, and chromatin according to the manufacturers recommendations (using 5 μ g of each respective antibody). IP was allowed to proceed overnight (~12 hours). Following the IP, tubes were placed in a magnetic stand to pellet magnetic beads at the bottom of the tubes. Tubes were removed from the stand and 500 μ L of wash buffer 1 was added and gently pipetted to resuspend. Tubes were incubated on a rotor for 30 minutes at RT. This was repeated for a second wash in ChIP buffer 1 and two washes using ChIP buffer 2. After the final wash, the solution was aspirated while the beads were on the magnetic stand, and the beads were resuspended in 50 μ L of Elution Buffer AM2 and incubated for 45 minutes at RT. Tubes were spun to pellet solution and beads in table top galaxy micro centrifuge (for 10 seconds) and 50 μ L of reverse cross-linking buffer was added. Tubes were placed in magnetic stand to retain beads and supernatant was moved to a new tube. To process input DNA, 12 μ L of chromatin (80 μ L of which was added to the IP step for the immunoprecipitation) was diluted in ChIP buffer 2, along with 4 μ L of 5M NaCl, to have the same volume (100 μ L) as other samples. All samples were then incubated overnight at 65°C to reverse cross-links. Tubes were then returned to RT and 1 μ L RNase A was added and tubes were incubated for 30 minutes at 37°C. Again tubes were returned to RT and 2 μ L of proteinase k was added and incubated for 1 hour at 37°C. Following proteinase k treatment, reaction was stopped by addition of 2 μ L of stop solution at RT. To purify DNA, 100 μ L each of chloroform and phenol saturated buffer (pH 7.9) was added, tubes were vortexed to mix,

then centrifuged for 15 min at 12,000 RPM at 4°C. The top layer was transferred to a new tube and 100 μ L chloroform was added, tubes were vortexed, and spun again. Supernatant was transferred to a new tube and 30 μ L NaO-Ac and 700 μ L of 100% EtOH was added and tubes were incubated at -20°C overnight. Tubes were then spun at maximum speed for 45 minutes, supernatant was aspirated, and pellet was **carefully** washed with 700 μ L of 70% EtOH. Tubes were spun again at max speed for 45 minutes, supernatant was aspirated, tubes were allowed to air dry for 3 minutes, and all samples were resuspended in 30 μ L DEPC treated dH₂O. This material was then used for ChIP-qRT-PCR and Agilent bioanalyzer analysis by the UTMB Molecular Genomics core, or for ChIP-sequencing Illumina library preparation by the UTMB Next Generation Sequencing core.

Differential Expression Analysis

NGS reads for RNA-sequencing analysis were sequenced at a depth of coverage of 40 million reads per sample. Results from these runs were processed by the core. Differential gene expression analyses were performed using both Cufflinks and DSeq, however the Cufflinks results were used for all downstream analysis.

Primary Hepatocyte Isolation

Primary hepatocyte isolation was performed exactly as previously described (Harper *et al.*, 2013). Primary hepatocytes were plated at of 8.5×10^4 cells per well on 6-well plates in Williams E media supplemented with Pennicillin (100 U/ml), Streptomycin (100 μ g/ml) and 5% fetal bovine serum. Hepatocytes were infected with the correct adenovirus construct at MOIs of 25-100 for 48 hours, and RNA isolated using TRIzol according to the manufacturers recommendations.

Semi-Quantitative PCR

Semiquantitative PCR was performed as discussed above (see **chapter 2**, materials and methods) using the appropriate primers.

Quantitative PCR

Quantitative PCR was performed as discussed above (see **chapter 2**, materials and methods) using the appropriate primers.

Primers

Primer sequences for ChIP PCR, qRT-PCR, and semi-quantitative PCR can be found in **Appendix 1**.

RESULTS

AhR Interaction With KLF6 Involves C-terminus Protein-Protein Interaction and N-terminal DNA-binding

A previous study assessing the AhR/KLF6 protein-protein interaction found that a C-terminal deletion (ΔC) of the human AhR protein (amino acids (AA) 424-805), lost the ability to interact with KLF6 (Wilson *et al.*, 2013). As such, we set out to more closely define the region of the AhR involved in the interaction with KLF6. To do this, we

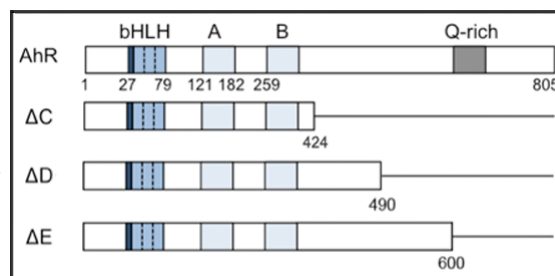


Figure 14: WT and C-terminal deletion mutants of the human AhR protein.

generated additional C-terminal deletion mutants of the AhR with sequentially longer additions onto the original ΔC mutant sequence (**Figure 14** and **Appendix 2**). We then confirmed expression of these mutants in our *in vitro* transcription/translation (TnT) system to ensure the proteins were expressed at the expected sizes via Western blot (**Figure 15**). Next, we performed co-immunoprecipitation (co-IP) experiments to assess the ability of the mutants to interact with KLF-6. We found that both the wild-type and ΔD forms of the human AhR protein co-IP'd with KLF6, while the ΔC deletion mutant of the AhR did not co-IP with KLF6 (**Figure 16**). These results show that AA 424-490 of the human AhR protein are necessary for the interaction with KLF6.

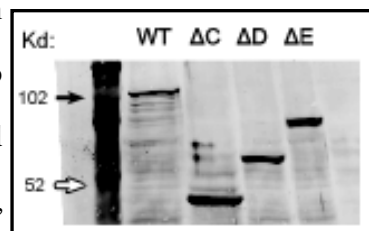


Figure 15: Expression of AhR mutants from **figure 14** in *in vitro* TnT system detected via Western Blot.

Previous studies by Wilson et al. (2013) tested several common deletions mutants of the AhR to determine what region of the protein is necessary to bind NC-XRE DNA sequences with KLF6. These studies found that deletion of the bHLH domain of the AhR, known to be vital for AhR DNA-binding to XRE DNA motifs with Arnt in the canonical pathway, did not affect AhR DNA-

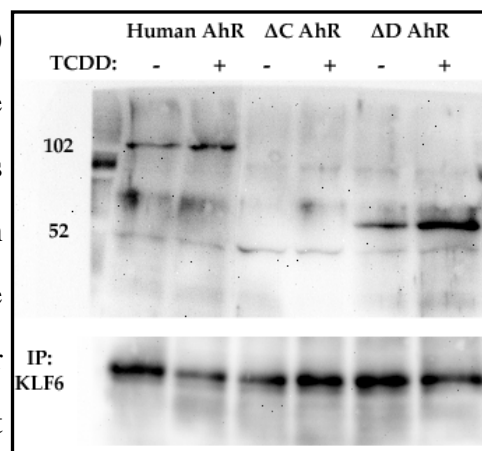


Figure 16: Co-IP of Human AhR mutant proteins from figure 15. Proteins were IP'd with anti-KLF6 antibody then blots for AhR were performed

found that none of the other AhR mutants tested, apart from the ΔC deletion (presumably due to the inability of the AhR to interact with KLF6), lost the ability to bind NC-XRE DNA sequences (Wilson *et al.*, 2013). We noted two regions of the AhR protein, AA 1-27 and AA 80-120 that were not assessed in these DNA-binding deletion studies. Upon further examination of the 1-27 AA region we found only four charged residues (AA 13-16 RKRR), which might be involved in NC-XRE DNA-binding by the AhR. It is important to note that basic residues have classically been involved in DNA-binding by the AhR, as this was the impetus for us to assess the presence of charged residues in

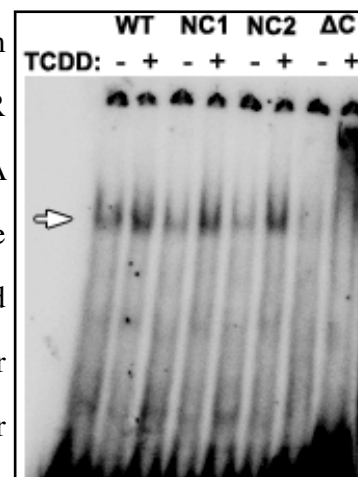


Figure 17: EMSA experiments on *in vitro* TnT generated NC1 and NC2 AhR alanine mutants or ΔC AhR deletion mutant with WT KLF6 and ³²P-ATP labeled NC-XRE DNA oligonucleotides. DNA-AhR/KLF6 complex is indicated by white arrow. Note the darkening in the top of the far right lane is spillover from a lane not shown in this figure

this region. Rather than generate a large N-terminal AhR deletion, we decided to perform site-directed mutagenesis to convert either two, RK→AA (NC1) or all four, RKRR→AAAA (NC2) charged residues to alanine. We confirmed the expression of these mutants in the TnT

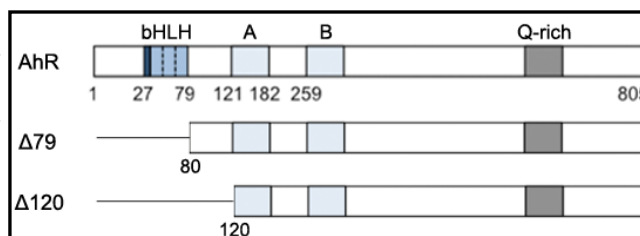


Figure 18: N-terminal AhR deletion mutants for future EMSA experiments to assess NC-XRE DNA-binding by the AhR with KLF6.

system and performed EMSA experiments using ^{32}P -ATP labeled NC-XRE DNA oligonucleotides with wild-type AhR, the NC1 mutant, the NC2 mutant, and the ΔC AhR deletion mutant (**Figure 17**). The results suggest that residues 13-16 of the AhR N-terminal region are not involved in AhR DNA-binding to NC-XRE DNA-motifs. As neutralizing the charged residues in the 1-27 AA region of the AhR did not affect NC-XRE DNA-binding, we generated larger N-terminal deletions of the AhR, focusing on regions not previously analyzed by Wilson et al. (2013) (**Figure 18**). Future studies of NC-XRE DNA-binding by the AhR will analyze these mutants via EMSA to assess whether or not they retain the ability to bind NC-XRE DNA sequences.

The AhR Directly Regulates Expression of Myriad Genes Following Activation by TCDD.

As previously discussed, the AhR is well known to transcriptionally regulate the expression of myriad genes in its function as a transcription factor. Indeed, recent work (described above) has shown this involves at least two different major protein partners (Arnt and KLF6) binding to two distinctly different DNA-motifs (the XRE and NC-XRE, respectively). Previous studies have employed microarray, and more recently NGS methodologies, to identify transcriptional targets of the AhR. However, due to the aforementioned constraints in the experimental paradigms these studies employed, we believe studies using RNA-sequencing to analyze changes in gene expression in livers of mice treated *in vivo* with vehicle or TCDD (20 $\mu\text{g}/\text{kg}$), will provide a more complete picture of AhR transcriptional targets. For our studies we used wild-type (WT) mice, which have normal AhR expression in the liver. We also utilized AhR conditional knock-out (AhR CKO) mice, which contain LoxP sites flanking exon 2 of the AhR and express Cre Recombinase under the control of the albumin

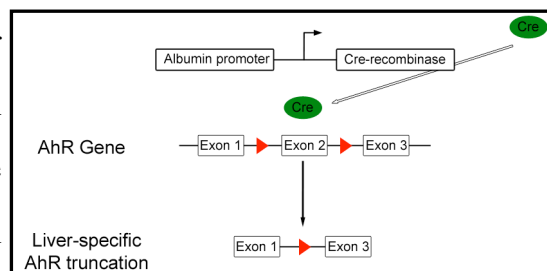


Figure 19: AhR conditional knock-out mouse model. Cre-recombinase is expressed under the control of the albumin promoter in primary hepatocytes. Cre-recombinase acts on LoxP sites (red triangles) flanking exon 2 to excise the flanked exon, generating a non-functional AhR protein

promoter (**Figure 19**). Note albumin expression is active during embryonic development, thus the loss of AhR in the liver occurs in mid-development. As such, these mice lack functional AhR expression in the primary hepatocytes of the liver. It should be noted however, these mice retain functional AhR expression in the non-parenchymal cells of the liver. While non-parenchymal cells account for only a modest fraction of the total cells in the liver, due to the robust changes in gene expression

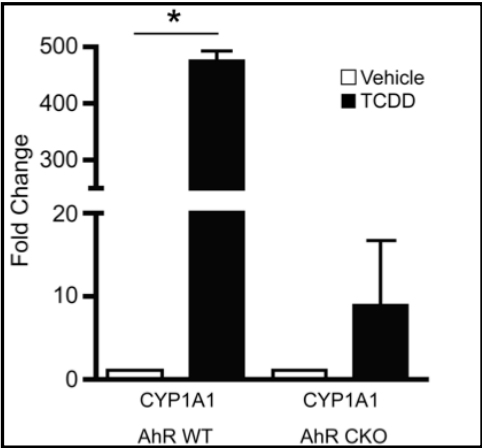


Figure 20: qRT-PCR quantification of Cyp1a1 message in mRNA from livers of WT and AhR CKO mice treated with vehicle or TCDD for 2 hours. Note the modest Cyp1a1 mRNA increases in AhR CKO mice treated with TCDD (relative to vehicle).

caused by the AhR, a very modest change in some AhR target genes (i.e Cyp1a1) can be seen (via qRT-PCR) in total liver RNA from AhR CKO mice treated with TCDD, relative to AhR CKO mice treated with vehicle (**Figure 20**).

We treated WT and AhR CKO mice with vehicle or TCDD via oral gavage for 2 hours (n=3 per genotype, per treatment). We then resected the livers, purified RNA, and performed RNA-sequencing on this material. The differential expression analysis on the RNA-sequencing dataset identified 190 genes which changed

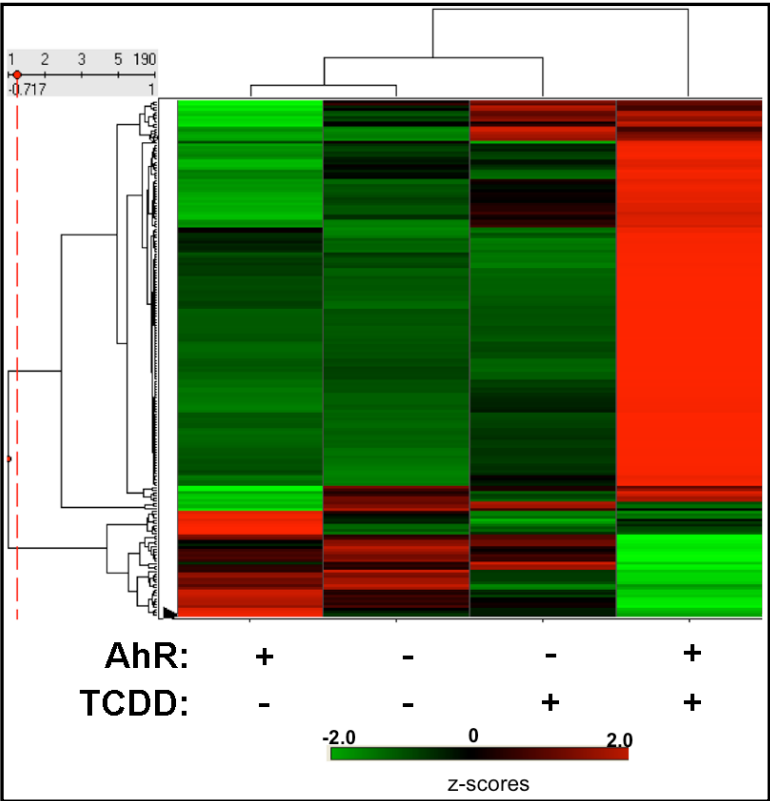


Figure 23: Average heat map of the 190 significant gene expression changes between WT mice treated with vehicle or TCDD. Heat map shows scaled FPKM values for both genotypes (WT and AhR CKO) and treatments (vehicle or TCDD), n=3 for all samples.

significantly in expression between the wild-type mice treated with vehicle or TCDD

(**Appendix 3**). In the same comparison on the AhR CKO mice, only 44 genes were found to be significantly different between the vehicle and TCDD treated mice (**Figure 21**). Between the two comparisons, of the 190 genes that change significantly in the WT mice and the 44 genes that change significantly in the AhR CKO mice, only 10 genes are the same between the two comparisons (**Figure 22**) 5 of which increase in WT mice treated with TCDD (relative to WT vehicle) and decrease in the AhR CKO mice treated with TCDD (relative to AhR CKO vehicle treatment). We generated a heat map of the 190 genes that changed significantly in the WT animals between the two treatments to visualize the expression changes, and compare the expression levels in the wild-type animals with the AhR CKO animals. As expected, the heat map shows that TCDD treatment in the AhR CKO animals, which lack the AhR in the liver, has little effect on gene expression, compared to the WT animals treated in the same way (**Figure 23**).

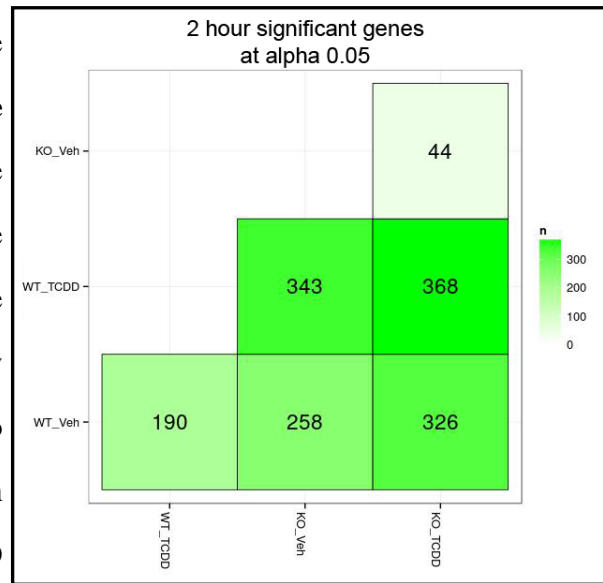


Figure 21: Significant gene expression changes matrix for differential expression analysis of RNA-sequencing performed on mRNA isolated from livers of WT and AhR CKO mice treated with vehicle or TCDD for 2 hours. n=3 for all samples.

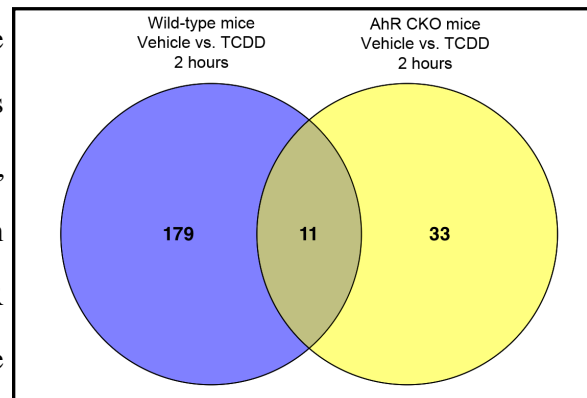


Figure 22: Venn diagram comparing significant gene expression changes in WT and AhR CKO mice (see **figure 21**) (vehicle vs. TCDD) treated for 2 hours.

Given that previous studies have identified a number of direct target genes for the AhR, we chose to validate our results by confirming changes in the expression of well-known AhR target genes in the WT animals treated with TCDD. The RNA-sequencing results identified significant changes in expression of Cyp1a1, Pai-1, p21, Tiparp, and

Maff, all of which are known direct AhR target genes following TCDD exposure (Jackson *et al.*, 2015). RNA-sequencing also identified (among others) significant differences in the expression of immediate early response 3 (Ier3), disheveled-binding antagonist of Beta catenin 2 (Dact2), sulfotransferase enzymes 1e1 and 2a1 (Sult1e1 and Sult2a1), and ubiquitin-specific protease 2 (Usp2)

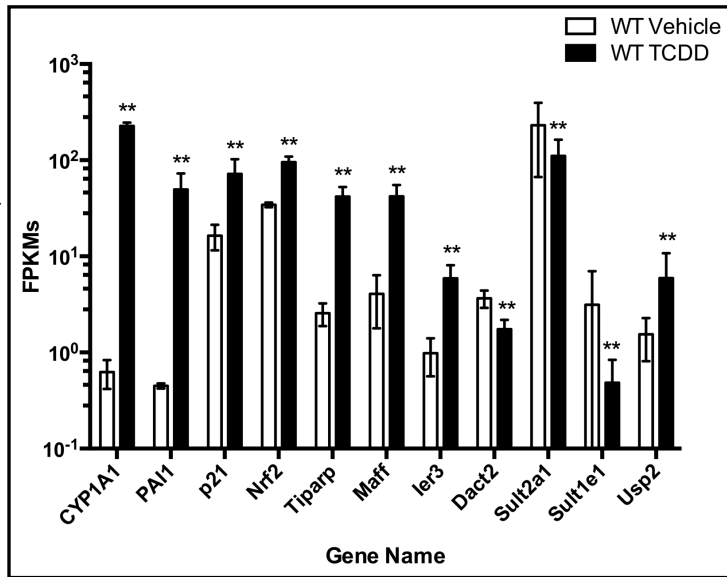


Figure 24: RNA-sequencing quantification (FPKM) of gene expression in RNA from livers of WT mice treated with vehicle or TCDD for 2 hours. * $q < 0.05$, ** $q < 0.01$ relative to vehicle. $n=3$ for all samples.

(**Figure 24**). Next, we collected new samples treated in the same way as for the RNA-sequencing experiments (WT and AhR CKO mice) and validated the RNA-sequencing results by assessing the aforementioned genes via qRT-PCR. qRT-PCR data showed significant differences (only in the WT mice, as expected) in the expression of Cyp1a1, Pai-1, p21^{Cip1}, Maff, Ier3, and Dact2. Note, Sult1e1, Sult2a1, and Usp2 were not significantly different statistically (two-tailed t-test, $p < 0.4$, $p < 0.2$, and $p < 0.23$, respectively) between the vehicle and TCDD treatments as measured by qRT-PCR (**Figure 25**).

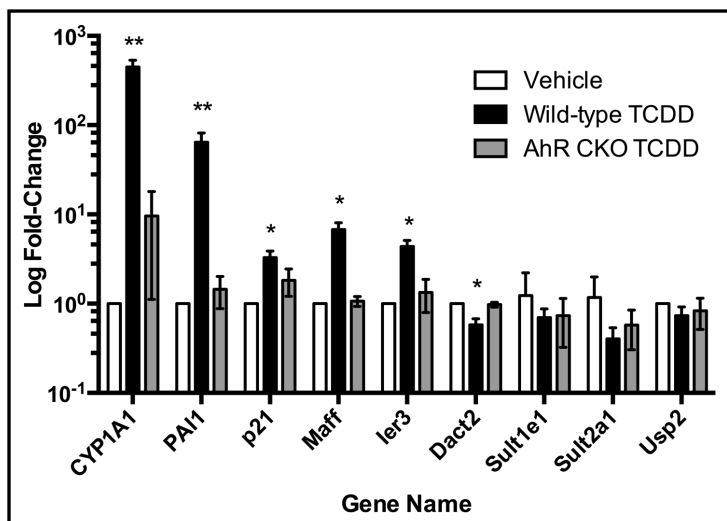


Figure 25: qRT-PCR validation of significant gene expression changes identified via RNA-sequencing (**figure 24**). RNA was isolated from livers of WT and AhR CKO mice treated with vehicle or TCDD for 2 hours. * $p < 0.05$, ** $p < 0.01$ relative to vehicle treatment. All genes normalized to 18S rRNA. $n=3$ for all samples.

We analyzed our dataset using Ingenuity Pathways

Analysis (IPA) to identify overarching cellular and physiological processes with which the gene changes in our RNA-sequencing dataset might be associated (**Appendix 4, 12-14**). The top signaling networks associated with our WT vehicle vs TCDD dataset (with any genes that also changed significantly in the AhR CKO vehicle vs TCDD comparison, removed) were cell death and survival, neurological disease, and cancer. The top diseases with which the gene changes may be associated were cancer, neurological disease, nutritional disease, and immunological disease. These findings are consistent with previous work in the AhR field, which has shown chronic exposure to xenobiotic AhR agonists can lead to immune dysfunction, nutritional and metabolic abnormalities, and cancer (Jackson *et al.*, 2015). On the molecular and cellular level, the dataset was correlated with cell death and cell survival signaling, cell growth and proliferation, and cellular development. On the physiological level, the RNA-sequencing dataset is associated with connective tissue diseases, hematological diseases, and changes to organ/tissue morphology. Again, these findings are consistent with studies of chronic exposure to xenobiotic AhR agonists, which have been associated with tissue fibrosis and cancer. The top canonical pathways, to which the gene changes in our dataset belong, include glucocorticoid signaling, AhR signaling, IGF-1 signaling, and PXR/RXR signaling pathways. Again, classic work in the field has implicated the AhR in various glucocorticoid signaling processes; indeed, the AhR is known to directly interact with the retinoic acid receptor at RXR/PXR regulated target genes, so these results are unsurprising (Jackson *et al.*, 2015). As far as upstream regulatory processes with which the gene expression changes are associated, IPA determined lipopolysaccharide, dexamethasone, IL-1B, and TNF as potential upstream regulators of the gene changes. This is interesting because lipopolysaccharide is well associated with KLF6 function in cell survival, and the AhR has previously been associated with IL-1B and TNF signaling (Jackson *et al.*, 2015).

Given that the 2 hour treatment time showed less than 200 genes to be significantly different in expression between WT animals treated with vehicle or TCDD, we employed the same experimental strategy using an 8 hour treatment time, to assess gene expression changes in the WT and AhR CKO mice. The 8 hour treatment was started at the same time of day as for the previous study using the 2 hour treatment. It is worth reiterating that the AhR belongs to the Per/Arnt/Sim (PAS) family of proteins, several of which play an important role in regulating gene expression concordant with circadian rhythms. While this process hasn't been fully studied, we attempted to account for possible circadian rhythm differences in our experiment, by treating all mice at the same time of the day. Though, it is obvious we can't both treat and euthanize the mice in the 8 hour study

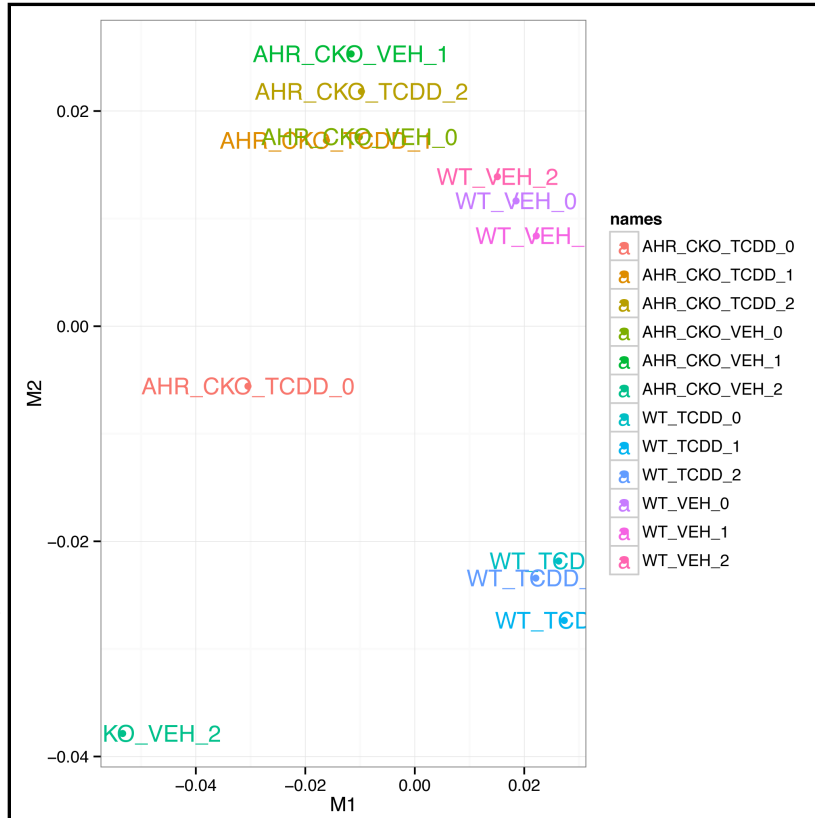


Figure 26: Multi-dimensional scaling plot of samples for RNA-sequencing, showing variance between samples and sample types. Each sample represents mRNA isolated from livers of WT and AhR CKO mice treated with vehicle or TCDD for 8 hours. Note that WT vehicle samples cluster closely together, as do WT TCDD samples. Conversely, there is more variance between the AhR CKO vehicle and TCDD treated samples. Note AhR CKO TCDD sample 0 and AhR CKO vehicle sample 2 cluster apart from samples with the same treatment, suggesting these samples may be outliers.

at the same times as in the 2 hour study; we did start the treatments at the same time of day.

The first thing we noted with regard to the RNA-sequencing results on the 8 hour dataset is that two of the six AhR CKO samples appeared to be outliers when assessed via multi-dimensional scaling plot (similar to principal component analysis) (**Figure 26**).

With these two samples removed from the analysis the samples cluster together more closely by treatment group (**Figure 27**). Interestingly, with regard to the AhR CKO samples, both the vehicle and TCDD treated samples appear to cluster more closely than the WT vehicle and TCDD treated samples, suggesting less differences between the two treatments in the AhR CKO genotype. This is reminiscent of the heat mapping (showing all four treatment groups) of the significant gene expression changes in the WT mice at 2 hours (**Figure 22**), which shows the largest differences in the dataset, relative to the other three treatments, occur in WT mice treated with TCDD.

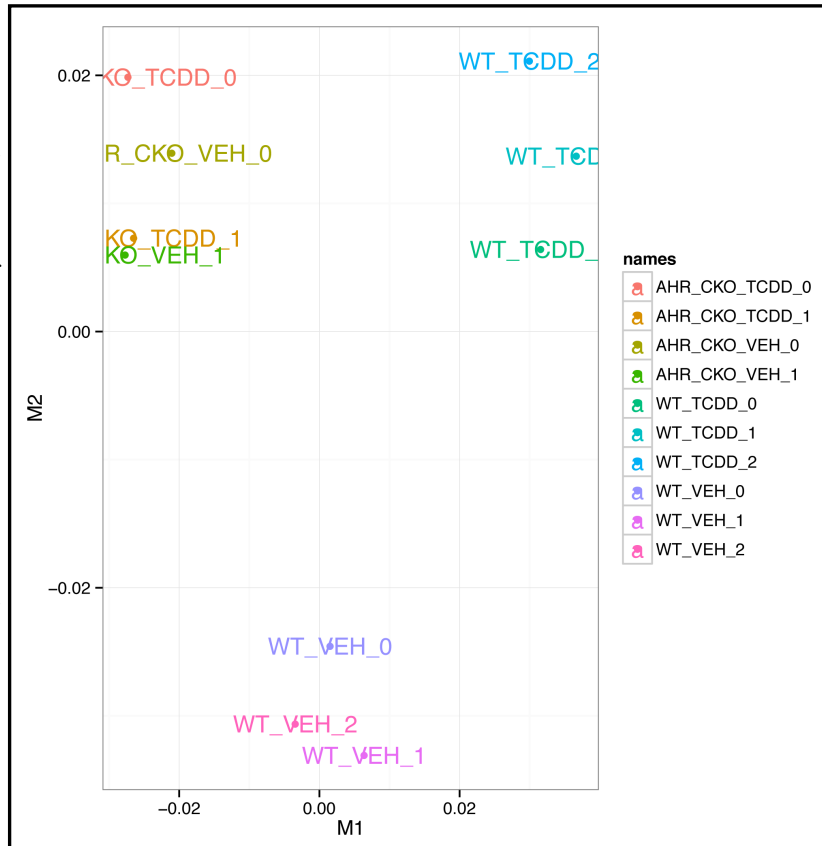


Figure 27: Multi-dimensional scaling plot of 8 hour samples for RNA-sequencing with AhR CKO vehicle sample 2 and AhR CKO TCDD sample 0 removed from the plot. Note with those 2 samples removed the groups cluster more closely with samples of the same type.

These findings underscore the hypothesis that TCDD induced gene expression changes in the liver largely depend on functional AhR expression. Next, we performed a principal component analysis on both the 2 hour and 8 hour datasets (**Figure 28**). This analysis suggests that there is larger variance in the 2 hour datasets than the 8 hour datasets. With respect to the 2 hour dataset, as with the the 8 hour datasets, again the AhR CKO samples cluster more closely (regardless of treatment with vehicle or TCDD) than the WT samples. These findings are not unexpected; the larger variance between the samples in the 2 hour dataset may reflect physiological differences in the mice. For example, a mouse with a full

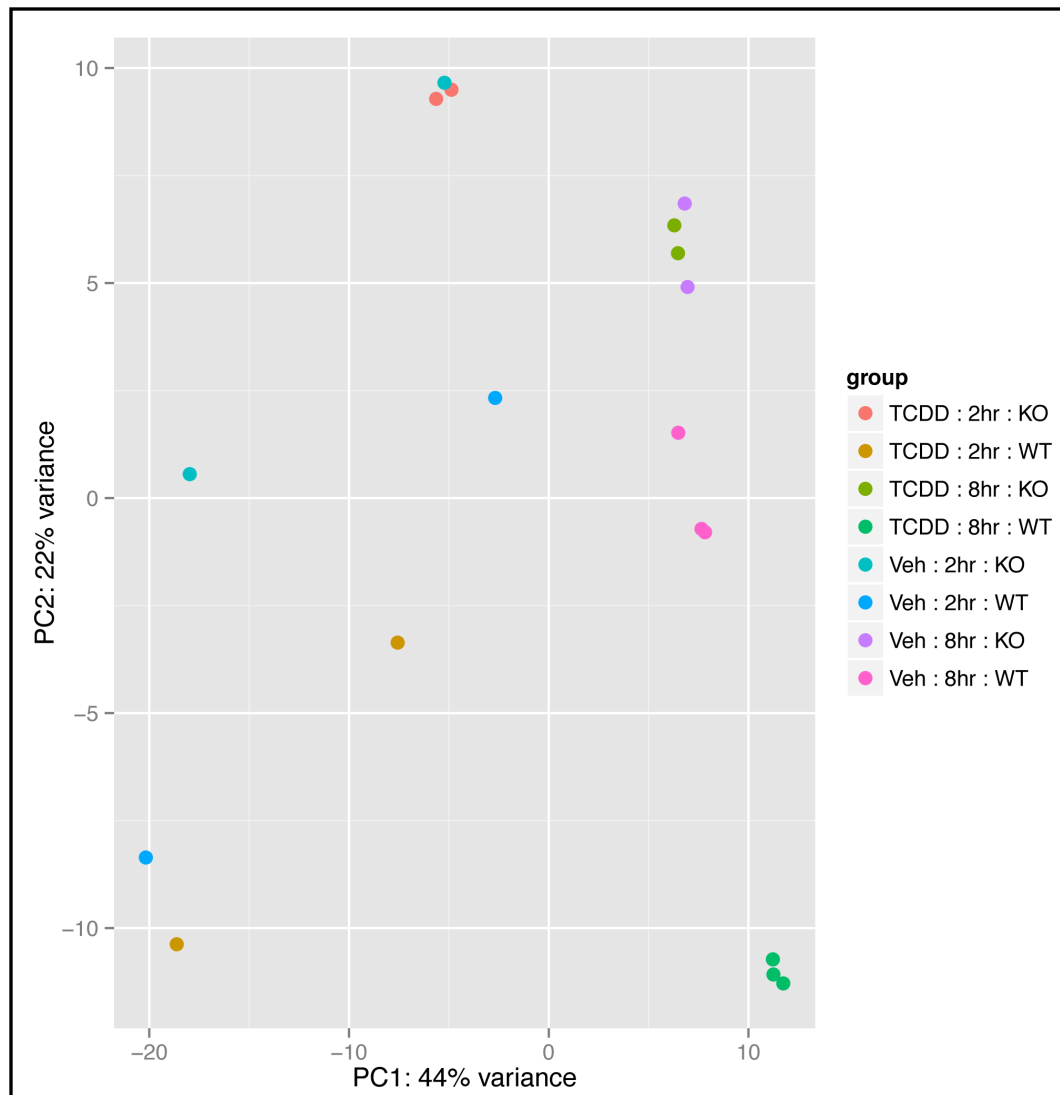


Figure 28: Principal component analysis of all samples (both 2 hour and 8 hour treatments) used for RNA-sequencing analysis, excluding AhR CKO vehicle sample 2 and AhR CKO TCDD sample 0. n=3 for all samples except vehicle and TCDD 8 hour where n=2. Note that the vehicle 8 hour WT samples and TCDD 8 hour WT samples cluster closely with each sample of the same treatment. Also note that the 8 hour CKO samples cluster closely together regardless of whether they were treated with vehicle or TCDD. The 2 hour WT and AhR CKO samples show large variance between samples of the same treatment than the 8 hour WT samples.

stomach may absorb the orally gavaged TCDD differently than a mouse with an empty stomach receiving the same treatment. This would be less apparent in the 8 hour treatment as the mice have more time to absorb the TCDD treatment into the blood stream. The fact that the nuclear form of the AhR is rapidly turned over and degraded (half-life of ~3 hours) may also contribute to larger differences in the two hour samples relative to the 8 hour samples. Nevertheless, with the two AhR CKO sample outliers removed from the analysis (one vehicle, one TCDD treated), we identified 1,497

significantly different genes in WT mice, and 565 significantly different genes in AhR CKO mice (**Figure 29** and **Appendix 10**). Between the two comparisons (four different treatments) 203 of the gene changes are significant in both the WT vehicle vs TCDD comparison and the AhR CKO vehicle vs TCDD comparison (**Figure 30**). However, of those 203 genes, not all change in the same manner (increase or decrease) in both comparisons (WT vehicle vs TCDD and AhR CKO vehicle vs TCDD). This interesting notion is further addressed below (see **Discussion**).

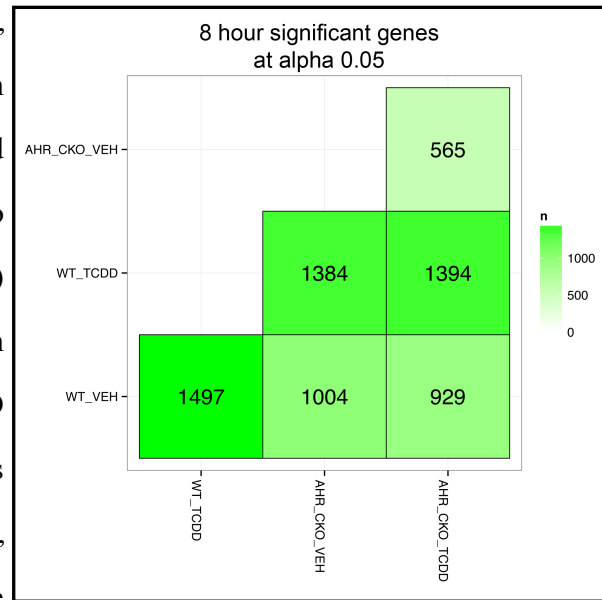


Figure 29: Significant gene expression changes matrix for differential expression analysis of RNA-sequencing performed on mRNA isolated from livers of WT and AhR CKO mice treated with vehicle or TCDD for 8 hours. n=3 for WT samples and n=2 for AhR CKO samples.

Given that we validated the 2 hour RNA-sequencing results via qRT-PCR analysis of several well-known AhR target genes, we first confirmed the significant changes in those previously identified genes, in the current dataset (**Figure 31**). Next, we treated new WT and AhR CKO mice for 8 hours with vehicle or TCDD (as for the RNA-sequencing experiments) and then collected total liver RNA and performed qRT-PCR for the aforementioned genes (**Figure 32**). The results confirm significant gene expression changes for all genes we measured, with the exception of *Dact2*, and the sulfotransferase enzymes *Sult1e1* and *Sult2a1*. In the 8 hour dataset, several other interesting gene changes were noted that also changed in the same manner in the 2 hour dataset, including *Cyr61*, *Ier2*, and *Lcn2* (further addressed in the discussion section).



Figure 30: Venn diagram comparing significant gene expression changes in WT and AhR CKO mice (see **figure 29**) (vehicle vs. TCDD) treated for 8 hours.

Given the large number of significant gene expression changes in the 8 hour RNA-sequencing datasets, we analyzed the results using venn diagrams, to compare the significant gene changes in multiple datasets, and IPA software to get some big picture insights on the processes with which the significant gene changes might be associated. Interestingly, there are significant differences in gene

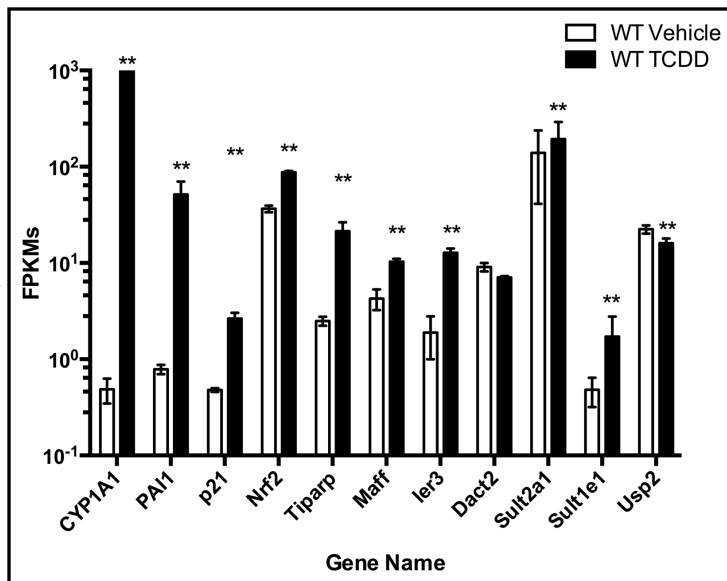


Figure 31: RNA-sequencing quantification (FPKM) of gene expression in RNA from livers of WT mice treated with vehicle or TCDD for 8 hours. * $p < 0.05$, ** $p < 0.01$ relative to vehicle. $n=3$ for all samples.

expression in the 2 hour WT vehicle vs TCDD comparison that are also seen in the 8 hour AhR CKO vehicle vs TCDD comparison but not in the 8 WT vehicle vs TCDD comparison (**Figure 33**). Of those 22 similar gene changes, none have previously been identified as AhR target genes, and many are serum proteins or sulfotransferase enzymes. The reason there are common significant gene expression differences between the 2 hour WT comparison and the 8 hour AhR CKO comparison, which are not also seen in the 8 hour WT comparison, is unclear at this point. It is also noteworthy that there are 32 significant gene expression changes that are identified in the 2 hour WT comparison, the 8 hour AhR CKO comparison, and the 8 hour WT comparison (**Figure 33**). Of these 32

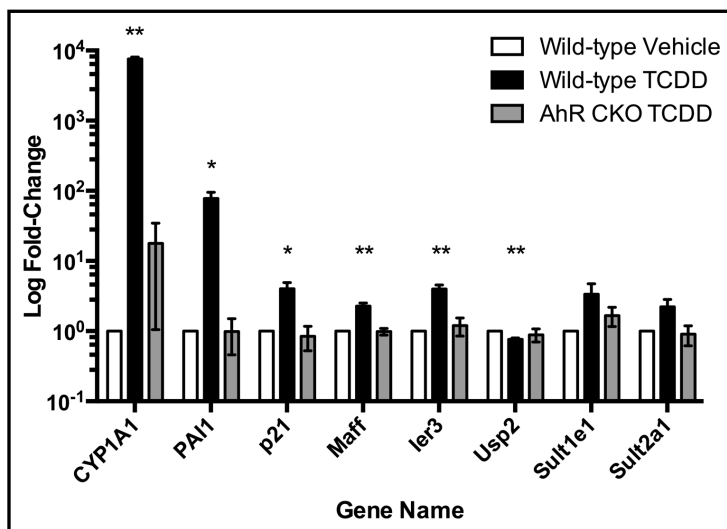


Figure 32: qRT-PCR validation of significant gene expression changes identified via RNA-sequencing (**figure 31**). RNA was isolated from livers of WT and AhR CKO mice treated with vehicle or TCDD for 8 hours. * $p < 0.05$, ** $p < 0.01$ relative to vehicle treatment. All genes normalized to 18S rRNA. $n=3$ for all samples.

elements common to all three comparisons, 10 have previously been identified as direct AhR target genes following TCDD treatment, including Cyp1a1, Pai-1, p21, Fos, Jun, and Cyp26b1. This is likely a ‘consequence’ of the AhR CKO model, which retains functional AhR expression in non-parenchymal cells of the liver, and thus those cells respond to TCDD and drive AhR-mediated transcriptional gene expression changes. The AhR induced gene expression changes in these liver cells in the AhR CKO genotype are likely sufficient enough to identified as significant changes given the exquisite sensitivity of RNA-sequencing methods. Indeed, several of these known AhR target genes identified to change significantly in these three comparisons (2 hour WT, 8 hour WT, and 8 hour AhR CKO) were identified as significant gene expression changes in both the 2 hour WT and 2 hour AhR CKO comparisons, supporting the notion that functional AhR expression in non-parenchymal cells of the liver is responsible for this observation that direct AhR target genes change in the AhR CKO animals (see **Figures 19 and 20**, discussion of AhR CKO genotype above).

We also compared significant differences in gene

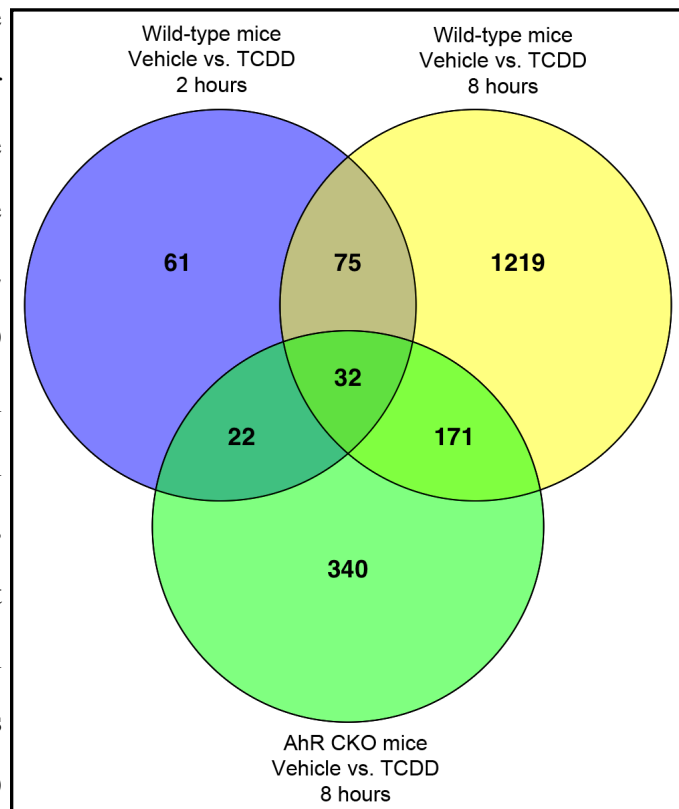


Figure 33: Venn diagram comparing significant gene expression changes in WT and AhR CKO mice (vehicle vs. TCDD) treated for 8 hours and WT mice (vehicle vs. TCDD) treated for 2 hours.

expression between the WT and AhR CKO mice that received 8 hours of vehicle treatment to significant differences in gene expression in the WT mice treated with vehicle or TCDD. This comparison is looking at significant differences in gene expression between the WT and AhR CKO genotypes- to determine how loss of the AhR

(in the AhR CKO mice) might affect gene expression in the liver in the absence of an exogenous ligand for the AhR- and how those differences compare to the significant differences in gene expression in WT mice treated with vehicle or TCDD (**Figure 34**).

Interestingly, there are a large number of differences in gene expression between WT and AhR CKO mice without any exogenous ligand, suggesting loss of the AhR affects basal gene expression levels in the livers of these mice, relative to WT mice. Interestingly, when

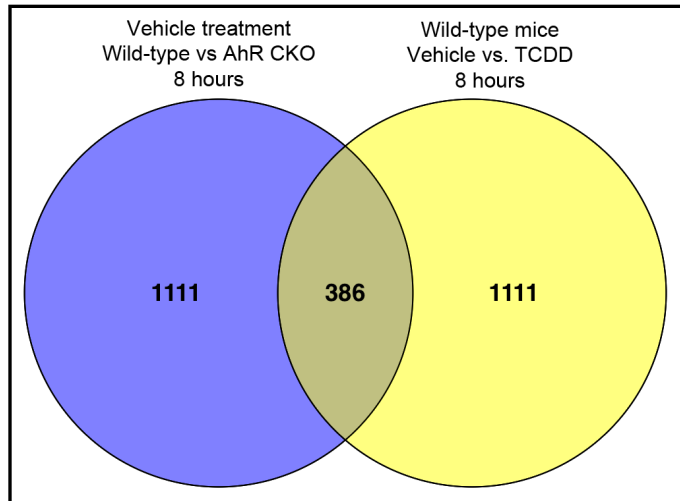


Figure 34: Venn diagram of significant gene expression differences between WT and AhR CKO mice, treated with vehicle for 8 hours, compared to significant gene expression differences between WT mice, treated with vehicle or TCDD for 8 hours.

these differences are compared to the significant gene expression changes induced in WT animals treated with TCDD for 8 hours (relative to vehicle), there are 386 common elements between the two comparisons (4 treatments, 2 in each comparison). This may suggest that direct AhR target genes, which change significantly in WT animals treated with TCDD (relative to vehicle) may have different levels of basal expression in the liver between the AhR CKO and WT genotypes. This is especially surprising given that between the WT mice treated with vehicle or TCDD for 8 hours and the AhR CKO mice treated with vehicle or TCDD for 8 hours, there are only 203 significant gene changes seen in both comparisons (**Figure 30**). The data suggest that there are more common gene expression changes between the WT vehicle vs AhR CKO vehicle comparison and the 8 hour WT vehicle vs TCDD comparison than the 8 hour WT vehicle vs TCDD and 8 hour AhR CKO vehicle vs TCDD comparison (386 common elements vs 203 common elements (**Figure 34** and **30**)). It is worth noting that we and others have found activation of the AhR by an exogenous ligand, as well as loss of the AhR, can both lead to increased expression of some AhR target genes, p21^{Cip1} for

example. This is especially evident with respect to cell cycle progression, as loss of the AhR as well as activation of the AhR with a xenobiotic ligand, both slow cell division (Kolluri et al. 1999). Given the similarities between the WT vs AhR CKO vehicle comparison and the WT vehicle vs TCDD comparison (**Figure 34**) this data may underscore the paradox where activation of the AhR by a xenobiotic has a similar effect on gene expression as loss of the AhR all together. While differences in basal gene expression between the WT and AhR CKO genotypes are not a major focus of this study, they represent a major avenue of research for future studies to determine what effects, if any, the differences in basal gene expression have on the physiology of AhR CKO mice relative to normal WT mice.

IPA analysis of the significant gene expression changes in the 8 hour WT vehicle vs TCDD comparison identified the top canonical pathways with which the dataset was associated to be LPS/IL-1 mediated inhibition of RXR function, PXR/RXR activation, nicotine degradation, and xenobiotic metabolism signaling. This is interesting because historic work in the AhR field has identified the AhR to be involved in regulating IL-1, PXR/RXR function, and of course xenobiotic metabolism (Jackson *et al.*, 2015). Further, LPS has been associated with modifying KLF6 transcription factor function and KLF6 has also been shown to regulate some IL-1 related genes. These findings suggest that NC-XRE regulated gene expression changes driven by the AhR/KLF6 interaction may represent a significant portion of the total AhR mediated transcriptional changes in various contexts, including both exogenous and endogenous ligand activation of the AhR. The major upstream regulators identified by IPA for the significant gene expression changes in the WT mice at 8 hours were TNF, PPAR α , dexamethasone, and methylprednisolone. These results implicate the AhR in modifying gene expression associated with immune cell function. The top diseases and disorders with which the dataset are associated include inflammatory response signaling, GI and hepatic diseases, metabolic abnormalities, and nutritional diseases. The top molecular and cellular

functions for the gene changes in the dataset include lipid metabolism, molecular transport, small molecule biochemistry, cell death and survival, and cell growth and proliferation. Indeed, the AhR, and in fact xenobiotic ligands for the AhR, have been associated with immunotoxicity and nutritional diseases. Previous work by ourselves and others has also identified the AhR to regulate cell-cycle progression to control cell growth and proliferation (Kolluri *et al.*, 1999; Jackson *et al.*, 2014). Our lab has also shown the AhR to play an important role in cytoprotection from oxidative and metabolic stress. Finally, the gene changes in the dataset (as for the 2 hour dataset) were associated with cardiac disfunction, various hepatotoxic processes (including steatosis, necrosis, and hyperplasia), and nephrotoxicity. The findings in this IPA analysis corroborate our RNA-sequencing results, given that they are consistent with historical work in the AhR field. This suggests that additional work on the RNA-sequencing datasets, to further characterize these transcriptional changes by determining which are XRE mediated targets and which are NC-XRE mediated targets, will lend insight on both the physiological and pathophysiological functions of the AhR (**Appendix 5**).

It's worth noting the potential for indirect gene expression changes to be occurring in the animals treated with TCDD for 8 hours. Given the multitude of target genes the AhR is known to regulate, previous studies using microarray and NGS based transcriptomic analyses have shown direct gene expression changes induced by the AhR can subsequently drive indirect gene activation or repression (Puga, *et al.*, 2000; Boverhof *et al.*, 2005; Dere *et al.*, 2011). While this is likely the case for some portion of the significant gene expression changes in the 8 hour experiment, this is less likely to be true in the two hour experiment, given the much shorter treatment time. Nevertheless, when we originally set out to perform the NGS analysis of AhR induced transcriptomic changes, our goal was to perform a complementary ChIP-sequencing analysis of AhR/DNA-binding at the 2 and 8 hour treatment times. Anchoring the transcriptomic changes induced by the TCDD activated AhR would allow us to characterize functional AhR

DNA-binding at target gene promoters, thus describing target gene activation relative to upstream promoter AhR binding. Our attempts at performing ChIP-sequencing in this paradigm are further discussed in the discussion section.

Murine KLF6 Knock-out Models are Not Viable for RNA-sequencing Studies

We also wish to address one other goal we initially had in utilizing RNA-sequencing to identify AhR-mediated transcriptomic changes in the mouse liver following TCDD treatment, anchored to ChIP-sequencing based identification of AhR/DNA-binding following the same TCDD treatment. As previously discussed, for our RNA-sequencing experiments we utilized wild-type mice and AhR conditional knock-out mice, which lack functional AhR expression in the liver, to identify gene expression changes following TCDD treatment that depend on functional AhR expression. We initially intended to also perform RNA-sequencing experiments using KLF6 conditional knockout (CKO) mice, with a liver-specific loss of functional KLF6 expression, to assess AhR mediated gene expression changes following TCDD treatment, in the absence of KLF6. KLF6 Fx/Fx mice, containing Flanking loxP (Floxed; Fx) sites around exons 2 and 3 of KLF6, have previously been generated, reported, and used in studies of KLF6 in the prostate (Leow *et al.*, 2009). Indeed, previous studies have utilized KLF6 Fx/Fx mice with the Alb/Cre genotype to generate KLF6 CKO mice, with liver specific loss of KLF6 expression (Bechmann *et al.*, 2012). We obtained KLF6 Fx/Fx mice and crossed them to mice expressing a tamoxifen inducible Cre/ErT transgene under the control of the Albumin promoter, to generate a tamoxifen inducible liver specific loss of KLF6. However, following further studies with these mice, even though the genotyping confirmed the presence of the Cre/ErT trans-gene and two floxed KLF6 alleles, we could not obtain 100% KLF6 truncation with tamoxifen treatment. Furthermore, when we treated these mice with TCDD and looked at TCDD induced expression of AhR/KLF6 target genes in the liver, we saw no loss of Pai-1 or p21 gene induction, as would be expected if functional KLF6 expression in the liver were lost (**Figure 35 A and B**). Next,

we isolated primary hepatocytes from the KLF6 Fx/Fx Cre/ErT mice to assess whether or not infection with an AdCre-GFP adenovirus construct could induce KLF6 Fx/Fx element excision. We infected primary hepatocytes with a non targeting (no gene)-GFP control virus, or AdCre-GFP virus at multiplicities of infection (MOI) of 25, 50, or 100 for 48 hours. We then isolated RNA from these cells, using TRIzol, and prepared cDNA for semi-quantitative RTPCR. Subsequent RTPCR to check KLF6 excision and GAPDH expression showed a maximum of 50% excision of the KLF6 floxed exons 2 and 3 with an AdCre-GFP adenovirus infection MOI of 50 and 100 (**Figure 35C**). We confirmed

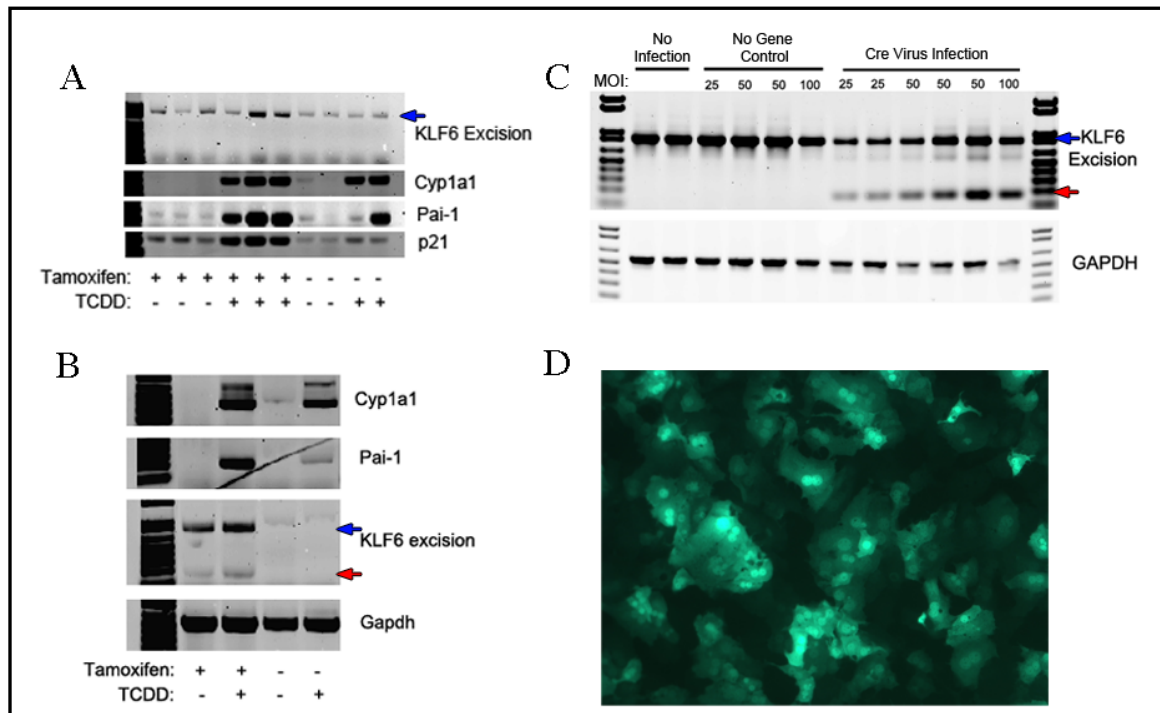


Figure 35: **A)** Semi-quantitative RTPCR analysis of Cyp1a1, Pai-1, p21^{Cip1} and full length (blue) or excised (red) KLF6 expression in mRNA isolated from livers of KLF6 Fx/Fx/Alb^{Cre/ErT} mice treated with or without tamoxifen (via oral gavage every 24 hours for 3 days) and with vehicle or TCDD for 2 hours. Note the lack of any detectable excised KLF6 mRNA in any of the samples (should appear above primer dimers at the leading edge of the gel). **B)** Semi-quantitative RTPCR analysis of Cyp1a1, Pai-1, Gapdh, and full-length or excised KLF6 expression in mRNA isolated from livers of KLF6 Fx/Fx/Alb^{Cre/ErT} mice treated with or without tamoxifen (via oral gavage every 24 hours for 5 days) and with vehicle or TCDD for 2 hours. Note the faint presence of excised KLF6 mRNA (indicated by red arrow) in the samples from tamoxifen treated mice. **C)** Semi-quantitative PCR analysis of Gapdh and full length or excised KLF6 expression in mRNA from primary hepatocytes isolated from KLF6 Fx/Fx/Alb^{Cre/ErT} mice and treated with no infection, infection with a no gene AdGFP adenovirus or infection with an AdCre-GFP, Cre-recombinase expressing virus at MOIs of 25, 50, or 100. Note the band indicating the modest presence of excised KLF6 in primary hepatocytes isolated from KLF6 Fx/Fx/Alb^{Cre/ErT} mice infected with the Cre-recombinase expressing virus. **D)** Detection of GFP expression, via light microscopy, in AdCre-GFP infected KLF6 Fx/Fx/Alb^{Cre/ErT} mouse primary hepatocytes used in **C**. Detection of GFP expression indicates successful viral infections in these experiments.

viral infection of all cell cultures by assessing GFP expression via microscopy (**Figure 35D**). These results suggest KLF6 Fx/Fx element excision in the Cre/ErT mice is, at best,

50%. It is worth noting, in retrospect, the presence of three different sizes of KLF6 band in **Figure 35C**. The middle band in this RTPCR imputes that Cre-Recombinase expression drives excision of a ~120bp element in the KLF6 gene. This is further discussed below, but suggests the presence of more than 2 LoxP elements in the KLF6 gene.

Given the possibility that the tamoxifen inducible Cre-recombinase was inefficient in excising the LoxP sites, for some unknown reasons, we crossed KLF6 Fx/Fx mice with Alb^{Cre} expressing mice to generate a KLF6 CKO mouse not involving the Cre/ErT tamoxifen inducible Cre trans-gene. After obtaining mice containing one KLF6 Fx/Fx allele (heterozygous) expressing Cre recombinase under the control of the albumin promoter, we mated pairs of these cre-expressing KLF6 Fx/WT heterozygotes to generate mice with two floxed KLF6 alleles (Fx/Fx) expressing Cre. However, after mating 18 heterozygote pairs, we failed to identify a single offspring homozygous for the Fx/Fx KLF6 allele and expressing Cre. Indeed, based on previous litter sizes from these animals, we concluded that there was a significant decrease in the number of viable off-spring from the KLF6 heterozygote crosses. This finding suggested that the liver specific KLF6 CKO genotype is embryonic lethal; a notion which is somewhat supported by previous attempts in another lab to generate global KLF6 knock-out mice, which determined global loss of KLF6 to be embryonic lethal (Matsumoto *et al.*, 2006).

Previous studies of a global KLF6 (+/-) heterozygous mouse genotype have reported aberrations to liver development, among other developmental abnormalities (Narla *et al.*, 2007). Nevertheless, following our inability to generate the KLF6 CKO genotype, we discovered a minor article correction had been published following the initial study describing the KLF6 Fx/Fx mice. This correction described two aberrations to the KLF6 floxed allele in the KLF6 Fx/Fx genotype we obtained. First, rather than obtaining mice with 3 loxp elements (two elements flanking a PGK/NEO cassette on the 5' side of exon 2, and a third loxP element on the 3' side of exon 3, which generate a loss

of exons 2 and 3 when excised by Cre), the lab had obtained mice with 4 loxP elements containing a duplication of the loxP element on the 5' side of exon 2. Second, the loxP element on the 3' side of exon 3 was inverted, and thus not compatible with efficient Cre-mediated loxP element excision (see Leow et al. 2009, supplemental figure) (Leow *et al.*, 2009). As a result, the floxed KLF6 allele could not be efficiently excised in the tamoxifen inducible Alb/CreErT expressing mice, explaining why we never saw 100% excision of KLF6 exons 2 and 3 in that line. The authors noted that in certain cases this genotype could still result in excision of exons 2 and 3 for both KLF6 alleles. We now believe that in the case of the Alb/Cre crosses to generate KLF6 CKO mice, there was indeed efficient excision in both KLF6 alleles, resulting in loss of KLF6 in the liver during development, which was subsequently lethal for an as yet unknown reason.

Nevertheless, we assessed the possibility of using Alb/Cre expressing mice heterozygous for a KLF6 Fx allele to determine if loss of one KLF6 allele sufficiently decreased KLF6 expression to be used for our RNA-sequencing studies. These studies of

both the F2 and F5 generations of KLF6 heterozygotes expressing Cre-recombinase, showed that mice containing a single KLF6 allele in the liver retained sufficient KLF6 protein expression to significantly up-regulate AhR-mediated NC-XRE target genes in the liver following TCDD treatment (Figure 36). In light of these findings, we abandoned the

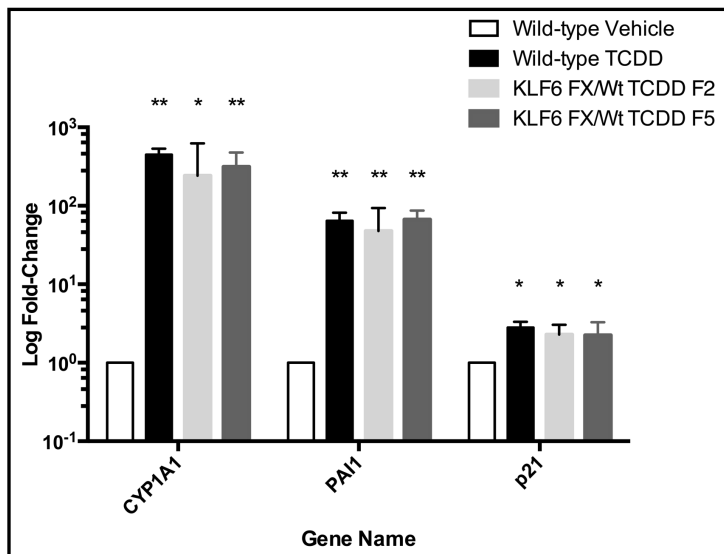


Figure 36: qRT-PCR quantification of Cyp1a1, Pai-1, and p21 in mRNA isolated from WT or KLF6 Fx/Wt heterozygotes (from F2 generation or F5 generation) treated with vehicle or TCDD for 2 hours. n=3 for all samples *p<0.05, **p<0.01 relative to vehicle. Note that loss of 1 KLF6 allele in the KLF6 heterozygous mice does not significantly diminish TCDD induced AhR-mediated transactivation of Pai-1 or p21.

attempts to use KLF6 CKO mice for our RNA-sequencing studies. Future RNA-

sequencing studies will utilize Arnt CKO mice (Arnt Fx/Fx Alb/Cre), lacking Arnt gene expression in the liver, to assess TCDD induced AhR mediated gene expression changes in the liver that occur without Arnt. This study will complement the RNA-sequencing studies in the AhR CKO mice by describing NC-XRE mediated gene expression changes in the same context, since XRE-mediated AhR-induced gene expression changes that require functional Arnt expression, should not occur in the Arnt CKO animals.

DISCUSSION

The AhR/KLF6 Protein Interaction

Through studies using C-terminal deletion mutants of the AhR, we have determined amino acids 424-490 of the protein are necessary for the interaction with KLF6. Previous studies of NC-XRE DNA-binding by the AhR found the bHLH domain was not necessary for AhR/KLF6 heterodimerization and subsequent DNA-binding; though the bHLH domain is necessary for DNA binding to XRE DNA-motifs. Follow up studies using alanine mutagenesis to neutralize charged residues in the first 27 amino acids of the AhR also found these changes had no effect on AhR NC-XRE DNA-binding. The findings, (including those by Wilson et al. 2013) impute other charged residues in the N-terminal 120 amino acids of the AhR are involved in AhR DNA-binding to NC-XRE DNA sequences (Wilson *et al.*, 2013). It is noteworthy that the involvement of these regions of the AhR and KLF6 are departures from historical studies, which have shown the bHLH and PAS A and B domains in the AhR to be necessary for DNA-binding and protein-protein interactions in the XRE pathway. Similarly, the zinc finger region of KLF6 was shown to be required for DNA-binding in other KLF6 signaling processes. Conversely, in it's role in the NC-XRE pathway we have shown arginine residues in KLF6, lying outside the zinc finger region, to be involved in NC-XRE DNA-binding. In fact, the entire zinc finger region is dispensable for DNA binding in the NC-XRE pathway *in vitro* (Wilson *et al.*, 2013; Jackson *et al.*, 2015). It is tempting to speculate that given the involvement of novel AhR and KLF6 protein regions for the protein-

protein interaction and DNA-binding, as well as the novel DNA motif to which these proteins bind, the function of the AhR/KLF6 transcription complex represents a functionally distinct signaling pathway for both the AhR and KLF6. However, further study is needed to more fully understand the AhR/KLF6 interaction and its DNA-binding. Indeed, it's possible the AhR/KLF6 interaction involves hitherto unknown additional protein partners, necessary for DNA-binding in the NC-XRE pathway. Given the well documented hallmarks of variance in KLF6 (and KLF6 splice variant) expression in many different aggressive cancers (discussed above), and the fact that some KLF6 variants lack the AhR interaction region and/or the NC-XRE DNA-binding domain, it's also possible future work may implicate the NC-XRE pathway in tumorigenesis and cancer metastasis.

RNA-sequencing Identification of Potentially Novel AhR Target Genes

Previous studies in the AhR field have attempted to characterize the transcriptional targets of the AhR. As discussed above, this includes early transcriptomic approaches such as microarray analysis of TCDD treated mouse and human hepatoma and breast cancer cell lines, among others. Recent studies show the AhR binds a novel DNA motif (the NC-XRE) *in vivo* via an interaction with KLF6, to regulate novel AhR target genes like Pai-1 and p21. This work along with studies by others, suggests the current picture of AhR-mediated gene expression changes following TCDD treatment is incomplete. Thus, we performed RNA-sequencing experiments on RNA isolated from livers of WT or AhR CKO mice treated with vehicle or TCDD for 2 or 8 hours. A broad summary of these results using Ingenuity Pathways analysis is consistent with the historical work in the AhR field, suggesting roles for the AhR in cell death and survival, cell growth and proliferation, metabolic and nutritional homeostasis, and liver homeostasis as well. Our approach utilized both WT and AhR CKO mice, so that any genes that changed significantly with TCDD treatment in both the WT and AhR CKO mice (lacking the AhR) could be removed from the WT vehicle vs TCDD significant gene

list. In the 2 hour dataset we identified 190 significant changes in WT mice, and 44 in AhR CKO mice, with 10 gene changes significant in both datasets, two of which are known AhR target genes (an artifact of the AhR CKO model type, discussed extensively above). Of the 190 significant gene changes, at least 10 have previously been associated with AhR mediated transactivation following treatment with a xenobiotic ligand for the AhR. The large difference in the number of significant gene changes between the WT and AhR CKO genotypes is illustrative of the notion that the AhR is the principle mediator of TCDD- induced gene expression changes in our system.

In our 2 hour dataset, we were interested in the finding that *Ier3* and *Dact2* are potential AhR target genes- as suggested by significant expression changes with TCDD treatment in WT animals and not in AhR CKO animals. *Ier3* is a compelling result because it has been shown in several contexts to be cytoprotective against oxidative stress induced mitochondrial damage and cell death (Arlt and Schäfer, 2011). In our RNA-sequencing dataset and when analyzed via qRT-PCR, *Ier3* gene expression increased significantly by ~5-fold with TCDD treatment, (relative to vehicle) at both 2 hour and 8 hour treatment times. This increased expression following TCDD treatment was absent in AhR CKO mice treated with TCDD (assayed by both RNA-seq and qRT-PCR). *Ier3* is also interesting in that, other than a NLS and a PEST sequence, it shows neither protein structure nor protein sequence homology with any other known vertebrate protein, yet the protein sequence is highly conserved in all extant eutherians (Arlt and Schäfer, 2011). *Ier3* has also been shown to have a role in preventing viral infection on a cellular level in several immune cell types. This study found that loss of *Ier3* enhanced susceptibility to *Leishmania* infection (Akilov *et al.*, 2009). Studies have also shown that *Ier3* over expression in T-cells prolongs T-cell life, which can lead to a lupus-like autoimmune disease (Arlt and Schäfer, 2011). *Ier3* is especially interesting in this context, given historical work in the AhR field showing TCDD and other AhR ligands to cause immunotoxicity. Another study has linked *Ier3* to modulation of the Nrf2 response

pathway (Stachel *et al.*, 2014), which is intriguing because the AhR is also known to regulate Nrf2 expression (Wang *et al.*, 2013; Jackson *et al.*, 2015). Ier3 has also been shown to synergize both pro and anti apoptotic signaling induced by signaling pathways, yet it has no activity in either pro or anti-apoptotic processes on its own (Arlt and Schäfer, 2011). Curiously, the Ier3 promoter contains four XRE DNA motifs within 5kb of the transcription start site (TSS), and two NC-XRE like sequences (GGGAGGGA). Dact2 is a candidate tumor suppressor gene, also identified in our RNA-sequencing experiments as a significant change in expression. In WT animals treated with TCDD Dact2 gene expression decreased significantly relative to vehicle treatment. Both the RNA-sequencing and qRT-PCR validation show TCDD treatment decreases Dact2 expression by ~2-fold in WT mice but not in AhR CKO mice. Dact2 functions as a tumor suppressor through inhibition of Wnt/ β -catenin signaling, and has been identified as a prognostic marker for squamous cell carcinoma, hepatocellular carcinoma, and colon cancer (Su *et al.*, 2007; Li *et al.*, 2013). The Dact2 promoter contains four XRE DNA motifs and three NC-XRE DNA motifs within 10kb of the TSS; other noteworthy gene expression changes in the RNA-sequencing dataset include E2f8, Id1, Hilpda, Cyr61, Ier2, Lcn2, and Pik3r1.

E2f8 has been shown to have a role in regulating cyclin D and E2F activation to control S-phase cell cycle progression (Christensen *et al.*, 2005). In our RNA-sequencing experiments, TCDD treatment significantly decreased E2F8 expression relative to vehicle. Over-expression of E2f8 is associated with enhanced cell proliferation, tumorigenicity, and colony formation, while loss of E2f8 inhibits cell proliferation and colony formation (Deng *et al.*, 2010). Indeed, previous work by ourselves and others have shown the AhR to be an important regulator of cyclin D/cdk activity and G₁/S phase cell cycle progression (Kolluri *et al.*, 1999; Jackson *et al.*, 2015), which is similar to the role of E2f8 in controlling S-phase cell cycle progression. Id1 has been implicated in regulating glucose and insulin homeostasis, cell differentiation, and lipid homeostasis,

and all three of these processes have previously been associated with the AhR (Satyanarayana *et al.*, 2012; Jackson *et al.*, 2015). In our 2 hour dataset, TCDD treatment reduced Id1 gene expression relative to vehicle treatment. The E2f8 promoter contains six XRE DNA motifs and four NC-XRE DNA motifs within 10kb of the TSS, while the Id1 promoter contains five XRE DNA motifs and seven NC-XRE DNA motifs within 10kb of the TSS. Hilpda is both a HIF-1 and PPAR target gene, and has been implicated in promoting renal cell carcinoma and colorectal cancer progression (Konda *et al.*, 2008). We found that TCDD treatment significantly increases Hilpda gene expression. It is noteworthy that there is a direct relationship between Hilpda and Arnt (aka HIF-1 β), as hypoxia induced activation of Hif-1 is known to mediate Hilpda transactivation. It is also interesting that Hilpda is most notably expressed in lipid droplets, which change in size and number in response to hypoxia (Gimm *et al.*, 2010). Indeed, previous studies of Arnt have shown Arnt to play a role in adipose function, lipid homeostasis, and it is known to be an important component in β -cell survival in pancreatic islets (Lalwani *et al.*, 2014). This is especially striking given that a recent study found cardiac specific loss of Arnt caused lipodystrophy and cardiac hypertrophy (Wu *et al.*, 2014). The Hilpda promoter contains two XRE DNA motifs and three NC-XRE DNA motifs within 10kb of the TSS. Interestingly, one of the three NC-XRE motifs in the Hilpda promoter is ~700bp upstream of the TSS and mirrors the Pai-1 NC-XRE motif exactly (GGGAGGGAGGGAGGGA), suggesting Hilpda may be an NC-XRE regulated AhR target gene following TCDD treatment.

Cysteine-rich protein 61, (Cyr61) is known to promote macrophage infiltration in the liver and has also been implicated in driving liver fibrosis. Cyr61 is also an interesting potential target gene for the AhR given it's well known important roles in proper organ development (Bian *et al.*, 2013). Cyr61 has seven XRE DNA motifs and three NC-XRE DNA motifs within 10kb of the TSS. In WT animals at both 2 and 8 hours after TCDD treatment Cyr61 gene expression is decreased, relative to vehicle treated mice. However,

Cyr61 expression is un-changed following TCDD exposure in the AhR CKO mice. Immediate early response gene 2 (Ier2) is involved in promoting cell motility, and has been implicated as a marker for increased cell growth and metastasis in several cancers; Ier2 also plays an important role in several developmental processes (Neeb *et al.*, 2012). In both the 2 hour and 8 hour RNA-sequencing datasets Ier2 gene expression is decreased in WT mice treated with TCDD, relative to vehicle treatment; Ier2 gene expression does not decrease with TCDD at either time point in the AhR CKO mice. Ier2 has ten XRE motifs and no NC-XRE DNA motifs within 10kb of the TSS. Lipocalin 2 (Lcn2) is known to drive inflammatory macrophage polarization in the liver, it is also known to be elevated in serum, by the liver, following partial hepatectomy surgery (Xu *et al.*, 2015). Lcn2 also regulates lipid droplet formation in the liver, blood glucose homeostasis, and brown fat activation (Zhang *et al.*, 2014). Studies have also shown Lcn2 to play a role in driving several autoimmune diseases, which is interesting given the observation that TCDD treatment can lead to immune toxicity (Nam *et al.*, 2014). The Lcn2 promoter contains five XRE DNA motifs and two NC-XRE DNA motifs within 10kb upstream of the TSS. In both the 2 and 8 hour datasets, Lcn2 gene expression was significantly increased following TCDD treatment in the WT mice, however it was not significantly increased in the AhR CKO mice. Pik3r1 is a PI3 kinase regulatory subunit. It has been shown to be an LPS inducible gene, which causes aberrations to insulin sensitivity. It is also known to play an important role in the early response for liver regeneration following partial hepatectomy (Jackson *et al.*, 2008; Wakayama *et al.*, 2014). The Pik3r1 promoter contains four XRE DNA motifs and no NC-XRE DNA-motifs within 10kb of the TSS.

While more work is needed to fully investigate the genes discussed above, for example, the significance of the XREs and NC-XREs identified above via *in silico* analysis, there are some very interesting gene expression changes in both the 2 and 8 hour

RNA-sequencing datasets with the potential to shed new light on the physiological roles of the aryl hydrocarbon receptor both specifically in the liver, and more generally in additional cell types. Furthermore, future studies using this same experimental paradigm to study Arnt CKO mice will anchor our current results and lend insight on how these gene expression changes may be related to the AhR XRE and NC-XRE pathways in particular.

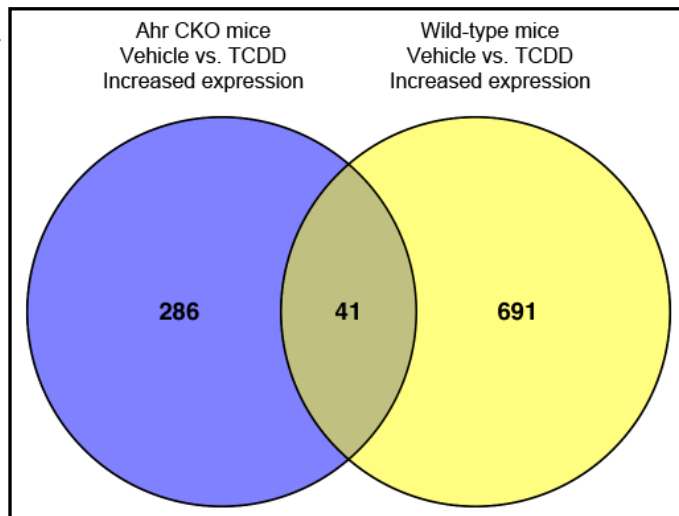


Figure 37: Venn diagram comparing similarities, between WT and AhR CKO RNA-sequencing datasets, only in genes showing a significant **increase** in expression following TCDD treatment (relative to vehicle treatment) for 8 hours.

Common Elements Between AhR CKO and WT RNA-sequencing Datasets May be Misleading

With respect to the 8 hour dataset, we identified 1,497 significant changes in gene expression between WT mice treated with vehicle or TCDD, and only 565 significant gene expression changes in the AhR CKO mice treated with vehicle or TCDD. Of those changes, 203 of the significant changes were seen in both the WT and AhR CKO comparisons. However, the aforementioned comparison between WT and AhR CKO datasets did not take into account the direction of the significant gene change (i.e. increased with TCDD treatment in WT mice yet decreased with TCDD treatment in AhR CKO mice...etc). When the comparison is made assessing significant changes that are the same between genotypes (increased with TCDD treatment in both genotypes, or decreased in both genotypes) the results are quite different. For genes that increase with TCDD treatment there were 732 in the WT comparison and 327 in the AhR CKO comparison, yet only 41 are increased in both datasets (**Figure 37**). Of those 41, 2 are known AhR targets, and thus likely artifacts of the AhR CKO mouse model (as

previously discussed). Conversely, for genes that decrease following TCDD treatment, there were 765 in the WT comparison and 238 in the AhR CKO comparison, yet only 38 were the same in both datasets (**Figure 38**). Thus, when the comparison between the AhR CKO and WT RNA-sequencing datasets is made only considering significant changes in the same direction (increases with TCDD or decreased with TCDD), there are only 79 common changes (compared to the original 203 common elements) between the two genotypes. It is difficult to speculate on the significance or the meaning of the differences between these

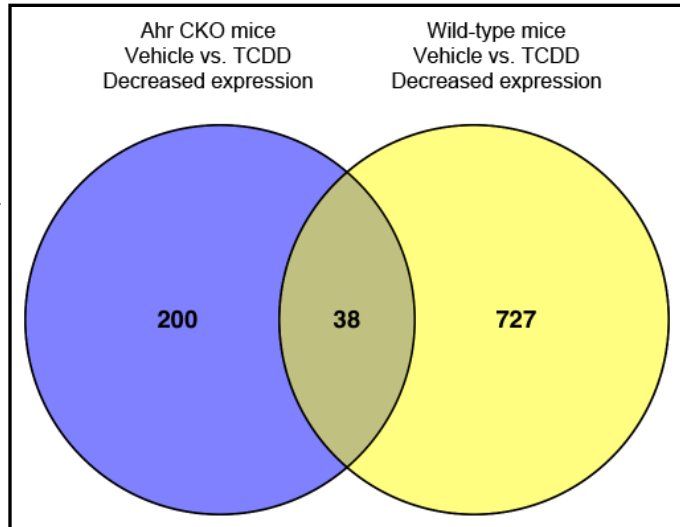


Figure 38: Venn diagram comparing similarities, between WT and AhR CKO RNA-sequencing datasets, only in genes showing a significant **decrease** in expression following TCDD treatment (relative to vehicle treatment) for 8 hours.

comparisons. Given that the AhR is the only known transcription factor to respond to TCDD (and as evidenced by the small number of significant gene expression changes in the AhR CKO animals at 2 hours), it is unlikely that in the absence of the AhR, Arnt or KLF6 are responding to TCDD and modifying gene expression in the opposite direction as when the AhR is present; though, this would explain why in the absence of the AhR (AhR CKO) a gene might decrease in expression following TCDD treatment (relative to vehicle), yet in the presence of the AhR (WT) the gene increases in expression following TCDD treatment (relative to vehicle). It is possible that as previously mentioned, the basal levels of gene expression are higher or lower in the AhR CKO mice (relative to WT mice), and that this is in some way impacting data interpretation in the vehicle vs. TCDD differential expression comparison. It is also possible that some unknown genetic, epigenetic, metabolic, or circadian rhythm factors may explain this interesting phenomenon. Alternatively, functional AhR expression, retained in non-parenchymal

liver cells in the AhR CKO mice, may be responding to TCDD treatment in the AhR CKO mice, which then might affect gene expression in primary hepatocytes of these mice through some unknown paracrine signaling mechanism. Nevertheless, as previously stated, TCDD is not currently known to activate any other receptors or transcription factors; thus, it is unclear at this point, why these differential gene expression changes occur with TCDD treatment between the two mouse genotypes.

Correlations Between RNA-sequencing and ChIP-Sequencing

Following our RNA-sequencing experiments, one of the goals for this work was to perform ChIP-sequencing on AhR immunoprecipitated DNA sequences to identify AhR DNA-binding in close proximity to the promoters of genes that change in expression significantly following TCDD treatment. This work is further discussed below, but it worth noting a recent publication by Raymond Lo and Jason Matthews (Lo and Matthews, 2012), detailing ChIP-sequencing of AhR and Arnt bound DNA sequences in MCF7 breast cancer cells following 2 or 24 hour treatment with TCDD (10 nM). While our RNA-sequencing studies were performed in the liver, we noted some interesting correlations between our RNA-sequencing results in the liver and the Lo and Matthews ChIP-sequencing in breast cancer cells. Their study identified two lists of genes, by determining the closest mapped gene to either an AhR bound DNA region or an AhR and Arnt bound DNA region. Note, this study defined a DNA sequence as being bound by both the AhR and Arnt when the reads had 1) 100% sequence similarity and 2) >50% width of the smallest region for both, between ChIP-sequencing reads on DNA immunoprecipitated with an antibody against the AhR or ChIP-sequencing reads on DNA immunoprecipitated with an antibody against Arnt (Lo and Matthews, 2012). We compared both our 2 hour and 8 hour RNA-sequencing datasets in WT and AhR CKO mice with the AhR and AhR/Arnt bound regions identified by ChIP-sequencing. For the 2 hour RNA-sequencing results, 33 of the genes that change significantly in the WT vehicle vs TCDD comparison were also identified as the closest gene to an AhR bound region of

DNA in the ChIP-sequencing study. Conversely, in the 2 hour RNA-sequencing results on the AhR CKO vehicle vs TCDD comparison, only 3 significant gene expression changes were also identified as the closest gene in proximity with an AhR bound DNA region. Furthermore, when these WT and AhR CKO significant gene changes were compared with genes in closest proximity to both AhR and Arnt bound DNA regions, 17 genes were the same in the WT dataset, while only 2 genes were the same in the AhR CKO dataset (compared to ChIP-sequencing results) (**Appendix 6**). For the 8 hour datasets, there were 155 common genes between the WT vehicle vs TCDD significant gene expression changes and AhR bound DNA regions identified by ChIP-sequencing, while there were only 62 common genes for the AhR CKO vehicle vs TCDD comparison and the genes closest to an AhR bound DNA-region. Furthermore, when the significant gene expression changes for the WT (vehicle vs TCDD) and AhR CKO (vehicle vs TCDD) comparisons were compared to the list of genes in closest proximity to an AhR and Arnt bound DNA region, 79 WT genes were similar to the ChIP-sequencing list, while only 23 AhR CKO genes were similar to the ChIP-sequencing list (Lo and Matthews, 2012) (**Appendix 7**). It is important to note that these studies were performed on different experimental paradigms (*in vitro* vs. *in vivo* and human cells vs. mouse tissue) and thus the results are not necessarily indicative of AhR and/or Arnt DNA-binding near the genes identified to change significantly with TCDD treatment via RNA-sequencing. Furthermore, the Lo and Matthews study did not identify AhR DNA-binding in close proximity to either p21 or Pai-1, both of which have been identified as AhR NC-XRE target genes. However, it is also noteworthy that this could be a result of aberrant KLF6 expression, or differential expression of KLF6 splice variants, some of which lack the NC-XRE DNA-binding domain and/or the KLF6 region necessary for the AhR/KLF6 protein-protein interaction. Whatever the case may be, the interesting connections between our RNA-sequencing results and the Lo and Matthews ChIP-sequencing results underscore the need for further transcriptomic and even proteomic studies of the AhR in several experimental paradigms.

These studies hold the potential to shine new light on the roles of the AhR in several different contexts, potentially contributing to novel therapeutics for a whole host of pathologies, with which the AhR, Arnt, and/or KLF6 have been associated. Indeed, the broad spectrum Ingenuity Pathways analyses of both the 2 hour and 8 hour RNA-sequencing results suggest the changes in our dataset are consistent with a number of previously studied diseases and disorders associated with the Ah receptor and its myriad ligands.

ChIP-sequencing Can Be Used to Anchor the RNA-sequencing Results to Functional AhR DNA-binding Events.

As mentioned above, one goal for this study was to anchor the RNA-sequencing results to ChIP-sequencing data to correlate TCDD-induced AhR mediated gene expression changes with functional AhR binding sites upstream of the genes that change in expression. Our first attempt at performing ChIP-sequencing on AhR or KLF6 immunoprecipitated DNA, from vehicle or TCDD treated (2 hour) mice livers, employed a 95°C incubation (a condition suitable for the semi-quantitative ChIP) for 15 minutes as our reverse cross-linking step, following immunoprecipitation of protein bound DNA sequences. Unfortunately, the use of the 95°C temperature caused the DNA fragments to melt and preferentially re-anneal at base repeat sites within the sheared DNA fragments. This artifact compromised the synthesis of the library and thus we preferentially sequenced these base repeat sequences in our NGS run. Ultimately, the NGS data could not be used for an accurate peak finding analysis, meaning the experiment was flawed.

While we know the 95°C temperature is the most efficient temperature for reversing protein/DNA cross-links, ChIP-Seq methods call for a 65°C reverse cross-linking incubation overnight for 6-8 hours instead. With this in mind, we continued optimizing the experiment to obtain the best possible immunoprecipitation enrichment of AhR or KLF6 bound DNA sequences in our ChIP workflow. To assess IP enrichment, we employed qRT-PCR to assess the presence of known DNA sequences bound by the AhR,

including a portion of the Cyp1a1 promoter, a portion of the Pai-1 promoter, and a portion of the p21 transcript 2 promoter. We ultimately obtained samples that passed this quality control step and performed the library preparation steps on said material. We also analyzed the ChIP material used to generate the libraries via Agilent bioanalyzer to assess the sizes of DNA fragments in our library. When we analyzed the libraries to confirm IP enrichment via qRT-PCR, as we had done on the starting material before the library prep, we found a significant decrease in the enrichment of all three known AhR-bound DNA sequences in the ChIP-sequencing library for the AhR IP'd material from TCDD treated animals. Due to the loss of enrichment after library preparation, we went back to the the Agilent analysis of the ChIP material we initially submitted. The Agilent analysis showed three bands of larger size DNA fragments in the input material, suggesting a flaw in the DNA shearing steps of our ChIP workflow (**Figure 39**), however these larger bands were

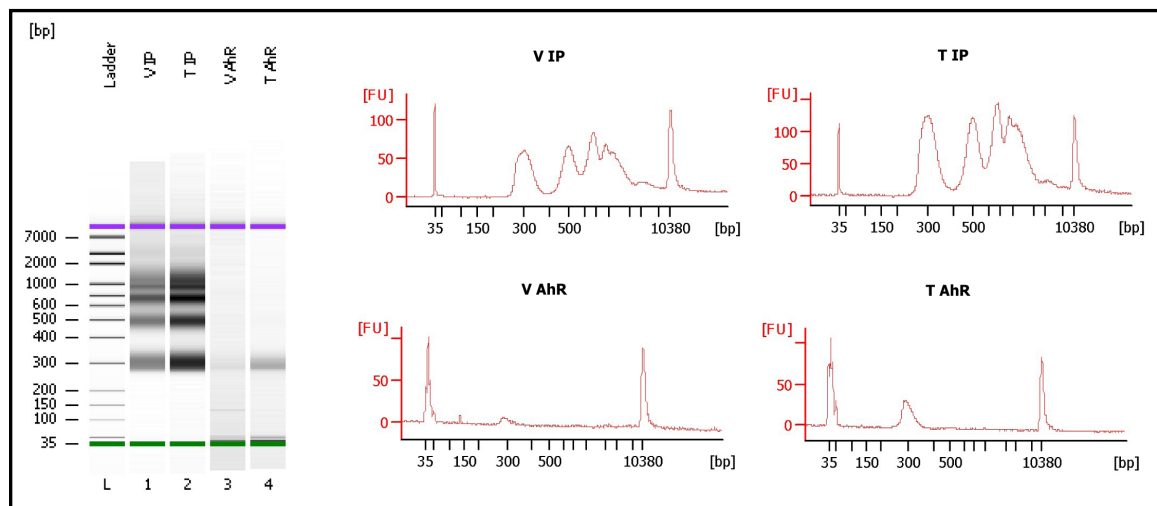


Figure 39: High-sensitivity Agilent Bioanalyzer analysis of DNA fragment size in input and AhR immunoprecipitated DNA samples from ChIP. ChIP experiment was performed using chromatin isolated from mice treated *in vivo* with vehicle or TCDD, sheared with enzymatic micrococcal nuclease.

not present in the AhR IP'd chromatin.

With these points in mind we pushed on with the ChIP-sequencing, on the basis that we could not explain the reason for the loss of IP enrichment after the library preparation, and thus couldn't be sure this was not an artifact of the qRT-PCR analysis, and as such not an accurate depiction of the DNA sequences in our samples. The peak

finding analysis in the subsequent NGS dataset identified low-quality peaks (low peak-height and wide peak width) in our samples. This peak finding also did not identify AhR/DNA-binding at the aforementioned known AhR binding sites in the promoters of the Cyp1a1, Pai-1, and p21 transcript 2 genes. Our conclusions were two-fold: 1) our then current method of DNA-shearing using micrococcal nuclease based enzymatic shearing, was biased to certain fragment sizes (which were not within the optimal 300-500bp range) and thus might be generating fragments too large to be properly processed in the library preparation step. This would explain why we saw an enrichment for the known AhR-bound DNA sequences in the qRT-PCR analysis prior to the library preparation, but did not see that enrichment in a similar qRT-PCR analysis after library preparation. 2) Our IP against the AhR to enrich DNA-sequences bound by the AhR was not sufficient to preferentially enrich the AhR bound sequences above background DNA present after the IP.

To address the first technical problem, we switched from enzymatic DNA shearing to Covaris acoustic sonication for a more concise and reproducible fragmentation, and optimized the DNA shearing conditions to generate DNA fragments in the 300-500bp size range (**Figure 40**). We also changed our protein/DNA cross-linking step as there were several discussions suggesting that our formaldehyde (Fisher Scientific) may be degrading over time, leading to variations in cross-linking. It was also noted that methanol present in the formaldehyde from that manufacturer could cause inconsistent cross-linking, and/or decrease the efficiency of the following step to halt the cross-linking process by incubating the tissue in 0.5 M glycine. As such, we began to use single-use 1mL ampule aliquots of methanol free formaldehyde to ensure we were using a consistent quality and concentration of formaldehyde in the cross-linking step. To address the second technical problem, we increased the stringency with which we washed the antibody-AhR/DNA-bound protein A/G- beads following the IP step. The bead washing protocol was changed from 3 washes incubated at room-temperature for 5

minutes each, to 4 washes incubated on a rotor at room-temperature for 20 minutes each, in an effort to remove any background DNA coming down in the IP. It should also be noted that to this point, quantitation of DNA concentration in the final material (used for qRT-PCR loading, and DNA loading for library preparation) after the IP and cleanup steps, were performed using a Nanodrop nanospectrophotometer. Given the relatively low DNA concentration after the ChIP-experiment (from 2ng/ μ L for IgG IP'd DNA- 200ng/

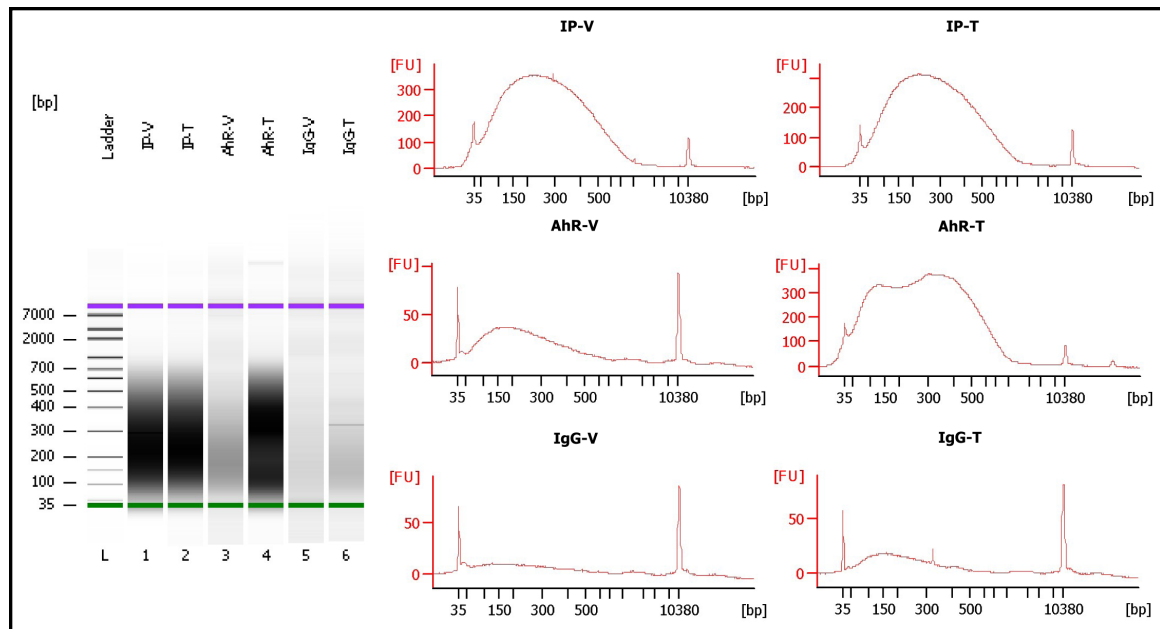


Figure 40: High-sensitivity Agilent Bioanalyzer analysis of DNA fragment size in input, AhR immunoprecipitated, or IgG immunoprecipitated DNA samples from a ChIP experiment. Experiment was performed using chromatin isolated from mice treated *in vivo* with vehicle or TCDD, sheared with Covaris acoustic micro-cavitation shearing method.

μ L for input DNA) and the potential for contamination by RNA in the final material, it's difficult to near impossible to obtain reliable DNA concentration measurements. Though it should be noted, there is no reason to believe there would be such large differences in composition between each sample in the same experiment (as far as RNA or other chemicals present) that differences in composition might affect the accuracy of the DNA concentration quantitation. Nevertheless, while we were in the process of addressing the aforementioned technical difficulties, the molecular genomics core acquired the ability to quantify ChIP'd DNA using the fluorometric dye based Qubit methodology (Simbolo *et al.*, 2013). Qubit quantification is specific to double-stranded DNA and is thus a more

accurate way to quantify DNA concentrations in ChIP'd material. Indeed, we compared Nanodrop and Qubit DNA quantitation and found a consistent difference in the results, with Nanodrop over-estimating the DNA concentration by up to a factor of 16 in some samples (**Table 1**). It is also worth noting that we added a control in the qRT-PCR validation of our ChIP'd material. ChIP-sequencing is based on the identification of peaks of a specific size in the sequenced material, these peaks are fragments of DNA that

are enriched (relative to background) in the immunoprecipitation step. Thus, a true peak in the ChIP-sequencing experiment represents a piece of DNA that was bound

	95°C reverse cross-linking		65°C reverse cross-linking	
Quantification (ng/μL):	Qubit	Nanodrop	Qubit	Nanodrop
Input Vehicle	24	22	76	14
Input TCDD	86	105	183	98
(AB) AhR Vehicle	1.2	6	0.7	2
(AB) AhR TCDD	4.9	20	0.5	8
(SC) AhR Vehicle	0.2	2	1.4	4
(SC) AhR TCDD	1.3	12	0.8	9

Table 1: Comparison of Qubit and Nanodrop quantifications of DNA amounts in samples from ChIP. ChIP was performed using chromatin isolated from mice treated *in vivo* with vehicle or TCDD. Samples represent input DNA or DNA immunoprecipitated with either an Abcam (ab) or Santa Cruz (sc) antibody against the AhR.

to the protein targeted during the IP. This means that the success of a ChIP-sequencing experiment depends on those protein bound DNA fragments being present at greater frequency than any other piece of DNA not bound by the protein of interest. While qRT-PCR can accurately quantify the amount of a known DNA-sequence following a ChIP experiment, this quantitation does not lend any insight on the amount of that known sequence relative to unbound, or background, DNA sequences present in the sample. In experiments up to this point, we were comparing the quantity of a known DNA sequence (specifically sequences in the Cyp1a1, Pai-1 and p21 transcript 2 promoters) in AhR immunoprecipitated DNA from livers of mice treated with TCDD, to the quantity of that same DNA sequence in: 1) input DNA for that same AhR immunoprecipitation, 2) AhR immunoprecipitated DNA from livers of mice treated with vehicle (and thus little to no AhR is present in the nucleus and bound to DNA), and 3) IgG immunoprecipitated DNA

(in this case the IgG antibody used for the IP shouldn't target any proteins and thus only background DNA should be present) to calculate enrichment with the AhR IP in the experiment. Because we were comparing the amount of that specific DNA sequence between different samples, we were not comparing each sample to itself to assess the amount of that DNA sequence relative to background DNA, which is vital in the ChIP-sequencing analysis to see a peak of that DNA sequence above background. As such, we designed primers against a DNA sequence 1kb away from any known AhR bound DNA sequences in the Cyp1a1 promoter. Thus, qRT-PCR quantitation of this unbound DNA sequence could be used to compare the quantity of AhR-bound DNA sequences in each sample to the amount of this unbound DNA sequence to confirm enrichment relative to background in the sample. As a result of the protocol improvements we, 1) optimized the DNA-shearing step, 2) increased the stringency with which we wash the beads following the IP step, 3) switched to using single-use aliquots of methanol-free formaldehyde, 4) switched to using Qubit to quantify DNA concentrations in the ChIP'd material rather than Nanodrop, and 5) employed the use of qRT-PCR primers against sequences of DNA that should not be bound by the AhR in our experimental paradigm, to control for background DNA-binding in the IP step.

Following all these technical changes, we performed ChIP experiments and assessed the amount of AhR bound vs unbound DNA sequences in AhR ChIP'd DNA from livers of mice treated with TCDD, compared to the presence of these two types of DNA sequences (AhR bound vs unbound) in 1) input DNA from livers of mice treated with or without TCDD, 2) histone H3 immunoprecipitated DNA from livers of mice treated with or without TCDD, 3) IgG immunoprecipitated DNA from livers of mice treated with or without TCDD, and 4) AhR immunoprecipitated DNA from livers of mice treated only with vehicle (little to no nuclear AhR means little to no AhR-bound DNA following the IP). qRT-PCR quantitation (plotted as CT values, where a lower CT means more target is present) of these different DNA sequences in the different samples (input

A)

qPCR target	Cyp1a1 #1 CT	Cyp1a1 #2 CT
Input Vehicle	30.02	27.96
Input TCDD	30.23	28.25
AhR Vehicle	29.43	27.44
AhR TCDD	30.26	28.17
H3 Vehicle	30.60	28.07
H3 TCDD	30.39	27.73

B)

qPCR target	Cyp1a1 #1 CT	Cyp1a1 #2 CT	Reg1 CT	Prss3 CT
Input Vehicle	23.25	21.21	31.0	19.16
Input TCDD	23.2	21.31	30.55	19.17
AhR TCDD	23.12	21.17	31.49	19.18

C)

	95°C reverse cross-linking		65°C reverse cross-linking	
qPCR target	Cyp1a1 #1 CT	Cyp1a1 1100 CT	Cyp1a1 #1 CT	Cyp1a1 1100 CT
Input Vehicle	27.9	24.1	29.8	26.1
Input TCDD	27.4	24.1	29.1	25.6
(ab) AhR Vehicle	29.3	24.5	29.3	25.9
(ab) AhR TCDD	28.1	24.4	28.3	25.8
(sc) AhR Vehicle	28.2	25.4	30.5	26.4
(sc) AhR TCDD	28.7	24.7	29.8	26.1

Table 2: A) qRT-PCR quantitation (CT value, lower value means higher amount) of 2 different regions of the Cyp1a1 promoter in ChIP material, both regions have previously been shown to be AhR DNA-binding sites following TCDD treatment. qRT-PCR quantitation was performed by loading the same amount (ng ChIP sample per reaction) of ChIP DNA template for each qRT-PCR reaction (DNA quantified by Qubit). Note the minute differences in CT value between the samples B) qRT-PCR quantitation of AhR DNA-binding regions in ChIP material as in A, compared to qRT-PCR quantitation of 2 regions not known to be bound by the AhR (exon 1 of Reg1 and Prss3). Note the Prss3 region appears to be present at greater amounts than either Cyp1a1 promoter region known to be bound by the AhR. C) qRT-PCR comparison of AhR bound (Cyp1a1 #1) and unbound (cyp1a1 1100) DNA regions in ChIP material obtained using either a 95°C or a 65°C reverse cross-linking step (see methods) and two different antibodies against the AhR: Abcam (ab) or Santa Cruz (sc).

DNA, H3 IP'd DNA, or IgG IP'd DNA from chromatin isolated from either vehicle or TCDD treated mouse livers) shows the AhR/DNA immunoprecipitation on chromatin isolated from TCDD treated mouse livers has little enrichment for AhR bound sequences relative to unbound (background) DNA sequences (**Table 2**). Based on these findings, the data suggest the AhR immunoprecipitation is not sufficiently enriching AhR bound DNA sequences above background DNA, and thus the ChIP is not sufficiently efficient for ChIP-sequencing to successfully identify AhR-binding sites (peaks) with the current

experimental conditions. This is likely indicative of either a poor-quality antibody being used for the AhR IP step however, this could also be indicative of excessive protein-DNA cross-linking with formaldehyde early in the workflow. Future work with the ChIP-sequencing experimental workflow will test 1) other AhR antibodies to assess whether they have greater enrichment of AhR bound sequences relative to background and 2) different protein-DNA cross-linking conditions to assess whether decreased cross-linking time increases the ChIP efficiency for enriching AhR bound DNA sequences relative to background.

Two things are important to note here. The first is that we are attempting to perform ChIP-sequencing experiments using livers from mice treated *in vivo* with vehicle or TCDD. This is noteworthy because most studies reporting successful ChIP-sequencing experiments reflect ChIP experiments on chromatin isolated from *in vitro* cell culture experiments, however successful ChIP-sequencing on material from *in vivo* treatments has been reported. Thus, successfully generating protein-DNA cross-linked chromatin from tissues is more difficult than generating protein-DNA cross-linked chromatin from cell culture. Based on this difficulty, it is worth reiterating the necessity of using a reverse cross-linking temperature that does not denature the IP'd DNA fragments. While we have had the greatest efficiency with a 95°C temperature we adapted to a 65°C temperature. Though, it is possible a higher temperature than 65°C may be useful, assuming there is no DNA denaturation, as we have found that the efficiency of the reverse cross-linking step is a function of the temperature. The second thing to note, is that we consistently obtain substantially more DNA from AhR immunoprecipitations performed on chromatin isolated from livers of mice treated with TCDD, than we obtain from immunoprecipitations using the exact same antibody (and same amount of said antibody) performed on chromatin from livers of mice treated with vehicle (**Table 3**). The greater amount of DNA in the AhR IP on TCDD treated material (relative to the amount of DNA in the AhR IP on vehicle treated material) would suggest that more DNA is being IP'd

following TCDD treatment, than vehicle treatment, and thus more AhR is bound to DNA. Since this comparison is being made using the same antibody (differing only in the type, and not the amount, of input chromatin)

this result is likely not due to the antibody binding to background DNA. Since we

Quantification (ng/ μ L):	20 May 2015	29 June 2015	14 August 2015
Input Vehicle	67.5	173	24.0
Input TCDD	68.0	275	86.0
AhR Vehicle	2.01	3.36	1.2
AhR TCDD	34.7	78.50	4.9
H3 Vehicle	3.14	0.41	***
H3 TCDD	1.50	1.32	***
IgG Vehicle	2.02	0.18	***
IgG TCDD	2.01	0.19	***

Table 3: Qubit quantitation of DNA concentrations following 3 separate ChIP experiments. Following the final step in the ChIP workflow, DNA is ethanol precipitated and then all samples are resuspended in an equal volume of nuclease free ddH₂O. Note the large difference in DNA concentrations between the AhR vehicle and AhR TCDD samples relative to the difference between input vehicle and input TCDD DNA concentrations. *** indicates DNA concentration could not accurately be quantified using Qubit.

resuspend the ChIP'd DNA from all input and IP'd samples in the same volume of water, it's reasonable to suggest that loading an equal volume (μ L), rather than an equal amount (ng), of material for the qRT-PCR analysis is an acceptable method of quantifying the amount of a DNA sequence in each sample. Indeed, when this is done we see far greater amounts of our known AhR-bound DNA sequences in the AhR IP on TCDD treated chromatin, than we see in the AhR IP on vehicle treated chromatin. Furthermore, we see greater amounts of the AhR bound DNA sequences in the AhR IP on TCDD treated

Quantification (ng/ μ L):	DNA conc.	Cyp1a1 #1 qPCR CT	Cyp1a1 #2 qPCR CT	Cdkn1a qPCR CT	Pai-1 qPCR CT
Input Vehicle	93.5	24.52	22.49	23.41	25.67
Input TCDD	103.0	25.74	24.73	27.07	27.08
AhR Vehicle	36.0	28.11	29.15	27.19	28.75
AhR TCDD	38.0	24.83	23.17	23.43	25.49
IgG Vehicle	6.0	37.61	37.06	31.27	36.00
IgG TCDD	4.0	36.00	>40.0	31.66	35.44

Table 4: qRT-PCR for 2 Cyp1a1 regions, 1 p21 region, and 1 Pai-1 region, all known to be bound by the AhR following TCDD treatment. Column 2 (DNA concentration) represents the amount of DNA in 1 μ L of sample (all samples resuspended in 30 μ L), and 1 μ L of each sample was used for each qRT-PCR reaction. Note the greater presence of each DNA region known to be bound by the AhR in the AhR TCDD sample than the AhR vehicle and IgG samples.

chromatin than we see in the IgG IP on either vehicle or TCDD treated chromatin (**Table 4**). While these results suggest the AhR IP is enriching for AhR bound DNA sequences, as previously discussed, this comparison does not accurately reflect the process by which ChIP-sequencing works. Namely, that ChIP-sequencing identifies amounts of DNA sequences that are present in greater amounts than background DNA in a single sample. This enrichment, via IP, for AhR-bound DNA sequences is vital to the success of the ChIP-sequencing experiment. Future experiments in this endeavor will keep these points in mind, and attempt to optimize the experimental workflow by addressing the aforementioned cross-linking and antibody technical considerations.

CONCLUSIONS

We have demonstrated that AA 424-490 of the AhR are necessary for the protein interaction with KLF6. We have also shown that NC-XRE DNA-binding by the AhR does not involve charged residues in the AhR N-terminal 27 amino acids, and instead likely involves other charged residues in the the N-terminal 120 amino acids. Our RNA-sequencing experiments have identified TCDD induced gene expression changes at 2 and 8 hours following TCDD treatment in both WT and AhR CKO mice, and IPA analyses of the two datasets suggest the gene expression changes are consistent with historical studies of the AhR and TCDD in mice. Ultimately, these IPA findings suggest that incorporation of RNA-sequencing experiments on Arnt CKO mice (using the same treatment paradigm), to characterize significant gene expression changes in WT mice as either XRE-mediated or NC-XRE mediated, hold the potential to identify the significance of the two pathways, and determine what TCDD induced pathophysiologies are a result of which of the two distinct AhR pathways. Further, by performing ChIP-sequencing with AhR and/or KLF6 immunoprecipitated DNA, these expression changes can be anchored to functional DNA-binding by the AhR and KLF6 to 1) confirm which genes are XRE or NC-XRE mediated, 2) identify novel DNA-binding motifs in AhR target gene promoters,

and 3) assess AhR DNA-binding locations relative to confirmed gene expression changes via RNA-sequencing.

As discussed above, future directions for this work should focus on RNA-sequencing experiments in Arnt CKO mice and ChIP-sequencing on AhR and KLF6 immunoprecipitated DNA. It would also be valuable to further study the AhR/KLF6 interaction to determine whether or not other proteins are a part of this transcription factor complex. While not discussed above, there is more than a modicum of evidence which imputes that target genes for the AhR can vary depending on the ligand by which the AhR is activated. Indeed, a recent report by our lab has identified stanniocalcin 2 (STC2) as a novel AhR target gene (Harper *et al.*, 2013). Further studies of this target have shown that the novel AhR ligand, cinnabarinnic acid, can specifically target the AhR to preferentially transactivate STC-2 gene expression, but not other known AhR target genes like Cyp1a1 and Pai-1 (Joshi *et al.*, 2015). In light of these findings, it's worth noting that the experimental strategy employed in the studies described herein, namely RNA and ChIP sequencing, would be valuable in 1) identifying other AhR target genes differentially activated following cinnabarinnic acid treatment and 2) assessing other known AhR ligands to identify additional ligand specific target genes for the AhR. Indeed, it is possible that other known AhR ligands may stimulate novel protein interactions between the AhR and as yet unidentified protein partners, which may regulate gene expression through as yet unidentified DNA-motifs. These studies hold the potential to fully define the repertoire of genes regulated by the AhR and, hopefully, to finally lend insight on both the physiological roles of the AhR and any high affinity endogenous ligands for the AhR that are yet to be discovered.

Chapter 4: A CALUX Based Assessment of Petrogenic PAH Contamination in Gulf Seafood Following the Deepwater Horizon Oil Disaster

INTRODUCTION

Background

On April 20th, 2010 an explosion onboard the *Deepwater Horizon* (DWH) drilling rig at the Macondo Prospect in the Gulf of Mexico, led to the largest oil spill in US history (United States Coast Guard National Response Team, 2011). In the months following the explosion, ~5 million barrels of oil were released into the Gulf of Mexico, (~800,000 barrels of which were collected at spill site) before the flow was stopped on July 15, 2010 (McNutt *et al.*, 2012; Reddy *et al.*, 2012). During the spill, state and federal authorities closed portions of Gulf fisheries beginning in May, 2010 in expectation of coastal and shore oiling (based on NOAA models), to prevent harvesting of potentially contaminated seafood (United States Coast Guard National Response Team, 2011). At its peak in early June, fisheries closures affected almost 40% of federally owned waters in the Gulf of Mexico (Upton, 2011). In the wake of the spill, survey teams identified more than 1000 miles of oiled US coastline (Upton, 2011). As of April 2011, all areas closed to fishing by federal authorities were reopened to the public (United States Coast Guard National Response Team, 2011).

In addition to the vast oil release, approximately 2 million gallons of chemical dispersants were used in subsurface and aerial applications at the spill site to break up the oil and aid in cleanup (Kujawinski *et al.*, 2011; United States Coast Guard National Response Team, 2011; Reddy *et al.*, 2012). The use of chemical dispersants was controversial (Wilson *et al.*, 2015), with critics pointing to the lack of basic toxicology studies on the chemicals and suggestions that dispersants might present an increased risk for deleterious health effects on several marine species (Ramachandran *et al.*, 2004; Schein *et al.*, 2009; Allan *et al.*, 2012). Indeed, it has been suggested that dispersants increase PAH absorption by fish (Ramachandran *et al.*, 2004; Wilson *et al.*, 2015). In

addition to the controversy about dispersants, the conspicuous obstacles to halting the oil release encountered by the responsible parties during the spill led to a negative public perception of the spill response. Furthermore, the inconsistent messages to the public and Gulf communities regarding the risks posed by consuming potentially contaminated seafood further complicated the situation and heightened public scrutiny. Collectively, the negative public perception, the large amount of oil released, and the use of chemical dispersants generated widespread concern about the economic, ecologic, and environmental impacts of the spill and led to questions regarding human health risks associated with contaminated seafood. In fact, it was recently reported that in one of the Gulf communities in particular, more than 80% of those surveyed reported decreasing their Gulf shrimp consumption for 5 months after the DWH spill; more than 40% reported decreasing their consumption for 12 months (Wilson *et al.*, 2015).

PAHs in Crude Oil

Crude oil composition varies widely between oil reservoirs, containing thousands of specific compounds ranging from a single carbon moiety to greater than 40 carbon moieties in size. Crude oil contains a number of different environmental contaminants, levels of which vary between reservoirs (Wardlaw *et al.*, 2008). The principle contaminants of concern in crude oil are polycyclic aromatic hydrocarbon compounds (PAHs). PAHs in the environment principally come from either pyrogenic or petrogenic sources. While the pyrogenic PAHs typically do not have substitutions to the aromatic rings, petrogenic PAHs tend to include alkyl, oxygen, and nitrogen substitutions (Wickliffe *et al.*, 2014). Crude oil may contain more than 100 different PAHs (Xia *et al.*, 2012), which typically range in size from 2-7 rings, with 2-3 ring structures being more abundant (Law and Hellou, 1999; Wickliffe *et al.*, 2014). In general, 2-3 ring PAHs tend to be more water soluble (Reddy *et al.*, 2012) than the 4-5 ring structures, making them more likely to be found in marine organisms following an oil spill (Law and Hellou, 1999). The smaller 2-3 ring PAHs are more easily degraded by various weathering

processes than the larger 4-6 ring compounds. PAHs are well known to accumulate in several species, with accumulation in crustaceans and mollusks being most common given their decreased ability to clear the compounds compared to chordates (Ylitalo *et al.*, 2012; Xia *et al.*, 2012; Wilson *et al.*, 2015).

Following the closures of Gulf fisheries, the U.S. FDA and NOAA set out to assess PAH contamination oil-stricken areas (U.S. Food and Drug Administration, 2010). This testing involved organoleptic sensory analysis and gas chromatography/mass spectroscopy (GC/MS) in several seafood species (U.S. Food and Drug Administration, 2010). As a part of this strategy, the FDA developed levels of concern (LOC) for shrimp/crab, finfish, and oysters based largely on studies and protocols from several previous oil spills, including the Exxon Valdez spill (Yender *et al.*, 2002). The LOC represents a maximum amount of benzo[a]pyrene toxic equivalency (BaPTEQ) in seafood that is acceptable for human consumption given a number of accepted values (i.e. body weight, increased cancer risk, exposure duration etc...). BaPTEQ is calculated by quantitatively determining levels (wt/wt) of specific PAHs in the samples and multiplying these amounts by toxic equivalence factors (TEF), to convert the total PAH levels into a toxicologically equivalent amount of BaP (Nisbet and LaGoy, 1992; U. S. Environmental Protection Agency, 1993; WR Reeves *et al.*, 2001). This method ultimately identifies a BaPTEQ for each sample, which informs risk-assessments of seafood consumption based on historical studies of BaP toxicology in animal models (Chen and Chu, 1991; Nisbet and LaGoy, 1992; Yender *et al.*, 2002). There have been several criticisms of the FDA's LOC methodology, including critiques regarding the average body weight and seafood consumption rate values used in the LOC calculations (Rotkin-Ellman *et al.*, 2011; Wilson *et al.*, 2015). The concern is that these assumptions do not account for sensitive sub-populations of people in the Gulf communities affected by the spill, who consume greater than average amounts of seafood and have a broad range of body weights (Dickey, 2012). These problems with the federal report have underscored the need for

studies assessing PAH contamination relative to those sensitive Gulf communities (Rotkin-Ellman *et al.*, 2011; Wickliffe *et al.*, 2014; Wilson *et al.*, 2015).

Toxic Equivalency Factors in Quantifying PAH Contamination

The TEF approach was first developed for studying polychlorinated dibenzofurans and polychlorinated dibenzodioxins. It was chosen for evaluating PAH toxicity based on the existence of several studies characterizing BaP toxicology as well as the relative lack of studies on other PAHs (Nisbet and LaGoy, 1992). Thus, by its very nature the TEF approach acknowledges gaps in understanding the fundamental toxicological characteristics of many PAHs (Nisbet and LaGoy, 1992). The TEF approach requires that the PAHs being evaluated must have concrete empirically derived TEFs relative to BaP. These values exist for the 16 US EPA priority PAHs, which are unsubstituted ‘parent PAH compounds’. However, given that unsubstituted PAHs represent a relatively small fraction of the total PAHs present in oil (Saha *et al.*, 2009; Wickliffe *et al.*, 2014), it is difficult to say for sure how the various substitutions to these parent compounds affect their toxic potency. There is data to suggest that substituted PAHs (i.e. 5-methylchrysene) are more carcinogenic than the unsubstituted parent compound (Hecht *et al.*, 1978; Hong *et al.*, 2015) (unpublished observations) and that certain compounds in weathered oil are more toxic than those in non-weathered oil (Hong *et al.*, 2012). This is an especially important consideration given the opportunity for various weathering processes to affect oil released during the DWH spill (Farwell *et al.*, 2009; Hong *et al.*, 2012; Wickliffe *et al.*, 2014; Hong *et al.*, 2015).

Given the significant lack of basic toxicological information, especially for petrogenic (rather than pyrogenic) PAHs, we set out to assess PAH contamination in Gulf seafood using a mechanistic approach. It is well accepted that the Aryl Hydrocarbon Receptor (AhR) is required for PAH toxicity to occur (Mimura *et al.*, 1997; Peters *et al.*, 1999; Matikainen *et al.*, 2001; Nebert *et al.*, 2004; Denison *et al.*, 2011; U. S. Environmental Protection Agency, 2012; Tuyen *et al.*, 2014). The AhR is a cytosolic

ligand activated transcription factor that translocates to the nucleus and activates various target genes, including several phase I and II metabolic enzymes, through binding to cis-DNA motifs in promoter regions (Denison *et al.*, 2011). Activation of the AhR by myriad structurally diverse PAH ligands is well documented and accepted as the basic toxic mechanism (Denison and Nagy, 2003; Windal *et al.*, 2005; Nguyen and Bradfield, 2008). With this in mind, Garrison et al. developed several stable Chemically Activated Luciferase eXpression (CALUX) reporter cell lines. The CALUX bioassay, is an EPA approved low cost effect-based, high-throughput method for assessing H/PAH contamination in myriad different sample types (Schechter *et al.*, 1999). We employed the CALUX assay to evaluate PAH contamination using PAH extracts from seafood samples collected by our partners. These extracts were evaluated in the assay in comparison to BaP (our reference compound). Note we report the results of the CALUX assay in ng BaPTEQ/g seafood as an overall representation of PAH contamination. Ultimately, we used the results to inform conservative seafood consumption guidelines tailored to the needs of our community partners based on their desired endpoint, which was potential increased cancer-risk associated with consuming contaminated seafood.

MATERIALS AND METHODS

Sample Collection

(For more information see **Appendix 8**) In keeping with the CBPR approach, we established a network of three major hubs for coordination of a community field science network of fishermen. These sampling hubs were located at Houma, Louisiana (United Houma Nation), Gulfport, Mississippi (*Mississippi Vietnamese Community Partner*) and Coden / Bayou la Batre, Alabama (South Bay Communities Alliance / Alabama Fisheries Cooperative). For sample collection by the fisherfolk in these hubs, we developed a standardized sampling procedure in order to maintain sample purity, accurate data on collection site (GPS, date, time), and maintenance of sample chain-of-custody. Sampling protocols were derived from EPA-approved procedures. Over the course of the seafood-

sampling period, community fishermen successfully collected samples of shrimp (brown and white), blue crab, oysters and a variety of finfish within the tri-state coastal area. We collected additional samples from sites in Galveston Bay for use as controls.

Method of extraction

5g of seafood (meat) was placed in a 50 ml falcon tube, 12 ml of water was added and the sample was homogenized. Deuterated phenanthrene was added to this mixture as a recovery standard and vortexed for 1 minute. To this mixture, 15 ml acetonitrile was added and the mixture was vortexed for 15 minutes. We then added the QuEChERS extract pouch contents containing MgSO₄ and NaCl (Agilent p/n 5982-6555) and shook vigorously for 15 minutes. The mixture was then centrifuged and 8 ml of acetonitrile layer was transferred to an Agilent AOAC fatty sample dSPE 15 ml tube (Agilent p/n 5982-5158) and vortexed for 1 minute. The sample was centrifuged and the acetonitrile layer was transferred to a glass tube and the volume was reduced under a gentle stream of nitrogen to 500µL. 100µL of this extract was taken and the running standards (deuterated naphthalene, anthracene and perylene) were added. A blank with all the added standards were run in parallel with the samples. These extracts and blanks were used for treatments in the CALUX assay, with the deuterated ‘running standards’ used as a vehicle control for the seafood extracts. The extraction procedure was adapted from Agilent technical note 5990-6668N.

Chemicals

Certified Reference grade Benzo[a]pyrene (#CRM40071 Sigma-Aldrich, St. Louis, MO) and TCDD (Cerilliant, Round Rock Texas) were dissolved in acetonitrile (Acros Organics Morris Plains, NJ) and diluted to stock concentrations for use in *in vitro* CALUX experiments. Acetonitrile CALUX treatments were used as vehicle controls for the standard curve treatments. Luciferase reagents were purchased from Promega and used according to the manufacturers recommendations (described below) (Promega Corp., Madison, WI).

Cell Culture

Hepa1c1c7 cell lines stably expressing the pGudluc reporters (termed H1L1.1c2 or H1L6.1c3 cells) were a generous gift from Dr. Michael Denison (University of California, Davis). Cells were cultured in MEM α supplemented with 10% FBS (Atlanta Biologicals, Norcross, GA), 1% Penicillin/Streptomycin and 250 μ g/ml active G418 (Cellgro Manassas, VA). Cells were grown to 90% confluency, trypsinized and pelleted (1,000RPM for 4 minutes), resuspended in fresh pre-warmed media, then seeded onto 12-well plates and allowed to attach overnight. Cells were rinsed with 300 μ L of room-temperature (RT) 1x phosphate buffered saline (PBS) and 2mL of pre-warmed media was added. Cells were treated with BaP stock solutions or acetonitrile (vehicle) (at an equal volume) to generate duplicate BaP standard curves, which were averaged together following normalization to protein. Seafood extracts (from above) were assayed in biological triplicate. Cells treated for 24 hours, rinsed with 300 μ L RT 1xPBS and lysed in 250 μ L pre-warmed 1x Passive Lysis Buffer (PLB) (Promega Corporation, San Luis Obispo, CA) for 15 minutes then frozen at -80°C. Following the freeze step, lysates were thawed and transferred to 1.5ml microcentrifuge tubes. Tubes were vortexed for 10 seconds and cleared via spin at 12,000 RPM for 30 seconds at RT. Cleared lysates were transferred to new tubes and used immediately for luciferase assays.

Luciferase Assays

For luciferase assays, 10 μ L of cleared cell lysate (from above) was plated per well on a 96-well white bottom plate. Each lysate was assayed in technical duplicate and the averaged. Luciferase assays were read on Synergy H4 Hybrid Microplate reader (BioTek, Winooski, VT) using Gen 5 Data analysis software. To assay luciferase activity, 50 μ L of luciferase assay reagent was added per well and luciferase activity was read for 10-seconds following a 5-second delay.

Protein Assays

Protein concentration was assayed in duplicate using the DC protein assay according to the manufacturers specifications (Bio-Rad Laboratories, Inc., Hercules, CA). Briefly, cleared lysates were seeded onto 96-well plates, diluted 1:1 with RT 1x PBS, and assay reagents were added (according to the manufacturers recommendations) then measured using a Flex Station III reader (Molecular Devices, Sunnyvale, CA) with Soft Max Pro 5 software. For BSA standard curves, a master mix was generated for each of 5 different protein concentrations and distributed to each 96-well plate (following the 15 minute incubation) in order to have a consistent standard curve for each plate.

Experimental Design

To assess PAH contamination in seafood samples we compared two mouse hepatoma (Hepa 1c1c7) CALUX cell lines stably expressing either the pGL 1.1 or pGL 6.1 CALUX reporter (H1L1.1c2 and H1L6.1c3, respectively) (Garrison *et al.*, 1996; Denison *et al.*, 2004; Windal *et al.*, 2005). We found the H1L1.1c2 cell line to give the most reproducible dose-response to our standard compounds (BaP and TCDD), over a large range of agonist concentrations (**Figure 46 A-C**). We also noted that the CALUX reporter is ~1,000 fold more responsive to TCDD than to BaP (**Figure 46D**). Using this assay we tested 4 treatment times (6, 12, 24, and 48 hours) and found the 24 hour treatment to provide the most consistent response in the most convenient experimental regimen (data not shown). These data empirically led us to the following experimental paradigm: H1L1.1c2 cells were treated with a standard range of BaP concentrations (1nM-300nM) or seafood extract (in biological triplicate for each extract) for 24 hours, cells were lysed, then luciferase activity and protein amounts were quantified. For analysis, the luciferase activity (RLU) was normalized to protein (RLU/mg protein), and vehicle luciferase was subtracted. Normalized values for the BaP treatments were plotted and used to generate a logarithmic regression trendline and the equation of the line was used to solve for BaPTEQ for each sample based on the average RLU/mg protein (n=3)

induced in cells treated with seafood extracts at the same time. Standard curves represent the average of 3 biological replicates and 2 technical replicates, and were generated each time a new set of seafood extracts was analyzed, to control for variability between treatments. The BaP standard curve LOD was <100 pg/ml.

Statistical Analysis

Data were analyzed using SPSS v20. All boxplots represent average values of 3-5 samples taken at a specific site (same time and location). Significant differences between groups were statistically analyzed using one-way Analysis of Variance (for 3 or more comparisons) or student's t-test (comparing only two groups). All data for analysis was transformed via the base 2 logarithm to make it more normally distributed. Results were considered significant when the p-value is <0.05. Tukey's HSD test was used to determine differences when the one-way ANOVA results were significant.

Results

In meeting with our community partners during the initial design phase of our study, we identified a widespread concern throughout many Gulf communities, which questioned the possibility of oil contamination, following the spill, in the seafood they commonly ate. This was because: 1) there were large disparities in the body weights of our community partners and the body weight values used by the FDA in their analysis of seafood safety, 2) the consumption values used in the FDA analysis were less than the amounts our community partners commonly consume, and 3) there was a persistent distrust of the government's reported results among our community partners (Rotkin-Ellman *et al.*, 2011; Ylitalo *et al.*, 2012; Wilson *et al.*, 2015).

Seafood Sample Collection

Through our community partners (see **Materials** above and **Appendix 8**), we collected blue crab, oyster, shrimp (brown and white), and finfish samples from community-relevant fishing locations throughout Galveston, Louisiana, Alabama, and Mississippi. Collection date and location data were recorded for each sample, and this

weight/day (Gohlke *et al.*, 2011; Ylitalo *et al.*, 2012). Based on historical reports that PAH toxicity through the AhR depends on persistent rather than transient Ah receptor activation (Windal *et al.*, 2005; Mitchell *et al.*, 2006; Schecter *et al.*, 2006; Mitchell and Elferink, 2009; White and Birnbaum, 2009; Nukaya *et al.*, 2010), we presented our consumption guidelines on a weekly (rather than daily) time scale (**Figure 45**).

CALUX Assessment of PAH Contamination

To determine whether PAH contamination was elevated in samples following the Deepwater Horizon oil spill, we analyzed average BaPTEQ levels (BaPTEQ/gram) in seafood over the course of the study. We found significantly higher levels of PAHs in the samples collected from 3 August 2010 to 2 February 2011, compared to all other time periods for which we had samples (**Figure 42A**). We also evaluated differences in

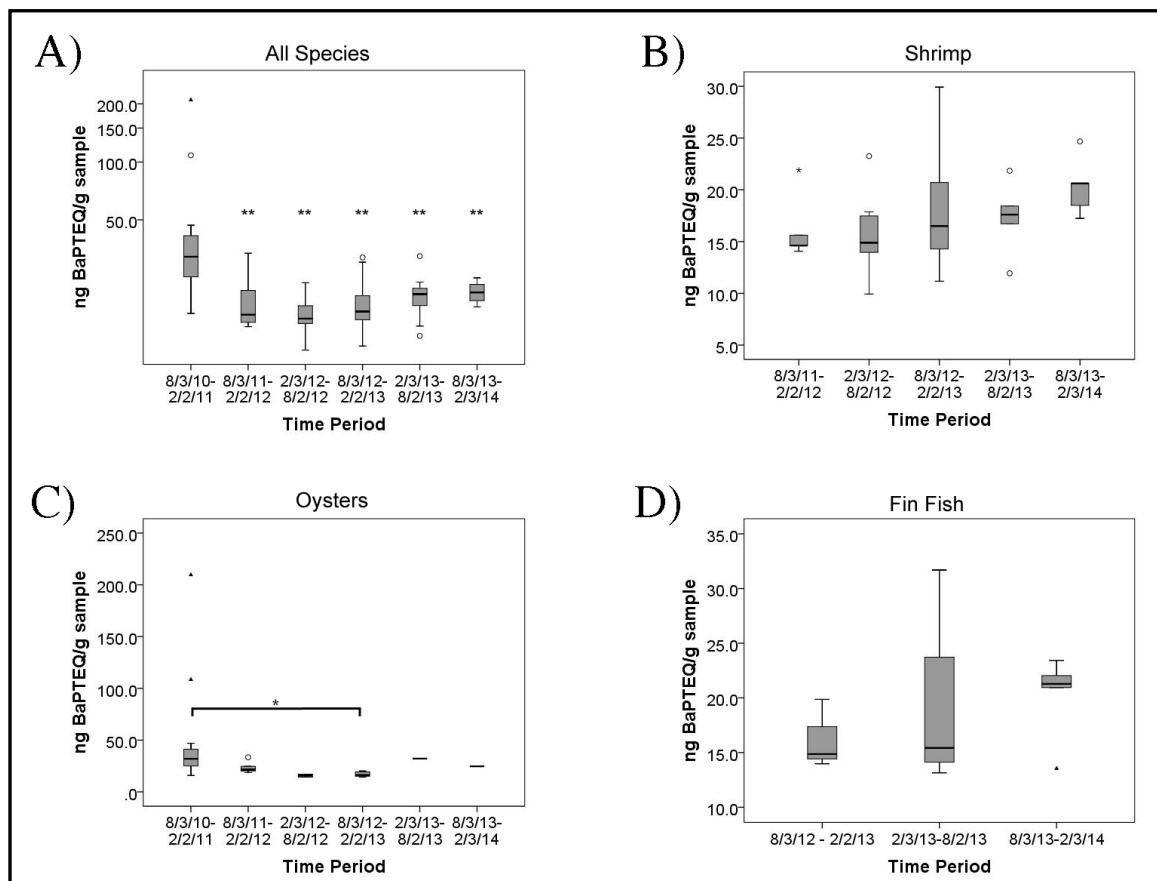


Figure 42: Box plots of of PAH contamination in Gulf seafood over time. (A) PAHs in all species, regardless of collection location, over time. (B) Analysis of PAH levels in shrimp samples over time, regardless of collection location. (C) Analysis of PAH levels in oyster samples over time, regardless of collection location (D) Analysis of PAH levels in finfish samples over time, regardless of collection location. For all graphs, asterisks indicate significance compared to the first time period or times connected by a solid bar under the asterisk. For all graphs, significance is indicted by asterisk where * $p < 0.05$, ** $p < 0.01$.

BaPTEQ levels over time for shrimp, oysters, and finfish alone. We found no significant differences in shrimp over time (**Figure 42B**), though it is worth noting we did not collect shrimp samples in 8/10-2/11. We did find that PAH levels in oysters collected during the earliest time period were significantly higher than those in oysters collected between August 2012 and February 2013 (**Figure 42C and D**) We saw no significant difference in finfish samples over time, however we did not collect finfish from 8/10-8/12.

After assessing differences in PAH levels over time in the study, we next analyzed differences between various species, regardless of when or where the samples

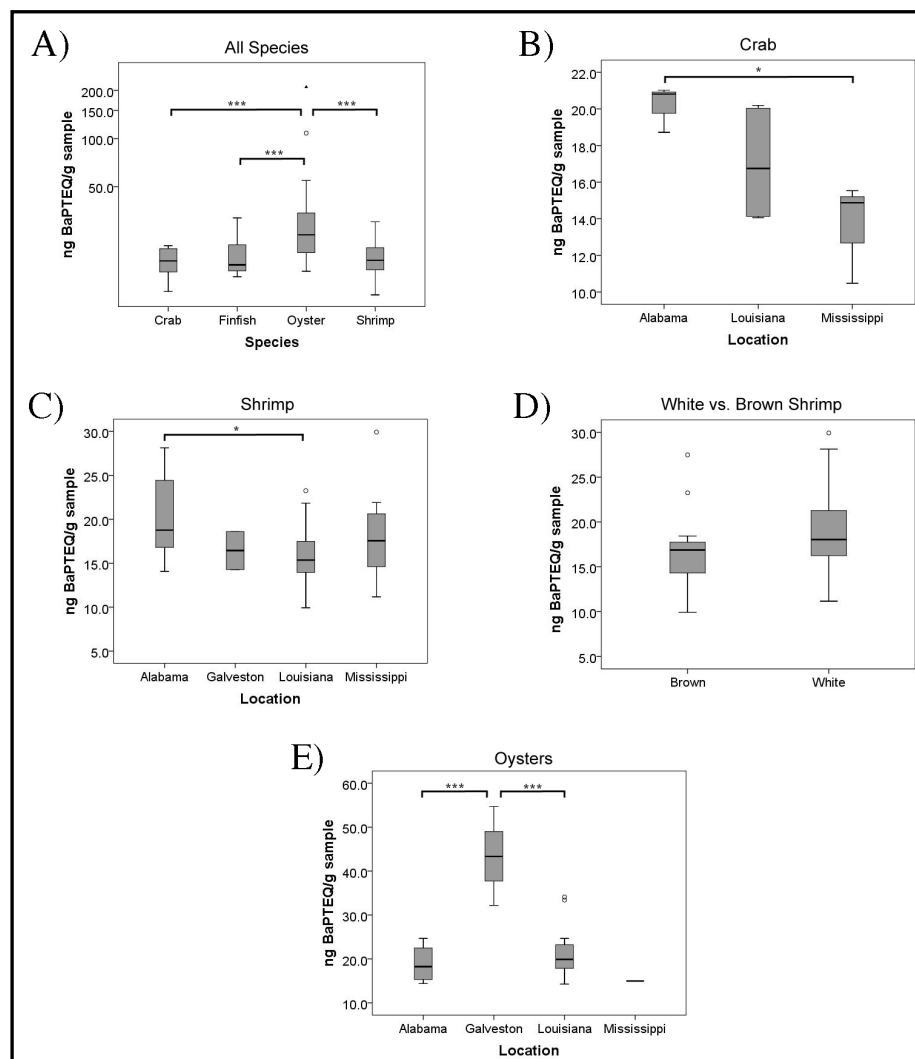


Figure 43: Box plots of PAH levels in Gulf seafood by species. (A) PAHs in Gulf seafood by species, regardless of sample collection location or time. (B) PAHs in crab samples from three different states. (C) PAHs in shrimp from four different states (D) PAHs in shrimp samples from (C), by sub-species (E) PAHs in Oysters from 3 different states excluding samples from 2010. For all graphs, significance is indicated by asterisk where * $p < 0.05$, ** $p < 0.01$, *** $p < 0.005$.

were collected, to test the hypothesis that oysters exhibit higher levels of PAH contamination than shrimp or crabs. We found BaPTEQ levels to be significantly higher in oysters than in crab, finfish, or shrimp (**Figure 43A**). When we then looked at differences between a single species across different states, we found that the levels were significantly higher in crabs from Alabama compared to crabs from Mississippi (**Figure 43B**). We also noted a significant difference in PAH levels between Alabama and Louisiana shrimp, with those from Alabama having higher levels (**Figure 43C**). We compared BaPTEQ levels between white and brown shrimp. We did not find one species of shrimp to contain significantly higher PAH levels than the other (**Figure 43D**). When we compared PAH levels in oysters (not including 2010 samples), between different states we found the oysters from Galveston were significantly higher than those collected in either Louisiana or Alabama (**Figure 43E**).

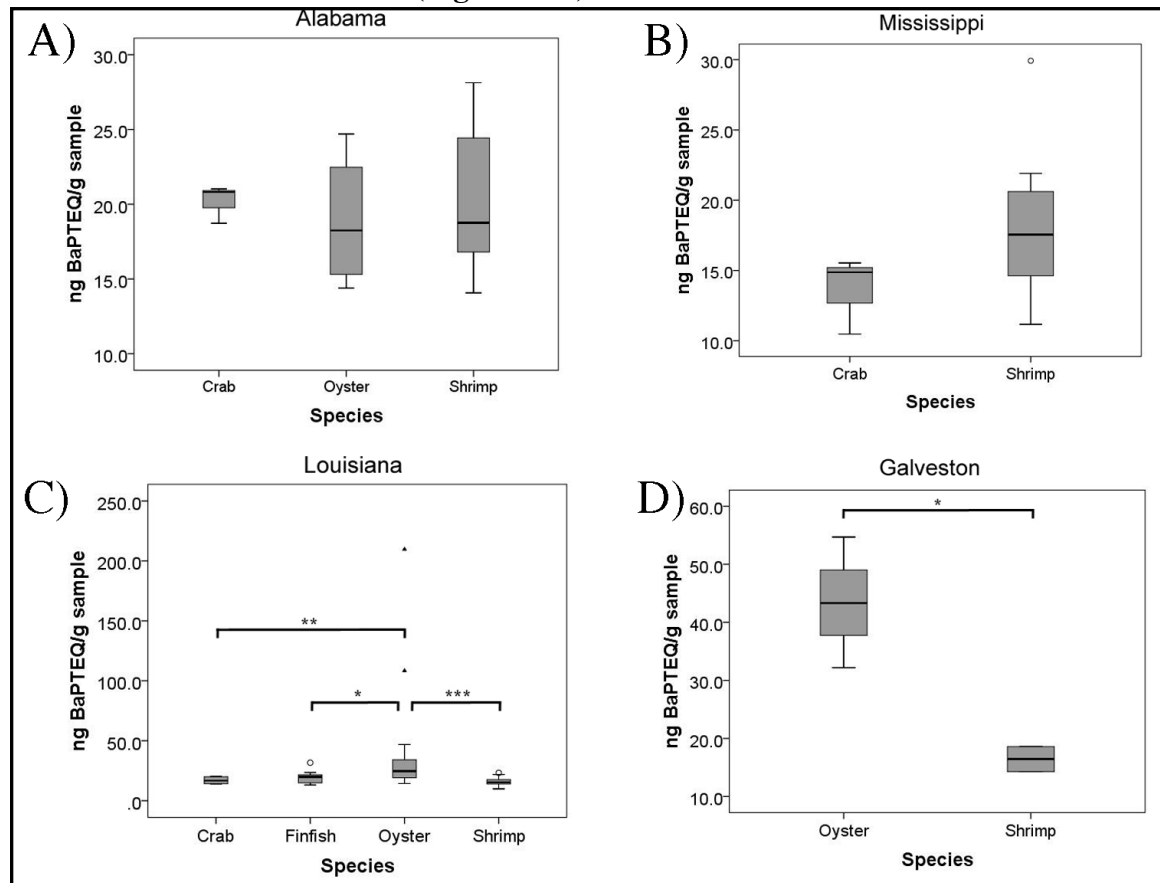


Figure 44: Differences in PAH contamination in several Gulf seafood species by state. (A) PAHs in three separate seafood species from Alabama (B) PAHs in Mississippi crab and shrimp (C) PAHs in Louisiana seafood samples by species. (D) PAH levels in Galveston shrimp and oyster samples. For all box plots, significance is indicated by asterisk where * $p < 0.05$, ** $p < 0.01$, *** $p < 0.005$.

Max weekly seafood consumption (lbs.) by body weight (without 2010)										
Species	ng BaPTEQ/ gram	100lbs		150lbs		200lbs		250lbs		# of Samples
Exposure Duration (years)		5	10	5	10	5	10	5	10	
Shrimp	17.64	0.09 0.90 9.01	0.046 0.456 4.559	0.13 1.35 13.51	0.068 0.684 6.836	0.18 1.80 18.80	0.095 0.951 9.513	0.23 2.25 22.53	0.114 1.140 11.400	208
Crab	16.90	0.09 0.92 9.21	0.047 0.466 4.660	0.14 1.38 13.82	0.070 0.699 6.992	0.18 1.84 18.43	0.093 0.933 9.326	0.23 2.30 23.30	0.118 1.179 11.789	64
Oyster	23.47	0.07 0.73 7.30	0.037 0.369 3.694	0.11 1.09 10.95	0.055 0.554 5.541	0.15 1.46 14.61	0.074 0.739 7.392	0.18 1.83 18.26	0.092 0.924 9.239	95
Finfish	18.34	0.09 0.87 8.73	0.044 0.442 4.417	0.13 1.31 13.09	0.062 0.623 6.624	0.17 1.75 17.46	0.088 0.883 8.835	0.22 2.18 21.83	0.110 1.104 11.046	43

Figure 45: Weekly seafood consumption (in lbs.) guidelines by body weight, excluding samples collected from sites in 2010. Guidelines were calculated based on the maximum allowable daily intake of BaPTEQ from the FDA's cancer risk equation (BaP cancer slope factor) using either a 5 or 10 year exposure duration and an increase cancer incidence risk of 1×10^{-4} (red), 1×10^{-5} (black), or 1×10^{-6} (blue).

After evaluating overall differences in the same species between different states, we next assessed differences in relative BaPTEQs between species collected in the same state. We found no significant differences between the species sampled in either Alabama or Mississippi (**Figure 44 A and B**). With respect to samples collected in Louisiana, there is a significant difference in BaPTEQ levels between oysters and the three other species we assayed (**Figure 44C**). We also found significantly higher levels of PAH contamination in Galveston oysters compared to shrimp, however no crabs or finfish were collected in Galveston (**Figure 4D**). Overall, the differences between species for each state are similar to the comparisons between species without regard to where the samples were collected (**Figure 43A**); oysters have the highest PAH levels, followed by shrimp, crab, and finfish samples, with no significant differences between crab, shrimp, or finfish.

Given that Galveston was not directly oiled by the DWH spill, we were surprised to see Galveston oysters exhibiting higher levels of PAHs than oysters from other areas. Based on our results, we hypothesized that the greater CALUX activity in Galveston oysters was attributable to the presence of PCBs and/or dioxins, which has previously been reported for the Galveston Bay area. Indeed, when we assessed CALUX activity in

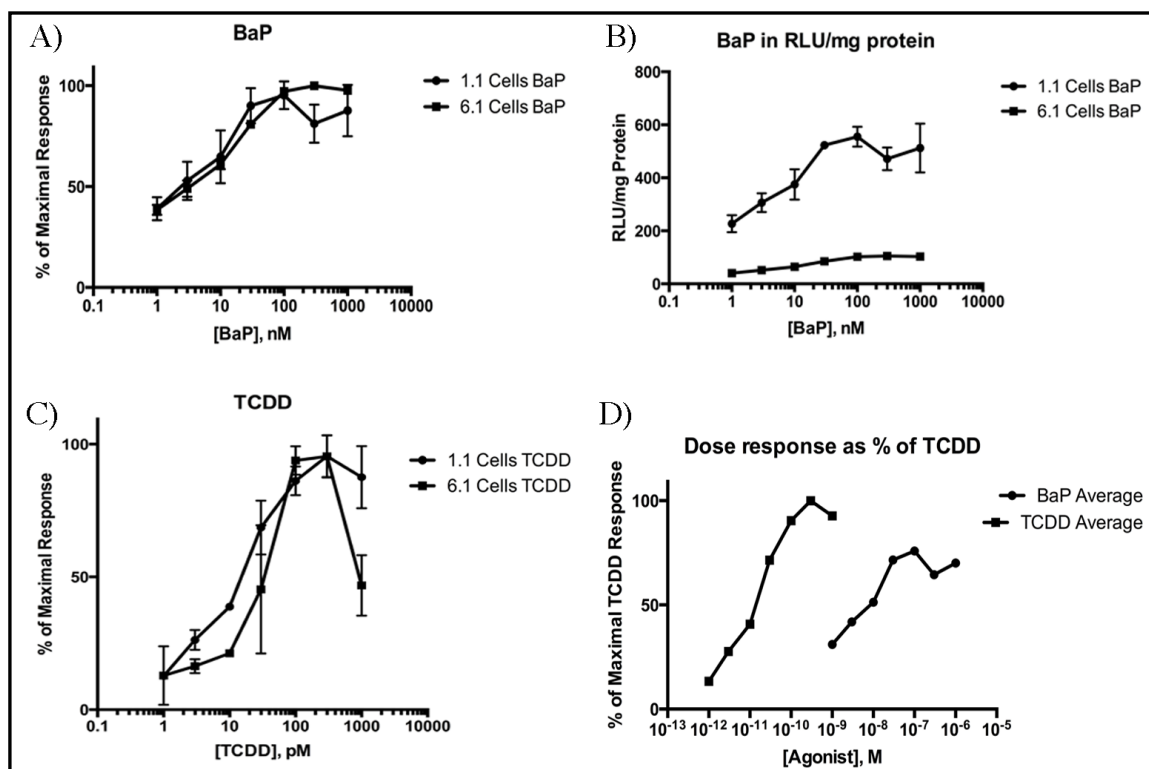


Figure 46: BaP vs TCDD dose response curves in CALUX Hepa 1.1 or Hepa 6.1 cells. (A) Dose response of BaP in two different CALUX cell lines, as a percent of the maximal response for each cell line. (B) BaP dose response as in (A), normalized to protein. (C) Dose response as in (A) using TCDD rather than BaP. (D) Comparison of TCDD and BaP dose response curves (as a percent of the maximal TCDD response) in the CALUX Hepa 1.1 cell line. Data plotted as mean of 4 individual replicates for each treatment, error bars are 1 standard deviation.

4 Louisiana Oysters and 2 Galveston Oysters (n= 3 replicates per oyster sample) over time, we found Galveston samples to elicit CALUX activity over a longer treatment time than the Louisiana oysters (**Figure 47**). Given that the CALUX activity decreased sharply over time in treatments with Louisiana oyster sample extracts, the results support the notion of metabolically resistant agonists present in Galveston oyster samples. It should be noted that we only obtained 5 oyster samples (1 site) from Mississippi and no crab samples from Galveston. As such, these data were not included in the aforementioned comparisons (**Figures 43E** and **43B**, respectively).

DISCUSSION

Previous studies assessing PAH contamination have reported oysters to contain higher PAH levels than shrimp or crabs (Law and Hellou, 1999; Law *et al.*, 2002; Gohlke *et al.*, 2011); our results are consistent with these observations. There are several

hypotheses as to why PAH levels are higher in oysters than shrimp or crabs. It has been suggested that oysters have less phase I and II metabolic enzyme expression than shrimp or crabs, and thus they metabolize PAHs more slowly (Law and Hellou, 1999; Law *et al.*, 2002; Gohlke *et al.*, 2011; Xia *et al.*, 2012). Alternatively, it has been suggested that oysters contain higher levels of PAH contamination

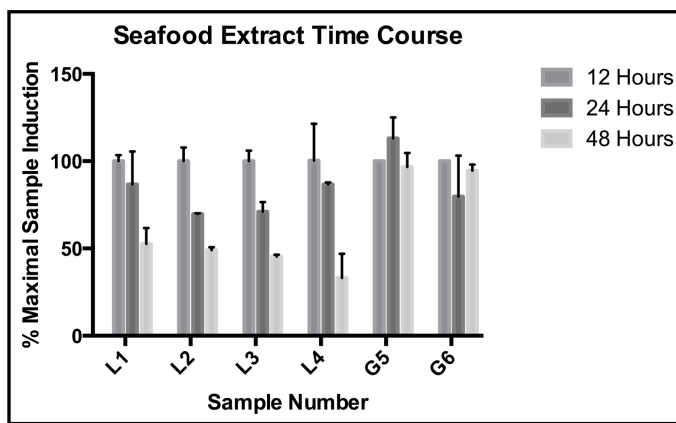


Figure 47: CALUX response of Louisiana (L1-L4) and Galveston (G5-G6) oyster samples over time (12-48 hours) data are RLUs normalized to protein then plotted as a percent of the CALUX activity at 12 hours. Data are the mean of 4 individual replicates for each time point, error bars are 1 standard deviation.

because they cannot move away from oil in the marine environment like shrimp, crabs, and finfish (Carls *et al.*, 2001; Peterson *et al.*, 2003). It is noteworthy that oysters collected in one of the early sites were identified as statistical outliers (**Figure 42A**). The samples from this site were collected in August of 2010 and showed ~2x greater activity in the CALUX assay than oysters collected around the same time at a different site. Because we only collected 6 oyster samples (3 different collection sites) from that time point, it is difficult to say why that site showed a greater response in the CALUX assay. It is possible these oysters were directly exposed to oil released during the Deepwater Horizon oil spill and thus had significantly higher PAH contamination as a result.

The data show that PAH levels in our samples were elevated immediately following the 2010 Deepwater Horizon disaster and the levels were significantly lower 1 year after the spill. It should be noted that other studies have investigated the effects of the DWH spill, and indeed some of these studies have reported short term changes as a result of the oil spill (Whitehead *et al.*, 2011; Xia *et al.*, 2012; Allan *et al.*, 2012). Indeed, Allan *et al.* identified significant increases in the amount of bioavailable PAHs along Gulf of Mexico beaches immediately following direct oiling (Allan *et al.*, 2012). Our results show that BaPTEQ levels found for the period 1 year after the spill are not significantly

different from any other time periods except the earliest one. One interpretation of the results is that PAH levels decreased over a 1 year period after the spill and remained relatively consistent thereafter. It is worth mentioning that Xia *et al.* (2012) concluded that PAH levels in oysters at 1 year after the DWH spill were not significantly different than the PAH levels reported in NOAA's 10-year Mussel Watch Program (Kimbrough *et al.*, 2008; Xia *et al.*, 2012). It is also noteworthy that the significant increases in bioavailable PAHs reported by Allan *et al.*, had returned to pre-oiling levels by March of 2011 (Allan *et al.*, 2012). Based on our results, we conclude that a 'background' or 'baseline' PAH contamination exists in Gulf seafood. It should be noted that our study did not include samples collected prior to the DWH spill, thus it is unknown how the PAH levels we report compare to pre-spill PAH levels. As such, it is possible the background levels we identified are related to the DWH spill. Given that a substantial portion of the oil released during the DWH spill remains unaccounted for (Valentine *et al.*, 2014; Chanton *et al.*, 2015), it is possible the background PAH levels are related to oil not removed from the Gulf after the spill (Allan *et al.*, 2012). In light of the Galveston results, the data suggest PAH contamination may be present in seafood from areas not directly oiled by the DWH disaster. While evidence does support the notion of a 'baseline' level of PAH contamination in Gulf seafood, it remains heretofore unclear how this is related (if at all) to the DWH spill, and what exactly the baseline values are for each species. Background PAH contamination in Gulf seafood can be explained by both natural and anthropogenic sources of PAHs. This includes natural seeps from oil reservoirs in the Gulf of Mexico, commercial shipping operations throughout the Gulf, industrial operations in Gulf cities, leaks from historic as well as current industrial drilling operations (Law and Hellou, 1999), and PAH input from U.S. waterways draining into the Gulf (i.e. the Mississippi river) (Santschi *et al.*, 2001; Eisler, 2004; Overton *et al.*, 2004).

We were initially surprised to find that Galveston oyster samples exhibited significantly higher levels of CALUX activity than oysters from Louisiana and Alabama, because Galveston was not directly oiled following the Deepwater Horizon spill. Consequently, we hypothesized the CALUX activity in the Galveston oyster samples may be indicative of PCB contamination. Indeed, when we measured the Galveston and Louisiana oyster extracts over a 48 hour time course, we found the Galveston samples to show smaller decreases in CALUX activity over time than were seen with Louisiana samples (**Figure 47**). We attribute the higher CALUX response in Galveston samples to the well-documented presence of PCBs and dioxins in the Galveston Bay area, which are not necessarily present in other sampling locations (Yeager *et al.*, 2007; Lakshmanan *et al.*, 2010). Unlike other PAH ligands for the AhR, PCBs and dioxins are long lived in the environment and resistant to metabolism. As such, PCBs are able to persistently activate the AhR both *in vitro* and *in vivo*. Thus, when they are present in seafood extracts, the CALUX response will persist at longer treatment times compared to extracts which don't contain PCBs (see **Figure 47**). Indeed, we were also surprised to find that Alabama crabs and shrimp showed significantly higher CALUX activity compared to crabs from Mississippi and Shrimp from Louisiana, respectively. While we did not investigate this difference further, it is possible that halogenated hydrocarbons are present in the Alabama samples. In fact, Alabama was at one time home to paper pulp bleaching factories, which used chlorine in the pulp bleaching process. Paper pulp bleaching has been shown to release persistent HAHs, including among others TCDD and TCDF (Johnston, 2005).

The CALUX Bioassay for Measuring PAH Contamination

As the CALUX system is an AhR-driven reporter assay, it is worth briefly addressing the potential presence of endogenous AhR ligands in the samples we collected. While possible, it could reasonably be assumed that any endogenous ligands would be present in similar amounts in all samples of the same species. Thus, differences in PAH levels between shrimp samples, for example, would have little to do with any

endogenous ligand, as said ligands would likely be equally present in both samples. Given that we tested several seafood extracts which showed no measurable CALUX activity, we conclude that contributions to the CALUX assay response by endogenous ligand(s) in the extracts are, at best, modest. It is also worth addressing the potential presence of AhR antagonists in the seafood extracts, which might blunt the overall CALUX response and thus under-represent the amount of true CALUX activity (and thus BaPTEQ) present in the extract. While many AhR agonists have been identified (Denison and Nagy, 2003; Nguyen and Bradfield, 2008), AhR antagonists- including the mechanisms by which they function and their metabolic fates- are not well studied (Denison *et al.*, 2011). Thus, it is difficult to say for sure how these compounds might be affecting our results. Hong *et al.* 2015 recently reported on studies of the 2007 *Hebei Spirit* oil tanker spill, in which they used a CALUX bioassay coupled with GC-MS to assess AhR-active PAHs in crude oil and sediments affected by the oil spill. In this report the authors demonstrate CALUX activity induced by treatment with a crude oil sample. Interestingly, when the authors compared the CALUX activity of the crude oil extract to the CALUX activity of 3 different silica gel fractions of that same crude oil extract, they found that fractions 2 and 3 (mainly consisting of aromatics, resins, and polar compounds) induced ~9 fold greater CALUX activity than treatment with the crude extract alone (Hong *et al.*, 2015). These findings may be explained by the presence of AhR antagonists in fraction 1, accounting for the larger induction in fraction 2 and 3, relative to induction by the raw extract. However, it should be noted that the authors do not clearly indicate how they accounted for concentration differences in the make up of each fraction relative to the raw extract, and the potential for this difference to obfuscate the results. For example, if a raw extract were split into three fractions, each of those fractions would have to be assayed in the CALUX system at 1/3rd of the volume used for the raw extract CALUX assessments. Otherwise, the results could be a product of an

enrichment, or greater concentration, of certain agonists in treatments with fractions 2 and 3.

While it's possible AhR antagonists may be present in our seafood extracts, it's difficult to know for sure the extent to which they may affect the signal by PAHs in the extracts. It's also difficult to say how these antagonists might behave *in vivo* in humans, as they may not be absorbed well, or may be rapidly metabolized. Thus, more work is needed to understand how complex PAH mixtures affect the bioassay. Specifically, it will be necessary to characterize AhR antagonists in crude and weathered oil, as well as the effective concentrations of these compounds to understand how they might affect the CALUX assay. Given our findings of a background PAH contamination across several locations (especially in Galveston, which was not directly oiled by DWH), it is tempting to speculate that levels of AhR antagonists wouldn't have significant variance between sampling locations. Whatever the case may be, the difficulties posed by AhR antagonists and endogenous agonists underscore the technical difficulties of working with chemical mixtures.

The CALUX bioassay signaling mechanisms have been extensively characterized, however, 'mixtures toxicology' studies are inherently difficult to conduct and interpret due to the complex chemical interactions at work. In fact, while TEFs are available for a number of PAHs, relatively little is known about how these TEFs might change when compounds are present as parts of a mixture (Reeves *et al.*, 2001; Martins *et al.*, 2015). These inherent difficulties- in concert with the thousands of individual compounds in oil - further obfuscate downstream attempts to reconcile the toxicology data with human health impacts (Nisbet and LaGoy, 1992; Reeves *et al.*, 2001). These difficulties underscore the historic justification of the TEF approach for studying PAH toxicology, which functions to translate toxicology data for myriad PAH compounds into equivalencies of a well-studied 'reference' PAH species (Nisbet and LaGoy, 1992). While the TEF approach has been widely used, the available human toxicology data for even the

commonly used reference PAHs (BaP and TCDD) is minimal (Reeves *et al.*, 2001; Wilson *et al.*, 2015). This includes a lack of basic pharmacokinetics and dose-response data for toxicities associated with these compounds. In many cases this lack of data limits the deduction of human health relevant conclusions. For example, early studies of the *in vivo* dose-dependent carcinogenic potential of BaP (from which the BaP cancer slope factors are derived) are both dated and limited and thus the data used to inform human health risk-assessments for excess cancer incidence (due to BaP exposure) has not been rigorously validated. As such, studies using the TEF approach may be under or over estimating the risks associated with PAH exposure. This limitation is further evident in attempts to correlate toxicity of non-genotoxic, carcinogenic PAHs and non-carcinogenic PAHs to human health. Thus, while AhR antagonism and the potential for endogenous AhR agonists in the seafood extracts need to be taken into consideration when drawing conclusions from the data, more emphasis should be placed on clearly defining human-health relevant toxic endpoints (including cancer and non-cancer endpoints) and elucidating the chemicals (and relevant concentrations) which evoke them.

Seafood Consumption Guidelines Based on CALUX Results

The main focus of our study was to assess PAH contamination in Gulf seafood, to inform conservative seafood consumption guidelines for our community partners who consume greater than average amounts of seafood (above the 90th percentile of the NHANES study) (Wilson *et al.*, 2015). These guidelines are based on a risk assessment using a 1:100,000 increase in cancer incidence over a 5 year exposure duration, however we also calculated consumption guidelines for both an order of magnitude higher and an order lower cancer risk as well as for a 10 year exposure duration (**Figure 45**). As with any risk assessment, it is important to note these consumption guidelines do not account for other sources of PAH contamination, which may be considerable depending on individual diet, local environment, and a plethora of other lifestyle choices. For example, there are reports that grilled and smoked food, in particular meats, can contain myriad

PAHs; this includes commercially available smoked meat products (Xia *et al.*, 2012; Hitzel *et al.*, 2013; Chen *et al.*, 2014). Studies have also shown that cigarette smoke is another substantial source of PAH contamination (Ding *et al.*, 2007). As PAHs (in particular the long-lived persistent organic pollutants) are commonly found in the environment, it is possible that environmental sources of PAH contamination might influence an individual's consumption guidelines. It is also noteworthy these guidelines are only based on the results from the samples we collected (concluded collection in February 2014); continued monitoring of PAH levels in Gulf of Mexico seafood would be needed to keep the consumption guidelines up to date.

CONCLUSIONS

Given the many sources of PAH contamination in everyday life today, more work is needed to fully determine the effects of PAH contamination in humans and how these compounds affect population health with respect to various PAH-induced pathologies like cancer. In light of recent reports that environmental exposures may in fact contribute to a number of common human health conditions (i.e autoimmune disease), a deeper understanding of basic toxicology data for a broad spectrum of parent (in particular petrogenic) PAHs must be made a research priority. Empirically defined PAH exposure limits and toxic endpoints from such studies, coupled with a greater understanding of where and to what extent PAH exposures occur in humans as a result of oil spills, will allow more accurate and informed risk assessments to reduce and ultimately abrogate human health conditions resultant from environmental PAH exposure.

Chapter 5: Galveston Texas Seafood Before and After the 2014 Houston Ship Channel Bunker Oil Spill: An Assessment of Petrogenic PAH Contamination and Associated Toxicology

INTRODUCTION

Background

On March 22, 2014 at 1230hrs, an oil-tank barge dubbed the Kirby 27706, carrying roughly one million gallons of heavy fuel oil, (bunker oil) collided with the bulk carrier ship M/V Summer Wind in the Houston Ship Channel (HSC), Galveston Bay, Texas. The collision punctured the #2 oil tank of the barge, which released an estimated 168,000 gallons of heavy fuel oil into the bay. The spilled oil quickly contaminated nearby beaches and marshlands, eventually extending further into the Gulf along the Texas coastline from Galveston to Matagorda. Cleanup efforts were quickly mobilized and the remaining oil was lightered from the stricken barge. During the cleanup period, shipping operations in the Houston Ship channel remained closed through 26 March. There are currently no estimates on the amount of oil recovered through the cleanup efforts and thus it is unclear how much oil remains unaccounted for in the Gulf waters (United States Coast Guard Public Affairs Detachment Houston, 2014).

Bunker Oil Composition

The *Kirby* oil barge was transporting marine fuel oil (RMG-380) which is predominantly heavy fuel oil with a small amount of light oil added to meet physical characteristic requirements for viscosity and pour point (Hwang *et al.*, 2014; NOAA Office of Response and Restoration, 2015). While the high viscosity and ‘stickiness’ of bunker oil can be beneficial for the success of skimming operations following spills, the characteristic components of heavy fuel oils are generally stable and thus do not readily degrade like the components in the ‘Light’ Louisiana Sweet (LLS) crude oil spilled during the 2010 Deepwater Horizon (DWH) oil spill. RMG-380 heavy fuel oil is low in volatile organic compounds (which evaporate readily) and significantly richer in polycyclic aromatic hydrocarbons (PAHs), including naphthalenes, phenanthrenes,

fluorenes, and higher molecular weight PAHs like fluoranthene, benz(a)anthracene, benzo[a,e]pyrene and chrysene (Wang *et al.*, 2003). For comparison, it is estimated that bunker oil contains as much as 50-fold more benzo[a]pyrene than the LLS crude (Wang *et al.*, 2003) released by DWH. In fact, a recent study found the BaP concentration to be more than 100 times higher in the oil from the HSC spill than a DWH spill sample (40 mg/kg and 0.43 mg/kg, respectively) (Yin *et al.*, 2015). As the principal chemicals of environmental and toxicological concern in crude oil are the PAHs, bunker oil presents a substantially greater risk for causing long lasting negative ecological, economical, and human health impacts. While it was initially suggested that the bunker oil would remain on the surface where it could easily be removed (NOAA Office of Response and Restoration Restoration, 2015), this phenomenon depends greatly on the chemical characteristics of sea water where the oil is spilled. Indeed, slight changes to water density can cause bunker oil to sink to the seafloor (NOAA Office of Response and Restoration, 2015). It is also worth noting, the specific gravity of heavy fuel oil renders it easily susceptible to mixing with sediment, which enhances the potential for bunker oil to sink (Lee *et al.*, 2003). Indeed, some have speculated that unknown amounts of the spilled oil did sink and thus may still be found on the Galveston Bay seafloor. In the weeks following the spill, overflight observations by NOAA and others identified mats of the spilled oil moving out of the bay and south along the Texas Gulf coast. These operations identified beached oil as far south as Matagorda Island, however there are currently no estimates on how much, if any, of the spilled oil sank to the seafloor in the Galveston bay (NOAA Office of Response and Restoration, 2015).

Pre-spill Baseline Data for PAH Levels in Galveston Seafood

As a result of the 2010 DWH oil spill, we developed a NIEHS U19 funded consortium to study petrogenic PAH contamination in several seafood species in the Gulf of Mexico. This study focused on seafood from Mississippi, Louisiana, Alabama, and Galveston, with Galveston samples collected as experimental controls to assess PAHs in

an area not directly oiled by the DWH spill. These samples were used to generate PAH-enriched organic extracts (PAH extracts, seafood extracts) to measure PAHs in seafood, which we analyzed by GC-MS and the EPA-approved *in vitro* Chemically Activated LUCiferase eXpression (CALUX) bioassay (Garrison *et al.*, 1996). The CALUX bioassay is a reporter assay driven by the Aryl Hydrocarbon Receptor (AhR). It is well accepted that the principal toxic effects of PAH exposure are mediated through the AhR (Fernandez-Salguero *et al.*, 1996; Jackson *et al.*, 2015).

While the use of GC-MS is valuable for detecting and identifying a wide range of PAH contaminants, the CALUX bioassay complements GC-MS analyses by assessing the overall AhR activation response of a PAH mixture. This quantified AhR activation can be compared to the dose response curve of a number of well-characterized AhR ligands to calculate the toxic equivalency (TEQ) of said PAH extracts. The resultant TEQs provide valuable insight on the overall biotoxicity of complex PAH mixtures which can be used to calculate exposure guidelines and human health risk-assessments for various toxic endpoints associated with exposure to PAHs in the collected seafood samples (Garrison *et al.*, 1996; Murk *et al.*, 1996; Schecter *et al.*, 1999; Denison *et al.*, 2004; Windal *et al.*, 2005; Wickliffe *et al.*, 2014). Because our previous studies of the DWH spill included the collection of samples from the Galveston area, we have obtained pre-spill baseline data for PAH levels in Galveston shrimp, crab, oysters, and finfish (atlantic croaker, speckled trout, and sand trout). As such, we are uniquely poised to study PAHs in Galveston seafood in the wake of the HSC spill. Thus, when the HSC spill occurred we leveraged pre-approved sample collection protocols and community partnerships to obtain seafood samples in the weeks following the spill, several months following the spill, and 1 year after the spill. We generated PAH extracts, using the QuEChers procedure, from these samples and analyzed PAH levels using GC-MS methods complemented by the CALUX bioassay, which was anchored to the Benzo[a]pyrene (BaP) reference standard. We report herein, baseline PAH levels in Galveston samples, which were significantly higher in the

immediate wake of the HSC spill, and remained above the pre-spill baseline values for the entirety of our one year post-spill study period. Furthermore, we note the apparent lack of any alternative natural or anthropogenic PAH sources in the area, which might account for our findings.

MATERIALS AND METHODS

Materials and Methods are described in further detail above (see **Chapter 4 Materials and Methods**) and are briefly described below.

Sample Collection

Briefly, we developed sample collection protocols with the help of community partners in our previous study. Sample collections were documented to include species, date, GPS location, and time of sample collection information for each site. Samples were stored on ice until they could be frozen, and collected from the community partners for transport to UTMB. A site consists of 5-10 samples taken from the same GPS location 1-5 of which (5 grams wet weight) were used in our analysis.

Seafood PAH Extracts

PAH extracts from seafood samples were extracted using procedure previously described (Jackson et al. 2015 submitted), methods were adapted from Agilent Technologies technical note 5990-6668N. Each sample (n=1-5 per site) represents a PAH extract generated from 5 grams (wet weight) of tissue as the starting material.

Chemicals and Reagents

Benzo[a]pyrene (#CRM40071 Sigma-Aldrich, St. Louis, MO) was diluted to stock concentrations (120 nM - 400 μ M) in acetonitrile (Acros Organics Morris Plains, NJ) for use in *in vitro* CALUX experiments. Acetonitrile was used as a vehicle control for the BaP standard curve treatments. Luciferase reagents were purchased from Promega and used according to the manufacturers recommendations (described below) (Promega Corp., Madison, WI).

Cell Culture and CALUX assays

Hepa1c1c7 cells stably expressing the pGudLuc1.1c2 construct were a generous gift from Dr. Mike Denison (University of California, Davis). Cells were maintained in MEM α supplemented with 10% FBS (Atlanta Biologicals, Norcross, GA), 1% Pennicillin/Streptomycin and 250 μ g/ml active G418 (Cellgro Manassas, VA). For the CALUX assay, cells from a 90% confluent T-75 flask were trypsinized with 0.25% trypsin-EDTA (Gibco, Life Technologies, Grand Isle, NY) and washed with 9ml pre-warmed media then pelleted at 1,000RPM for 4 minutes in a 15ml conical bottom tube. Trypsin containing media was aspirated and the cells were resuspended in 10ml pre-warmed MEM α media supplemented with 1% Pennicillin/Streptomycin and 10% FBS. Resuspended cells were seeded onto 12-well plates and allowed to attach overnight. The next morning cells were rinsed with 300 μ L of room-temperature (RT) 1x phosphate buffered saline (PBS) and 2mL of pre-warmed media was added. Next, cells were treated for 24 hours with an equal volume (5 μ L) acetonitrile, BaP standards ranging in concentration (5 μ L), or seafood PAH extracts (5 μ L), all assayed in triplicate. Note that all new samples (not previously reported in Jackson et al. 2015) collected during and post HSC spill were assayed together in one single experiment to minimize variance. After treatment, wells were rinsed with 300 μ L of room-temperature (RT) 1x PBS and lysed in 250 μ L pre-warmed 1x Passive Lysis Buffer (PLB) (Promega Corporation, San Luis Obispo, CA) for 15 minutes, then frozen at -80°C. Following the freeze step, lysates were thawed slowly at RT and transferred to 1.5ml microcentrifuge tubes. Tubes were vortexed for 10 seconds and cleared via spin at 12,000 RPM for 30 seconds at RT. Cleared lysates were transferred to new tubes and used immediately for luciferase assays. 10 μ L of each lysate were added to half-area white bottom 96-well plates in technical duplicate. 50 μ L of luciferase assay reagent was added per well and luciferase activity was read for 10-seconds (following 5 second delay) on Synergy H4 Hybrid Microplate reader (BioTek, Winooski, VT) using Gen 5 Data analysis software, technical duplicate reads were

averaged together. Luciferase activity was normalized to protein content, which was also measured in technical duplicate. Cleared lysates were diluted 1:1 with 1x RT PBS and quantified using Biorad DC protein assay (Bio-Rad Laboratories, Inc., Hercules, CA) according to manufacturers recommendations and measured using a Flex Station III reader (Molecular Devices, Sunnyvale, CA) with Soft Max Pro 5 software. A master BSA standard curve was generated (0-2mg/ml BSA) and mixed with protein assay reagents, then divided to each 96-well plate containing CALUX cell lysates, to have exactly the same standard curve for each 96-well plate. Technical duplicate readings of protein concentration for each biological replicate were averaged together (as before for technical duplicate readings of luciferase activity).

BaPTEQ calculations

BaPTEQ calculations were performed as described above. RLU values (normalized to protein) for BaP standards were averaged and plotted (pg BaP vs RLU/mg protein). A logarithmic regression trend-line was added to generate an equation for the dose response curve, and the equation of the line was used to convert RLU/mg protein values, for the seafood PAH extracts measured via CALUX, to pg BaPTEQ. The results were then calculated to give values for ng BaPTEQ/ gram of seafood sample for each PAH extract. As previously stated all BaP standard concentrations and seafood PAH extracts were analyzed in 'biological' triplicate, and each of those biological replicates were analyzed in 'technical' duplicate for luciferase activity as well as for protein quantification. All technical replicates were averaged to calculate RLU/mg protein for each biological replicate, and all three biological replicates were averaged together to determine average RLU/mg protein for each PAH extract or BaP standard. The BaP standard curve LOD was <75 pg/ml (300pm BaP in 2mL media) and >250ng/ml (1000nm BaP in 2ml media). The standard curve concentrations were 1nM, 3nM, 10nM, 30nM, and 100nM. 300pM and 300nM BaP concentrations were analyzed in each experiment (but not included in the standard curve calculation via log. regression) to ensure the

dynamic range of the CALUX bioassay extended well beyond the BaP concentrations used to generate the BaP standard curve.

Statistical Analysis

As data were found to be non-normally distributed, nonparametric tests were used to analyze significance. The Kruskal-Wallis test was used to examine differences due to time of sample collection (individual time points, or pre – spill, at-spill, and post-spill) (**Figure 49**). Dunn’s test was used to identify specific time points that were different from others. The method of Benjamini-Hochberg was used to control the false discovery rate for the individual time of sample collection analyses (**Figure 50**). $p < 0.05$ was used as the level of significance for all tests. All statistical tests were carried out using SPSS v20 by a biostatistician.

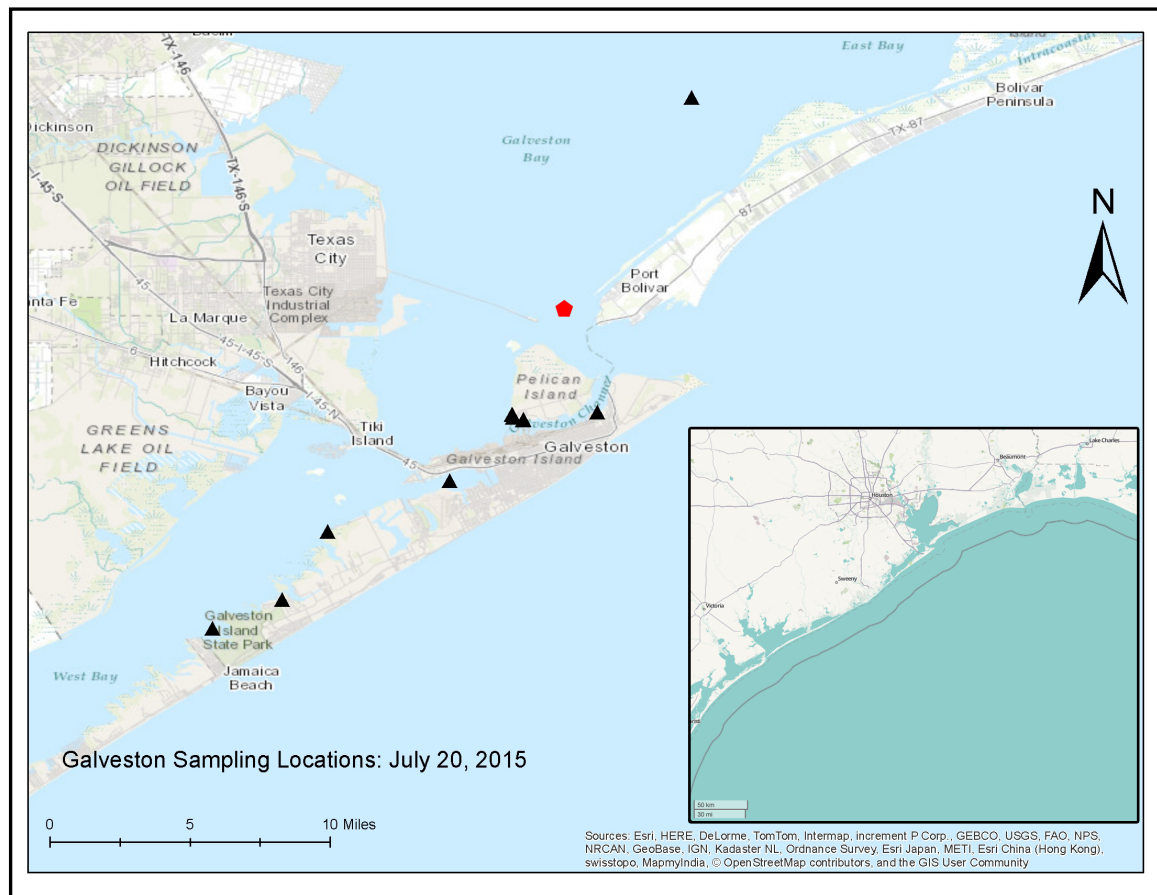


Figure 48: Map of Galveston seafood sample collection sites, indicated by dark filled triangles. HSC oil spill site is indicated by red pentagon. Outset shows Galveston in the context the larger perspective of the whole Gulf of Mexico.

RESULTS

PAH Extract CALUX Activity Was Elevated During and After HSC Oil Spill

We have previously analyzed PAH extracts from seafood samples collected in the Galveston Bay, to serve as control values in assessing Gulf seafood PAH levels resultant from the 2010 DWH spill (Jackson et al. in preparation). These baseline values were obtained using the *in vitro* CALUX bioassay and GC/MS analysis to quantify individual PAHs (naphthalenes, acenaphthene, fluorene etc...) or total PAH levels (ng/g seafood wet weight) and Benzo[a]Pyrene (BaP) toxic equivalency (ng BaPTEQ/g seafood wet weight). We leveraged these baseline data to assess changes in total PAH content,

composition, and AhR activity in shrimp, oyster, and fin fish samples collected during and after the 2014 HSC bunker oil spill (Figure 48).

First, we compared BaPTEQ/gram sample for all samples of the same species collected before 20 March 2014 (collectively termed “pre-spill” collection) to samples collected within 30 days of the HSC

spill (termed “at spill” collection) and all samples of the same species collected 1 month or more after the

spill (termed “post-spill” collection). We identified statistically significant increases in PAH levels, in all three species, for ‘at-spill’ and ‘post-spill’ samples, relative to PAHs in ‘pre-spill’ samples. (Figure 49). Not surprisingly, the largest increase in PAH levels among the 3 species was in oyster samples, which showed an increase by up to two orders of magnitude at the time of the spill compared to pre-spill samples. No samples

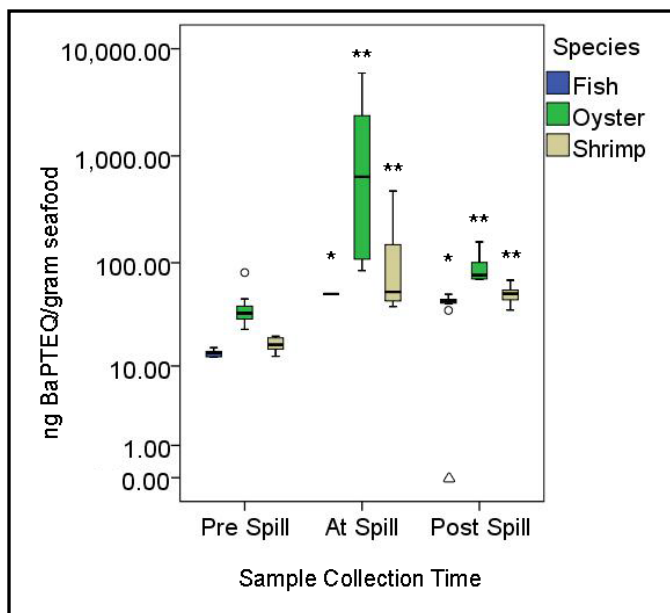


Figure 49: Box plots of average CALUX activity (BaPTEQ/g sample) of shrimp, oyster, and fin fish sites collected before the spill, at the time of the spill (within 30 days of March 22, 2014), and after the spill. Data represent average of all samples between multiple sites (all samples were assayed in biological triplicate, n=5 samples per site, each sample represents a PAH extract from 5g wet weight starting tissue). * p<0.05, ** p<0.001 compared to pre-spill sites. Open triangles indicate samples determined to be outliers.

were significantly different when comparing ‘at spill’ samples to ‘post-spill’ samples, however they appear to be trending towards a decrease in PAH content when comparing ‘at spill’ samples to post-spill sample PAH levels (shrimp $p<0.16$, oyster $p<0.43$).

PAH Levels Increase After HSC spill, Trend Toward Decreases Over Time Thereafter

We assessed PAH levels in each species over time. We found statistically significant increases in PAHs in the first shrimp samples collected after the spill, compared to samples collected in 2012 as well as to commercial samples (from local market) from around the same time. The increased PAH levels seen after the spill remained significantly higher than samples collected in 2012, from March 2014 to July 2014. While the shrimp collected roughly one year after the spill exhibited higher PAH levels than samples collected in August and November of 2012, the differences in PAH levels between those times and levels one year after the spill were not significantly different ($p<0.33$,

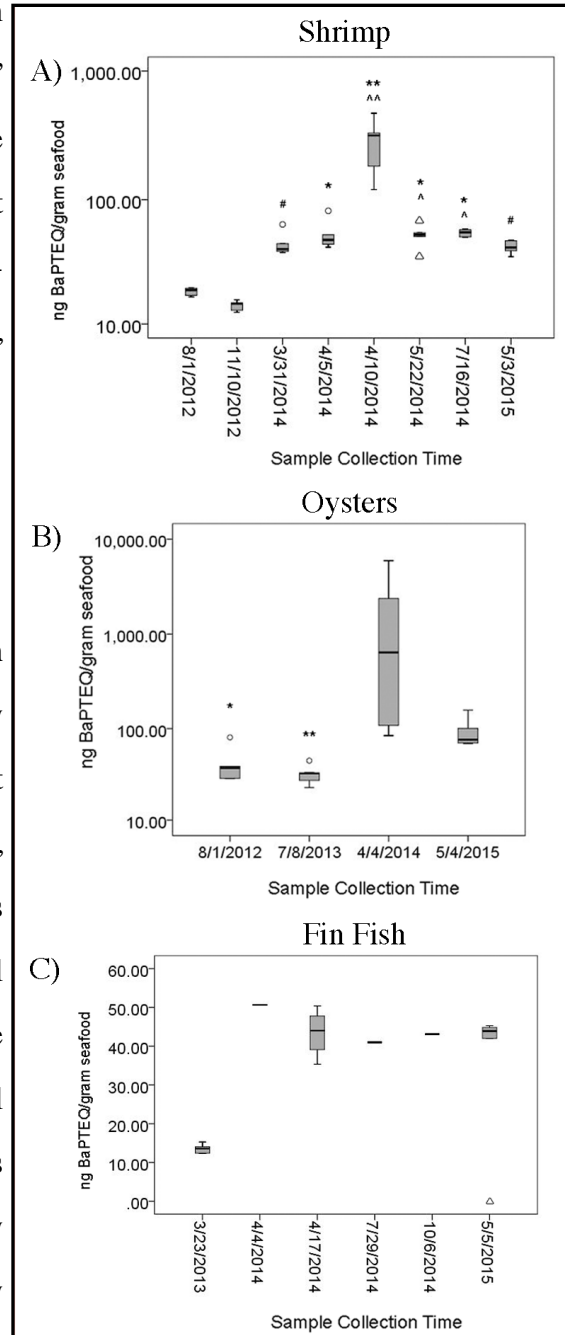


Figure 50: BaPTEQ/g sample from collection sites by date. Open triangles indicate samples determined to be outliers **A:** Average of all shrimp samples by site (all samples were assayed in biological triplicate, $n=5$ samples per site, each sample represents a PAH extract from 5g wet weight starting tissue). $^{\wedge}$ $p<0.05$, $^{\wedge\wedge}$ $p<0.001$ compared to samples from 8/1/2012 site. * $p<0.05$, ** $p<0.001$ compared to samples from 11/10/2012 site. $^{\#}$ $p<0.05$ compared to samples from 4/10/2014 site. **B:** Data represent average of all oyster samples by site, $n=4-5$ samples per site * $p<0.05$, ** $p<0.001$ compared to samples from 4/4/2014 sites. **C:** Data represent average of all finfish samples by site, $n=1-5$ samples per site.

Samples:	Individual PAHs (ng/g)								Total PAH (ng/g):
	Nap	C1nap	C2nap	C3nap	Acenap	Flu	Phe	Fluor	
07/10/2012 (n=5)!	8.17 ± 2.39	9.85 ± 1.80	7.22 ± 0.82	12.02 ± 1.71	-	0.75 ± 0.17	-	-	38.00 ± 5.34
11/10/2012 (n=5)	20.46 ± 8.94	4.49 ± 2.10	-	7.21 ± 1.16	5.29 ± 0.71	1.25 ± 0.66	2.56 ± 1.15	2.06 ± 0.88	43.33 ± 12.01
03/31/2014 (n=5)	7.69 ± 1.34	3.52 ± 0.77	28.5 ± 7.73	17.5 ± 3.26	2.23 ± 0.47	2.58 ± 0.45	3.54 ± 1.34	-	65.56 ± 9.89
04/05/14 (n=5)	58.28 ± 5.52	28.29 ± 2.34	41.34 ± 4.82	33.21 ± 2.12	27.57 ± 1.62	11.66 ± 1.14	16.20 ± 4.80	5.47 ± 3.51	222.02 ± 12.76
04/10/2014* (n=3)	60.64 ± 7.01	25.25 ± 2.48	53.09 ± 6.66	32.59 ± 3.85	8.39 ± 0.99	-	-	-	179.96 ± 28.92
04/10/2014* (n=4)	31.04 ± 4.78	19.25 ± 0.66	35.97 ± 2.58	20.37 ± 0.94	9.21 ± 0.95	2.62 ± 0.41	3.01 ± 0.73	-	121.46 ± 8.74
05/22/14 (n=5)	55.20 ± 7.01	27.11 ± 1.56	38.64 ± 2.15	33.66 ± 3.17	26.09 ± 2.51	12.87 ± 1.50	15.23 ± 1.23	6.46 ± 0.76	215.26 ± 12.03
07/16/14 (n=5)	49.56 ± 2.66	26.29 ± 1.02	32.66 ± 3.08	32.26 ± 1.50	19.26 ± 4.65	11.13 ± 1.13	12.35 ± 0.91	4.07 ± 0.44	187.59 ± 3.14
05/03/15 (n=5)	48.27 ± 8.10	24.55 ± 1.81	29.80 ± 3.43	29.85 ± 3.73	19.78 ± 1.32	10.56 ± 1.25	11.52 ± 2.66	1.90 ± 0.90	176.23 ± 14.54

Table 5: GC/MS quantification of individual and total PAH levels in Galveston shrimp collected before and after the HSC oil spill. Total PAH data obtained before the spill were less than 50 ng/g wet weight. Of the total PAH values reported, the major compounds identified in all species were unalkylated and alkylated naphthalenes.

$p < 0.13$ respectively) (**Figure 50A**). The CALUX data is further supported by a complementary GC/MS analysis of the same samples, which shows a ~5-fold increase in total PAH content in the shrimp samples collected two weeks after the spill. The PAH composition in samples collected after the HSC spill also varied compared to shrimp collected in 2012. Shrimp from 2012 contained little to no acenaphthylene, fluorine, or phenanthrene however, all three PAHs were found in much larger quantities, with higher naphthalene and alkylated naphthalenes, in samples collected after the HSC spill. It is also worth noting that total PAH levels remained significantly higher in all samples collected up to one year after the HSC spill, relative to pre-spill samples (**Table 5**). With respect to oyster samples, those collected shortly after the spill exhibited significantly higher PAH levels than oysters collected in 2012 or 2013. It is noteworthy that PAH levels in oysters collected roughly one year after the spill were not significantly higher than 2012 or 2013 oyster samples (after Benjamini-Hochberg adjustment, $p < 0.2$, $p < 0.063$ respectively) (**Figure 50B**). The GC/MS complement analysis for these samples, relative to the oyster CALUX data, supported the findings of increased PAH levels in post-spill oyster samples. In the GC/MS analysis of oyster samples, we saw a ~5-fold increase in total

Samples:	Individual PAHs (ng/g)										Total PAH (ng/g)
	Nap	C1nap	C2nap	C3nap	Acenap	Flu	Phe	Fluor	Benz/Chry	B[a]P	
07/08/2013 (n=5)	3.69 ± 1.06	1.97 ± 0.58	8.22 ± 4.13	-	2.05 ± 0.37	3.79 ± 0.35	3.11 ± 1.13	-	-	-	22.83 ± 5.69
07/08/2013 (n=7)	18.03 ± 5.41	-	-	-	6.6 ± 0.89	-	-	-	-	-	24.63 ± 5.35
04/04/2014 (n=4)	25.84 ± 5.89	15.18 ± 0.68	19.09 ± 3.73	28.49 ± 4.41	4.50 ± 0.70	4.80 ± 0.72	11.07 ± 1.57	9.63 ± 2.20	BDL	BDL	118.61 ± 18.08
04/04/2014 (n=5)*	29.69 ± 1.77	15.83 ± 1.39	38.05 ± 3.22	26.62 ± 2.94	9.32 ± 0.85	7.29 ± 1.51	6.84 ± 1.56	21.90 ± 4.71	4.39 ± 0.91	0.77 ± 0.32	160.70 ± 9.16
05/04/15 n=5	46.79 ± 6.19	26.50 ± 4.14	33.74 ± 7.09	36.23 ± 7.60	7.61 ± 0.87	7.77 ± 0.89	12.77 ± 1.23	7.36 ± 2.39	-	-	178.77 ± 24.76

Table 6: GC/MS quantification of individual and total PAH levels in Galveston oysters collected before and after the HSC oil spill. The representative SIM ion chromatograms used for quantification of the PAH's are given in Supplemental figure 1. Total PAH data obtained before the spill were less than 30 ng/g wet weight. Of the total PAH values reported, the major compounds identified in all species were unalkylated and alkylated naphthalenes.

PAH levels in all oysters collected after the HSC spill, relative to pre-spill oyster samples. With respect to the composition of PAHs present, samples collected after the spill had increased levels of C1, C2, and C3 naphthalenes, fluorine, phenanthrene, and fluorene relative to pre-spill samples. It is noteworthy that the initial GC/MS analysis of two separate collections of oyster samples (both collected on 4/4/14) did not account for the large difference in the CALUX response induced by one of the sample sets, which was absent in the other (**Table 6**). A subsequent re-examination via GC/MS identified higher levels of 3 different PAHs, accounting for the CALUX data, as discussed below. Because of the low numbers of individual samples for sites where fin fish samples were collected, we could not assess statistical significance for comparisons between collection dates for these samples. However, the PAH levels appear to increase immediately after the 2014 HSC spill and remain above the values measured in a 2013 collection, for the remainder of the study period (**Figure 50C**). These findings are supported by the GC/MS analysis of the same samples, which showed a 3-5 fold increase in total PAH levels between samples collected before and after the spill. We also noted increases in C1, C2, and C3 naphthalenes, fluorine, and phenanthrene in fin fish collected after the spill, compared to pre-spill samples (**Table 7**). Compared to the pre-spill values, PAH levels in the finfish samples do not appear to trend toward a decrease for any of the sample collections after the spill as measured by both GC/MS and the CALUX assay. In fact, the GC/MS analysis

Samples:	Individual PAHs (ng/g)								Total PAH (ng/g)
	Nap	C1nap	C2nap	C3nap	Acenap	Flu	Phe	Anth	
03/23/2013 (n=5)	10.11 ± 6.81	2.84 ± 1.06	-	6.35 ± 1.29	4.65 ± 1.01	1.31 ± 0.17	2.06 ± 0.17	1.31 ± 0.74	28.63 ± 9.71
04/03/2014 (n=2)	20.19	13.77	30.97	18.59	7.76	8.24	-	-	99.52
04/17/14 (n=3)	39.32 ± 16.44	21.97 ± 6.80	45.87 ± 6.80	29.96 ± 3.18	11.08 ± 0.44	9.47 ± 0.57	14.36 ± 1.61	-	172.03 ± 33.72
07/29/14 (n=1)	13.00	11.33	32.71	24.57	7.45	8.29	11.68	-	109.03
10/06/14 (n=1)	50.81	29.02	57.60	31.34	10.74	9.45	11.79	-	200.75
05/05/15 (n=5)	45.79 ± 14.55	26.06 ± 7.96	40.59 ± 7.36	34.97 ± 5.13	17.60 ± 7.17	10.94 ± 1.38	11.09 ± 3.16	-	187.04 ± 36.85

Table 7: GC/MS quantification of individual and total PAH levels in Galveston fin fish collected before and after the HSC oil spill. Total PAH data obtained before the spill were less than 30 ng/g wet weight. Of the total PAH values reported, the major compounds identified in all species were unalkylated and alkylated naphthalenes.

of all three species groups does not show a trend toward a decrease in total PAH levels over time in samples collected after the spill. Thus, while the CALUX data suggest BaPTEQ may trend toward a decrease over time after the spill in shrimp and oyster samples, total PAH levels measured via GC/MS do not display such a trend.

PAH Extract Color Correlates With CALUX Activity

Over the course of this and a previous study (Jackson et al. in preparation) , researchers noted several interesting trends between the color of the seafood PAH extract and the AhR activation potential of the extracts in the CALUX bioassay. Interestingly, extracts that appeared light orange, amber, or golden in color tended to exhibit greater CALUX activity than extracts which lacked any apparent color. The most stark differences in color and CALUX activity were seen in oyster samples collected from two different sites (on the same day, 4 April 2014) in Galveston, shortly after the HSC spill. We noted that PAH extracts from 4 oysters collected at the G36 sampling site showed little to no color, while PAH extracts from 5 oysters collected at the G35 sampling site showed varying degrees of a deep golden-amber color (**Figure 51A**). The obvious difference in color of PAH extract between the two sites was directly correlated with the CALUX activity of those samples, with the golden-amber G35 oysters exhibiting roughly an order of magnitude greater activity in the CALUX assay than the clear/colorless G36

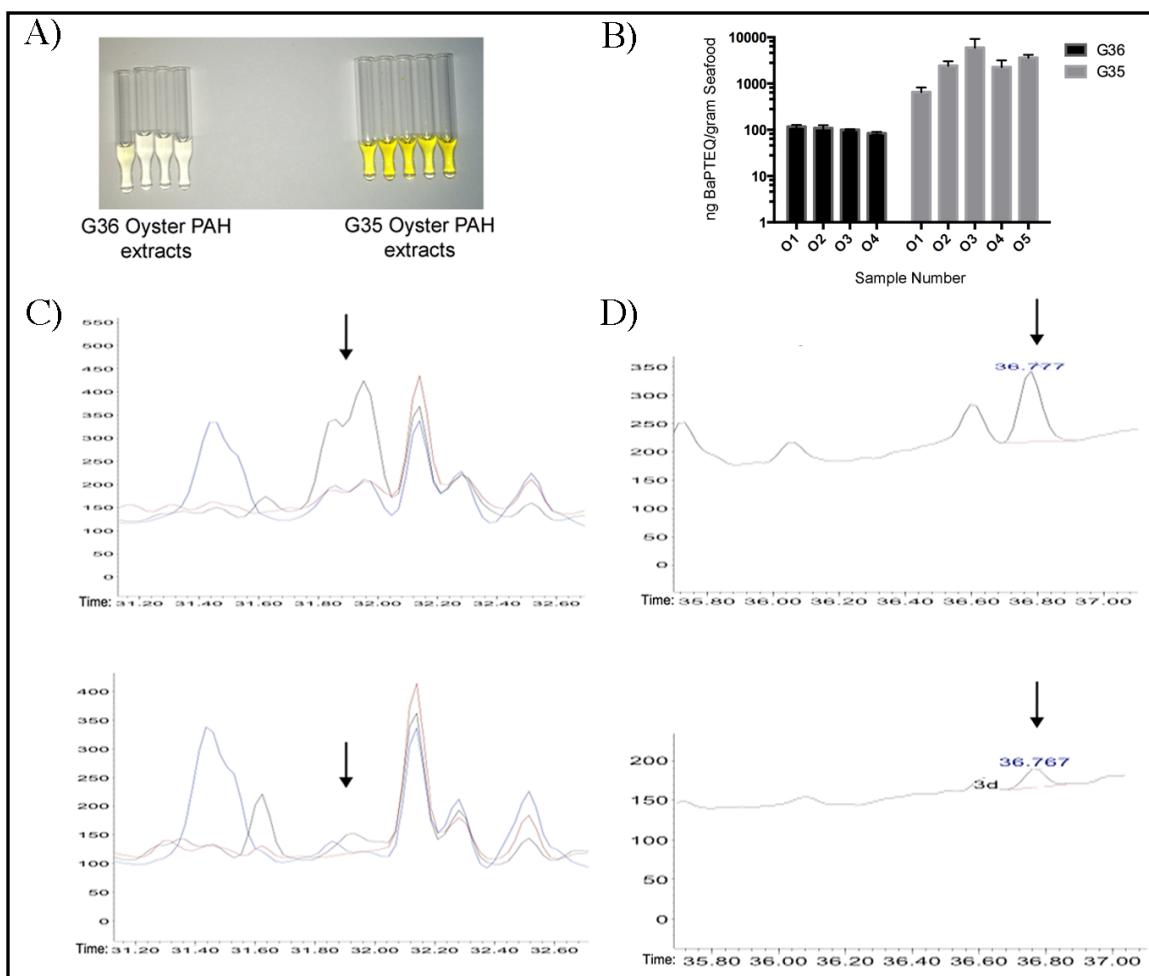


Figure 51: PAH extracts generated from oysters collected at two different sites on the same day, 4 different G36 site oysters vs 5 different G35 site oysters **A:** Photograph of G36 and G35 PAH extracts. Note the stark difference in color between the samples collected on the same day from two different locations. **B:** CALUX activity (normalized to protein and relative to BaP reference standard) of G36 vs G35 oyster samples. Data represent an average of $n=4$ biological replicates per sample (each sample represents a PAH extract from 5g wet weight starting tissue), plotted as mean \pm 1 std. **C:** Representative chromatogram of G35 and G36 oysters between 31.2 and 32.6 retention time. The masses monitored were m/z 228 (black), m/z 226 (blue) and m/z 229 (red). The m/z 226 and m/z 229 masses supported the presence of benz[a]anthracene/chrysene. Black arrow indicates double-peak for Benz[a]anthracene/chrysene **D:** Representative SIM ion chromatograms of G35 and G36 oysters between 35.8 and 37.0 retention time. Black arrow indicates peak for benzo[a]pyrene (m/z 252).

oyster PAH extracts (**Figure 51B**). It is worth noting that the oysters collected at the G35 sampling site were smaller in size than other oyster collections. Where in previous collections, a single oyster sample represented enough tissue for a single 5 gram (wet weight) seafood extract, for G35 oysters we had to use more than one oyster for each 5 gram (wet weight) seafood extract, though the same amount (by weight, 5 grams per sample) of oyster tissue was still used for each seafood extract sample. Based on this interesting relationship between color and CALUX activity, we next looked at the GC-

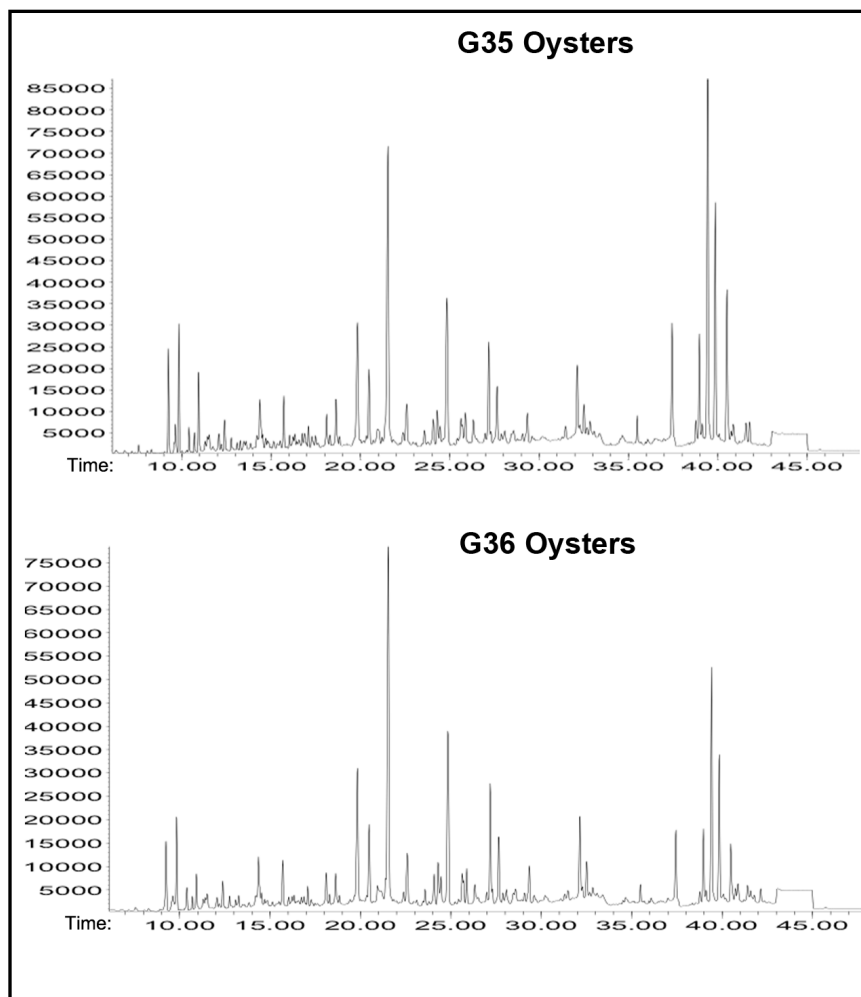


Figure 52: Representative SIM ion chromatograms for G35 and G36 oysters.

MS results for these samples to determine if any differences in PAH quantities could explain the color. Our initial GC-MS analysis identified roughly the same amount of total PAHs (ng PAHs/g oyster sample) for the G35 and G36 collections (**Table 6, Figures 52 and 54**). Upon further analysis, we determined that unidentified peaks in the chromatograms, at the high molecular weight range, may have masked the identification of some larger petrogenic PAHs, for example BaP. It is noteworthy that the levels of several high molecular weight petrogenic PAHs, which are well known to be toxic, are at much higher levels in the heavy fuel oil spilled in the HSC spill compared to the light crude released during the DWH oil spill in 2010. As previously mentioned, it is estimated that the HSC heavy fuel oil contained ~100 times more BaP than the crude oil from the

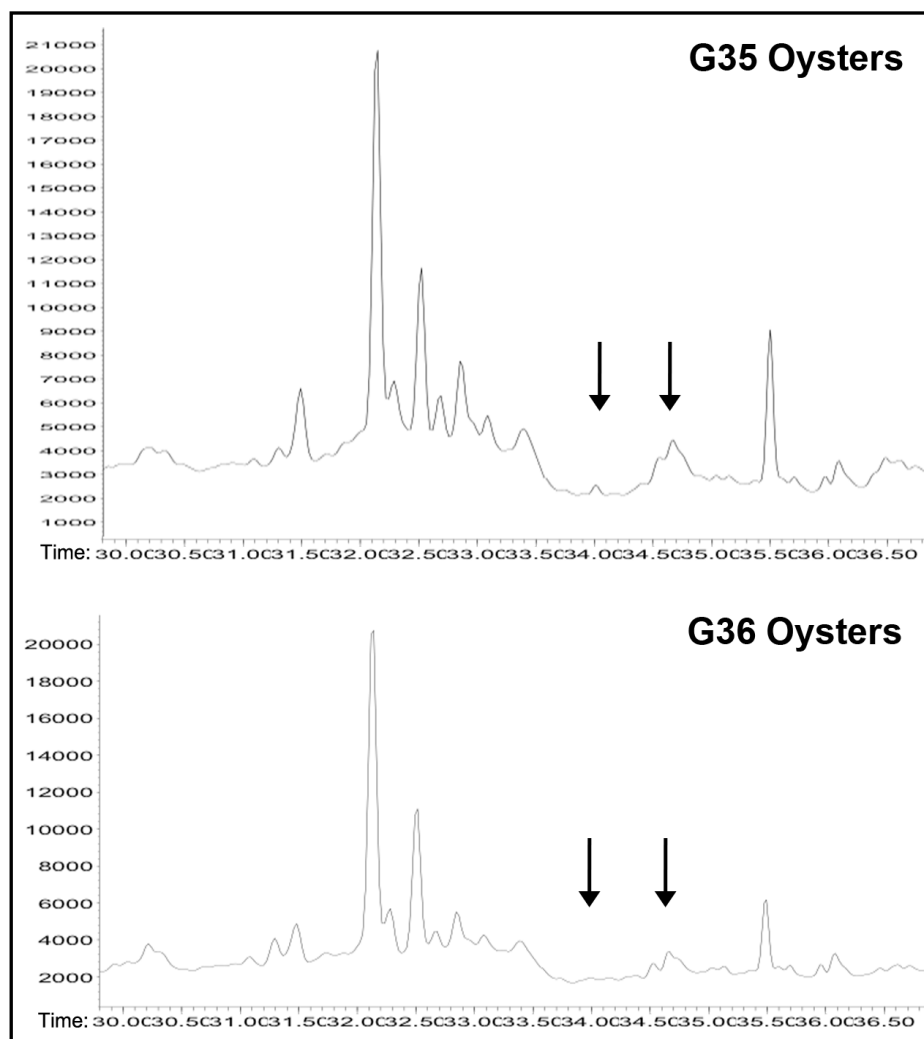


Figure 53: Representative SIM ion chromatograms for G35 and G36 oysters showing selective large ring PAHs.

DWH spill (Yin *et al.*, 2015). As such, we re-examined the G35 and G36 oyster samples via GC-MS to assess differences in the levels of any higher weight PAHs, between the two collection sites, which weren't seen in the initial GC/MS analysis. This subsequent analysis identified higher levels of Benz[a]anthracene (BA)/chrysene (**Figure 51C**) and BaP (**Figure 51D**) in the 5 G35 oysters compared to the 4 G36 oysters (**Figure 53**). Interestingly, BaP exhibits a deep amber-golden color in both pure form, and at various concentrations when dissolved in the acetonitrile used in our study as a vehicle (data not shown). As such, it is possible that while total PAH levels were not largely different between the G35 and G36 oysters (118 ng/g and 160 ng/g, respectively), the stark

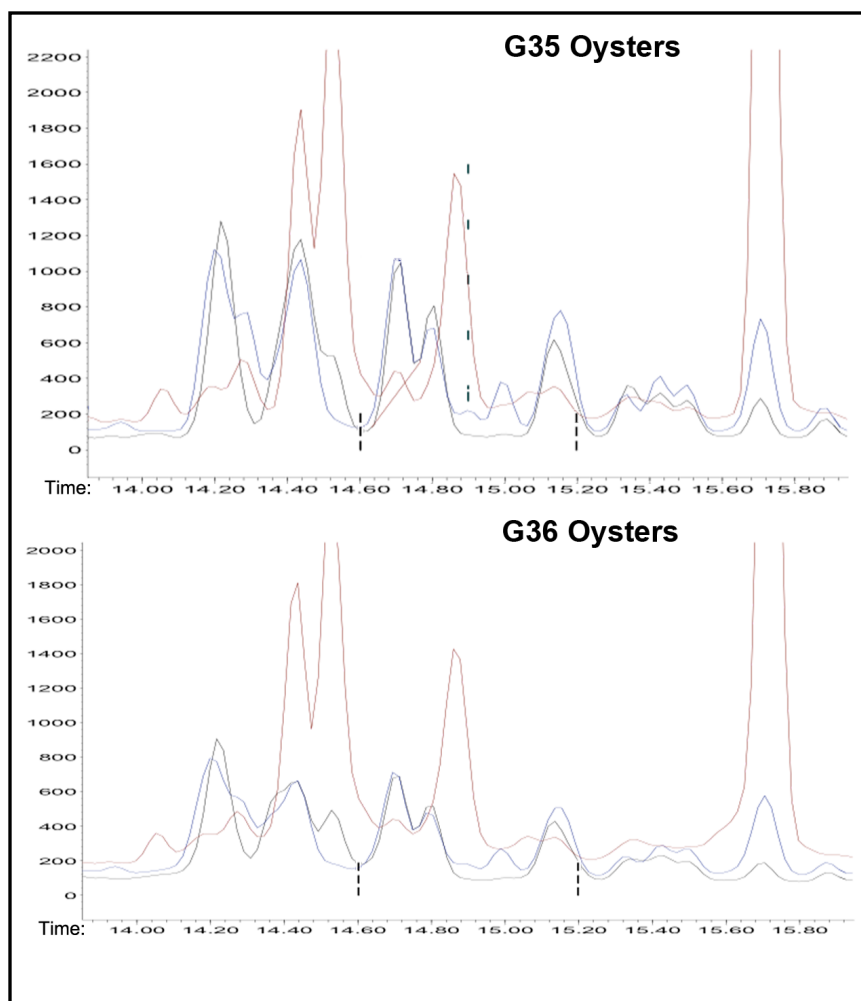


Figure 54: Representative SIM ion chromatograms for G35 and G36 oysters of the C2-naphthalene region.

difference in the color of the two extracts (**Figure 51A**) is due to the presence of BaP and/or BA and chrysene in the G35 samples, which are beyond detection limits in the G36 oysters. It is difficult to say why PAH composition is different between the two sets of samples given that they are the same species, collected on the same day, and differing only by size and the location from which they were collected. It is possible that the oysters collected from the G35 site had recently been exposed to HSC oil, and thus did not have sufficient time to metabolize the BaP, BA, and chrysene from such an exposure. It is also possible that larger oysters metabolize PAHs more readily. As we used the same amount of starting sample (5 grams) for all species when making the PAH extracts, this is not an artifact of having more or less sample used in the extraction process. One can

speculate given that the G35 oysters were somewhat smaller in size than the G36 oysters, that the G35 oysters were younger in age and thus expressed less of the phase I and II metabolic enzymes needed to clear BaP and other high molecular weight petrogenic PAHs present in the HSC oil. However, to our knowledge, there are no studies reporting on the expression levels of phase I and II enzymes in oysters, relative to age. Thus, while it is difficult to say for sure why PAH composition varied between the two collections, future studies should be aware of the possible impact of oyster (and possibly shrimp, crab and finfish) age/size on PAH composition following exposure to petrogenic PAHs, and note that the color of the PAH extracts generated for such samples may be an indicator of PAH contamination as well as the composition of PAHs in the samples.

DISCUSSION

PAHs and Methods of Quantification

As a group, the PAH family of multi-ring aromatic compounds represents a massive number of individual chemical structures. While some of the more common PAHs have been extensively studied to characterize their toxic manifestations in animal models (more commonly for pyrogenic than petrogenic PAHs), it is difficult to speculate on the complete spectrum of toxic effects PAHs may exert in marine organisms exposed to spilled crude oil and humans who consume PAH contaminated seafood (Nebert *et al.*, 2004; Xia *et al.*, 2012; Lee *et al.*, 2013; Martins *et al.*, 2015). This is largely because of the vast number of different PAH compounds and the fact that toxicities (and dose of those toxicities) caused by said PAHs can vary greatly between chemical species. Indeed, the large number of different PAH species and the discovery that many act through a common mechanism (the AhR) was the impetus for the development of the Toxic Equivalency Factor (TEF) approach. This TEF approach to assess PAH toxicity (North Atlantic Treaty Organization, 1988; Nisbet and LaGoy, 1992) was initially implemented in defining the toxicities of polychlorinated dibenzodioxins. The TEF approach employs equivalency factors to convert mathematically amounts (ng) of a certain PAH to a

toxicologically equivalent amount of a well studied reference standard such as BaP or TCDD. As such, this method is based on the same principles underlying the CALUX assay (Garrison *et al.*, 1996; Nagy *et al.*, 2002; Denison and Nagy, 2003; Denison *et al.*, 2004).

Activity of Parent PAHs in the CALUX Assay

The TEF method can be coupled to GC-MS quantifications of PAH levels to develop risk-assessments and exposure limits for an oil-contaminated sample; while this method has its advantages, GC-MS has its limitations as well. For example, the CALUX assay is sensitive to a broad range of chemical compounds that exert toxicities through the AhR. However, our (and often others) GC-MS analyses focus only on 43 PAHs. We analyzed the CALUX activity of several individual petrogenic PAHs, quantified by GC-MS in our study (naphthalene, including C1, and C2, acenaphthene, phenanthrene, fluoranthene, fluorene, and pyrene) and found they had little to no activation in the CALUX bioassay (data not shown). Further, we made ‘artificial’ mixtures mimicking our shrimp and oyster PAH extracts, containing the same amount of naphthalenes (C1 and C2), phenanthrene, fluoroanthene, and pyrene that were present in several shrimp or oyster samples collected for our study, and analyzed these ‘synthetic’ extracts in the CALUX assay. The ‘artificial’ shrimp and oyster mixtures had little to no activity in the CALUX assay, relative to the responses given by PAH extracts obtained from shrimp and oysters (data not shown). Our results suggest that these PAHs are not responsible for the CALUX activity in PAH extracts from our shrimp and oysters, thus we speculate that unidentified chemical compounds present in extracts of the seafood samples must be responsible for the CALUX response. This is not surprising given that crude oil contains 1000’s of different compounds at varying concentrations.

It is noteworthy that even though our data show these standard PAHs do not drive AhR activation *in vitro*, this does not mean the compounds are devoid of toxic effects. It is possible that the PAHs that do not activate the AhR, can synergize the toxic effects of

other PAHs which do activate the AhR, by contributing to metabolic stress following AhR mediated transactivation of phase I and II enzymes (Martins *et al.*, 2015). These results underscore the difficulty of assessing the toxic effects of complex mixtures of PAHs, and suggest that simply quantifying PAH levels by GC-MS fails to account for complex interactions occurring *in vitro* and *in vivo*. Indeed, it is difficult to nearly impossible to quantify all PAH compounds (including oxygenated, conjugated, and alkylated forms of parent compounds), in extracts from the seafood samples we collected, using only GC-MS analyses. The limited potential of GC-MS methods in quantifying large numbers of PAH compounds, and the data describing variability in the toxic manifestations of PAHs when present with myriad other PAH compounds, highlight the value of the CALUX assay in this context. Furthermore, the CALUX approach by its nature removes the need to convert quantities of many different individual PAHs (using TEFs) to toxicologically equivalent amounts of a reference compound (i.e BaP equivalence) to make risk-assessments for exposures. Given the multitude of previous studies showing that PAH toxicities are largely driven through aberrant activation of the AhR- even in cases where a compound doesn't directly activate the AhR, yet causes indirect toxic changes through the AhR, for example to the cellular environment in the presence of AhR trans-activated enzymes- we believe these notions underscore the value of the CALUX assay in assessing PAH contamination in seafood. As such, we feel a more thorough method of assessing PAH contamination in seafood samples involves the use of GC-MS analysis anchored to the CALUX assay, assessing AhR activation by the PAH extracts relative to a standard compound, to complement the GC-MS findings.

We employed the *in vitro* CALUX bioassay, anchored to GC-MS analyses, to assess PAH contamination in Galveston seafood following the 2014 HSC bunker oil spill. The results were compared to past studies assessing PAH levels in Galveston bay seafood, which were completed as part of our U19 GC-HARMS consortium studying the 2010 DWH oil spill. In those studies of samples before the HSC spill, we identified what

we concluded were baseline levels of PAH contamination in Galveston Bay seafood and in other Gulf of Mexico areas as well. Baseline PAH levels were generally higher in Galveston samples than in other areas (Jackson et al. 2015, in preparation). However, based on published seafood consumption values and increased cancer incidence risk-assessment calculations (Rotkin-Ellman *et al.*, 2011; Gohlke *et al.*, 2011; Ylitalo *et al.*, 2012; Dickey, 2012; Wilson *et al.*, 2015), the levels were not high enough to present a general cause for concern to human health (Jackson et al. 2015, in preparation). At the terminus of our initial study, the 2014 HSC spill of bunker oil was the impetus for us to continue collecting Galveston seafood samples to document PAH contamination after the spill. We felt it was especially important to study the spill because we were in the unique position of having already obtained baseline data for PAH levels before the spill; this pre-spill data was, unfortunately, almost universally lacking in studies of PAH contamination after the DWH spill. Over the course of the current study we identified significant increases in PAH contamination immediately following the 2014 HSC spill. The increased PAH levels we identified immediately following the spill decreased slightly over time in some cases; however, for the most part, PAH levels remained significantly higher than pre-spill levels in seafood samples collected as long as one year after the spill. We were surprised by our initial findings in samples collected within two weeks of the spill, as we had not seen CALUX activity that high in previously tested samples (Jackson et al. 2015, in preparation). It is worth noting that in our DWH study the need for protocol approval, funding appropriation, and partnership development limited our ability to immediately begin sample collection. As such, we only had access to a few seafood samples from 2010, immediately after the DWH spill. While we did observe what appeared to be elevated PAH levels in those early samples in the DWH study, the bulk of the samples for that study were collected beginning in August 2011, and it appeared the PAH levels had decreased significantly by that time (Jackson et al. 2015, in preparation).

Elevated PAH Levels in Seafood After the HSC Spill

In the case of the HSC study, PAH levels were immediately elevated in samples collected after the spill, relative to pre-spill samples. This rapid increase was statistically significant for all three species when analyzed with sample collection sites grouped into pre-spill, at-spill (samples collected within 30 days of the spill), and post-spill categories (**Figure 49**). PAH levels were also statistically significantly higher in both oysters and shrimp, when comparing individual collection sites immediately following the spill to pre-spill collection sites (**Figure 50A and B**). This comparison could not be made to assess PAH levels in fin fish samples (comparing specific collection sites after the spill to pre-spill sites) (**Figure 50C**), as the sample sizes for fin fish collection sites after the spill were fewer than the normal 3 to 5 samples collected per site before the spill. Nevertheless, these findings suggest that in general, PAH levels in the seafood samples we collected were elevated as a result of the HSC spill. While PAH levels appeared to trend toward a decrease with time over the course of the study in shrimp and oysters, none of the samples collected within one year of the spill had statistically significant lower PAH levels than the samples within 30 days of the spill (**Figure 49**). We were surprised by the results of this comparison because our previous DWH study found that PAH levels had decreased significantly in the seafood samples by one year after the spill.

Persistence of Elevated PAH Levels in Galveston Seafood After the HSC Spill

The persistence of PAH level elevations in the current study could be a result of several factors. It is noteworthy that the heavy fuel oil spilled during the HSC spill contained significantly higher levels of the toxic high molecular weight PAHs known to cause cancer and activate the AhR, than the light crude spilled during the 2010 DWH spill. Not only are many of those large PAHs resistant to metabolism, many are also highly lipophilic and thus they have long half lives in both the environment and *in vivo*. Indeed, this may explain the persistence of elevated PAH levels over time observed in this study, and not seen in the 2010 DWH study. It is also worth mentioning that the HSC

spill occurred closer to shore than the DWH spill and thus, PAHs and other chemical components of heavy oil had less time to weather. The spill response after the HSC spill also did not involve the use of dispersants, which were heavily applied in the DWH spill response (Yin *et al.*, 2015). It is also worth noting that if any of the bunker oil spilled during the HSC spill sank to the bottom of the bay, it may still be present in some quantity and thus may contribute to continued PAH contamination in Galveston Bay seafood. Given the differences in PAH turnover with time in the HSC spill relative to the DWH spill, continued monitoring of PAH levels in Galveston seafood may lend some insight on how and when PAH contamination in seafood returns to pre-spill levels. Nevertheless, further assessment of PAH levels in Galveston Bay seafood is necessary to more fully assess the extent of PAH contamination and determine what, if any, potential negative human health impacts might be associated with said contamination. Further study of PAHs in Galveston samples will also provide a broader picture of PAH levels in the Galveston bay area, by increasing sample size and including samples from areas other than where our samples were collected (**Figure 48**).

It is important to acknowledge that our study represents a relatively modest sample size, (27 pre-spill samples and 51 during/post-spill samples) representing three separate species (shrimp, oyster, and finfish). While all our samples were assayed in triplicate, the sample number pales in comparison to the >400 samples analyzed for our U19 GC-HARMS consortium study. This small sample number is a result of several factors, including the smaller size of the spill (relative to the DWH spill) and the lack of defined financial resources to assess the HSC spill. As previously mentioned, based on the early findings in our previous study following the DWH spill, we were surprised by the results of the HSC study. However, in retrospect, given that the oil spilled in the HSC spill contained greater quantities of PAHs (and in particular higher molecular weight PAHs known to be toxic) than the DWH spill, and given that the HSC spill occurred in closer proximity to shore than the DWH spill, PAH contamination in Galveston Bay

seafood as a result of the spill isn't entirely unexpected. In light of the small sample size, it is too early to suggest any broad recommendations on limiting seafood consumption until further studies can be completed.

The Value of Pre-spill Data Describing PAH Levels Before a Spill

We feel it is imperative to note that our studies would not have been as meaningful without the availability of pre-spill data describing PAH levels in Galveston Bay seafood before the HSC spill. Pre-spill data describing PAH levels in seafood from other regions of the Gulf of Mexico before the DWH spill were not available in our previous study (Jackson et al. 2015, in preparation). As such, our assessments, which suggested elevated PAH levels immediately following the DWH spill, could not compare PAH contamination levels in the study area before the spill to PAH levels after the DWH spill. Given that we used Galveston seafood samples as an 'unexposed' control for our previous GC-HARMS study, we were in the unique position of having pre-spill data for PAH contamination in Galveston seafood before the HSC spill. Having these pre-spill values for PAH contamination in three different species groups allowed us to determine that PAH levels were significantly increased immediately following, and up to one year after the HSC spill. It is also worth noting the importance of rapidly responding to oil spills from a research standpoint. Ideally, such rapid response to the spill would allow researchers to immediately begin sample collection. These early samples would then provide insight on the immediate effects of environmental releases and contribute to a more full understanding of how quickly contamination accumulates in the surrounding environment.

We believe the findings in the current study underscore the need for further studies to assess PAH levels in seafood from other regions of the Gulf of Mexico and throughout the United States. These studies can help inform risk-assessments and seafood consumption guidelines across the U.S. Furthermore, studies documenting PAH levels in seafood from all areas of the U.S. can provide baseline data on PAH contamination in the

event of future oil spills. Such information will be useful in determining the full extent of ecological and economic impacts of future oil spills by allowing comparisons of PAH levels before and immediately after such environmental releases of crude oil and other PAH containing mixtures. Our findings in this study support the need for such baseline information, and underscore the potential for PAHs to accumulate in seafood species following marine oil spills. Our study also highlights the value of the CALUX assay in assessing such PAH contamination and suggests the CALUX method is a vital complement to GC-MS and other TEF based methods of quantifying PAH contamination in the environment.

Chapter 6: Dissertation Conclusion

INTRODUCTION

As discussed above, recent work in the AhR field has identified a novel signaling pathway for the AhR, dubbed the NC-XRE. In this pathway, the AhR interacts with a novel protein partner, KLF6, to bind a non-consensus DNA motif (the NC-XRE) in novel AhR target gene promoters to regulate gene expression. We have further shown this novel branch of AhR signaling regulated p21^{cip1} gene expression following TCDD treatment and in the absence of an exogenous ligand during liver regeneration. Indeed, we have reported that during liver regeneration in mice lacking functional p21^{cip1} expression in the liver, AhR signaling is dysregulated suggesting that loss of an NC-XRE target gene can have a negative effect on XRE target gene expression (**Figure 12**). All together, these findings, as discussed below, suggest cross-talk between the XRE and NC-XRE pathways, which is vital for proper AhR gene transactivation. Indeed, it is also possible that aberrations in AhR signaling in either pathway could disrupt this cross-talk, contributing to any number of different pathophysiological processes with which aberrant Ah receptor signaling has classically been associated. As such, further characterization of the repertoire of genes the AhR regulates, which we report above, can be used to understand the role of the AhR in a physiological context and ultimately, contribute to novel therapeutic approaches to both preventing and treating the deleterious health conditions associated with the AhR. In this light, the results we report based on our molecular approaches to studying the AhR are complemented by additional studies we have completed assessing environmental sources and levels of PAHs. This work is directly related to the molecular biology of the AhR given that the toxic effects of many halogenated and polycyclic aromatic hydrocarbon carbons are driven through the AhR. We believe the studies *en toto*, reported herein: 1) demonstrate cross-talk between the NC-XRE and XRE signaling pathways of the AhR, and highlight importance of such cross-talk, 2) provide convincing evidence that baseline PAH levels in Gulf seafood

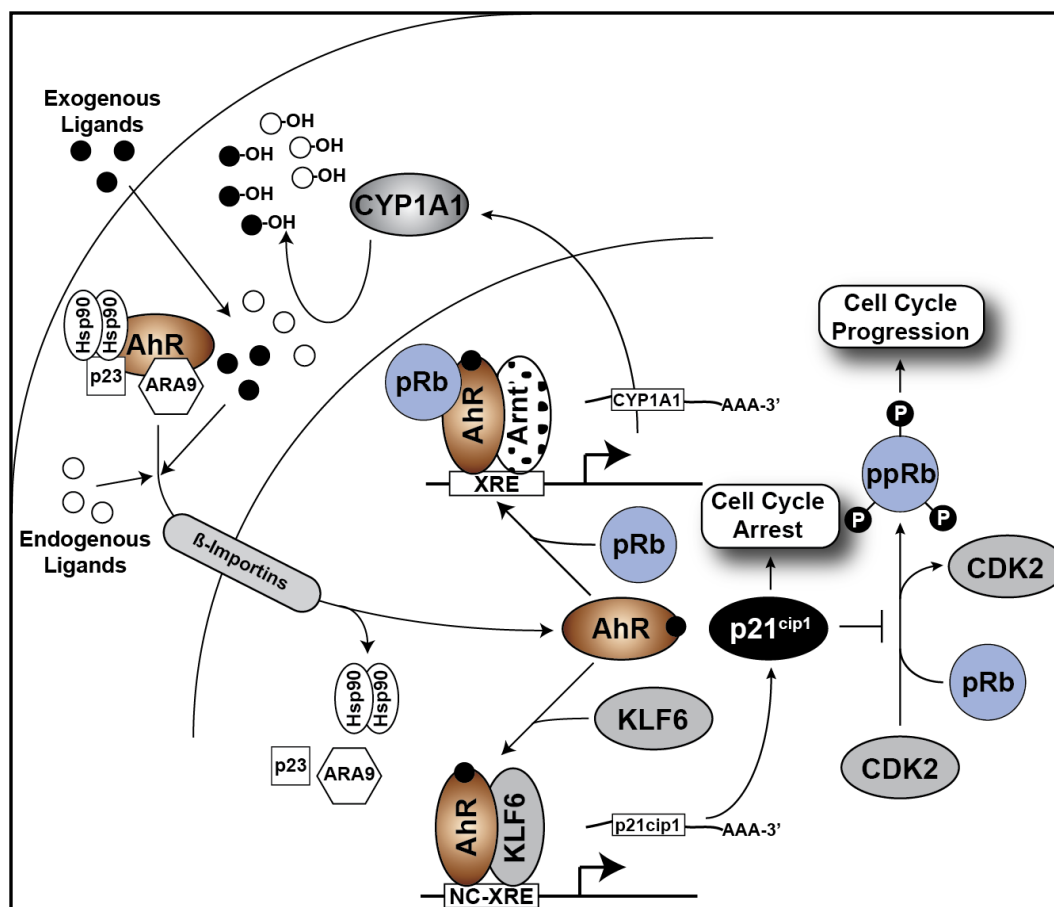


Figure 55: AhR activation and nuclear translocation results in induction of XRE- and NC-XRE-driven target genes. In cycling cells, prolonged activation of the AhR results in enhanced p21^{cip1} expression and inhibition of cyclin-dependent kinase 2 (CDK2) activity, thus preventing pRb inactivation resulting in cell cycle arrest. Induction of CYP1A1—which is enhanced by the AhR interaction with pRb—results in metabolic clearance of receptor ligands and subsequent inactivation of the AhR. This in turn, silences p21^{cip1} expression allowing CDK2 to inactivate pRb by hyperphosphorylation, thus facilitating G₁ phase cell cycle progression. The equilibrium between the XRE and NC-XRE pathways and consequent effects on AhR activity thus influences passage through G₁ phase.

underscore the need for further studies to continue monitoring Gulf seafood as well as to investigate additional environmental sources of PAH contamination, 3) provide a broad (if potentially incomplete) picture of AhR-mediated transcriptional changes in the mouse liver following TCDD treatment, and 4) suggest a need for future studies, using NGS methodologies, of both the physiological and pathological roles of the AhR, in an effort to understand how PAH exposure and deleterious changes to AhR signaling contribute to the myriad negative human health conditions with which the AhR is known to play a role.

Cross-talk between the XRE and NC-XRE pathways

The AhR is known to function in regulating cell cycle progression involving both XRE- and NC-XRE-driven mechanisms (Gottlicher and Wiebel, 1991; Wiebel *et al.*, 1991; Ma and Whitlock, 1996; Jackson *et al.*, 2014). The evidence showing that the AhR and Arnt are necessary for proper AhR mediated cell cycle progression (Elizondo *et al.*, 2000; Shimba *et al.*, 2002), coupled with our finding that AhR-mediated p21^{cip1} expression involves the NC-XRE (Jackson *et al.*, 2014), suggests that the NC-XRE and XRE pathways conspire in their control of G₁-phase cell cycle progression. p21^{cip1} expression decreases CDK2 activity (Harper *et al.*, 1995), leading to decreased CDK2-mediated pRb hyperphosphorylation and inactivation (Giacinti and Giordano, 2006). One downstream consequence of NC-XRE mediated p21^{cip1} induction is the prolonged presence of hypophosphorylated ‘active’ pRb (**Figure 55**). Since this form of pRb interacts with the AhR to facilitate XRE-mediated target gene expression, it is tempting to speculate that the NC-XRE might synergize XRE-driven target gene expression, most notably of Cyp1a1 (Levine-Fridman *et al.*, 2004) (**Figure 12**). Such a scenario predicts that maximal induction of Cyp1a1 would lead to enhanced metabolic clearance of AhR ligands and provide a counter balance to prevent sustained AhR signaling and subsequent deleterious consequences.

In the context of G₁-phase cell cycle progression, the evidence clearly shows that sustained AhR activity in response to TCDD induction results in cell cycle arrest. This occurs because TCDD resists metabolic degradation and thus constitutes a persistent agonist that sustains AhR activity. Why loss of the AhR also leads to prolonged cell doubling time is less clear (Elizondo *et al.*, 2000; Tohkin *et al.*, 2000). One possibility is that the AhR contributes to growth promoting processes during G₁-phase that are lost when the receptor is absent. Indeed there is evidence to support this notion, including recent studies showing AhR induced cell proliferation in cancer cell lines (Xie *et al.*, 2012; Chen *et al.*, 2012) possibly through a mechanism involving the Akt pathway

(Goode *et al.*, 2013; Xu *et al.*, 2014). There is also evidence to suggest that AhR activation up-regulates the proliferative transcription factor c-Myc through an NF- κ B element via the AhR/RelA interaction (Kim *et al.*, 2000). Finally, it is known that AhR activation leads to increased expression of the early response proto-oncogenes *Fos* and *Jun* (Puga *et al.*, 1992; Ashida *et al.*, 2000), possibly through activation of the p38 MAPK pathway (Weiss *et al.*, 2005). The implication is that the AhR regulates both positive and negative growth promoting signals that provide balance to an orchestrated program regulating passage through G₁-phase of the cell cycle while ensuring that entry into S phase does not occur prematurely. The evidence for endogenous AhR activation during liver regeneration following PH—and possibly during cellular proliferation in general—is entirely consistent with that viewpoint. We previously observed in the p21^{cip1} knock out mice, that the absence of p21^{cip1} expression in the regenerating liver also prevented the transient AhR-mediated induction of Cyp1a1 (Jackson *et al.*, 2014) (**Figure 12**). This suggests that the absence of p21^{cip1} hastens G₁-phase pRb inactivation due to enhanced CDK-mediated hyperphosphorylation, which in turn curtails Cyp1a1 induction. This interplay between p21^{cip1} and Cyp1a1 induction further highlights the cross-talk between NC-XRE and XRE driven transcriptional events. Although our findings with the p27^{kip1} knock out mouse model indicated that this CDK inhibitor plays no role in the TCDD-induced growth inhibition during liver regeneration (Jackson *et al.*, 2014), p27^{kip1} is a known AhR target gene in cell lines, suggesting that it may yet play a role in G₁-phase passage *in vivo* under certain conditions (Kolluri *et al.*, 1999; Levine-Fridman *et al.*, 2004; Faust *et al.*, 2013). Our results with the PH model and the proposed signaling pathway (**Figure 55**) predict that liver regeneration would be delayed in liver specific conditional AhR knock out mice subjected to PH. However, these experiments have not been performed to date.

The recent discovery of the NC-XRE and the research showing its role in regulating novel AhR target genes has shed new light on the landscape of AhR-mediated

transcriptional regulation. While our picture of AhR signaling likely remains incomplete, we believe that NC-XRE mediated genes represent a functionally distinct and hitherto uncharacterized class of AhR target genes. This is especially intriguing given transcriptomic studies noted above showing large percentages of TCDD induced AhR target genes lacking known AhR DNA-binding motifs (Puga, *et al.*, 2000; Kinehara *et al.*, 2008; Dere *et al.*, 2011; Lo *et al.*, 2011; Lo and Matthews, 2012). While none of these studies have directly investigated the connection between the AhR and KLF6, a 2011 study by Dere *et al.* found via RegionMiner analysis that KLF6 and ZF9 (another name for KLF6) transcription factor matrices were over-represented in AhR enriched regions at both 2 and 24 hours post TCDD treatment (1.41 and 1.37 fold for KLF6 matrices, 1.78 and 1.74 for ZF9 matrices, respectively) (Dere *et al.*, 2011). Interestingly, they also noted an over-representation of KLF6 binding-sites within 50 base pairs of a XRE at 2 and 24 hours following TCDD treatment (2.36 and 2.87 fold respectively) (Dere *et al.*, 2011). Further, it was noted in a 2012 study using ChIP-Seq that KLF family binding sites are over-represented in AhR/Arnt target genes in MCF-7 cells treated with TCDD, though these results do not specify which KLF family member binding-site is over-represented (supplemental information) (Lo and Matthews, 2012). These are not the only striking commonalities between the KLF6 and AhR fields. Studies assessing the role of KLF6 in cell-cycle progression suggest that KLF6 controls G₁ phase cell cycle progression through a mechanism which affects pRb hyperphosphorylation (Benzeno *et al.*, 2004; Sirach *et al.*, 2007). Specifically, it has been reported that akin to the AhR, loss of KLF6 prolongs cell doubling time (Matsumoto *et al.*, 2006). These studies suggest that while KLF6 up-regulates p21^{cip1} expression in a number of experimental paradigms, like the AhR, KLF6 also plays an important role in driving the G₁/S-phase transition in dividing cells (Benzeno *et al.*, 2004; Sirach *et al.*, 2007; D'Astolfo *et al.*, 2008; Liu *et al.*, 2010). Interestingly, studies have also reported that loss of KLF6 leads to tumor promotion following chronic diethylnitrosoamine (DEN) exposure, with increases in hepatocellular

carcinoma and these tumors mirroring the gene signatures of highly aggressive human hepatocellular carcinoma (Tarocchi *et al.*, 2011; Vetter *et al.*, 2012). Tumor promotion following DEN treatment has also been shown for the AhR in combination with various exogenous ligands (Poland *et al.*, 1982; Davis *et al.*, 2000; Kennedy *et al.*, 2014). Further, KLF6 has recently been suggested to function in T-cell activation (Palau *et al.*, 2013) and in NF- κ B signaling via p65-dependent transcription (Li *et al.*, 2014); the AhR has also been implicated in T-cell activation (Prigent *et al.*, 2014) and in NF- κ B signaling with p65 (Vogel *et al.*, 2014). Moreover, while total knock-out of the AhR in mice is not lethal, it does result in significantly decreased litter sizes, whereas total KLF6 knock-out mice are embryonic lethals. Furthermore, the livers in AhR^{-/-} and KLF6^{+/-} mice exhibit phenotypic commonalities (Fernandez-Salguero *et al.*, 1995; Schmidt *et al.*, 1996; Matsumoto *et al.*, 2006; Narla *et al.*, 2007). These examples serve to highlight the parallels that exist between AhR and KLF6 action, consistent with their role as a transcriptional complex. They underscore mounting evidence as well as the studies described above, to suggest that characterization of the NC-XRE pathway and anchoring AhR induced gene expression changes (identified via RNA-sequencing) to ChIP-sequencing studies (identifying functional AhR DNA-binding throughout the genome) will provide great insight on Ah receptor function and the importance of this large signaling pathway in normal physiological processes.

Environmental PAH contamination in Gulf of Mexico seafood

Through our work assessing PAH contamination in seafood following two recent oil spills, we have identified what we believe are baseline levels of PAHs in Gulf seafood. Our data suggests that PAHs are present in the Gulf, even in the absence of major oil spills. While these levels are likely not high enough to represent a cause for concern for most seafood consumers, our findings underscore the need for further work characterizing environmental sources of PAH exposure and the amount of PAHs present in those sources. This is especially important given the myriad toxicities and deleterious human

health conditions associated with aberrant AhR signaling and PAH exposure. Such health conditions include developmental abnormalities, nutritional and metabolic diseases, liver fibrosis, and cancer. Indeed, recent studies have reported evidence of a link between environmental exposures and both immune diseases and neurodegenerative diseases (Esser, 2012), suggesting (among other contaminants) persistent chemicals like pyrethroids and carbamate pesticides may contribute to the pathophysiology of several autoimmune and neurodegenerative diseases. As such, identifying environmental sources and quantification of PAH levels can inform risk-assessments and exposure limits for these compounds, ultimately facilitating the prevention of PAH and AhR associated human health conditions.

RNA-sequencing identification of AhR target genes

We have reported above on our studies assessing AhR-mediated gene expression changes following TCDD treatment, in an effort to identify the complete repertoire of AhR target genes. We also discussed several interesting novel potential AhR target genes identified in these studies, given the known function of said genes and the similarities between those gene functions and historical studies of the AhR and AhR ligands. Furthermore, while we have not yet anchored our transcriptomic studies to ChIP-sequencing studies identifying genome wide AhR DNA-binding, we were able to make some comparisons between our results and the results of a 2012 AhR ChIP-sequencing study in a breast cancer cell line (Lo and Matthews, 2012). Based on these comparisons and a basic *in silico* search for XRE and NC-XRE DNA-motifs in the promoters of several potential AhR target genes from our results, there is evidence to suggest functional AhR DNA-binding in close proximity to the genes we identified. Indeed, these interesting correlations underscore the need for future work to anchor transcriptomic studies of the AhR (in several different experimental paradigms) to ChIP-sequencing studies of the AhR and its protein partners in the XRE and NC-XRE pathways, Arnt and KLF6, respectively. Nevertheless, a broad spectrum analysis of our results using IPA

shows the significant gene expression changes in our dataset are consistent with historical studies of the AhR and PAHs, which implicate the AhR in modifying gene expression consistent with roles in driving carcinogenesis, nutritional and metabolic diseases, liver dysfunction, cardiac toxicity, immune disease, and neurological disease. While more work is indeed necessary to understand these results, our findings underscore the notion that environmental health studies identifying human health relevant sources of PAH exposure will contribute to the prevention of many PAH and AhR induced health conditions. Likewise, a more full understanding of AhR-mediated gene expression changes and AhR signaling will complement the environmental health studies and contribute to prevention or novel therapeutic approaches for treating AhR induced pathophysiologies like neurodegenerative diseases, cancer, and immune disease.

CONCLUSIONS

Given that almost four decades of research in the AhR field has yet to identify the precise role of the AhR in TCDD toxicity, it is our contention that a greater emphasis on the AhR/KLF6 complex bound to NC-XRE sites will fill some of the existing gaps in understanding as it relates to TCDD toxicity and AhR action in general. Accordingly, the identification of the AhR/KLF6 complex and NC-XRE recognition site constitute a paradigm shift in AhR biology. Future studies focused on this novel complex should be considered a research priority, and hold promise to reward the field with unanticipated discoveries that have eluded the field to date. While we have clearly demonstrated the role of the NC-XRE in the regulation of several genes using CHIP—and we have identified a host of new potential AhR target genes using RNA-sequencing—future studies should leverage the considerable power of the ‘omics’ approaches to characterize the NC-XRE pathway at the genomic, transcriptomic, and proteomic levels. Such an approach can determine the extent to which novel gene regulation through the NC-XRE—and conceivably hitherto unknown AhR DNA-binding motifs—is involved in the well-known but poorly understood functions of the AhR. These technologies can be employed

to address old questions about AhR function, like the proliferative role of the AhR in the G₁/S transition or the pathophysiologies of TCDD induced wasting syndrome. The recent observations in the studies that examined the NC-XRE also highlighted the cross-talk that exists between NC-XRE- and XRE-driven AhR target genes to regulate complex signaling pathways. This interplay is clearly exemplified by the cell cycle control studies, but it is likely that similar observations will be made for the repertoire of genes involved in other signaling cascades regulated by the AhR.

FUTURE DIRECTIONS

Future experiments for this project should focus on transcriptomics and genomics. The two major focuses, in particular, should be to perform ChIP-Sequencing on the AhR and KLF6 to anchor the transcriptomics data from chapter 3 to functional DNA-binding by the AhR and KLF6. The other major focus for this project should be performing RNA-sequencing on Arnt conditional knock-out mouse livers treated with vehicle or TCDD, to identify TCDD induced gene expression changes in this paradigm, that occur in the absence of Arnt. Significant TCDD induced gene expression changes that occur in the absence of Arnt, and the presence of the AhR, would suggest those changes are mediated by the AhR/KLF6 interaction and thus, are NC-XRE mediated changes. A significant focus should also be a thorough characterization of the NC-XRE DNA motif, and this could be elucidated as a part of the ChIP-Sequencing experiments suggested above. Finally, given that the NC-XRE motif in the Pai-1 gene promoter resembles a DNA sequence capable of forming a G-quadruplex, future work should investigate the possibility for higher order DNA structures, forming at NC-XRE regulated gene promoters, to be involved in the processes which regulate NC-XRE-mediated gene expression. Given the link between G-quadruplexes and their importance in G₁/S-transition and DNA replication in S-phase, it is possible that these DNA-structures may represent a novel role for the AhR in controlling cell cycle progression.

Appendices

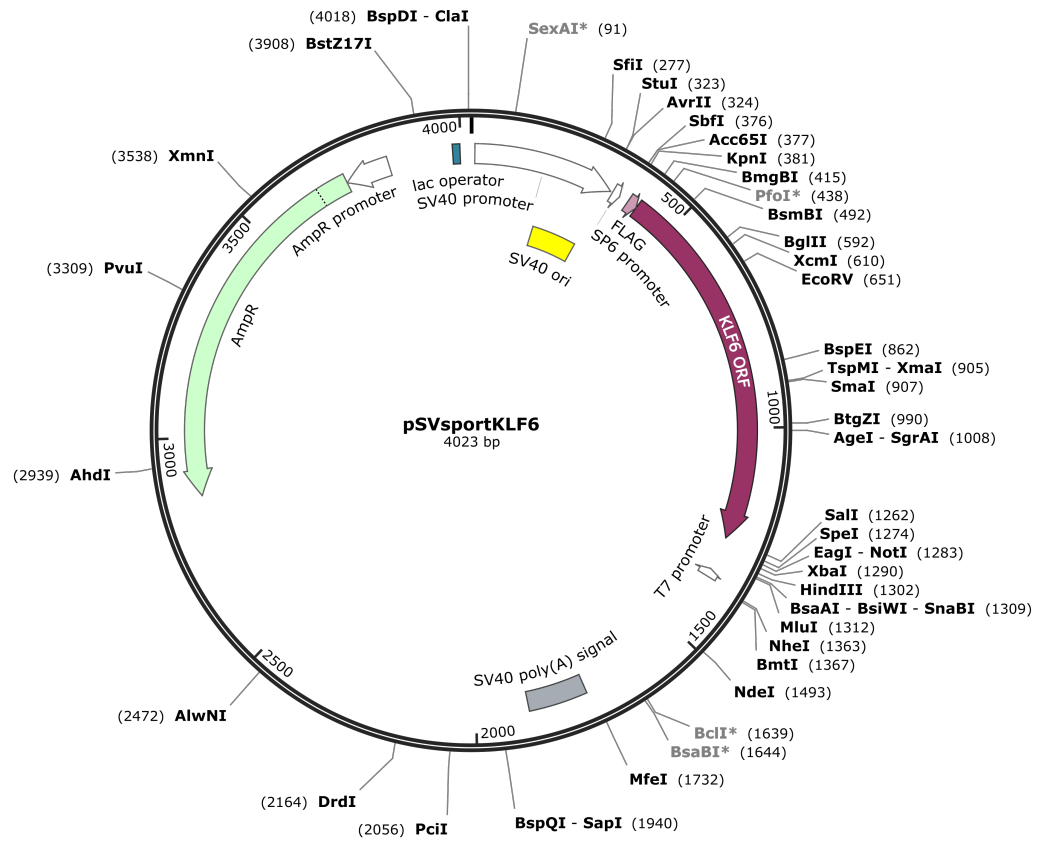
Appendix I: Primers

Application	Primer Name	Sequence (5'-3')	Amplicon (bp)
ChIP qPCR	Cdkn1a Forward	GTGACAAGAGAATAGCCCAGGTG	139
ChIP qPCR	Cdkn1a Reverse	CCACTCCTTCACCGATCCC	***
ChIP qPCR	Cyp1a1 #1 Forward	CAGGAGAGCTGGCCCTTTAAG	135
ChIP qPCR	Cyp1a1 #1 Reverse	GTTGCGTGAGAAGAGCCTGG	***
ChIP qPCR	Cyp1a1 #2 Forward	AGCAGGCTTACGCACGCTAG	121
ChIP qPCR	Cyp1a1 #2 Reverse	GTATGGTGGAGGAAAGGGTGG	***
ChIP qPCR	Pai-1 Forward	GTCCCAGCAAGTCACTGGGAGG	234
ChIP qPCR	Pai-1 Reverse	CTGGAGGCGGGTGTGCGGCG	***
ChIP qPCR	Cyp1a1 550 Forward	AGTGCTCTTTTGTACTATGCCTGTC	91
ChIP qPCR	Cyp1a1 550 Reverse	ATACTCCTTTGACGAAGCTTACCC	***
ChIP qPCR	Cyp1a1 1100 Forward	GACAGAAAGGATTTCACATTCTGAGAG	103
ChIP qPCR	Cyp1a1 1100 Reverse	CAGACCCCTATTGATCCCCAG	***
ChIP Semiquant. PCR	CDH1 Forward	GGGTCAGAGCACAGCTAGG	220
ChIP Semiquant. PCR	CDH1 Reverse	TGGGAACTCAGTAGTGCGCC	***
ChIP Semiquant. PCR	Cyp1a1 ChIP Forward	CTATCTCTTAAACCCACCCCAA	350
ChIP Semiquant. PCR	Cyp1a1 ChIP Reverse	CTAAGTATGGTGGAGGAAAGGGTG	***
ChIP Semiquant. PCR	p21 ChIP Forward	GCTGGGCAGCCAGGAGCCTG	269
ChIP Semiquant. PCR	p21 ChIP Reverse	CTGCTCACACCTCAGCTGGC	***
ChIP Semiquant. PCR	Pai-1 ChIP Forward	GTCCCAGCAAGTCACTGGGAGG	234
ChIP Semiquant. PCR	Pai-1 ChIP Reverse	CTGGAGGCGGGTGTGCGGCG	***
SYBR qPCR	Cyp1a1 Forward	GCCTAACTCTCCCTGGATGC	132
SYBR qPCR	Cyp1a1 Reverse	TCAATGAGGCTGTCTGTGATGTC	***
SYBR qPCR	Pai-1 Forward	GGTCAGGATCGAGGTAAACGAG	101
SYBR qPCR	Pai-1 Reverse	ATCGGTCTATAACCATCTCCGTG	***
SYBR qPCR	p21 Forward	TGTCTTGCACTCTGGTGTCTGAG	119
SYBR qPCR	p21 Reverse	CAATCTGCGCTTGGAGTGATAG	***
SYBR qPCR	p27 Forward	TCCAGGGATGAGGAAGCG	113
SYBR qPCR	p27 Reverse	CTCCACAGTGCCAGCGTTC	***
SYBR qPCR	Dact2 Forward	AGGCCTTGATAGTGACAGCAG	95
SYBR qPCR	Dact2 Reverse	GCAAACAGATGCGCAGGAG	***
SYBR qPCR	Ier3 Forward	GTGTCCACCGCGCGTT	137
SYBR qPCR	Ier3 Reverse	GCGAACAGGAGAAAGAGGACC	***
SYBR qPCR	Maff Forward	TGGATCCCTTATCTAGCAAAGCC	100
SYBR qPCR	Maff Reverse	TCGCGCACCGACAGC	***

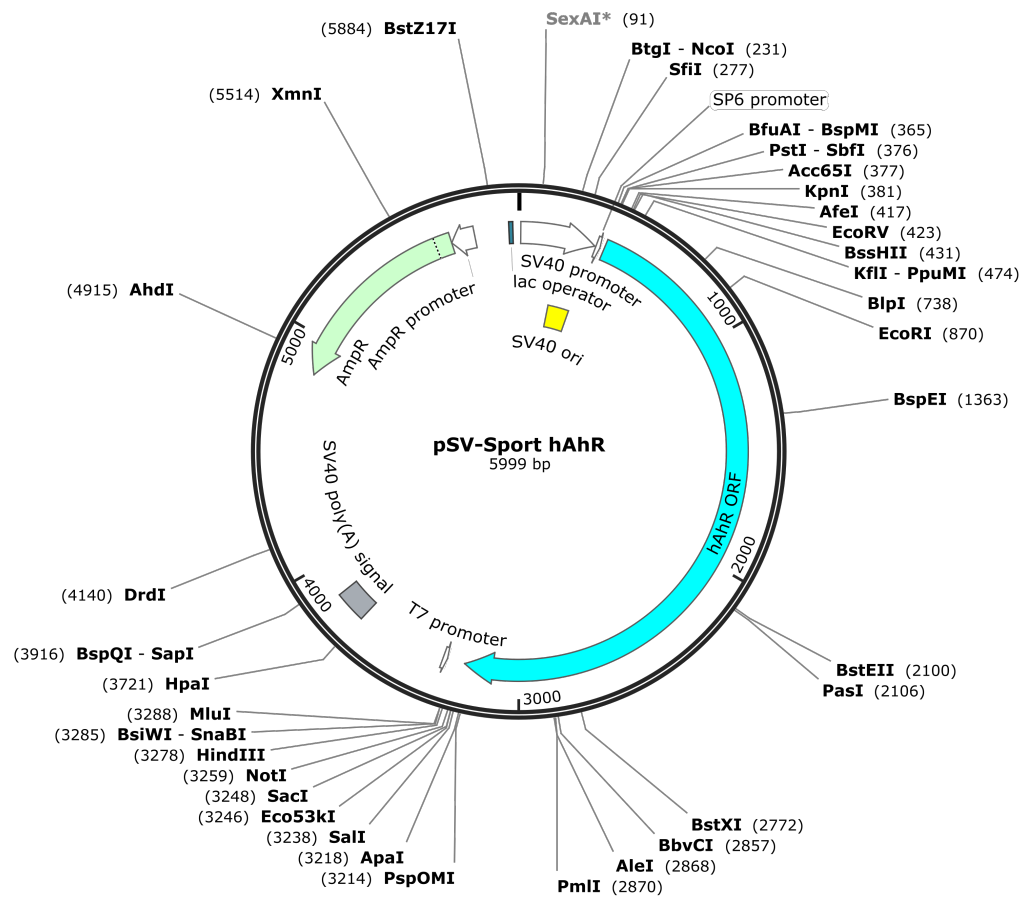
Appendix I (continued)

Application	Primer Name	Sequence (5'-3')	Amplicon (bp)
SYBR qPCR	Sult1e1 Forward	TTATACAATGATGCCAGAGGAAATG	103
SYBR qPCR	Sult1e1 Reverse	CCTCAGGGCTTCTGGGAAG	***
SYBR qPCR	Sult2a1 Forward	ATGGTTCCTCAAAGGAAATGTTCTA	90
SYBR qPCR	Sult2a1 Reverse	ACCAAAAAGTTGTCCCATTCTCTC	***
SYBR qPCR	Usp2 Forward	CCGGTTACAGGCGAATGG	133
SYBR qPCR	Usp2 Reverse	CTCAATGCTACATACGGGAGGG	***
semi-quantitative PCR	p21 Variant 1 Forward	AGCAGCCGAGAGGTGTGAGC	248
semi-quantitative PCR	p21 Variant 1 Reverse	ACCAGAGTGCAAGACAGCGACAAG	***
semi-quantitative PCR	p21 Variant 2 Forward	GGAGCATGAATGGAGACAGAGACC	150
semi-quantitative PCR	p21 Variant 2 Reverse	ACCAGAGTGCAAGACAGCGACAAG	***
semi-quantitative PCR	KLF6 excision 1 Forward	GGATGTGCTCCCAATGTGTA	full = 861
semi-quantitative PCR	KLF6 excision 1 Reverse	CTGCTCCTTCAGAGGTGCCT	excised = 151
semi-quantitative PCR	KLF6 excision 2 Forward	TGTCTTTTCCAACCCGACAT	full = 880
semi-quantitative PCR	KLF6 excision 2 Reverse	CCTCTGCTCCTTCAGAGGTG	excised = 200
EMSA	XRE EMSA Forward	GATCTGAGCTCGGAGTTGCGTGAGAA GAGCCG	
EMSA	XRE EMSA Reverse	GATCCGGCTCTTCTCACGCAACTCCG AGCTCA	
EMSA	NC-XRE EMSA Forward	GTCCCAGCAAGTCACTGGGAGGGAG GGAGGGAGGGGGG	
EMSA	NC-XRE EMSA Reverse	CTCCCCCCCCTCCCTCCCTCCCTCCC AGTGACTTGCTG	
PCR Deletion Mutagenesis	Delta C Forward	CCCTTTTCCTGCCATAATGTAACCCTTA CCTAAGGACT	
PCR Deletion Mutagenesis	Delta C Reverse	AGTCCTTAGTGGTAAGGGTTACATTAT GGCAGGAAAAGGG	
PCR Deletion Mutagenesis	Delta D Forward	GAAAACAACTTTTTCAACGAATCTATGT AAGAATGCAGAAATTGGCAAGATAATA CT	
PCR Deletion Mutagenesis	Delta D Reverse	AGTATTATCTTGCCAATTTCTGCATTCT TACATAGATTGTTGAAAAAGTTGTTTT C	
PCR Deletion Mutagenesis	Delta E Forward	CTCCCTTCATACCTTCAGATTATTAACA GCAACAGTCCTT	
PCR Deletion Mutagenesis	Delta E Reverse	AAGGACTGTTGCTGTTAATAATCTGAA GGTATGAAGGGAG	

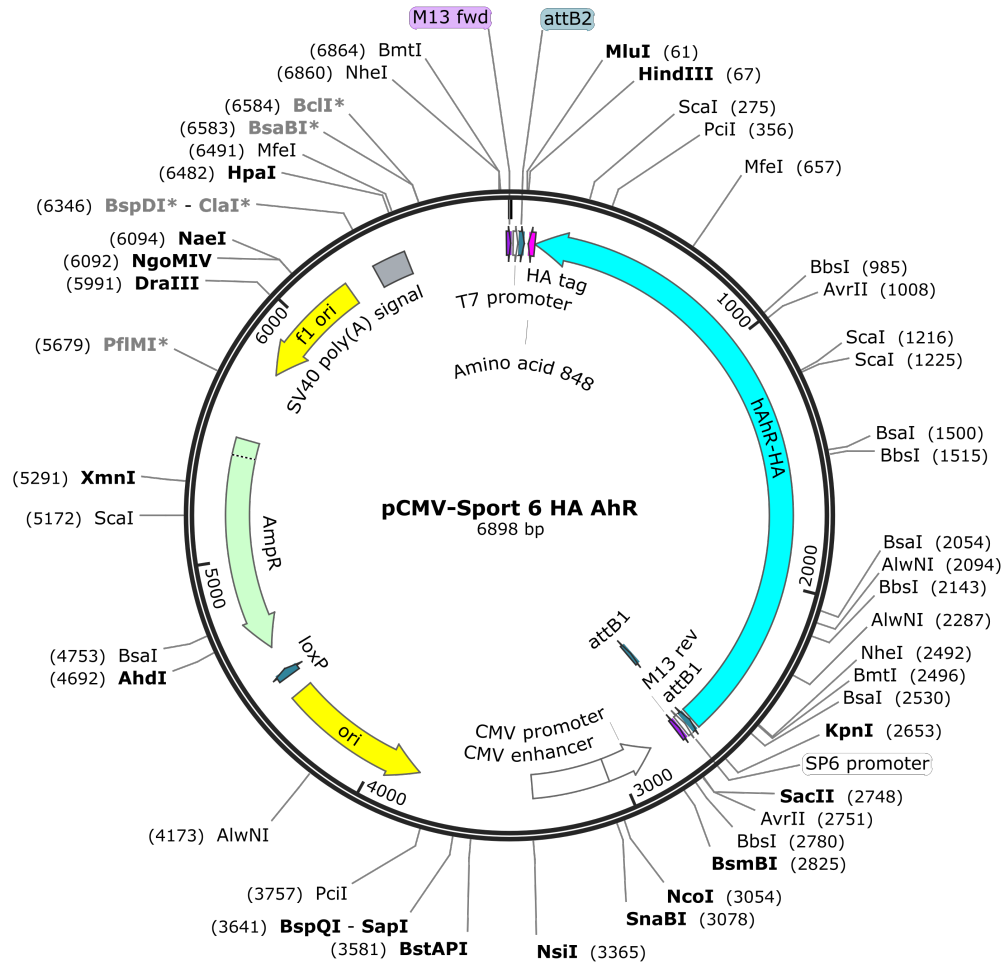
Appendix II: KLF6 and AhR Vector maps



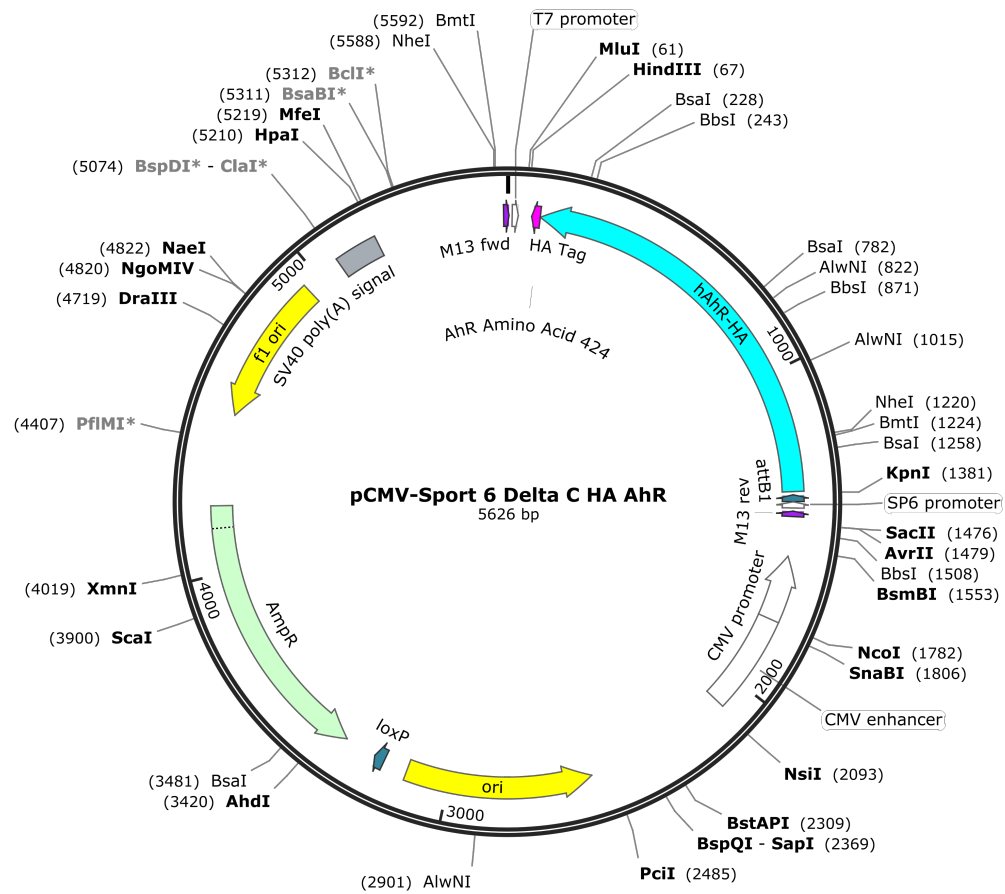
Appendix II (continued)



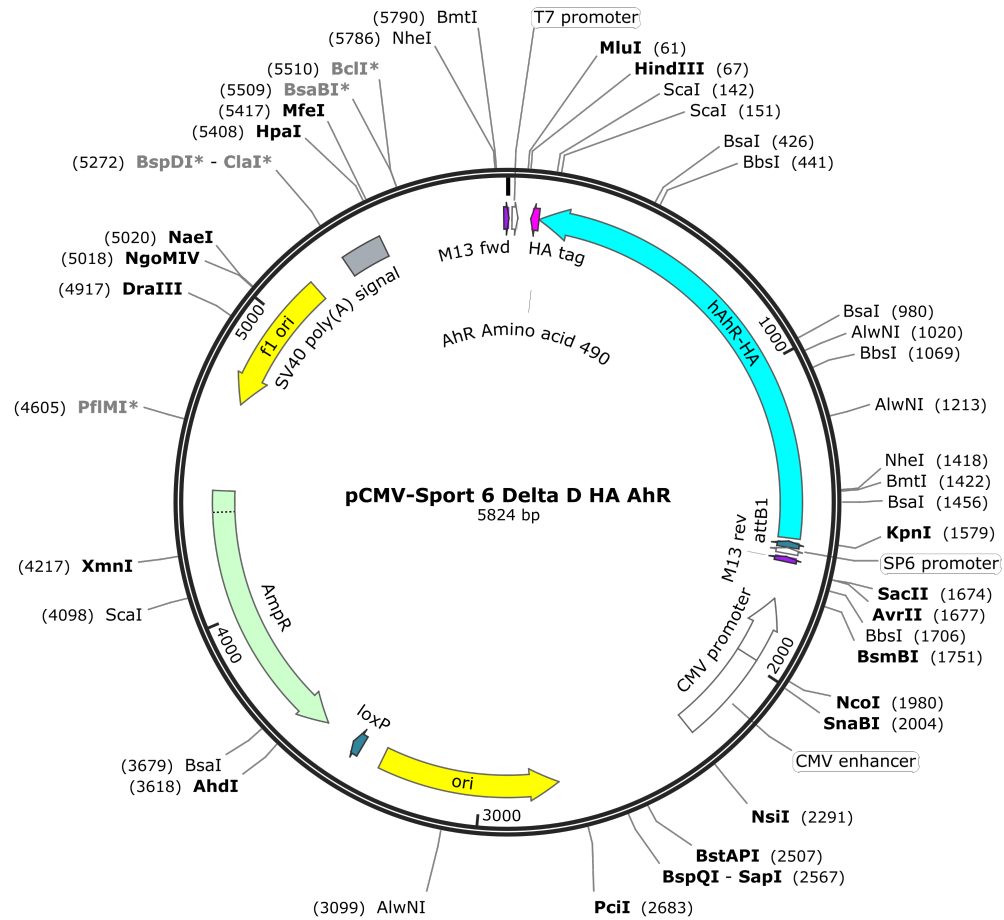
Appendix II (continued)



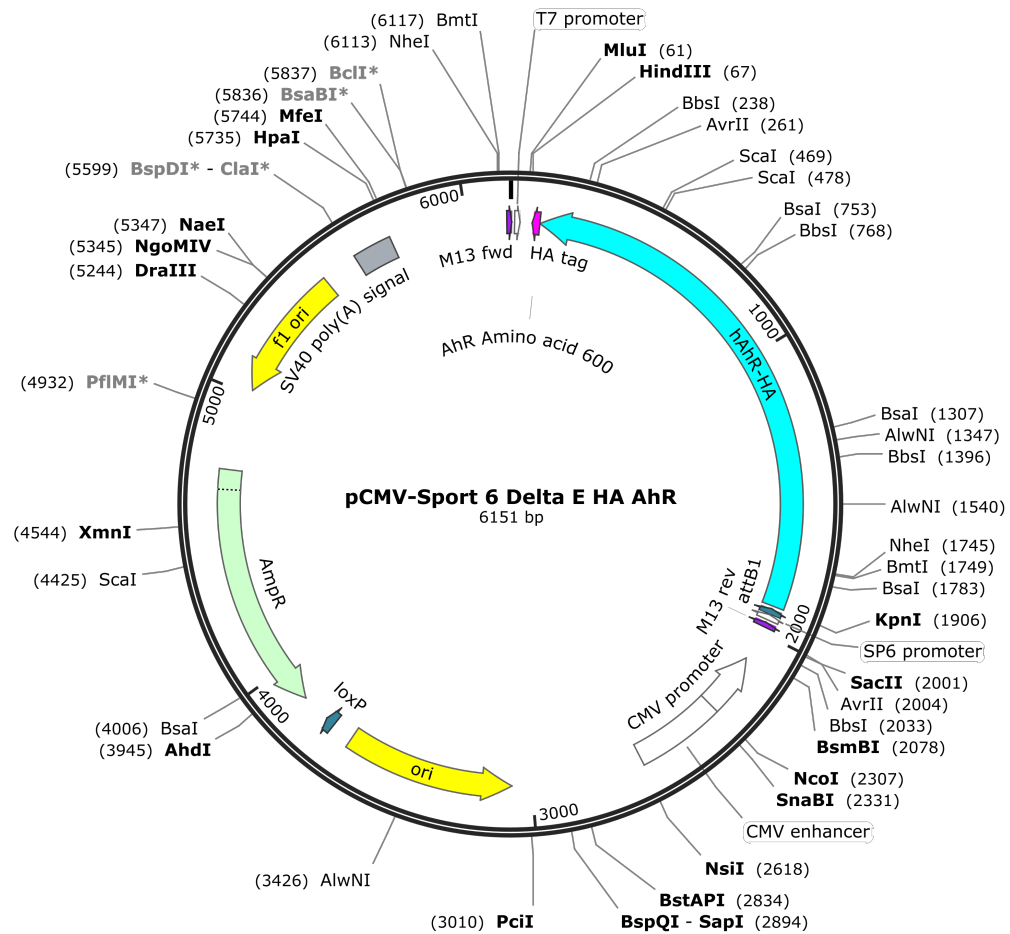
Appendix II (continued)



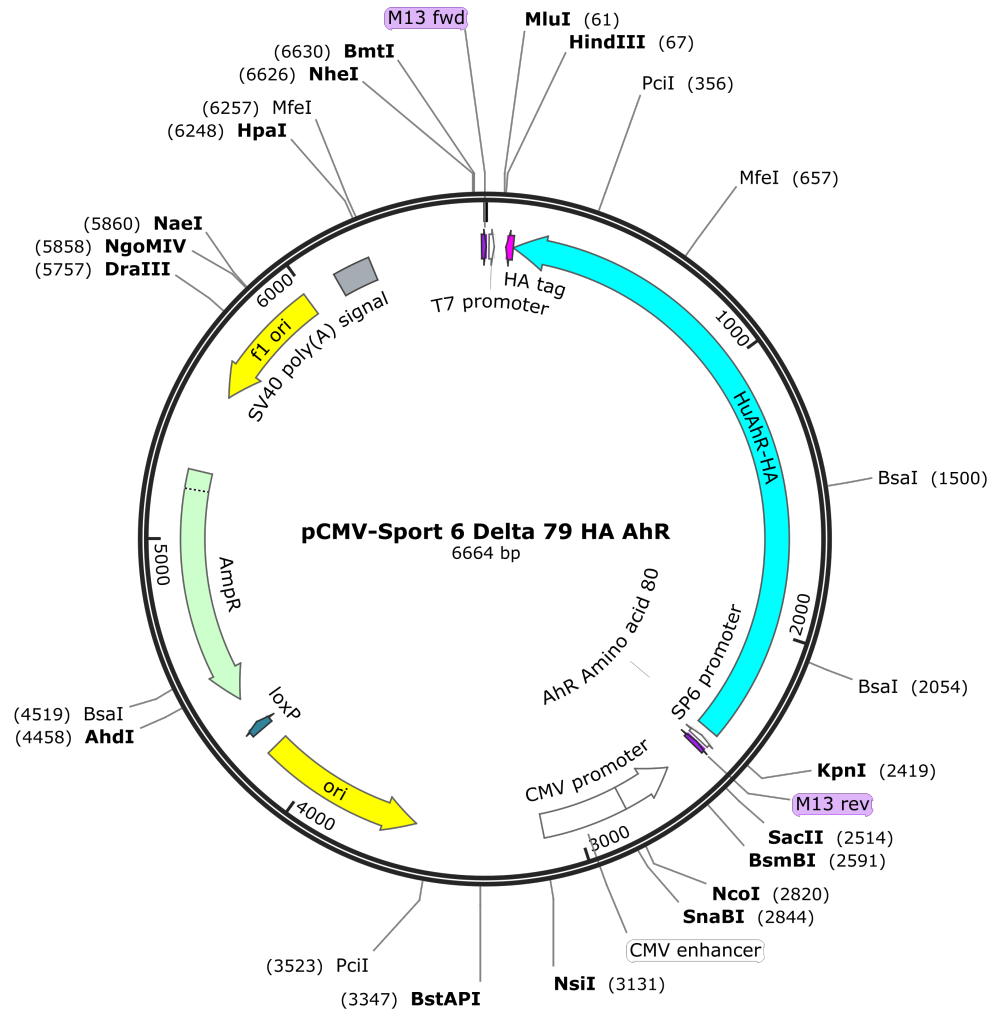
Appendix II (continued)



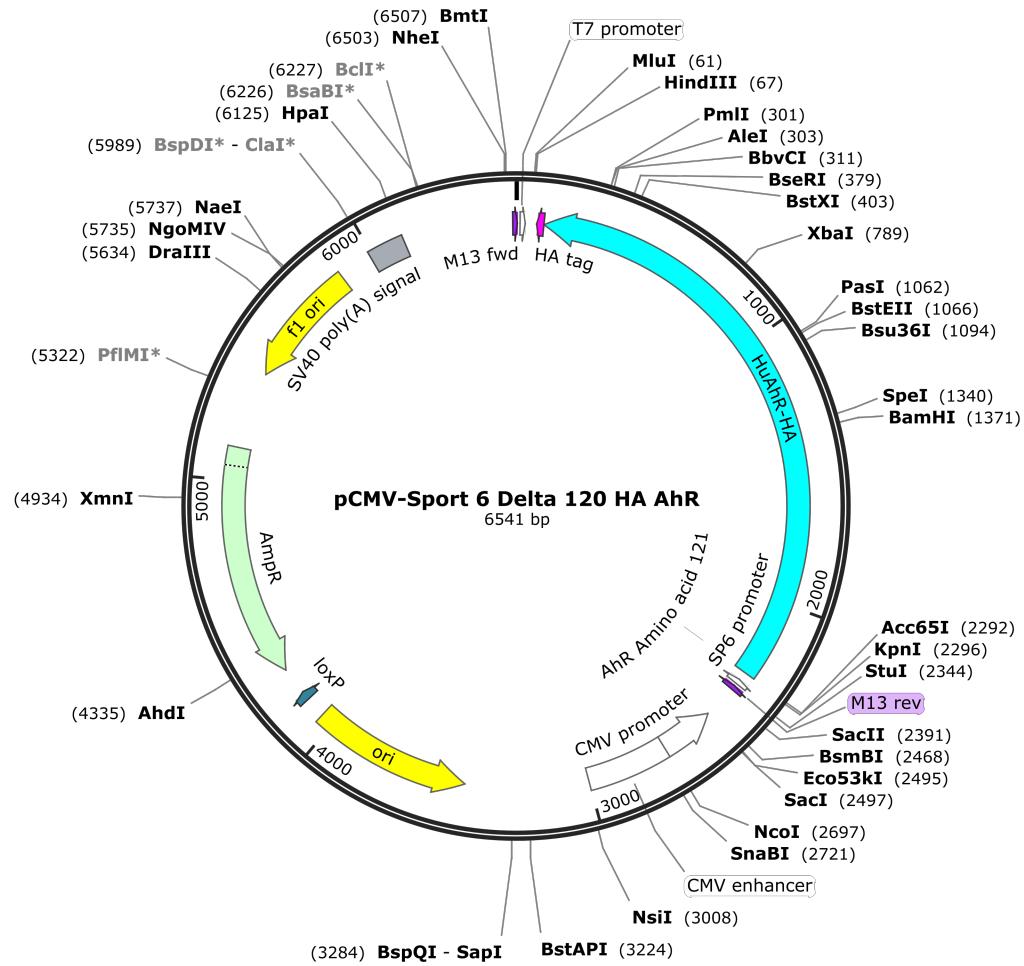
Appendix II (continued)



Appendix II (continued)



Appendix II (continued)



Appendix III: Significant Gene Expression Changes in Wild-type Mice at 2 Hours

gene_id	WT_TCDD	WT_Veh	log2(fold_change)	q_value
Cyp1a1	224.692	0.643	-8.448	0.00408383
Serpine1	49.457	1.194	-5.372	0.00408383
Tiparp	45.537	2.818	-4.014	0.00408383
Maff	44.871	4.479	-3.325	0.00408383
Ccno	8.026	0.901	-3.155	0.00408383
Gadd45g	456.783	60.025	-2.928	0.00408383
Igfbp1	1004.390	136.189	-2.883	0.00408383
Tnfaip8l3	1.882	0.295	-2.675	0.00408383
Ier3	6.304	1.041	-2.599	0.00408383
Gadd45b	57.429	9.877	-2.540	0.00408383
Sebox	2.507	0.461	-2.442	0.00408383
Cyp1a2	1826.110	336.506	-2.440	0.00408383
Tchh	0.441	0.084	-2.394	0.00408383
Gm129	3.310	0.729	-2.182	0.00408383
Hilpda	27.121	6.194	-2.130	0.00408383
Hspa2	5.292	1.229	-2.106	0.00408383
Cib3	3.444	0.825	-2.062	0.0165264
Usp2	6.506	1.701	-1.936	0.00408383
Zfp36l1	317.186	82.997	-1.934	0.00408383
Edc3	15.038	4.041	-1.896	0.00408383
BC057022	23.275	0.892	-1.876	0.00408383
Pim3	228.778	62.482	-1.872	0.00408383
Notch1	9.827	2.710	-1.858	0.00408383
Mafb	60.997	16.903	-1.851	0.00408383
Zfp941	0.943	0.267	-1.820	0.00408383
Hjurp	11.674	3.481	-1.746	0.00408383
Cyp1b1	0.769	0.232	-1.726	0.00408383
Bmf	4.461	1.397	-1.675	0.00408383
Lipg	15.509	4.893	-1.664	0.00408383
Tat	1589.930	507.044	-1.649	0.00408383
Pmm1	8.732	2.785	-1.649	0.00408383
Sgk1	18.884	6.081	-1.635	0.00408383
Jun	39.615	12.823	-1.627	0.00408383
Cdkn1a	78.694	26.408	-1.575	0.00408383
Ddit4	15.143	5.141	-1.559	0.00408383
Ccrn4l	20.115	6.845	-1.555	0.00408383
Sphk1	0.714	0.245	-1.541	0.035699
Hmgb2	3.954	1.368	-1.531	0.00408383
Acpp	4.205	1.461	-1.525	0.00408383
Fos	14.340	5.002	-1.520	0.00408383
Btg2	23.713	8.327	-1.510	0.00408383
Nfe2l2	99.876	35.706	-1.484	0.00408383

Appendix III (continued)

Cebpb	283.388	102.602	-1.466	0.00408383
Junb	154.643	56.161	-1.461	0.00408383
Tmem100	1.195	0.437	-1.451	0.0137082
Srrm4	6.970	2.569	-1.440	0.00408383
Ppp1r15a	10.600	3.962	-1.420	0.00408383
Slc38a2	98.347	37.860	-1.377	0.00408383
Atf3	3.040	1.180	-1.365	0.00408383
Socs3	30.759	12.038	-1.353	0.00408383
Lcn2	68.996	27.395	-1.333	0.00408383
Lpin1	87.183	35.498	-1.296	0.00408383
Itprp	0.672	0.275	-1.291	0.0218495
Egr1	73.139	30.197	-1.276	0.00408383
Adcy1	0.763	0.318	-1.262	0.00762098
Sap30	6.178	2.578	-1.261	0.00408383
Adrb2	2.191	0.925	-1.244	0.0218495
Wipf3	5.476	2.322	-1.237	0.00408383
Lrp4	6.521	2.794	-1.223	0.00408383
Foxo3	5.846	2.514	-1.218	0.00408383
Slc46a3	21.103	9.225	-1.194	0.00408383
Zfp36	244.985	108.604	-1.174	0.00408383
Atoh8	28.613	12.853	-1.155	0.00408383
1810011O10	64.738	29.146	-1.151	0.00408383
G6pc	284.316	128.027	-1.151	0.00408383
Fbxw9	21.749	9.806	-1.149	0.00408383
Dclk3	5.135	2.324	-1.144	0.00408383
Dusp1	45.014	20.39	-1.143	0.00408383
Akap5	0.410	0.186	-1.142	0.0335815
Fzd7	10.285	4.712	-1.126	0.00408383
Ripk4	3.317	1.527	-1.119	0.00408383
Cldn14	34.002	15.68	-1.117	0.00408383
Bcl2l11	2.859	1.32	-1.109	0.00408383
Sds	559.192	260.9	-1.100	0.00408383
Rasgef1b	9.988	4.686	-1.092	0.00408383
Lpin2	102.069	49.17	-1.054	0.00408383
Per2	3.882	1.880	-1.046	0.00408383
Gdf15	49.083	23.95	-1.035	0.00408383
Gcc1	8.599	4.198	-1.034	0.00408383
Slc20a1	24.051	11.838	-1.023	0.00408383
Pfkfb3	3.141	1.555	-1.015	0.00408383
Mt2	4048.770	2026.680	-0.998	0.00408383
Acer2	5.204	2.628	-0.986	0.00408383
Csrnp1	5.308	2.701	-0.975	0.00408383

Appendix III (continued)

Tmem101	10.078	5.144	-0.970	0.00408383
Hes1	29.538	15.286	-0.950	0.00408383
Tnfrsf1b	12.232	6.393	-0.936	0.00408383
Tsc22d3	95.698	50.187	-0.931	0.00408383
Nr0b2	92.714	49.147	-0.916	0.00408383
Nfkbiz	9.938	5.303	-0.906	0.00408383
Sdc4	417.968	223.494	-0.903	0.0191513
Trib1	18.921	10.165	-0.896	0.00408383
Shroom1	30.738	16.516	-0.896	0.00408383
Gpr97	4.461	2.410	-0.888	0.00762098
Ppp1r3c	49.324	26.845	-0.878	0.00408383
Tbx2	2.253	1.234	-0.869	0.0379532
Tnfaip8l1	23.959	13.139	-0.867	0.00408383
Axin2	5.230	2.894	-0.854	0.00408383
Upp2	206.718	114.407	-0.853	0.0165264
Fbxo31	29.684	16.590	-0.839	0.00408383
Spry4	4.916	2.748	-0.839	0.00408383
Eml4	5.120	2.866	-0.837	0.00408383
Gm14403	4.440	2.486	-0.836	0.0107546
Josd1	21.411	11.998	-0.836	0.00408383
N4bp2l1	45.968	25.869	-0.829	0.00408383
Slc25a25	108.532	61.101	-0.829	0.0191513
Plk3	37.071	20.931	-0.825	0.00408383
2900026A02	32.665	18.450	-0.824	0.00408383
Nags	101.528	57.489	-0.821	0.00408383
Etnk2	226.705	128.398	-0.820	0.0137082
Tfric	7.485	4.240	-0.820	0.00408383
Rassf1	8.198	4.646	-0.819	0.0137082
Rhbdd2	8.627	4.892	-0.818	0.00408383
Coq10b	25.231	14.315	-0.818	0.00408383
BC031353	45.917	26.113	-0.814	0.00408383
Pcp4l1	53.046	30.173	-0.814	0.00408383
Slc7a2	87.373	49.799	-0.811	0.0400101
Il1r1	28.595	16.592	-0.785	0.00408383
Rcan1	14.821	8.693	-0.770	0.00408383
A1bg	74.371	43.662	-0.768	0.0137082
Klf13	12.099	7.197	-0.749	0.00762098
Serpina4	24.583	14.641	-0.748	0.0441711
Selenbp2	23.494	14.057	-0.741	0.0165264
Vcam1	4.668	2.794	-0.740	0.0289181
Ier2	65.983	39.584	-0.737	0.0165264
Slc22a5	29.460	17.769	-0.729	0.00762098

Appendix III (continued)

Ppp1r10	14.922	9.012	-0.727	0.00408383
Wsb1	48.272	29.315	-0.720	0.0107546
Lpar6	20.915	12.716	-0.718	0.0400101
Pptc7	8.305	5.092	-0.706	0.0191513
Gpcpd1	40.414	24.910	-0.698	0.00762098
Rhobtb1	21.921	13.567	-0.692	0.0137082
Zfp568	2.744	1.706	-0.685	0.0335815
1810055G02	35.723	22.470	-0.669	0.0289181
Irf2bp2	36.385	22.907	-0.668	0.0335815
Rfx7	4.447	2.811	-0.662	0.0267149
Tnfaip2	12.715	8.050	-0.660	0.0267149
Ifrd1	14.445	9.152	-0.658	0.035699
Foxo1	12.512	8.011	-0.643	0.0441711
Pla2g12a	16.867	10.870	-0.634	0.0441711
Grpel2	31.231	20.196	-0.629	0.035699
Htatip2	60.661	39.284	-0.627	0.035699
Mast3	13.816	8.956	-0.625	0.0379532
Foxq1	20.287	13.221	-0.618	0.042147
Pik3r1	12.716	8.444	-0.591	0.0400101
Prkd3	16.072	24.324	0.598	0.035699
Dnajb9	24.112	38.028	0.657	0.0289181
Clec2d	102.460	161.663	0.658	0.0400101
Plcxd2	6.255	9.909	0.664	0.0107546
Id1	20.519	34.164	0.736	0.0165264
E2f8	2.229	3.818	0.776	0.0191513
Sult2a2	199.399	344.453	0.789	0.0218495
Mid1ip1	16.172	28.160	0.800	0.00408383
Hsph1	11.468	20.127	0.812	0.00408383
Fam84b	3.210	5.800	0.853	0.00408383
Klf10	11.209	20.455	0.868	0.00408383
Gas1	3.471	6.395	0.882	0.00408383
Serpina7	15.009	28.229	0.911	0.00762098
Dct	1.565	2.950	0.914	0.045894
Cyr61	3.903	7.487	0.940	0.00408383
Socs2	10.166	19.687	0.954	0.00408383
Bbc3	3.248	6.324	0.962	0.00408383
H2-K2	10.696	21.010	0.974	0.00408383
8430408G22	26.881	52.929	0.977	0.00408383
Sowahb	1.010	2.034	1.010	0.0165264
Gsta2	20.508	42.491	1.051	0.00408383
Rasl11b	1.434	2.974	1.053	0.0400101
Sult2a1	121.562	253.078	1.058	0.00408383

Appendix III (continued)

Mvd	17.864	37.600	1.074	0.00408383
Dact2	1.944	4.142	1.091	0.00408383
Hist2h3c1	2.243	5.195	1.212	0.00408383
Ckm	6.715	15.903	1.244	0.00762098
D930048N14	1.952	4.637	1.248	0.00408383
Inhbe	12.186	35.280	1.534	0.00408383
Klhdc7a	1.069	3.158	1.563	0.00408383
Cyp26b1	0.446	1.320	1.566	0.00408383
Zfp503	0.162	0.503	1.632	0.0165264
Sult2a7	5.714	20.597	1.850	0.00408383
Myl3	0.575	2.353	2.033	0.0191513
Sult1e1	0.533	3.576	2.746	0.00408383
Arrdc3	6.018	48.822	3.020	0.00408383
Myh4	0.067	1.007	3.913	0.00408383

Appendix IV: IPA Analysis of 2 hour WT RNA-Sequencing

Top Networks		
ID	Associated Network Functions	Score
1	Cell Death and Survival, Neurological Disease, Cancer	42
2	Cell Signaling, Post-Translational Modification, Cellular Function and Maintenance	36
3	Endocrine System Development and Function, Small Molecule Biochemistry, Drug Metabolism	27

Top Diseases and Bio Functions		
Diseases and Disorders		
Name	p-value	# Molecules
Neurological Disease	3.88E-22 - 1.17E-04	42
Cancer	3.40E-09 - 9.61E-04	95
Immunological Disease	3.40E-09 - 4.27E-04	34
Organismal Injury and Abnormalities	1.21E-07 - 8.95E-04	37
Nutritional Disease	1.34E-07 - 2.90E-04	29
Molecular and Cellular Functions		
Name	p-value	# Molecules
Cell Death and Survival	4.45E-16 - 9.61E-04	74
Cellular Growth and Proliferation	1.74E-14 - 9.61E-04	79
Gene Expression	2.62E-14 - 9.35E-04	57
Cellular Development	5.01E-11 - 9.61E-04	74
Cell Morphology	1.96E-09 - 9.61E-04	48
Physiological System Development and Function		
Name	p-value	# Molecules
Connective Tissue Development and Function	5.01E-11 - 9.61E-04	43
Hematological System Development and Function	1.46E-10 - 8.97E-04	55
Tissue Morphology	1.46E-10 - 6.40E-04	54
Organ Morphology	3.74E-10 - 9.78E-04	47
Tumor Morphology	1.13E-09 - 1.95E-04	30

Top Canonical Pathways		
Name	p-value	Ratio
Glucocorticoid Receptor Signaling	2.12E-07	13/299 (0.043)
Aryl Hydrocarbon Receptor Signaling	2.11E-06	9/171 (0.053)
IL-17A Signaling in Fibroblasts	8.76E-06	5/40 (0.125)
IGF-1 Signaling	1.4E-05	7/107 (0.065)
PXR/RXR Activation	1.71E-05	6/92 (0.065)

Appendix IV (continued):

Top Molecules	
Log Ratio up-regulated	
Molecules	Exp. Value
CYP1A1	↑8.507
SERPINE1	↑5.444
APBA3	↑4.095
TIPARP	↑4.032
MAFF	↑3.368
CCNO	↑3.202
GADD45G	↑2.899
IGFBP1	↑2.860
Rhox5	↑2.735
TCHH	↑2.644
Log Ratio down-regulated	
Molecules	Exp. Value
PFAS	↓-3.996
ARRDC3	↓-3.039
SULT1E1	↓-2.691

Top Tox Lists		
Name	p-value	Ratio
Liver Necrosis/Cell Death	3.93E-13	19/262 (0.073)
Acute Renal Failure Panel (Rat)	2.43E-12	11/62 (0.177)
Renal Necrosis/Cell Death	1.24E-06	16/466 (0.034)
Primary Glomerulonephritis Biomarker Panel (Human)	1.31E-06	4/11 (0.364)
Aryl Hydrocarbon Receptor Signaling	6.32E-06	9/160 (0.056)

Appendix IV (continued):

Top Tox Functions		
Assays: Clinical Chemistry and Hematology		
Name	p-value	# Molecules
Increased Levels of Alkaline Phosphatase	2.39E-03 - 2.42E-02	5
Increased Levels of Hematocrit	4.56E-02 - 4.56E-02	3
Increased Levels of Red Blood Cells	4.56E-02 - 4.56E-02	3
Increased Levels of Bilirubin	4.77E-02 - 4.77E-02	1
Increased Levels of AST	9.32E-02 - 9.32E-02	1
Cardiotoxicity		
Name	p-value	# Molecules
Cardiac Hypertrophy	2.06E-04 - 2.42E-02	12
Cardiac Necrosis/Cell Death	5.22E-04 - 2.30E-01	8
Cardiac Infarction	1.51E-02 - 1.51E-02	5
Cardiac Damage	1.62E-02 - 7.82E-02	2
Cardiac Degeneration	1.62E-02 - 1.62E-02	1
Hepatotoxicity		
Name	p-value	# Molecules
Liver Necrosis/Cell Death	3.42E-13 - 1.22E-01	19
Liver Proliferation	5.44E-07 - 2.42E-02	10
Liver Damage	1.57E-06 - 3.21E-02	11
Liver Regeneration	1.43E-05 - 1.43E-05	6
Liver Steatosis	7.21E-05 - 2.42E-02	10

Nephrotoxicity		
Name	p-value	# Molecules
Renal Necrosis/Cell Death	8.86E-07 - 1.91E-01	16
Renal Proliferation	9.39E-06 - 4.77E-02	12
Kidney Failure	6.82E-05 - 1.08E-01	9
Renal Inflammation	1.49E-04 - 1.71E-01	10
Renal Nephritis	1.49E-04 - 1.71E-01	10

Appendix V: IPA Analysis of 8 hour WT RNA-Sequencing

Top Canonical Pathways		
Name	p-value	Overlap
LPS/IL-1 Mediated Inhibition of RXR Function	2.33E-14	21.9 % 48/219
PXR/RXR Activation	4.60E-10	31.3 % 21/67
Nicotine Degradation II	9.24E-10	31.7 % 20/63
Xenobiotic Metabolism Signaling	2.62E-09	16.6 % 45/271
Bupropion Degradation	9.59E-09	48.0 % 12/25
Top Upstream Regulators		
Upstream Regulator	p-value of overlap	Predicted Activation
TNF	3.94E-43	Inhibited
PPARA	4.66E-43	
dexamethasone	8.30E-42	
ACOX1	3.29E-39	Activated
methylprednisolone	1.88E-38	
Top Diseases and Bio Functions		
Diseases and Disorders		
Name	p-value	#Molecules
Inflammatory Response	1.87E-05 - 7.42E-18	291
Gastrointestinal Disease	1.98E-05 - 2.84E-15	850
Hepatic System Disease	1.98E-05 - 2.84E-15	525
Metabolic Disease	1.50E-05 - 2.84E-15	239
Nutritional Disease	6.97E-06 - 4.27E-14	138
Molecular and Cellular Functions		
Name	p-value	#Molecules
Lipid Metabolism	2.24E-05 - 1.61E-32	310
Molecular Transport	1.69E-05 - 1.61E-32	348
Small Molecule Biochemistry	2.24E-05 - 1.61E-32	372
Cell Death and Survival	2.25E-05 - 5.07E-25	479
Cellular Growth and Proliferation	1.59E-05 - 9.97E-23	514
Physiological System Development and Function		
Name	p-value	#Molecules
Organismal Development	2.02E-05 - 8.63E-19	463
Organismal Survival	9.73E-06 - 1.84E-18	365
Connective Tissue Development and Function	2.33E-05 - 1.76E-16	206
Tissue Morphology	2.33E-05 - 1.76E-16	338
Embryonic Development	9.97E-06 - 5.55E-16	255

Appendix V (continued):

Name	p-value	#Molecules
Lipid Metabolism	2.24E-05 - 1.61E-32	310
Molecular Transport	1.69E-05 - 1.61E-32	348
Small Molecule Biochemistry	2.24E-05 - 1.61E-32	372
Cell Death and Survival	2.25E-05 - 5.07E-25	479
Cellular Growth and Proliferation	1.59E-05 - 9.97E-23	514
Physiological System Development and Function		
Name	p-value	#Molecules
Organismal Development	2.02E-05 - 8.63E-19	463
Organismal Survival	9.73E-06 - 1.84E-18	365
Connective Tissue Development and Function	2.33E-05 - 1.76E-16	206
Tissue Morphology	2.33E-05 - 1.76E-16	338
Embryonic Development	9.97E-06 - 5.55E-16	255
Top Tox Functions		
Assays: Clinical Chemistry and Hematology		
Name	p-value	#Molecules
Increased Levels of Hematocrit	1.01E-03 - 1.01E-03	15
Increased Levels of Bilirubin	3.68E-01 - 4.01E-03	4
Increased Levels of Red Blood Cells	2.30E-01 - 2.25E-02	12
Increased Levels of Alkaline Phosphatase	1.78E-01 - 3.21E-02	10
Increased Levels of Creatinine	9.82E-02 - 4.50E-02	7

Appendix V (continued):

Name	p-value	#Molecules
Cardiac Infarction	3.68E-01 - 4.26E-06	35
Cardiac Hypertrophy	4.31E-01 - 1.45E-05	49
Cardiac Arteriopathy	5.73E-01 - 1.55E-04	38
Cardiac Necrosis/Cell Death	5.37E-01 - 1.87E-04	32
Heart Failure	1.29E-01 - 1.95E-04	32
Hepatotoxicity		
Name	p-value	#Molecules
Liver Steatosis	2.30E-01 - 2.84E-15	61
Liver Necrosis/Cell Death	1.45E-01 - 1.03E-07	42
Liver Proliferation	2.21E-01 - 1.96E-07	35
Liver Cholestasis	3.25E-01 - 1.36E-06	25
Liver Hyperplasia/Hyperproliferation	5.44E-01 - 3.34E-06	473
Nephrotoxicity		
Name	p-value	#Molecules
Renal Damage	5.50E-01 - 3.72E-14	48
Renal Tubule Injury	5.50E-01 - 3.72E-14	33
Kidney Failure	3.68E-01 - 1.89E-05	33
Renal Atrophy	4.80E-01 - 3.39E-04	8
Renal Necrosis/Cell Death	4.11E-01 - 8.51E-04	53

Top Networks		
ID	Associated Network Functions	Score
1	Metabolic Disease, Neurological Disease, Organismal Injury and Abnormalities	38
2	Gene Expression, RNA Post-Transcriptional Modification, Cell Morphology	38
3	Lipid Metabolism, Molecular Transport, Small Molecule Biochemistry	38
4	Cell Cycle, Cell Morphology, Hematopoiesis	36
5	Lipid Metabolism, Nucleic Acid Metabolism, Small Molecule Biochemistry	32
Top Tox Lists		
Name	p-value	Overlap
LPS/IL-1 Mediated Inhibition of RXR Function	3.28E-18	23.1 % 58/251
Xenobiotic Metabolism Signaling	5.69E-15	18.8 % 63/336
Cytochrome P450 Panel - Substrate is a Xenobiotic (Mouse)	7.34E-14	64.0 % 16/25
Fatty Acid Metabolism	1.51E-13	28.2 % 33/117
NRF2-mediated Oxidative Stress Response	1.82E-11	19.2 % 45/234

Appendix V (continued):

Log Ratio up-regulated	
Molecules	Exp. Value
Hsd3b4 (includes others)	↑ 3.772
IHH	↑ 3.380
ARL4D	↑ 2.808
Dsg1c	↑ 2.396
Hamp/Hamp2*	↑ 2.158
SLC13A2	↑ 2.037
HSD3B1*	↑ 2.002
TK1	↑ 1.940
CYP4A22	↑ 1.919
Clec2e/Clec2h	↑ 1.880
Log Ratio down-regulated	
Molecules	Exp. Value
CYP1A1	↓ -12.508
NPTX1	↓ -7.174
SERPINE1	↓ -6.034
CYP1B1	↓ -4.578
AHRR	↓ -4.446
CYP1A2	↓ -4.390
INSL6	↓ -4.138
CBR3	↓ -4.089
HSD3B2	↓ -4.049
MYOM1	↓ -3.444

Appendix VI: 2 hour RNA-sequencing compared to lo et al.

Common Between AhR Peaks and 2 hr Significant Genes			Common Between AhRARnt Peaks and 2 hr Significant Genes	
WT		AhR CKO	WT	AhR CKO
33 common		3 common	17 common	2 common
EDC3	TIPARP	CXCR7	EDC3	CXCR7
CYP1B1	ITPRIP	ONECUT1	CYP1B1	ONECUT1
PIK3R1	IRF2BP2	IGSF3	PIK3R1	
DNAJB9	ACPP		DNAJB9	
CEBPB	SLC38A2		GDF15	
GDF15	CSRNP1		CYP1A2	
CYP1A2	PPP1R15A		FAM84B	
FAM84B	DDIT4		BMF	
BMF	SLC22A5		FBXO31	
FBXO31	CIB3		CYP1A1	
NFE2L2	ADCY1		HES1	
CYP1A1	FOXQ1		NFE2L2	
SOCS2	AXIN2		SLC38A2	
HES1	KLHDC7A		DDIT4	
GSTA2	RFX7		SOCS2	
ID1	FOS		MID1IP1	
MID1IP1			FOS	

Appendix VII 8 hour RNA-sequencing compared to lo et al.

Common Between AhR only bound Peaks and 8 hr Significant Genes				Common Between AhR and Arnt Bound Peaks and 8 hr Significant Genes		
WT			AhR CKO	WT		AhR CKO
155 common			62 common	79 common		23 common
EDC3	NUDT7	TPD52L1	TSKU	EDC3	CYP1A2	TSKU
CYP1B1	TLE3	BTG1	KRT18	CYP1B1	PLEKHA7	KRT18
ATXN1	INSIG1	GSTP1	PPARG	ATXN1	CDYL2	PPARG
STARD13	GDF15	P2RY2	STARD13	STARD13	FBXO31	STARD13
ABLIM3	CYP1A2	GNA14	MID1	ABLIM3	ARL5B	FIGN
PLEKHF1	PLEKHA7	GPX3	FIGN	PLEKHF1	SULF2	RRS1
FAM174B	COL18A1	CABLES1	RRS1	FAM174B	CYP1A1	IGFBP5
KLF4	CDYL2	AHRR	WEE1	KLF4	ID4	CPEB4
FHIT	HIST1H1C	MME	IGFBP5	FHIT	PSPC1	GDF15
ERC2	COL4A1	STIM2	CPEB4	ERC2	KLF12	PYGL
ARHGEF10L	FBXO31	EFNA5	GDF15	ARHGEF10L	BZW2	FNDC3B
ST3GAL1	ARL5B	ABCC4	PYGL	ST3GAL1	FNDC3B	PHLDA1
DAB2	SULF2	HAAO	RAD51L1	DAB2	PHLDA1	HES1
ATP1B1	NFE2L2	AOX1	XRCC6BP1	ATP1B1	RERG	FBXO21
GPC6	CYP1A1	LIMA1	VTCN1	GPC6	LPHN2	PDXK
WEE1	ID4	SYNJ2	RARB	IGFBP5	NFE2L2	SORL1
IGFBP5	PSPC1	NEDD4L	FNDC3B	CXCR7	GSTP1	DDIT4
CXCR7	FAM129B	AGPAT9	PHLDA1	TRAFD1	P2RY2	WEE1
TRAFD1	BZW2	THEM4	HES1	CPEB4	GNA14	FAM102A
COL4A2	FNDC3B	TTC39A	FBXO21	TXNRD1	GPX3	BCL6
CPEB4	PHLDA1	TBC1D8	PDXK	NUDT7	CABLES1	MKX
RERG	PGPEP1	ARHGAP10	MME	TLE3	AHRR	MID1IP1
LPHN2	ARHGAP26	TTC39B	STIM2	INSIG1	ABCC4	ONECUT1
SLC16A7	PSEN2	ACSL3	QSOX1	GDF15	HAAO	

Appendix VII (continued)

Common Between AhR only bound Peaks and 8 hr Significant Genes				Common Between AhR and Arnt Bound Peaks and 8 hr Significant Genes		
WT			AhR CKO	WT		AhR CKO
PROM1	SVIL	ARSG	FAM102A	LIMA1	LIN7A	
DYSF	SORBS2	DNPEP	ACPP	SYNJ2	ONECUT1	
ZADH2	PAPSS2	PRKCA	SORL1	AGPAT9	SOD3	
FAM102A	LRFN3	PPP1R13B	TGFBR2	TTC39A	TCF7L2	
DLL1	SLC22A5	DAAM1	CD36	DLL1	MYOF	
OSMR	HS3ST6	MBL2	CSRNP1	FAM65B	FOS	
MYOF	DSTN	LIN7A	GJB2	FAM20C		
IRF2BP2	RGS3	ELOVL5	DDIT4	COL18A1		
FAM65B	ABHD2	ETHE1	UNG	P2RY6		
TBX3	FRMD6	NPR1	NCOR2	PDZRN3		
KYNU	PPFIBP1	ONECUT1	DPP9	TBC1D8		
FAM20C	GNA12	SOD3	BCL6	SLC16A7		
SARDH	RAPH1	NDRG1	MKX	TTC39B		
ACPP	TESK2	LEKR1	MID1IP1	EFNA5		
HS6ST1	THADA	TCF7L2	RALGPS2	WEE1		
P2RY6	NQO1	UBE2E2	LIFR	FAM102A		
TIMP3	RARS2	CD53	PVRL2	ABHD2		
TGFBR2	MID1IP1	AHR	HIVEP2	TESK2		
KAT2B	WDR93	ABR	LOXL1	SOCS2		
CD36	GPR110	ABHD4	RARG	THADA		
CSRNP1	EMP2		COL5A2	MID1IP1		
PDZRN3	UBE2CBP		NEK6	GPR110		
LMO7	TIPARP		BMPER	LMO7		
FBXO34	PLEKHM3		ELOVL5	DNPEP		
SUSD4	MYOM1		ONECUT1	NTN4		

Appendix VII (continued)

Common Between AhR only bound Peaks and 8 hr Significant Genes				Common Between AhR and Arnt Bound Peaks and 8 hr Significant Genes		
WT			AhR CKO	WT		AhR CKO
BCL3	ELTD1		NDRG1			
AXIN2	NTN4		DPT			
KLHDC7A	ATIC		FOXQ1			
FOS	ANPEP		FBXO33			
			SUSD4			
			BCL3			
			KLHDC7A			
			TET2			
			FBXL17			
			RTN4RL1			

Appendix VIII: GCHARMS Supplemental Methods

Realizing the importance of trust by the community and the benefits of active community involvement science, the NIEHS mandated that applicants for Deepwater Horizon Disaster Research Consortia: Health Impacts and Community Resiliency (U19) funding include a strongly supported community outreach and dissemination / liaison core in their proposals. Our university-community consortium that co-created *Gulf Coast Health Alliance: health Risks related to the Macondo Spilled (GC-HARMS)* resolved to frame their research on petrogenic PAH exposures and health impacts as Community-Based Participatory Research, to promote maximum empowerment for affected communities to collaborate with university science teams and address the health risks and economic damage stemming from the DWH disaster. A CBPR approach values, among other things the selection of a research focus that reflects community-identified needs, a commitment to trust and mutuality, and promotes inclusion and mutual respect among project collaborators for differences in priorities and points-of-view.

To include affected communities directly in formulating the study design, the UTMB NIEHS P30 Center in Environmental Toxicology Community Outreach & Engagement Core (COEC) staff conducted a pre-project phone survey of community organizations with which the COEC had established a prior working relationship. Suggestions from the original core of community partners expanded the range of this convenience sample, and eventually, 26 separate community-based organizations responded to informal queries on possible research priorities. The organizations were also asked to gauge their capacity and actual interest in serving as an active component of the research / resiliency-building team. The primary research needs identified in this process all related to the safety of the food web and natural ecosystems, the risks to human health from continued consumption of Gulf seafood, and resiliency challenges faced by fishing communities, given the harsh economic realities of fishing closures and a widespread national perception that Gulf seafood may no longer be safe to consume.

Appendix VIII (continued)

These expressed needs were integrated into a research proposal that focused on the health effects of exposure to petrogenic PAH components of crude oil and understanding how population health and social / economic factors may undermine or strengthen community resilience in the Gulf. Six community hubs were created across the tri-state area: three in Louisiana, two in Mississippi and one in Alabama.

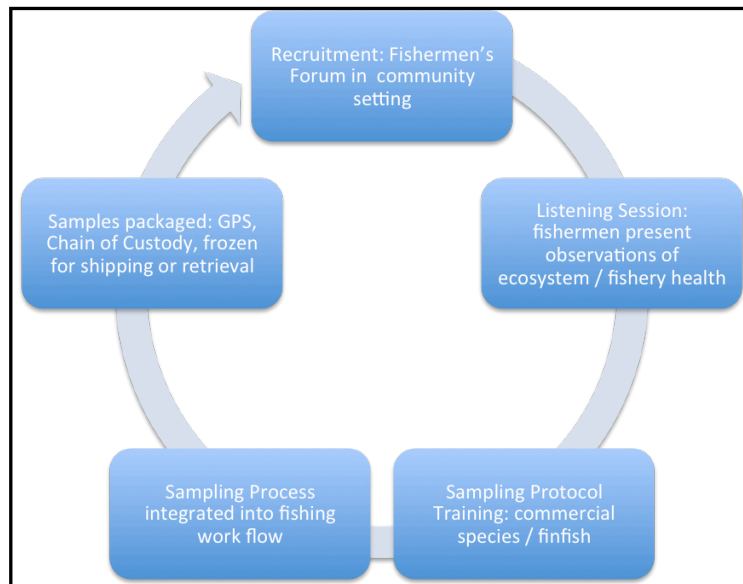
The project established a network of three major hubs for coordination of a community field science network of fishermen. These sampling hubs were located at Houma, Louisiana (United Houma Nation), Gulfport, Mississippi (Mississippi Vietnamese Community Partner) and Coden / Bayou la Batre, Alabama (South Bay Communities Alliance / Alabama Fisheries Cooperative). After notification by NIEHS that the GC-HARMS project would be funded, but just before the funding stream was officially established, the lead institution (University of Texas Medical Branch at Galveston TX) leveraged existing monies to launch a pilot project for developing and field testing a model for collaborating with local fishermen to obtain seafood samples for laboratory assays that would establish petrogenic polycyclic aromatic hydrocarbon content and toxicity. This model was developed primarily through collaboration between the GC-HARMS science team and the Louisiana Environmental Action Network. Sampling protocols were derived from EPA-approved procedures and incorporated into text, chart and power-point presentations geared toward an audience of working fishermen and concerned community members. Standardizing procedures for maintaining purity of samples, accurate collection of data on environmental conditions while sampling, careful recording of each site's geographical position (GPS coordinates), and maintenance of chain-of-custody were primary outcome goals for basic science. Enhancing regional environmental health literacy and building community hub capacity to understand and subsequently interpret the scientific concepts underlying GC-HARMS were equally important process-driven resiliency goals.

Appendix VIII (continued)

The pilot project launched in July 2011; project components included: 1) presentation of proposed project goals and objectives, 2) outline of sampling protocols / techniques / equipment for use on board fishing vessels, 3) overview of data collection, organization, recording, 4) explanation and maintenance of chain-of-custody throughout the process, 5) sample preparation for shipping and/or pickup, 6) project protocols for discussion of findings as the data evolves. The fishermen were also encouraged to log or otherwise report observations of changes in environmental conditions and were directly responsible for choosing sample sites which, in most cases, reflected the most productive seasonal fishing waters from past experience. Results of the pilot were overwhelmingly positive and fishermen feedback was incorporated into refinements of materials and process. Fishermen and hub coordinators were also instrumental in targeting specific finfish for capture, based on their knowledge of local consumption preferences.⁹

As soon as community hub organizations approved final versions of process protocols, the program officially rolled-out in December 2011. (see below: GC-HARMS Community Fishermen Training: Work Flow Process Map) Community forums for fishermen and concerned community residents were facilitated in five locations throughout the Louisiana United Houma Nation catchment area (Terrebonne / Lafourche, Jefferson, Plaquemines and St. Bernard Parishes). Similar forums were convened in Gulfport / Biloxi, Mississippi and Coden / Bayou la Batre and Theodore, Alabama. Despite some attrition within the fishermen's field science network during the formal seafood-sampling period (12 / 2011 – 4 / 2014), community fishermen successfully collected samples of shrimp (brown and white), blue crab, oysters and a variety of finfish species. Project staff collected an additional 10 sample sites in Galveston Bay for use as comparative controls.

Appendix VIII (continued)



Appendix IX: GCHARMS Seafood Sample Information

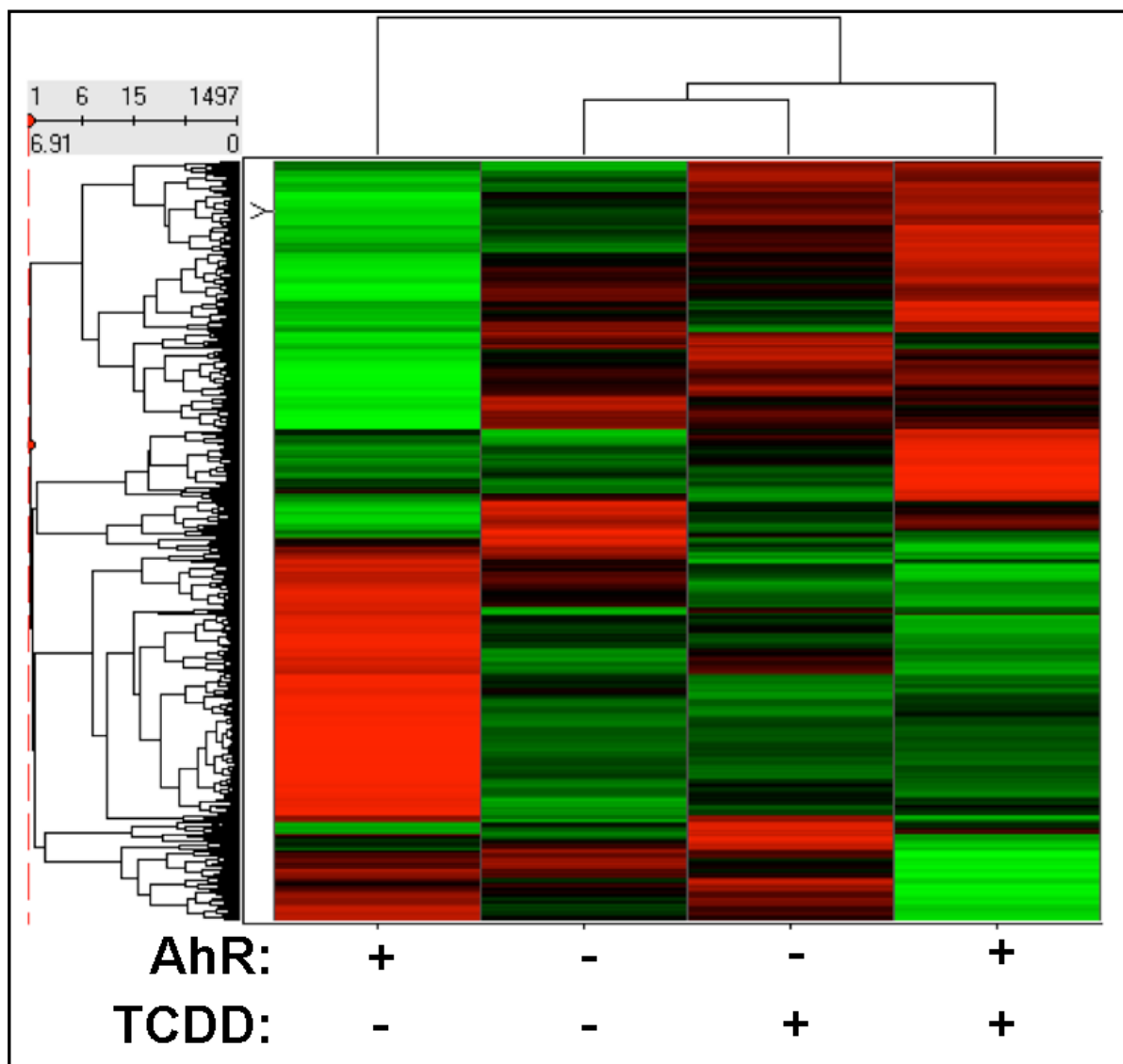
Site	Sample #	Species	Location	Date	N GPS	W GPS	Additional Geographic
SBCA 10	5	Shrimp	Alabama	8/10/12	30.18.386	88.01.674	W End of Ship Channel
SBCA 12	5	Shrimp	Alabama	8/10/12	30.18.386	88.01.940	N of Bay Bon Soucor
SBCA 16	5	Shrimp	Alabama	8/10/12	30.27.138	88.02.950	E End of Ship Channel
SBCA 17	5	Shrimp	Alabama	8/10/12	30.27.138	88.02.950	E End of Ship Channel
UHN 26	5	Shrimp	Louisiana	6/15/12	8:15:38	90.6495	Robinson Canal
UHN 29	5	Shrimp	Louisiana	6/21/12	29.52.758	89.38.242	Lake Borgne
UHN 80	5	Shrimp	Louisiana	5/9/12	29.30.98	90.10.48	Little Lake
UHN 81	5	Shrimp	Louisiana	5/20/12	29.30.31	90.4.23	Bayou St. Denis
UHN 78	5	Shrimp	Louisiana	5/26/12	29.9.64	90.30.73	Grand Lake / Barataria Bay
UHN 71	5	Finfish	Louisiana	4/20/11	29.3.30	90.42.77	Timbalier Island
UHN 70	5	Oyster	Louisiana	8/16/11	29.28.93	90.00.26	N Bay Jimmy
UHN 79	1	Shrimp	Louisiana	5/26/12	29.9.64	90.30.73	Grand Lake / Barataria Bay
Galveston O1	5	Oyster	Galveston	8/1/12	29°16'55"	94°51'19"	
UHN 38	5	Shrimp	Louisiana	10/11/12	29.20.104	90.22.277	Pointe-aux-Chenes
UHN 40	5	Crab	Louisiana	10/11/12	29.21.924	90.23.796	Comb Bay
UHN 41	5	Oyster	Louisiana	10/11/12	29.22.092	90.25.031	Comb Bay
Galveston O2	5	Oyster	Galveston	8/1/12	29°16'55"	94°51'19"	
Galveston S1	5	Shrimp	Galveston	11/10/12	29.19.02.6	94.46.43.5	
UHN 60	5	Oyster	Louisiana	11/1/12	30.04.794	89.29.806	Petit Passage (St. Bernard)
UHN 49	5	Oyster	Louisiana	10/20/12	29.20.193	90.35.613	Isle de Jean Charles
UHN 27	5	Oyster	Louisiana	6/21/12	29.51.29	89.40.40	Ycloskey Bayou
UHN 25	5	Crab	Louisiana	6/21/12	8:36:21	90.3853	Bay Sorrell
UHN 22	5	Oyster	Louisiana	6/15/12	5:26:01	91.13232	Comb Bay
UHN 35	3	Finfish	Louisiana	7/1/12	29.183.40	88.736.849	Main Pass 311
UHN 36	3	Finfish	Louisiana	7/1/12	29.183.40	88.736.849	Main Pass 311
UHN 34	3	Finfish	Louisiana	6/22/12	29.51.29	89.40.40	Ycloskey Bayou
UHN 32	5	Crab	Louisiana	6/22/12	29.59.747	89.15.776	Barasich Lease
UHN 68	5	Shrimp	Louisiana	12/10/12	30.158333	89.472917	St. Joe Pass Light

UHN 69	3	Crab	Louisiana	12/10/12	30.158333	89.472917	St. Joe Pass Light
UHN 48	5	Shrimp	Louisiana	10/18/12	29.24.970	90.26.874	Isle de Jean Charles
UHN 45	5	Oyster	Louisiana	10/25/12	29.43.476	89.36.343	Lake Calabash
MCV 8	5	Crab	Mississippi	8/2/12	30.12.651	89.23.530	Bay St. Louis
MCV 9	5	Shrimp	Mississippi	8/2/12	30.13.098	89.21.754	Bay St. Louis
UHN 23	5	Shrimp	Louisiana	6/15/12	8:36:21	90.3853	Pointe-aux-Chenes
MCV 18	5	Shrimp	Mississippi	8/3/12	30.22.045	89.58.911	Ocean Spring / Biloxi
UHN 45	5	Shrimp	Louisiana	10/25/12	29.43.476	89.36.343	Grand Pass
MCV 13	5	Shrimp	Mississippi	8/2/12	30.17.384	89.01.173	E of Gulfport
MCV 22	5	Shrimp	Mississippi	11/3/12	30.21.555	88.54.771	Biloxi / Pascagoula
SBCA 23	5	Shrimp	Alabama	12/14/12	30.20.719	88.01.593	Central Channel
SBCA 19	5	Oyster	Alabama	10/25/12	30.27.741	88.05.960	Fowl River / Mobile Bay
SBCA 21	5	Oyster	Alabama	11/7/12	30.18.26	88.08.41	Cedar Point / w side of Dauphin Island Bridge
MCV 35	5	Crab	Mississippi	12/15/12	30.18.8.12 8	89.15.654	Pass Christian
MCV 33	5	Oyster	Mississippi	11/9/12	30.15.266	89.15.425	Area 2c / Pass Christian
SBCA 17	5	Shrimp	Alabama	8/10/12	30.28.138	88.02.950	E End of Ship Channel
UHN A	5	Finfish	Louisiana	10/20/12			
MCV 29/32	4	Shrimp	Mississippi	11/3/12	30.18.316	89.11.760	Long Beach E of Gulfport
SBCA 17	5	Shrimp	Alabama	8/10/12			
UT1	5	Shrimp	Galveston	11/10/12	29.18.478	94.46.256	Yacht Basin
UT5	5	Finfish	Galveston	3/23/13	29.205517	94.9777011	Carancahua Cove
UHN B	5	Finfish	Louisiana	12/10/12			
UHN C	5	Finfish	Louisiana	10/20/12			
MCV 27	5	Shrimp	Mississippi	11/3/12	30.18.832	89.09.887	Long Beach
UHN 102	5	Shrimp	Louisiana	6/30/13	30.0827	89.4781	Le Petit Pass
MCV 27	5	Shrimp	Mississippi	11/3/12	30.18.832	89.09.887	Long Beach
UHN 101	5	Shrimp	Louisiana	6/30/13	30.0827	89.4781	Le Petit Pass
UHN 92	1	Finfish	Louisiana	6/13/13	29.30.037	89.45.344	Grand Bayou
UHN 98	1	Finfish	Louisiana	6/30/13	30.08.27	89.47.81	Le Petit Pass

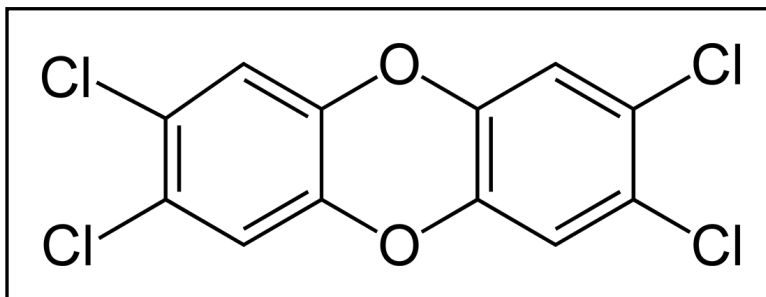
UHN 96	1	Finfish	Louisiana	6/13/13	29.30.713	89.45.956	Grand Bayou
UHN 100	1	Finfish	Louisiana	6/30/13	30.0827	89.4781	Le Petit Pass
UHN 99	1	Finfish	Louisiana	6/30/13	30.0827	89.4781	Le Petit Pass
MCV 32	3	Shrimp	Mississippi	1/4/12	30.14.328	89.23.480	Waveland / Pass Christian
SBCA 23	5	Shrimp	Alabama	12/14/12	30.20.719	88.01.593	Central Channel
UHN 97	5	Crab	Louisiana	6/13/13	29.30.713	89.45.956	Grand Bayou
UHN 93/95	5	Shrimp	Louisiana	6/13/13	29.30.037	89.45.344	Grand Bayou
UHN 91/94	5	Shrimp	Louisiana	6/13/13	29.30.037	89.45.344	Grand Bayou
MCV 42	5	Shrimp	Mississippi	8/24/13	30.14261	89.23242	Bay St. Louis
MCV 39/41	5	Shrimp	Mississippi	8/24/13	30.15.483	89.22.197	Bay St. Louis
MCV 40	4	Shrimp	Mississippi	8/24/13	30.12.249	89.24.147	LA / MS Border Water
UHN 89	3	Crab	Louisiana	5/3/13	29.24.586	90.24.168	(unspecified)
UHN 87	3	Crab	Louisiana	5/3/13	29.25.940	90.22.389	Bayou Buyou
UTMB	7	Oyster	Galveston	7/8/13	29.29	94.73	Lease 268
SBCA 36	5	Crab	Alabama	2/2/14	30.18.04	88.34.40	Mississippi Sound
SBCA 27	5	Crab	Alabama	2/1/14	30.29.98	88.03.49	W Side N Yard Island
SBCA 39	5	Oyster	Alabama	2/3/14	30.18.24	88.08.23	Cedar Point Reef
SBCA 28/31	5	Shrimp	Alabama	2/1/14	30.23.04	88.01.16	Between Channel Beacons 38-41
SBCA 32/33	5	Shrimp	Alabama	11/12/13	30.22.674	88.01.275	Between Channel Beacons 30-39
UHN78	3	Shrimp	Louisiana	5/26/12	29.9.64	90.30.73	Grand Lake / Barataria Bay
UHN 102	5	Shrimp	Louisiana	6/30/13	30.0827	89.4781	Le Petit Pass
UHN 104	2	Oyster	Louisiana	8/5/10	30.01.14	89.34.33	Lake Borgne
UHN 105	2	Oyster	Louisiana	8/5/10	30.02.21	89.21.10	3 Mile Bay
UHN 106	2	Oyster	Louisiana	8/5/10	29.53.19	89.17.31	Drum Bay
UHN 107	2	Oyster	Louisiana	8/5/10	29.14.43.7	91.03.18. 6	Mid-Bay Junop
UHN 108	2	Oyster	Louisiana	8/5/10	29.12.38.4	91.03.18. 2	Lower Bay Junop
UHN 109	2	Oyster	Louisiana	8/5/10	29.12.58.2	90.56.40. 2	Old Camp
UHN 110	2	Oyster	Louisiana	8/5/10	29.14.50.9	90.56.16. 9	Walkers Point
UHN 111	2	Oyster	Louisiana	8/3/10	29.40.022	89.30.828	Lake Fortuna

UHN 112	2	Oyster	Louisiana	8/3/10	29.34.9	89.37.317	Bay Gardene
UHN 113	2	Oyster	Louisiana	8/3/10	29.31.674	89.32.461	N California Bay
UHN 114	2	Oyster	Louisiana	8/5/10	29.25.05.5 2	90.02.08. 10	Middle Hackberry
UHN 115	2	Oyster	Louisiana	8/4/10	29.25.01.6 0	90.01.56. 90	NHB Seed Ground (label: Cult 6")
UHN 116	2	Oyster	Louisiana	8/4/10	29.431.824	89.904.55 6	W Bay Jimmy
UHN 11	5	Shrimp	Louisiana	1/11/12	28.37.84	89.33.18	federal waters
UHN 1	5	Oyster	Louisiana	12/13/11	29.24801	90.369093	"east reef"
UHN 14	5	Oyster	Louisiana	1/12/12	29.591046	89.642561	Bay Gardene
UHN 6	3	Oyster	Louisiana	12/16/11	29.6116	89.56145	Lonesome Island
UHN 9	2	Finfish	Louisiana	1/9/12	29.466711	90.367522	
SBCA 8	2	Finfish	Alabama	12/15/12	30.31942	88.07158	north bay
MCV 4	2	Shrimp	Mississippi	12/16/11	30.282443	88.338948	
MCV 6	3	Crab	Mississippi	12/16/11	30.282443	88.388948	
UHN 19	3	Crab	Louisiana	1/14/12	29.21832	91.1326	4 League Bay
UHN 17	3	Crab	Louisiana	1/12/12	29.544102	89.619227	Bay Crabe
UHN 8	4	Crab	Louisiana	1/9/12	29.466357	90.357051	
MCV 5	2	Shrimp	Mississippi	12/16/11	30.271009	88.365627	
SBCA 7	2	Crab	Alabama	12/17/11	30.400871	88.015804	south bay
UHN 18	5	Oyster	Louisiana	1/14/12	29.2215	91.13003	4 League Bay
SBCA 6	5	Shrimp	Alabama	12/17/11	30.363825	88.022415	south bay
SBCA 1	5	Oyster	Alabama	12/16/11	30.19061	88.074751	Cedar Point

Appendix X: Heat map of Significant WT Expression Changes, 8 hour Comparison



Appendix XI: TCDD Structure



Appendix XII: Signaling Pathways from 2 hour IPA Analysis

Biological Functions and Disease	Molecules
Neurological Disease	LRP4, SOCS3, PIM3, GADD45B, ZFP36, PLK3, GADD45G, HSPA1A/HSPA1B, SGK1, KLF10, HES1, SDC4, DNAJA1, USP2, TSC22D3, Bbc3, C10orf10, TRIB1, ARRD3, JUN, TIPARP, ITPRIP, TNFRSF1B, NFE2L2, MT1H, ADRB2, SLC25A25, ATF3, IER2, EGR1, IL1R1, IER3, MAFF, RCAN1, FOS, DUSP1, ADCY1, CDKN1A, NR4A1, G6PC, CYR61, HMG2
Cell Death and Survival	PER1, SOCS3, PLK3, SGK1, HSPA1A/HSPA1B, ZFP36L1, Hmga1, SDC4, HES1, TSC22D3, Rhox5, Bbc3, NR0B2, ITPRIP, C8orf4, TNFAIP2, IGF1, SERPINE1, MT1H, AXIN2, ATF3, DDIT4, LCN2, IER3, KLF13, MAFF, SULT2A1, APBA3, CCNO, DACT2, DUSP1, BTG2, TFRC, CYR61, NOTCH1, HMG2, PIM3, GADD45B, ZFP36, GADD45G, ACER2, KLF10, SOCS2, GDF15, TNFAIP8L1, DNAJA1, USP2, SELENBP1, TRIB1, JUN, PPP1R10, FOXO3, SPHK1, TNFRSF1B, NFE2L2, RASSF1, ADRB2, SLC20A1, GAS1, HSPH1, EGR1, H2-K2H2-Q9, PPP1R15A, CSRN1, IL1R1, CEBPB, DNAJB9, NFKBIZ, HSPA2, CYP1B1, RCAN1, FOS, NFE2, BMF, CDKN1A, NR4A1, G6PC, MAFB, BCL2L11
Cellular Growth and Proliferation	MVD, PER1, SOCS3, PLK3, HSPA1A/HSPA1B, SGK1, EML4, ZFP36L1, Hmga1, HES1, SDC4, TSC22D3, SPRY4, Bbc3, LPIN1, C8orf4, IGF1, SERPINE1, ACPP, MT1H, PFKFB3, AXIN2, ATF3, LCN2, IER3, KLF13, MAFF, SULT2A1, APBA3, CCNO, DACT2, DUSP1, BTG2, TFRC, CYR61, NO, TCH1, HMG2, HILPDA, PIM3, GADD45B, ZFP36, GADD45G, ACER2, KLF10, GDF15, SOCS2, DNAJA1, USP2, SELENBP1, TRIB1, ARRD3, JUN, PPP1R10, FOXO3, SULT1E1, SPHK1, LIPG, TNFRSF1B, NFE2L2, ADRB2, RASSF1, SLC20A1, CYP1A1, GAS1, EGR1, PPP1R15A, CEBPB, IL1R1, CYP1B1, RCAN1, FOS, BMF, NFE2, ADCY1, CDKN1A, NR4A1, MAFB, BCL2L11, FZD7
Gene Expression	SOCS3, PER1, HSPA1A/HSPA1B, SGK1, PLK3, ZFP36L1, Hmga1, HES1, TSC22D3, Rhox5, CYP1A2, LPIN1, NR0B2, MID1P1, IGF1, SERPINE1, AXIN2, ATF3, LCN2, HIST2H3C (includes others), SAP30, IER3, KLF13, MAFF, CCRN4L, DUSP1, INHBE, BTG2, PER2, NOTCH1, HMG2, ZFP36, GADD45G, KLF10, SOCS2, USP2, JUN, FOXO3, TNFRSF1B, NFE2L2, RASSF1, ADRB2, SLC20A1, CYP1A1, EGR1, CSRN1, IL1R1, CEBPB, NFKBIZ, CYP1B1, RCAN1, FOS, NFE2, CDKN1A, NR4A1, MAFB, FZD7
Cellular Development	SOCS3, SGK1, HSPA1A/HSPA1B, EML4, ZFP36L1, Hmga1, SDC4, HES1, TSC22D3, SPRY4, Bbc3, LPIN1, NR0B2, C8orf4, IGF1, SERPINE1, ACPP, MT1H, RIPK4, PFKFB3, AXIN2, ATF3, LCN2, IER3, KLF13, MAFF, SULT2A1, DACT2, DUSP1, SRRM4, BTG2, TFRC, CYR61, NOTCH1, HMG2, PIM3, GADD45B, ZFP36, GADD45G, KLF10, GDF15, SOCS2, SELENBP1, TRIB1, ARRD3, JUN, PPP1R10, TIPARP, FOXO3, SPHK1, SULT1E1, TNFRSF1B, NFE2L2, RASSF1, ADRB2, SLC20A1, CYP1A1, GAS1, EGR1, PPP1R15A, CEBPB, IL1R1, HSPA2, CYP1B1, FOS, RCAN1, NFE2, BMF, ADCY1, CDKN1A, NR4A1, MAFB, BCL2L11, FZD7
Connective Tissue Development and Function	PER1, SOCS3, PIM3, GADD45B, PLK3, HSPA1A/HSPA1B, GADD45G, KLF10, Hmga1, HES1, SDC4, TSC22D3, SELENBP1, LPIN1, JUN, FOXO3, SULT1E1, SPHK1, IGF1, TNFRSF1B, SERPINE1, NFE2L2, MT1H, RASSF1, ADRB2, SLC25A25, ATF3, GAS1, EGR1, PPP1R15A, IL1R1, CEBPB, IER3, FOS, DUSP1, NFE2, CDKN1A, BTG2, NR4A1, TFRC, PER2, NOTCH1, BCL2L11
Hematological System Development and Function	SOCS3, HSPA1A/HSPA1B, EML4, ZFP36L1, Hmga1, HES1, TSC22D3, Bbc3, LPIN1, NR0B2, IGF1, SERPINE1, ACPP, MT1H, ATF3, LCN2, KLF13, APBA3, DUSP1, BTG2, TFRC, CYR61, NOTCH1, HMG2, PIM3, GADD45B, ZFP36, GADD45G, KLF10, GDF15, SOCS2, JUN, TIPARP, FOXO3, SPHK1, LIPG, TNFRSF1B, NFE2L2, ADRB2, SLC20A1, CYP1A1, EGR1, PPP1R15A, IL1R1, CEBPB, NFKBIZ, FOS, RCAN1, NFE2, BMF, CDKN1A, NR4A1, MAFB, BCL2L11, FZD7
Tissue Morphology	SOCS3, PER1, LRP4, HSPA1A/HSPA1B, SGK1, ZFP36L1, Hmga1, SDC4, HES1, TSC22D3, Bbc3, LPIN1, ITPRIP, IGF1, SERPINE1, MT1H, ATF3, LCN2, KLF13, DACT2, DUSP1, TFRC, PER2, NOTCH1, PIM3, GADD45B, ZFP36, GADD45G, KLF10, GDF15, DNAJA1, JUN, FOXO3, SULT1E1, SPHK1, LIPG, TNFRSF1B, NFE2L2, ADRB2, SLC25A25, SLC20A1, CYP1A1, EGR1, PPP1R15A, IL1R1, CEBPB, RCAN1, FOS, NFE2, BMF, CDKN1A, NR4A1, MAFB, BCL2L11
Organ Morphology	PER1, SOCS3, LRP4, ZFP36, HSPA1A/HSPA1B, GADD45G, KLF10, Hmga1, HES1, SDC4, USP2, DNAJA1, TSC22D3, Bbc3, CYP1A2, NR0B2, FOXO3, SPHK1, SULT1E1, IGF1, SERPINE1, TNFRSF1B, NFE2L2, ADRB2, MT1H, RIPK4, CYP1A1, LMO7, GAS1, EGR1, PPP1R15A, NAGS, CEBPB, IL1R1, NFKBIZ, KLF13, CYP1B1, FOS, DUSP1, BMF, NFE2, CDKN1A, G6PC, MAFB, NOTCH1, PER2, BCL2L11
Tumor Morphology	SOCS3, PIM3, ZFP36, HSPA1A/HSPA1B, KLF10, GDF15, Bbc3, TRIB1, JUN, ARRD3, FOXO3, SPHK1, IGF1, SERPINE1, NFE2L2, RASSF1, ATF3, EGR1, LCN2, IL1R1, FOS, RCAN1, DACT2, DUSP1, BTG2, CDKN1A, NR4A1, CYR61, NOTCH1, BCL2L11
Cell Morphology	SOCS3, LRP4, PIM3, SGK1, HSPA1A/HSPA1B, PLK3, KLF10, GDF15, Hmga1, HES1, SDC4, USP2, DNAJA1, TSC22D3, SPRY4, Bbc3, CYP1A2, JUN, FOXO3, SULT1E1, SERPINE1, TNFRSF1B, NFE2L2, RASSF1, ADRB2, MT1H, ATF3, GAS1, EGR1, LCN2, PPP1R15A, IL1R1, CEBPB, KLF13, CYP1B1, RCAN1, FOS, DUSP1, BMF, NFE2, CDKN1A, NR4A1, TFRC, MAFB, CYR61, NOTCH1, BCL2L11, HMG2
Cancer	MVD, LRP4, PER1, SOCS3, HSPA1A/HSPA1B, SGK1, PLK3, EML4, GSTA5, Hmga1, HES1, TSC22D3, Bbc3, LPIN1, CYP1A2, NR0B2, TNFAIP2, LPIN2, IGF1, SERPINE1, ACPP, MT1H, RIPK4, PFKFB3, AXIN2, DDHD1, ATF3, DDIT4, IER2, EDC3, LCN2, CIB3, TAT, DCLK3, IER3, KLF13, APBA3, SLC46A3, ETNK2, DACT2, DUSP1, SLC22A5, BTG2, TFRC, PFAS, CYR61, NOTCH1, PER2, FAM214A, HILPDA, HMG2, GADD45B, ZFP36, GADD45G, KLF10, SOCS2, GDF15, DNAJA1, USP2, SELENBP1, TRIB1, ARRD3, JUN, PPP1R10, FOXO3, SPHK1, SULT1E1, TNFRSF1B, NFE2L2, RASSF1, ADRB2, CYP1A1, MAP3K6, LMO7, GAS1, N4BP2L1, EGR1, IL1R1, CEBPB, DNAJB9, NFKBIZ, HSPA2, A1BG, RHOB, TB1, CYP1B1, FOS, NFE2, BMF, CDKN1A, NR4A1, G6PC, MAFB, TCHH, BCL2L11, FZD7
Immunological Disease	SOCS3, GADD45B, ZFP36, GADD45G, HSPA1A/HSPA1B, Hmga1, SDC4, JUN, CYP1A2, FOXO3, SPHK1, TNFRSF1B, NFE2L2, MT1H, RASSF1, ADRB2, PFKFB3, EGR1, LCN2, CEBPB, IL1R1, IER3, KLF13, CYP1B1, A1BG, FOS, DUSP1, BMF, CDKN1A, SLC7A2, NR4A1, TFRC, PFAS, BCL2L11

Appendix XII: Signaling Pathways from 2 hour IPA Analysis (continued)

Biological Functions and Disease	Molecules
Endocrine System Development and Function	SOCS3,CYP1A1,CYP1A2,TIPARP,CDKN1A,SULT1E1,SERPINE1,NFE2L2,CYP1B1
Vitamin and Mineral Metabolism	CYP1A1,CYP1A2,TIPARP,NR0B2,SULT1E1,NR4A1,G6PC,SULT2A1,CYP1B1
Gastrointestinal Disease	ZFP36,SDC4,HES1,TSC22D3,LPIN1,JUN,NR0B2,FOXO3,IGFBP1,TNFRSF1B,SERPINE1,NFE2L2,MT1H,RASSF1,PFKFB3,EGR1,LCN2,IL1R1,CCRN4L,DUSP1,CDKN1A,SLC22A5,BTG2,NR4A1,TFRC,G6PC,CYR61
Hepatic System Disease	ZFP36,EGR1,SDC4,IL1R1,TSC22D3,CCRN4L,JUN,LPIN1,NR0B2,DUSP1,SLC22A5,CDKN1A,FOXO3,NR4A1,G6PC,IGFBP1,CYR61,SERPINE1,TNFRSF1B,NFE2L2,MT1H,RASSF1
Developmental Disorder	ATF3,HSPA1A/HSPA1B,Hmga1,CEBPB,HES1,IER3,CYP1B1,RCAN1,CYP1A2,JUN,DUSP1,FOXO3,CDKN1A,SULT1E1,SERPINE1,ADRB2,RASSF1
Behavior	PER1,SGK1,HSPA1A/HSPA1B,EGR1,NAGS,IL1R1,USP2,NFKBIZ,FOS,RCAN1,CYP1A2,JUN,DUSP1,ADCY1,CYR61,TNFRSF1B,NOTCH1,PER2,NFE2L2,ADRB2,ACPP
Reproductive System Disease	PFKFB3,CYP1A1,ZFP36,SGK1,HSPA1A/HSPA1B,EGR1,IL1R1,CEBPB,CYP1B1,FOS,C10orf10,JUN,CYP1A2,DUSP1,BMF,NR4A1,IGFBP1,CYR61,TNFRSF1B,BCL2L11,MT1H
Infectious Disease	SOCS3,ZFP36,GDF15,LCN2,CEBPB,IL1R1,APBA3,Bbc3,FOS,DUSP1,SPHK1,LPIN2,TNFRSF1B,SERPINE1,BCL2L11,ADRB2
Carbohydrate Metabolism	Mup1 (includes others),SOCS3,ATF3,PPP1R3C,PPP1R15A,TAT,CEBPB,USP2,NR0B2,DUSP1,NR4A1,G6PC,IGFBP1,SDS,ADRB2
Endocrine System Disorders	CYP1A1,ATF3,LCN2,CEBPB,HES1,CYP1B1,CYP1A2,JUN,DUSP1,FOXO3,BTG2,G6PC,IGFBP1,SERPINE1,TNFRSF1B,ADRB2
Hereditary Disorder	LRP4,CYP1A1,SGK1,HSPA1A/HSPA1B,EGR1,IER3,SDC4,USP2,DNAJA1,MAFF,CYP1B1,TSC22D3,FOS,RCAN1,CYP1A2,JUN,NR4A1,G6PC,ADRB2,HMGB2,MT1H
Organ Development	ZFP36,GADD45G,Hmga1,HES1,DNAJA1,TSC22D3,Bbc3,JUN,CYP1A2,TIPARP,NR0B2,FOXO3,IGFBP1,TNFRSF1B,SERPINE1,NFE2L2,ADRB2,MT1H,RASSF1,CYP1A1,LMO7,GAS1,EGR1,LCN2,CEBPB,IL1R1,HSPA2,CYP1B1,FOS,SRRM4,BMF,ADCY1,CDKN1A,NR4A1,TFRC,MAFB,CYR61,NOTCH1,BCL2L11,FZD7,HMGB2
Tissue Development	PER1,GADD45G,Hmga1,HES1,SDC4,DNAJA1,TSC22D3,SPRY4,Bbc3,LPIN1,JUN,TIPARP,FOXO3,TNFRSF1B,SERPINE1,MT1H,AXIN2,LMO7,GAS1,EGR1,LCN2,CEBPB,IL1R1,HSPA2,CYP1B1,RCAN1,FOS,SRRM4,BMF,CDKN1A,ADCY1,NR4A1,G6PC,MAFB,CYR61,NOTCH1,BCL2L11,HMGB2
Digestive System Development and Function	PER1,SOCS3,LRP4,ZFP36,Hmga1,HES1,SPRY4,JUN,CYP1A2,TIPARP,NR0B2,IGFBP1,TNFRSF1B,SERPINE1,NFE2L2,RASSF1,MT1H,SLC25A25,SLC20A1,AXIN2,CYP1A1,ATF3,GAS1,EGR1,CSRNP1,CEBPB,IL1R1,FOS,DUSP1,CDKN1A,G6PC,CYR61,NOTCH1,PER2,BCL2L11
DNA Replication, Recombination, and Repair	ATF3,FBXO31,HSPA1A/HSPA1B,SGK1,PLK3,GADD45G,PPP1R15A,SDC4,DNAJA1,Bbc3,CCNO,FOS,JUN,INHBE,DUSP1,FOXO3,CDKN1A,BTG2,SPHK1,NR4A1,IGFBP1,CYR61,HMGB2,RASSF1
Organismal Survival	SOCS3,LRP4,ZFP36,HSPA1A/HSPA1B,PPP1R3C,ZFP36L1,SDC4,HES1,SPRY4,Bbc3,CYP1A2,JUN,FOXO3,TNFRSF1B,SERPINE1,NFE2L2,ADRB2,MT1H,RASSF1,SLC25A25,SLC20A1,RIPK4,CYP1A1,LMO7,GAS1,LCN2,PPP1R15A,CSRNP1,NAGS,IL1R1,CEBPB,NFKBIZ,MAFF,APBA3,FOS,DUSP1,BMF,NFE2,CDKN1A,TFRC,G6PC,MAFB,CYR61,PER2,NOTCH1,BCL2L11
Renal and Urological System Development and Function	SOCS3,LRP4,ZFP36,GADD45G,EGR1,CEBPB,SDC4,TSC22D3,FOS,JUN,TIPARP,BMF,ADCY1,FOXO3,CDKN1A,NR4A1,G6PC,MAFB,TNFRSF1B,SERPINE1,BCL2L11,RASSF1,MT1H
Connective Tissue Disorders	PER1,SOCS3,GADD45B,ZFP36,HSPA1A/HSPA1B,SDC4,SELENBP1,JUN,CYP1A2,LPIN1,FOXO3,SPHK1,LPIN2,IGFBP1,SERPINE1,TNFRSF1B,ADRB2,LCN2,CEBPB,IL1R1,KLF13,A1BG,FOS,DUSP1,SLC7A2,CDKN1A,NR4A1,TFRC,PFAS,BCL2L11
Inflammatory Disease	SOCS3,PER1,GADD45B,ZFP36,GADD45G,HSPA1A/HSPA1B,SDC4,SELENBP1,CYP1A2,JUN,LPIN1,NR0B2,FOXO3,SPHK1,LPIN2,IGFBP1,SERPINE1,TNFRSF1B,NFE2L2,ADRB2,MT1H,RASSF1,EGR1,LCN2,CEBPB,IL1R1,KLF13,A1BG,FOS,DUSP1,SLC7A2,CDKN1A,NR4A1,TFRC,PFAS,CYR61,BCL2L11
Skeletal and Muscular Disorders	LRP4,SOCS3,PER1,GADD45B,ZFP36,HSPA1A/HSPA1B,SGK1,SDC4,DNAJA1,USP2,TSC22D3,SELENBP1,CYP1A2,JUN,LPIN1,FOXO3,SPHK1,LPIN2,IGFBP1,TNFRSF1B,MT1H,ADRB2,EGR1,LCN2,IL1R1,CEBPB,IER3,KLF13,MAFF,A1BG,RCAN1,FOS,DUSP1,CDKN1A,SLC7A2,NR4A1,TFRC,G6PC,PFAS,BCL2L11,HMGB2
Cardiovascular Disease	SOCS3,ZFP36,HSPA1A/HSPA1B,GDF15,Hmga1,Bbc3,CYP1A2,JUN,ITPRIP,FOXO3,SULT1E1,LIPG,SERPINE1,TNFRSF1B,NFE2L2,ADRB2,RASSF1,ATF3,EGR1,LCN2,IER3,IL1R1,RCAN1,FOS,DUSP1,CDKN1A,NR4A1,BCL2L11
Organismal Functions	PER1,Mup1 (includes others),HSPA1A/HSPA1B,EGR1,SDC4,IL1R1,CEBPB,CYP1A2,LPIN1,DACT2,DUSP1,NR4A1,LPIN2,TNFRSF1B,SERPINE1,PER2,MT1H,ADRB2
Humoral Immune Response	PIM3,GADD45B,ATF3,GADD45G,EGR1,LCN2,CEBPB,IL1R1,NFKBIZ,FOS,RCAN1,BMF,CDKN1A,SPHK1,TNFRSF1B,BCL2L11,MT1H
Nucleic Acid Metabolism	CYP1A1,CYP1A2,CYP1B1,ACPP
Nervous System Development and Function	PER1,SGK1,EGR1,PPP1R15A,CEBPB,HES1,IL1R1,USP2,RCAN1,FOXO3,ADCY1,TNFRSF1B,NOTCH1,PER2,ADRB2
Dermatological Diseases and Conditions	CYP1A1,ZFP36,SGK1,IER2,KLF10,PPP1R3C,HSPH1,EGR1,LCN2,CEBPB,IL1R1,CYP1B1,FOS,JUN,DUSP1,CDKN1A,SERPINE1,TNFRSF1B,NOTCH1,NFE2L2,ACPP,FZD7,RASSF1

Appendix XII: Signaling Pathways from 2 hour IPA Analysis (continued)

Biological Functions and Disease	Molecules
Psychological Disorders	LRP4,SGK1,HSPA1A/HSPA1B,EGR1,IER3,SDC4,USP2,DNAJA1,MAFF,TSC22D3,FOS,RCAN1,JUN,NR4A1,G6PC,ADRB2,HMGB2,MT1H
Visual System Development and Function	LMO7,GAS1,EGR1,LCN2,IL1R1,HES1,CYP1B1,FOS,ADCY1,CDKN1A,SERPINE1,TNFRSF1B,NOTCH1,MT1H
Energy Production	CYP1A1,CYP1A2,CYP1B1
Metabolic Disease	ZFP36,HSPA1A/HSPA1B,PPP1R3C,KLF10,GDF15,Hmga1,HES1,TSC22D3,JUN,LPIN1,NR0B2,FOXO3,IGFBP1,TNFRSF1B,SERPINE1,ADRB2,Mup1 (includes others),ATF3,LCN2,CEBPB,IL1R1,DUSP1,ADCY1,BTG2,CDKN1A,NR4A1,G6PC,BCL2L11
Renal and Urological Disease	GADD45B,HSPA1A/HSPA1B,GADD45G,SELENBP1,TRIB1,JUN,FOXO3,SERPINE1,TNFRSF1B,NFE2L2,MT1H,ADRB2,RASSF1,CYP1A1,ATF3,LCN2,CEBPB,IL1R1,FOS,DUSP1,NFE2,CDKN1A,BTG2,CYR61,BCL2L11,HILPDA
Cardiovascular System Development and Function	SOCS3,PIM3,ZFP36L1,HES1,SDC4,SPRY4,Bbc3,JUN,TIPARP,FOXO3,SPHK1,SERPINE1,NFE2L2,ADRB2,RASSF1,ATF3,MAP3K6,LCN2,PPP1R15A,CYP1B1,RCAN1,NFE2,CDKN1A,NR4A1,TFRC,CYR61,NOTCH1,HMGB2
Respiratory Disease	CYP1A1,GADD45B,LMO7,ZFP36,PLK3,GAS1,LCN2,HES1,CYP1B1,JUN,DACT2,FOXO3,CDKN1A,SPHK1,MAFB,CYR61,SERPINE1,NOTCH1,NFE2L2,ADRB2,RASSF1
RNA Damage and Repair	FOS,AXIN2,ZFP36,HSPA1A/HSPA1B,ZFP36L1
Amino Acid Metabolism	EGR1,SLC7A2,SLC22A5,TAT,NAGS,PFAS,SDS
Cell Signaling	SOCS3,AXIN2,GADD45B,MAP3K6,GADD45G,HSPA1A/HSPA1B,SDC4,CEBPB,CYP1B1,Bbc3,TRIB1,JUN,DUSP1,ADCY1,CDKN1A,SLC7A2,TNFRSF1B,NOTCH1,ADRB2
Cell-To-Cell Signaling and Interaction	PER1,HSPA1A/HSPA1B,EGR1,LCN2,PPP1R15A,IL1R1,JUN,FOXO3,CDKN1A,TNFRSF1B,SERPINE1,CYR61,NOTCH1,NFE2L2
RNA Post-Transcriptional Modification	FOS,AXIN2,ZFP36,ZFP36L1
Free Radical Scavenging	SOCS3,CYP1A1,DDIT4,CYP1B1,FOS,JUN,CYP1A2,DUSP1,NFE2,CDKN1A,FOXO3,NR4A1,TFRC,CYR61,NFE2L2,BCL2L11
Immune Cell Trafficking	SOCS3,PER1,HSPA1A/HSPA1B,EGR1,LCN2,PPP1R15A,IL1R1,NFKBIZ,APBA3,DUSP1,CDKN1A,SPHK1,G6PC,CYR61,TNFRSF1B,SERPINE1,NOTCH1,NFE2L2,ADRB2
Respiratory System Development and Function	GAS1,HES1,IL1R1,SPRY4,CYP1A2,NR0B2,DUSP1,CDKN1A,TNFRSF1B,SERPINE1,NOTCH1,NFE2L2,ADRB2

Appendix XIII: Canonical Pathways from 2 hour IPA Analysis

© 2000-2013 Ingenuity Systems, Inc. All rights reserved.	
Canonical Pathways	Molecules
Glucocorticoid Receptor Signaling	FOS,JUN,DUSP1,SGK1,HSPA1A/HSPA1B,FOXO3,CDKN1A,TAT,CEBPB,SERPINE1,HSPA2,TSC22D3,ADRB2
Aryl Hydrocarbon Receptor Signaling	FOS,CYP1A1,CYP1A2,JUN,NR0B2,GSTA5,CDKN1A,NFE2L2,CYP1B1
IL-17A Signaling in Fibroblasts	FOS,JUN,LCN2,CEBPB,NFKBIZ
IGF-1 Signaling	SOCS3,FOS,JUN,FOXO3,SOCS2,IGFBP1,CYR61
PXR/RXR Activation	CYP1A2,NR0B2,FOXO3,G6PC,IGFBP1,SULT2A1
Acute Phase Response Signaling	SOCS3,FOS,JUN,SOCS2,IL1R1,CEBPB,TNFRSF1B,SERPINE1
Aldosterone Signaling in Epithelial Cells	HSPA1A/HSPA1B,DUSP1,SGK1,HSPH1,DNAJB9,DNAJA1,HSPA2
Prolactin Signaling	SOCS3,FOS,JUN,SOCS2,CEBPB
IL-6 Signaling	SOCS3,FOS,JUN,IL1R1,CEBPB,TNFRSF1B
VDR/RXR Activation	CDKN1A,HES1,CEBPB,IGFBP1,SULT2A1
GADD45 Signaling	GADD45B,GADD45G,CDKN1A
NRF2-mediated Oxidative Stress Response	FOS,JUN,GSTA5,DNAJB9,DNAJA1,MAFF,NFE2L2
HMGB1 Signaling	FOS,JUN,IL1R1,TNFRSF1B,SERPINE1
PPAR Signaling	FOS,JUN,NR0B2,IL1R1,TNFRSF1B
ATM Signaling	JUN,GADD45B,GADD45G,CDKN1A
TNFR2 Signaling	FOS,JUN,TNFRSF1B
JAK/Stat Signaling	SOCS3,FOS,CDKN1A,SOCS2
LPS/IL-1 Mediated Inhibition of RXR Function	JUN,NR0B2,GSTA5,SULT1E1,IL1R1,TNFRSF1B,SULT2A1
IL-10 Signaling	SOCS3,FOS,JUN,IL1R1
Xenobiotic Metabolism Signaling	CYP1A1,CYP1A2,MAP3K6,GSTA5,SULT1E1,NFE2L2,SULT2A1,CYP1B1
Production of Nitric Oxide and Reactive Oxygen Species in Macrophages	FOS,JUN,PPP1R10,MAP3K6,PPP1R3C,TNFRSF1B
Ceramide Signaling	FOS,JUN,SPHK1,TNFRSF1B
GNRH Signaling	FOS,JUN,MAP3K6,EGR1,ADCY1
Insulin Receptor Signaling	SOCS3,PPP1R10,SGK1,PPP1R3C,FOXO3
Hepatic Cholestasis	JUN,NR0B2,ADCY1,IL1R1,TNFRSF1B
CDK5 Signaling	PPP1R10,PPP1R3C,EGR1,ADCY1
p53 Signaling	JUN,GADD45B,GADD45G,CDKN1A
IL-1 Signaling	FOS,JUN,ADCY1,IL1R1
CD27 Signaling in Lymphocytes	FOS,JUN,MAP3K6
HGF Signaling	FOS,JUN,MAP3K6,CDKN1A
UVB-Induced MAPK Signaling	FOS,JUN,HIST2H3C (includes others)
Type I Diabetes Mellitus Signaling	SOCS3,SOCS2,IL1R1,TNFRSF1B
Role of Macrophages, Fibroblasts and Endothelial Cells in Rheu Arthritis	SOCS3,FOS,JUN,IL1R1,CEBPB,TNFRSF1B,FZD7
Corticotropin Releasing Hormone Signaling	FOS,JUN,ADCY1,NR4A1
Type II Diabetes Mellitus Signaling	SOCS3,SOCS2,CEBPB,TNFRSF1B

Appendix XIV: Functional Pathways from 2 hour IPA Analysis

© 2000-2013 Ingenuity Systems, Inc. All rights reserved.			
ID	Top Diseases and Functions	Focus Molecules	Molecules in Network
1	Cell Death and Survival, Neurological Disease, Cancer	22	14-3-3, Akt, ATF3, Bcl2L1, BMF, BTG2, CCN0, Cyclin A, Cyclin E, CYR61, DDIT4, E2f, EDC3, EGR1, EML4, FOXO3, Foxo, GDF15, Hmga1, IER2, IER3, Igm, IL1R1, JINK1/2, MAFF, MAP2K1/2, p70 S6k, PDGF BB, PER2, PI3K (family), PPP1R15A, SERCA, ZFP36, ZFP36L1
2	Cell Signaling, Post-Translational Modification, Cellular Function and Maintenance	20	alcohol group acceptor phosphotransferase, Alpha catenin, CEP350, G6PC, GADD45B, GADD45G, GAS1, Growth hormone, HDL-cholesterol, ICN2, LDL, LDL-cholesterol, LIPG, LMOT, MAP3K6, MAP3K, Mup1 (includes others), NFkB (complex), NFkB2, Notch, NR0B2, Nr1h, PDIA4, PFAS, PFKFB3, PLK3, Plk, Pro-inflammatory Cytokine, Raf, RPK4, SAA, Sapk, SGK1, SLC38A2, TNFAIP2
3	Endocrine System Development and Function, Small Molecule Biochemistry, Drug Metabolism	16	ADCY1, Ahr-Amt, Ahr-aryl hydrocarbon-Amt, Cebp, CYP1A1, CYP1A2, CYP1B1, ERK1/2, ETS, GC-GCR dimer, Glucocorticoid-GCR, Gm-cst, GST, GSTA5, KLf13, MT1H, N-cor, PEPCCK, PIM3, Rar, Rxr, SAP30, SLC46A3, SOCS2, SPRY4, Stat3, Stat3, SULT1E1, SWI-SNF, TAT, Thyroid hormone receptor, TRIB1, TSC2D3, TSH, unspecific monooxygenase, VLDL-cholesterol
4	Cellular Assembly and Organization, Cellular Compromise, Cell-To-Cell Signaling and Interaction	16	APP, ARPP19, ASCC1, AXIN2, C10orf10, C1orf51, CD164, CRYBB3, CSRN1, ELAVL1, FAM84B, FBXW9, GILP2, GLIS2, GLOD4, GRB2, H2-K2/H2-Q9, IFNG, INHBE, MAT2B, NAGS, NAPB, NEFL, Neur3, NR1H4, PCP4L1, PTP4A1, RAB2B, RASL11B, SLC38A2, TMEM101, UPP2, VIM, xylool, ZKSCAN1
5	Hereditary Disorder, Neurological Disease, Dermatological Diseases and Conditions	15	ANKS1A, ARAF, ARHGGEF5, ARHGGEF17, C10orf24, CALML5, CEP57, COQ10B, DDHD1, DTX2, EDC3, E FHD1, FLG, GCC1, HILPDA, KIAA1217, LRRCC41, MELK, MPRIP, RACGAP1, RHBDD2, RHOBTB1, SFN, SHCBP1, SHROOM1, SLC25A25, SLC7A2, SYNPO, TCHH, TMEM100, TNFAIP8L1, UBC, YTHDC1, ZNF503, ZNF638
6	Cell Death and Survival, Liver Necrosis/Cell Death, Cancer	14	26s Proteasome, ACPP, Actin, ADCY, ARDC3, CCRN4L, CD3, Cg, Collagen(s), DNAJB9, Fgf, FOS, FSH, he moglobin, Histone h3, Hsp22/Hsp40/Hsp90, HSPA1A/HSPA1B, Insulin, Integrin, JUN, Lh, Mapk, Mmp, NFE2, NFE2L2, NOTCH1, PER1, RNA polymerase II, SELENBP1, SLC20A1, Sos, trypsin, Ubiquitin, USP2, Vegf
7	Cell Cycle, Nervous System Development and Function, Tissue Morphology	14	A1BG, Alp, Cbp/p300, Cdc2, CDKN1A, Creb, Cyclin B, ERK, estrogen receptor, Fc gamma receptor, GOT, Hdac, HES1, HISTONE, Histone H4, HMGB2, IGFBP1, IL-2R, ITPRIP, JUN, JUND, JUND, KLF10, LRP4, MAFB, RASSF1, Rb, Rhox5, SERPINE1, SLC22A5, Smad, SULT2A1, TCF, Tgf beta, thymidine kinase, TMSB4, VitaminD3-VDR-RXR
8	Drug Metabolism, Embryonic Development, Organismal Development	13	AHR, AIP, ARLB, ATOH8, B2W2, CACNA1A, CAMK2N2, CBR3, CCND1, CDKN2D, Ces2b/Ces2c, CYP1A1, DACT2, DCLK3, DNAJB5, EPO, FBXO31, HIST2H3C (includes others), HNF4A, HSPH1, KDM5C, KIF20A, LTBP3, MID1P1, MTTH, N4BP2L1, PMM1, SERPINA7, SLC35A2, SP2, SRRM4, TRIP11, TSPYL2, UGT1A6, vitamin A
9	Organismal Functions, Skeletal and Muscular System Development and Function, Tissue Morphology	13	ADRB, C8orf4, Calcineurin A, Calcineurin protein(s), Caspase 3/7, Ck2, cytochrome C, DUSP1, FAM110C, FAM214A, Fcgr1, Gsk3, Jnk, Laminin, LPIN1, MEK2, Mek, MVD, NFAT (complex), Nfat (family), NMDA Receptor, NR4A1, PARP, Pdof (complex), phosphatase, Pkc(s), PP1 protein complex group, PP2A, PPP1R10, PPP1R3C, PPTC7, Rap1, RCAN1, SDC4, TIPARP
10	Infectious Disease, Connective Tissue Disorders, Hematological Disease	8	AMPK, Ap1, APBA3, BCR (complex), DNAA1, Hsp27, Hsp70, HSP, HSPA2, Ifn, IFN Beta, Ige, IgG1, IgG, IgG2a, Ikb, IL1, IL12 (complex), IL12 (family), Immunoglobulin, Interferon alpha, LPIN2, NADPH oxidase, P38 MAPK, PI3K (complex), SOCS3, SPHK1, SRC (family), STAT3a/b, TCR, TFRG, Tfr, Tnf (family), TNFRSF1B, tyrosine kinase
11	Cell Signaling, Molecular Transport, Nucleic Acid Metabolism	5	ACER2, ADRA2A, ADRB2, Calmodulin, caspase, DCL1, ETNK2, Focal adhesion kinase, FZD3, FZD7, G2C, GIPR, GLP1R, GNRH, Gpr, GPR68, GPR155, HCAR1, HTR7, IKK (complex), LPHN3, MTNR1B, NOL3, NPS, NPY2R, P2RY2, PCNX, Pka, Rac, Ras, Ras
12	Cancer, Hematological Disease, Reproductive System Disease	1	homolog, S1PR2, SDS, STAT
13	Auditory Disease, Hereditary Disorder, Neurological Disease	1	CIB3, TUBB2A
		1	CASR, CLDN6, CLDN14, cldn

Permission to Publish



Council

Kenneth E. Thummel
President
University of Washington

David R. Sibley
President-Elect
Bethesda, Maryland

Annette E. Fleckenstein
Past President
University of Utah

Dennis C. Marshall
Secretary/Treasurer
Ferring Pharmaceuticals, Inc.

Charles P. France
Secretary/Treasurer-Elect
University of Texas Health Science
Center — San Antonio

Paul A. Insel
Past Secretary/Treasurer
University of California — San Diego

John D. Schuetz
Councilor
St. Jude Children's Research Hospital

Margaret E. Gnegy
Councilor
University of Michigan Medical School

Wayne L. Backes
Councilor
Louisiana State University Medical
Center

Mary E. Vore
Chair, Board of Publications Trustees
University of Kentucky

Brian M. Cox
FASEB Board Representative
Uniformed Services University
of the Health Sciences

Scott A. Waldman
Chair, Program Committee
Thomas Jefferson University

Judith A. Siuciak
Executive Officer

August 6, 2015

Dan Jackson
NRSA F31
Graduate School of Biomedical Sciences
University of Texas Medical Branch
106 Whiting Ave
Galveston, TX 77550

Email: dp3jacks@UTMB.EDU

Dear Mr. Jackson:

This is to grant you permission to include the following article in your doctoral dissertation entitled "A Rhapsody on the Aryl Hydrocarbon Receptor: Molecular and Environmental Health Insights Via Novel and Canonical Signaling Pathways" for the University of Texas Medical Branch, Galveston:

Daniel P. Jackson, Hui Li, Kristen A. Mitchell, Aditya D. Joshi, and
Cornelis J. Elferink, Ah Receptor-Mediated Suppression of Liver
Regeneration through NC-XRE-Driven p21^{Cip1} Expression, *Mol*
Pharmacol April 2014 85:533-541

On the first page of each copy of this article, please add the following:

Reprinted with permission of the American Society for Pharmacology
and Experimental Therapeutics. All rights reserved.

In addition, the original copyright line published with the paper must be shown
on the copies included with your thesis.

Sincerely yours,

Richard Dodenhoff
Journals Director

References

- Abdelrahim M, Ariazi E, Kim K, Khan S, Barhoumi R, Burghardt R, Liu S, Hill D, Finnell R, Wlodarczyk B, Jordan VC, and Safe S (2006) 3-Methylcholanthrene and other aryl hydrocarbon receptor agonists directly activate estrogen receptor alpha. *Cancer Research* **66**:2459–2467.
- Abdelrahim M, Smith R, and Safe S (2003) Aryl hydrocarbon receptor gene silencing with small inhibitory RNA differentially modulates Ah-responsiveness in MCF-7 and HepG2 cancer cells. *Molecular Pharmacology* **63**:1373–1381.
- Akilov OE, Ustyugova IV, Zhi L, Hasan T, and Wu MX (2009) Enhanced susceptibility to Leishmania infection in resistant mice in the absence of immediate early response gene X-1. *Journal of Immunology* **183**:7994–8003
- Albrecht JH, Meyer AH, and Hu MY (1997) Regulation of cyclin-dependent kinase inhibitor p21WAF1/Cip1/Sdi1 gene expression in hepatic regeneration. *Hepatology* **25**:557–563.
- Albrecht JH, Poon RY, Ahonen CL, Rieland BM, Deng C, and Crary GS (1998) Involvement of p21 and p27 in the regulation of CDK activity and cell cycle progression in the regenerating liver. *Oncogene* **16**:2141–2150.
- Alfred LJ, and Gelboin HV (1967) Benzpyrene hydroxylase induction by polycyclic hydrocarbons in hamster embryonic cells grown in vitro. *Science* **157**:75–76.
- Allan SE, Smith BW, and Anderson KA (2012) Impact of the Deepwater Horizon Oil Spill on Bioavailable Polycyclic Aromatic Hydrocarbons in Gulf of Mexico Coastal Waters. *Environmental Science and Technology* **46**:2033–2039.

- Andreoli V, Gehrau RC, and Bocco JL (2010) Biology of Krüppel-like factor 6 transcriptional regulator in cell life and death. *IUBMB Life* **62**:896–905.
- Arlt A, and Schäfer H (2011) Role of the immediate early response 3 (IER3) gene in cellular stress response, inflammation and tumorigenesis. *European Journal of Cell Biology* **90**:545–552.
- Arpiainen S, Raffalli-Mathieu F, Lang M, Polkonen O, and Hakkola J (2005) Regulation of the Cyp2a5 Gene Involves an Aryl Hydrocarbon Receptor-Dependent Pathway. *Molecular Pharmacology* **67**:1325–1333.
- Ashida H, Nagy S, and Matsumura F (2000) 2,3,7,8-tetrachlorodibenzo-p-dioxin (TCDD)-induced changes in activities of nuclear protein kinases and phosphatases affecting DNA binding activity of c-Myc and AP-1 in the livers of guinea pigs. *Biochemical Pharmacology* **59**:741–751.
- Auyeung DJ, Kessler FK, and Ritter JK (2003) Mechanism of rat UDP-glucuronosyltransferase 1A6 induction by Oltipraz: evidence for a contribution of the Aryl hydrocarbon receptor pathway. *Molecular Pharmacology* **63**:119–127.
- Baccarelli A, Pesatori AC, Masten SA, and Patterson DG Jr (2004) Aryl-hydrocarbon receptor-dependent pathway and toxic effects of TCDD in humans: a population-based study in Seveso, Italy. *Toxicology Letters* **149**:287–293.
- Backlund M, and Ingelman-Sundberg M (2005) Regulation of Aryl Hydrocarbon Receptor Signal Transduction by Protein Tyrosine Kinases. *Cellular Signaling* **17**:39–48.
- Barhoover MA, Hall JM, Greenlee WF, and Thomas RS (2010) Aryl Hydrocarbon Receptor Regulates Cell Cycle Progression in Human Breast Cancer Cells via a

Functional Interaction with Cyclin-Dependent Kinase 4. *Molecular Pharmacology* **77**:195–201.

Barry G, Cook JW, Haslewood GAD, Hewett CL, Hieger I, and Kennaway EL (1935) The Production of Cancer by Pure Hydrocarbons.--Part III. *Proceedings of the Royal Society B: Biological Sciences* **117**:318–351.

Bechmann LP, Gastaldelli A, Vetter D, Patman GL, Pascoe L, Hannivoort RA, Lee UE, Fiel I, Muñoz U, Ciociaro D, Lee Y-M, Buzzigoli E, Miele L, Hui KY, Bugianesi E, Burt AD, Day CP, Mari A, Agius L, Walker M, Friedman SL, and Reeves HL (2012) Glucokinase links Krüppel-like factor 6 to the regulation of hepatic insulin sensitivity in nonalcoholic fatty liver disease. *Hepatology* **55**:1083–1093.

Benzeno S, Narla G, Allina J, Cheng GZ, Reeves HL, Banck MS, Odin JA, Diehl JA, Germain D, and Friedman SL (2004) Cyclin-dependent kinase inhibition by the KLF6 tumor suppressor protein through interaction with cyclin D1. *Cancer Research* **64**:3885–3891.

Bian Z, Peng Y, You Z, Wang Q, Miao Q, Liu Y, Han X, Qiu D, Li Z, and Ma X (2013) CCN1 expression in hepatocytes contributes to macrophage infiltration in nonalcoholic fatty liver disease in mice. *Journal of Lipid Research* **54**:44–54.

Bieker JJ (2001) Kruppel-like Factors: Three Fingers in Many Pies. *Journal of Biological Chemistry* **276**:34355–34358.

Binder BR, Christ G, Gruber F, Grubic N, Hufnagl P, Krebs M, Mihaly J, and Prager GW (2002) Plasminogen Activator Inhibitor 1: Physiological and Pathophysiological Roles. *Physiology* **17**:56–61.

- Bock KW (2012) Ah receptor- and Nrf2 gene battery members: Modulators of quinone-mediated oxidative and endoplasmic reticulum stress. *Biochemical Pharmacology* **83**:833–838.
- Bock KW, and Köhle C (2006) Ah receptor: Dioxin-mediated toxic responses as hints to deregulated physiologic functions. *Biochemical Pharmacology* **72**:393–404.
- Botella LM, Sanz-Rodriguez F, Komi Y, Fernandez-L A, Varela E, Garrido-Martin EM, Narla G, Friedman SL, and Kojima S (2009) TGF- β regulates the expression of transcription factor KLF6 and its splice variants and promotes co-operative transactivation of common target genes through a Smad3–Sp1–KLF6 interaction. *Biochemical Journal* **419**:485–495.
- Boutros PC, Bielefeld KA, Pohjanvirta R, and Harper PA (2009) Dioxin-Dependent and Dioxin-Independent Gene Batteries: Comparison of Liver and Kidney in AHR-Null Mice. *Toxicological Sciences* **112**:245–256.
- Boverhof DR, Burgoon LD, Tashiro C, Chittim B, Harkema JR, Jump DB, and Zacharewski TR (2005) Temporal and Dose-Dependent Hepatic Gene Expression Patterns in Mice Provide New Insights into TCDD-Mediated Hepatotoxicity. *Toxicological Sciences* **85**:1048–1063.
- Bradfield CA, Glover E, and Poland A (1991) Purification and N-terminal amino acid sequence of the Ah receptor from the C57BL/6J mouse. *Molecular Pharmacology* **39**:13–19.
- Budinsky RA, Schrenk D, Simon T, Van den Berg M, Reichard JF, Silkworth JB, Aylward LL, Brix A, Gasiewicz T, Kaminski N, Perdew G, Starr TB, Walker NJ, and Rowlands JC (2014) Mode of action and dose-response framework analysis for

receptor-mediated toxicity: The aryl hydrocarbon receptor as a case study. *Critical Reviews in Toxicological* **44**:83–119.

Burbach KM, Poland A, and Bradfield CA (1992) Cloning of the Ah-receptor cDNA reveals a distinctive ligand-activated transcription factor. *Proceedings of the National Academy of Sciences* **89**:8185–8189.

Burns KA, Zorrilla LM, Hamilton KJ, Reed CE, Birnbaum LS, and Korach KS (2013) A Single Gestational Exposure to 2,3,7,8-Tetrachlorodibenzo-p-dioxin Disrupts the Adult Uterine Response to Estradiol in Mice. *Toxicological Sciences* **136**:514–526.

Carls MG, Heintz R, Moles A, Rice SD, and Short JW (2001) Long-Term Biological Damage: What is Known, and How Should that Influence Decisions on Response, Assessment, and Restoration? *Biodiversity and Bioremediation* 399-403

Carrier F, Owens RA, Nebert DW, and Puga A (1992) Dioxin-dependent activation of murine Cyp1a-1 gene transcription requires protein kinase C-dependent phosphorylation. *Molecular and Cellular Biology* **12**(4):1856–1863.

Carver LA, and Bradfield CA (1997) Ligand-dependent Interaction of the Aryl Hydrocarbon Receptor with a Novel Immunophilin Homolog in Vivo. *Journal of Biological Chemistry* **272**:11452–11456.

Chang C-C, Sue Y-M, Yang N-J, Lee Y-H, and Juan S-H (2014) 3-Methylcholanthrene, an AhR agonist, caused cell-cycle arrest by histone deacetylation through a RhoA-dependent recruitment of HDAC1 and pRb2 to E2F1 complex. *PLoS ONE* **9**:e92793–e92793.

- Chang C-Y, Smith DR, Prasad VS, Sidman CL, Nebert DW, and Puga A (1993) Ten nucleotide differences, five of which cause amino acid changes, are associated with the Ah receptor locus polymorphism of C57BL/6 and DBA/2 mice. *Pharmacogenetics and Genomics* **3**:312.
- Chang CY, and Puga A (1998) Constitutive activation of the aromatic hydrocarbon receptor. *Molecular and Cellular Biology* **18**:525–535.
- Chanton J, Zhao T, Rosenheim BE, Joye S, Bosman S, Brunner C, Yeager KM, Diercks AR, and Hollander D (2015) Using Natural Abundance Radiocarbon To Trace the Flux of Petrocarbon to the Seafloor Following the Deepwater Horizon Oil Spill. *Environmental Science and Technology* **49**:847–854.
- Chen CW, and Chu M (1991) *Dose–Response Analysis of Ingested Benzo[a]Pyrene* (CAS No. 50-32-8), Washington, DC.
- Chen HS, and Perdew GH (1994) Subunit Composition of the Heteromeric Cytosolic Aryl Hydrocarbon Receptor Complex. *Journal of Biological Chemistry* **269**:27554–27558.
- Chen P-H, Chang H, Chang JT, and Lin P (2012) Aryl hydrocarbon receptor in association with RelA modulates IL-6 expression in non-smoking lung cancer. *Oncogene* **31**:2555–2565.
- Chen Y, Shen G, Su S, Shen H, Huang Y, Li T, Li W, Zhang Y, Lu Y, Chen H, Yang C, Lin N, Zhu Y, Fu X, Liu W, Wang X, and Tao S (2014) Contamination and distribution of parent, nitrated, and oxygenated polycyclic aromatic hydrocarbons in smoked meat. *Environmental Science and Pollution Research* **21**:11521–11530.

- Chen YJ, Hung CM, Kay N, Chen CC, and Kao YH (2012) Progesterone receptor is involved in 2,3,7,8-tetrachlorodibenzo-p-dioxin-stimulated breast cancer cells proliferation. *Cancer Letters* **319**:223–231.
- Chopra M, and Schrenk D (2011) Dioxin toxicity, aryl hydrocarbon receptor signaling, and apoptosis-persistent pollutants affect programmed cell death. *Critical Reviews in Toxicology* **41**:292–320.
- Christensen J, Cloos P, Toftegaard U, Klinkenberg D, Bracken AP, Trinh E, Heeran M, Di Stefano L, and Helin K (2005) Characterization of E2F8, a novel E2F-like cell-cycle regulated repressor of E2F-activated transcription. *Nucleic Acids Research* **33**:5458–5470.
- Conney AH, Gillette JR, Inscoe ER, Trams ER, and Posner HS (1959) Induced Synthesis of Liver Microsomal Enzymes Which Metabolize Foreign Compounds. *Science* **130**:1478–1479.
- Conney AH, Miller EC, and Miller JA (1957) Substrate-Induced Synthesis And Other Properties Of Benzpyrene Hydroxylase In Rat Liver. *Journal of Biological Chemistry*. **223** 753-766
- Conney AH, Miller EC, and Miller JA (1956) The Metabolism of Methylated Aminoazo Dyes: V. Evidence For Induction of Enzyme Synthesis in the Rat by 3-Methylcholanthrene. *Cancer Research* **16**:450–459.
- Cook JW, Hewett CL, and Hieger I (1933) 106. The isolation of a cancer-producing hydrocarbon from coal tar. Parts I, II, and III. *Journal of the Chemical Society* 395–405.

- D'Astolfo DS, Gehrau RC, Bocco JL, and Koritschoner NP (2008) Silencing of the transcription factor KLF6 by siRNA leads to cell cycle arrest and sensitizes cells to apoptosis induced by DNA damage. *Cell Death and Differentiation* **15**:613–616.
- Davis BJ, McCurdy EA, Miller BD, Lucier GW, and Tritscher AM (2000) Ovarian Tumors in Rats Induced by Chronic 2,3,7,8-Tetrachlorodibenzo-p- Dioxin Treatment. *Cancer Research* **60**:5414–5419.
- Deng Q, Wang Q, Zong W-Y, Zheng D-L, Wen Y-X, Wang K-S, Teng X-M, Zhang X, Huang J, and Han Z-G (2010) E2F8 contributes to human hepatocellular carcinoma via regulating cell proliferation. *Cancer Research* **70**:782–791.
- Denis M, Wikström AC, and Gustafsson JA (1987) The molybdate-stabilized nonactivated glucocorticoid receptor contains a dimer of Mr 90,000 non-hormone-binding protein. *Journal of Biological Chemistry* **262**:11803–11806.
- Denison MS, and Nagy SR (2003) Activation of The Aryl Hydrocarbon Receptor by Structurally Diverse Exogenous and Endogenous Compounds. *Annual Review of Pharmacology and Toxicology* **43**:309–334.
- Denison MS, Fisher JM, and Whitlock JP (1988a) Inducible, receptor-dependent protein-DNA interactions at a dioxin-responsive transcriptional enhancer. *Proceedings of the National Academy of Science* **85**:2528–2532.
- Denison MS, Fisher JM, and Whitlock JP (1988b) The DNA recognition site for the dioxin-Ah receptor complex. Nucleotide sequence and functional analysis. *Journal of Biological Chemistry*. **263** 17221-17224

- Denison MS, Soshilov AA, He G, DeGroot DE, and Zhao B (2011) Exactly the same but different: promiscuity and diversity in the molecular mechanisms of action of the aryl hydrocarbon (dioxin) receptor. *Toxicological Sciences* **124**:1–22.
- Denison MS, Zhao B, Baston DS, Clark GC, Murata H, and Han D (2004) Recombinant cell bioassay systems for the detection and relative quantitation of halogenated dioxins and related chemicals. *Talanta* **63**:1123–1133.
- Dere E, Lo R, Celius T, Matthews J, and Zacharewski T (2011) Integration of Genome-Wide Computation DRE Search, AhR ChIP-chip and Gene Expression Analyses of TCDD-Elicited Responses in the Mouse Liver. *BMC Genomics* **12**:365
- Dickey RW (2012) FDA Risk Assessment of Seafood Contamination after the BP Oil Spill. *Environmental Health Perspectives* **120**:a54–a55.
- Dietrich C, and Kaina B (2010) The aryl hydrocarbon receptor (AhR) in the regulation of cell-cell contact and tumor growth. *Carcinogenesis* **31**:1319–1328.
- DiFeo A, Narla G, Camacho-Vanegas O, Nishio H, Rose SL, Buller RE, Friedman SL, Walsh MJ, and Martignetti JA (2006) E-cadherin is a novel transcriptional target of the KLF6 tumor suppressor. *Oncogene* **25**:6026–6031.
- DiNatale BC, Murray IA, Schroeder JC, Flaveny CA, Lahoti TS, Laurenzana EM, Omiecinski CJ, and Perdew GH (2010) Kynurenic acid is a potent endogenous aryl hydrocarbon receptor ligand that synergistically induces interleukin-6 in the presence of inflammatory signaling. *Toxicological Sciences* **115**:89–97.
- DiNatale BC, Schroeder JC, Francey LJ, Kusnadi A, and Perdew GH (2010) Mechanistic insights into the events that lead to synergistic induction of interleukin 6

- transcription upon activation of the aryl hydrocarbon receptor and inflammatory signaling. *Journal of Biological Chemistry* **285**:24388–24397.
- Ding YS, Ashley DL, and Watson CH (2007) Determination of 10 carcinogenic polycyclic aromatic hydrocarbons in mainstream cigarette smoke. *Journal of Agricultural and Food Chemistry* **55**:5966–5973.
- Dolwick KM, Schmidt JV, Carver LA, Swanson HI, and Bradfield CA (1993) Cloning and expression of a human Ah receptor cDNA. *Molecular and Cellular Biology* **4**:911–917.
- Duan R, Porter W, Samudio I, Vyhldal C, Kladde M, and Safe S (1999) Transcriptional Activation of c-fos Protooncogene by 17 β -Estradiol: Mechanism of Aryl Hydrocarbon Receptor-Mediated Inhibition. *Molecular Endocrinology* **13**:1511–1521.
- Dunn TJ, Lindahl R, and Pitot HC (1988) Differential gene expression in response to 2,3,7,8-tetrachlorodibenzo-p-dioxin (TCDD). Non-coordinate regulation of a TCDD-induced aldehyde dehydrogenase and cytochrome P-450c in the rat. *Journal of Biological Chemistry* **263**: 10878-10886.
- Durand M, Bodker JS, Christensen A, M DD, Hansen M, Jensen JK, Kjelgaard S, Mathiasen L, Pedersen KE, Skeldal S, Wind T, and Andreasen PA (2004) Plasminogen activator inhibitor-I and tumour growth, invasion, and metastasis. *Journal of Thrombosis and Haemostasis* **91**:438–449.
- Eaton DL, and Bammler TK (1999) Concise review of the glutathione S-transferases and their significance to toxicology. *Toxicological Sciences* **49**:156–164.

- Eisler R (2004) Polycyclic Aromatic Hydrocarbon Hazards to Fish, Wildlife, and Invertebrates: A Synoptic Review. *US Fish and Wildlife Service* **85**:81.
- Elferink CJ (2003) Aryl Hydrocarbon Receptor-mediated Cell Cycle Control. *Progress in Cell Cycle Research* **5**:261–267.
- Elferink CJ, and Whitlock JP (1990) 2,3,7,8-Tetrachlorodibenzo-p-dioxin-inducible, Ah receptor-mediated bending of enhancer DNA. *Journal of Biological Chemistry* **265**:5718–5721.
- Elferink CJ, Gasiewicz TA, and Whitlock JP (1990) Protein-DNA interactions at a dioxin-responsive enhancer. Evidence that the transformed Ah receptor is heteromeric. *Journal of Biological Chemistry* **265**:20708–20712.
- Elferink CJ, Ge NL, and Levine A (2001) Maximal aryl hydrocarbon receptor activity depends on an interaction with the retinoblastoma protein. *Molecular Pharmacology* **59**:664–673.
- Elizondo G, Fernandez-Salguero P, Sheikh MS, Kim G-Y, Fornace AJ, Lee KS, and Gonzalez FJ (2000) Altered Cell Cycle Control at the G2/M Phases in Aryl Hydrocarbon Receptor-Null Embryo Fibroblast. *Molecular and Cellular Biology* **57**:1056–1063.
- Esser C (2012) Biology and function of the aryl hydrocarbon receptor: report of an international and interdisciplinary conference. *Archives of Toxicology*, doi: 10.1007/s00204-012-0818-2.
- Evans BR, Karchner SI, Allan LL, Pollenz RS, Tanguay RL, Jenny MJ, Sherr DH, and Hahn ME (2008) Repression of aryl hydrocarbon receptor (AHR) signaling by

AHR repressor: role of DNA binding and competition for AHR nuclear translocator. *Molecular Pharmacology* **73**:387–398.

Evans BR, Karchner SI, Franks DG, and Hahn ME (2005) Duplicate aryl hydrocarbon receptor repressor genes (ahrr1 and ahrr2) in the zebrafish *Danio rerio*: Structure, function, evolution, and AHR-dependent regulation in vivo. *Archives of Biochemistry and Biophysics* **441**:151–167.

Evans MR, Card PB, and Gardner KH (2009) ARNT PAS-B has a fragile native state structure with an alternative β -sheet register nearby in sequence space. *Proceedings of the National Academy of Sciences* **106**:2617–2622.

Farwell C, Reddy CM, Peacock E, Nelson RK, Washburn L, and Valentine DL (2009) Weathering and the Fallout Plume of Heavy Oil from Strong Petroleum Seeps Near Coal Oil Point, CA. *Environmental Science and Technology* **43**:3542–3548.

Faust D, Kletting S, Ueberham E, and Dietrich C (2013) Aryl hydrocarbon receptor-dependent cell cycle arrest in isolated mouse oval cells. *Toxicology Letters* **223**:73–80.

Fenton SE, Hamm JT, and Birnbaum LS (2002) Persistent abnormalities in the rat mammary gland following gestational and lactational exposure to 2, 3, 7, 8-tetrachlorodibenzo-p-dioxin (TCDD). *Toxicological Sciences* **67**: 63-74

Fernandez-Salguero P, Pineau T, Hilbert DM, McPhail T, Lee SS, Kimura S, Nebert DW, Rudikoff S, Ward JM, and Gonzalez FJ (1995) Immune system impairment and hepatic fibrosis in mice lacking the dioxin-binding Ah receptor. *Science* **268**:722–726.

- Fernandez-Salguero PM, Hilbert DM, Rudikoff S, Ward JM, and Gonzalez FJ (1996) Aryl-hydrocarbon Receptor-Deficient Mice Are Resistant to 2,3,7,8-Tetrachlorodibenzo-p-dioxin-Induced Toxicity. *Toxicology and Applied Pharmacology* **140**:173–179.
- Forgacs AL, Dere E, Angrish MM, and Zacharewski TR (2013) Comparative analysis of temporal and dose-dependent TCDD-elicited gene expression in human, mouse, and rat primary hepatocytes. *Toxicological Sciences* **133**:54–66.
- Friedewald WF, and Rous P (1944) The Initiating and Promoting Elements in Tumor Production. *Journal of Experimental Medicine* **80**:101–126.
- Friling RS, Bensimon A, Tichauer Y, and Daniel V (1990) Xenobiotic-inducible expression of murine glutathione S-transferase Ya subunit gene is controlled by an electrophile-responsive element. *Proceedings of the National Academy of Sciences* **87**:6258–6262.
- Frueh FW, Hayashibara KC, Brown PO, and Whitlock JP (2001) Use of cDNA microarrays to analyze dioxin-induced changes in human liver gene expression. *Toxicology Letters* **122**:189–203.
- Fukunaga BN, Probst MR, Reisz-Porszasz S, and Hankinson O (1995) Identification of functional domains of the aryl hydrocarbon receptor. *Journal of Biological Chemistry* **270**:29270–29278.
- Garrison PM, Tullis K, Aarts JM, Brouwer A, Giesy JP, and Denison MS (1996) Species-specific recombinant cell lines as bioassay systems for the detection of 2,3,7,8-tetrachlorodibenzo-p-dioxin-like chemicals. *Fundamental and Applied Toxicology* **30**:194–203.

- Gartel AL, and Tyner AL (1999) Transcriptional Regulation of the p21 (WAF1/CIP1) Gene. *Experimental Cell Research* **246**:280–289.
- Gartel AL, Radhakrishnan SK, Serfas MS, Kwon YH, and Tyner AL (2004) A novel p21WAF1/CIP1 transcript is highly dependent on p53 for its basal expression in mouse tissues. *Oncogene* **23**:8154–8157.
- Gartel AL, Serfas MS, Gartel M, Goufman E, Wu GS, el-Deiry WS, and Tyner AL (1996) p21 (WAF1/CIP1) expression is induced in newly non-dividing cells in diverse epithelia and during differentiation of the Caco-2 intestinal cell line. *Experimental Cell Research* **227**:171–181.
- Gasiewicz TA, Elferink CJ, and Henry EC (1991) Characterization of multiple forms of the Ah receptor: recognition of a dioxin-responsive enhancer involves heteromer formation. *Biochemistry* **30**:2909–2916.
- Gasiewicz TA, Holscher MA, and Neal RA (1980) The effect of total parenteral nutrition on the toxicity of 2,3,7,8-tetrachlorodibenzo-p-dioxin in the rat. *Toxicology and Applied Pharmacology* **54**:469–488.
- Ge N-L, and Elferink CJ (1998) A Direct Interaction between the Aryl Hydrocarbon Receptor and Retinoblastoma Protein. *Journal of Biological Chemistry* **273**:22708–22713.
- Giacinti C, and Giordano A (2006) RB and cell cycle progression. *Oncogene* **25**:5220–5227.
- Gielen JE, Goujon FM, and Nebert DW (1972) Genetic Regulation of Aryl Hydrocarbon Hydroxylase Induction. *Journal of Biological Chemistry* **247**:1125–1137.

- Gillesby BE, Stanostefano M, Porter W, Safe S, Wu ZF, and Zacharewski TR (1997) Identification of a Motif within the 5' Regulatory Region of pS2 Which Is Responsible for AP-1 Binding and TCDD-Mediated Suppression. *Biochemistry* **36**:6080–6089.
- Gimm T, Wiese M, Teschemacher B, Deggerich A, Schödel J, Knaup KX, Hackenbeck T, Hellerbrand C, Amann K, Wiesener MS, Höning S, Eckardt K-U, and Warnecke C (2010) Hypoxia-inducible protein 2 is a novel lipid droplet protein and a specific target gene of hypoxia-inducible factor-1. *FASEB J* **24**:4443–4458.
- Gohlke JM, Doke D, Tipre M, Leader M, and Fitzgerald T (2011) A review of seafood safety after the deepwater horizon blowout. *Environmental Health Perspectives* **119**:1062–1069.
- Goode GD, Ballard BR, Manning HC, Freeman ML, Kang Y, and Eltom SE (2013) Knockdown of aberrantly upregulated aryl hydrocarbon receptor reduces tumor growth and metastasis of MDA-MB-231 human breast cancer cell line. *International Journal of Cancer* **133**:2769–2780.
- Gottlicher M, and Wiebel FJ (1991) 2,3,7,8-Tetrachlorodibenzo-p-dioxin causes unbalanced growth in 5L rat hepatoma cells. *Toxicology and Applied Pharmacology* **111**:496–503.
- Gouédard C, Barouki R, and Morel Y (2004) Dietary polyphenols increase paraoxonase 1 gene expression by an aryl hydrocarbon receptor-dependent mechanism. *Molecular and Cellular Biology* **24**:5209–5222.
- Greenlee WF, and Poland A (1979) Nuclear Uptake of 2,3,7,8-tetrachlorodibenzo-p-dioxin in C57BL/6J and DBA/2J mice. Role of the Hepatic Cytosol Receptor Protein. *Journal of Biological Chemistry* **254**:9814–9821.

- Gu YZ, Hogenesch JB, and Bradfield CA (2000) The PAS superfamily: sensors of environmental and developmental signals. *Annual Review of Pharmacology and Toxicology* **40**:519–561.
- Guenthner TM, and Nebert DW (1977) Cytosolic receptor for aryl hydrocarbon hydroxylase induction by polycyclic aromatic compounds. Evidence for structural and regulatory variants among established cell cultured lines. *Journal of Biological Chemistry* **252**:8981–8989.
- Gupta BN, Vos JG, Moore JA, Zinkl JG, and Bullock BC (1973) Pathologic effects of 2, 3, 7, 8-tetrachlorodibenzo-p-dioxin in laboratory animals. *Environmental Health Perspectives* 125–150.
- Hahn ME (2002) Aryl hydrocarbon receptors: diversity and evolution. *Chemico-Biological Interactions* **141**:131–160.
- Hanahan D, and Weinberg RA (2011) Hallmarks of Cancer: The Next Generation. *Cell* **144**:646–674.
- Hankinson O (1983) Dominant and recessive aryl hydrocarbon hydroxylase-deficient mutants of mouse hepatoma line, Hepa-1, and assignment of recessive mutants to three complementation groups. *Somatic Cell Genet* **9**:497–514.
- Hankinson O (1981) Evidence that Benzo(a) pyrene-resistant, aryl hydrocarbon hydroxylase-deficient variants of mouse hepatoma line, Hepa-1, are mutational in origin. *Somatic Cell Genetics* **7**:373–388.
- Hankinson O (2005) Role of co-activators in transcriptional activation by the Aryl hydrocarbon receptor. *Archives of biochemistry and biophysics* **433**:379–386.

- Hankinson O (1979) Single-Step Selection of Clones of a Mouse Hepatoma Line Deficient in Aryl Hydrocarbon Hydroxylase. *Proceedings of the National Academy of Sciences* **76**:373–376.
- Hankinson O (1995) The Aryl Hydrocarbon Receptor Complex. *Annual Review of Pharmacology and Toxicology* **35**:307–340.
- Hankinson O, Andersen RD, Birren BW, Sander F, Negishi M, and Nebert DW (1985) Mutations affecting the regulation of transcription of the cytochrome P1-450 gene in the mouse Hepa-1 cell line. *Journal of Biological Chemistry* **260**:1790–1795.
- Hannah RR, Nebert DW, and Eisen HJ (1981) Regulatory gene product of the Ah complex. Comparison of 2,3,7,8-tetrachlorodibenzo-p-dioxin and 3-methylcholanthrene binding to several moieties in mouse liver cytosol. *Journal of Biological Chemistry* **256**:4584–4590.
- Hao N, Lee KL, Furness SGB, Bosdotter C, Poellinger L, and Whitelaw ML (2012) Xenobiotics and loss of cell adhesion drive distinct transcriptional outcomes by aryl hydrocarbon receptor signaling. *Molecular Pharmacology* **82**:1082–1093.
- Harper JW, Elledge SJ, Keyomarsi K, Dynlacht B, Tsai LH, Zhang P, Dobrowolski S, Bai C, Connell-Crowley L, and Swindell E (1995) Inhibition of cyclin-dependent kinases by p21. *Molecular Biology of the Cell* **6**:387–400.
- Harper TA, Joshi AD, and Elferink CJ (2013) Identification of Stanniocalcin 2 as a Novel Aryl Hydrocarbon Receptor Target Gene. *Journal of Pharmacology and Experimental Therapeutics* **344**:579–588.
- Hartel M, Narla G, Wente MN, Giese NA, Martignoni ME, Martignetti JA, Friess H, and Friedman SL (2008) Increased alternative splicing of the KLF6 tumour suppressor

- gene correlates with prognosis and tumour grade in patients with pancreatic cancer. *European Journal of Cancer* **44**:1895–1903.
- Hecht SS, Loy M, Mazzaresse R, and Hoffmann D (1978) Study of chemical carcinogenesis. 7. Synthesis and mutagenicity of modified chrysenes related to the carcinogen, 5-methylchrysene. *Journal of Medicinal Chemistry* **21**:38–44.
- Helin K, Harlow E, and Fattaey A (1993) Inhibition of E2F-1 transactivation by direct binding of the retinoblastoma protein. *Molecular and Cellular Biology* **13**:6501–6508.
- Henck JM, New MA, Kociba RJ, and Rao KS (1981) 2,3,7,8-Tetrachlorodibenzo-p-dioxin: Acute oral toxicity in hamsters. *Toxicology and Applied Pharmacology* **59**:405–407.
- Henry EC (2003) Agonist but Not Antagonist Ligands Induce Conformational Change in the Mouse Aryl Hydrocarbon Receptor as Detected by Partial Proteolysis. *Molecular Pharmacology* **63**:392–400.
- Henry EC, Rucci G, and Gasiewicz TA (1989) Characterization of multiple forms of the Ah receptor: comparison of species and tissues. *Biochemistry* **28**:6430–6440.
- Higgins GM, and Anderson RM (1931) Experimental Pathology of the Liver: Restoration of the Liver of the White Rat Following Partial Surgical Removal. *Archives of Pathology* 186–202.
- Hitzel A, Pöhlmann M, Schwägele F, Speer K, and Jira W (2013) Polycyclic aromatic hydrocarbons (PAH) and phenolic substances in meat products smoked with different types of wood and smoking spices. *Food Chemistry* **139**:955–962.

- Hoffman EC, Reyes H, Chu FF, Sander F, Conley LH, Brooks BA, and Hankinson O (1991) Cloning of a factor required for activity of the Ah (dioxin) receptor. *Science* **252**:954–958.
- Hollingshead BD, Beischlag TV, DiNatale BC, Ramadoss P, and Perdew GH (2008) Inflammatory signaling and aryl hydrocarbon receptor mediate synergistic induction of interleukin 6 in MCF-7 cells. *Cancer Research* **68**:3609–3617.
- Hong S, Khim JS, Ryu J, Park J, Song SJ, Kwon B-O, Choi K, Ji K, Seo J, Lee S, Park J, Lee W, Choi Y, Lee KT, Kim C-K, Shim WJ, Naile JE, and Giesy JP (2012) Two Years after the Hebei Spirit Oil Spill: Residual Crude-Derived Hydrocarbons and Potential AhR-Mediated Activities in Coastal Sediments. *Environmental Sciences and Technology* **46**:1406–1414.
- Hong S, Lee S, Choi K, Kim GB, Ha SY, Kwon B-O, Ryu J, Yim UH, Shim WJ, Jung J, Giesy JP, and Khim JS (2015) Effect-directed analysis and mixture effects of AhR-active PAHs in crude oil and coastal sediments contaminated by the Hebei Spirit oil spill. *Environmental Pollution* **199**:110–118.
- Huang G, and Elferink CJ (2012) A novel nonconsensus xenobiotic response element capable of mediating aryl hydrocarbon receptor-dependent gene expression. *Molecular Pharmacology* **81**:338–347.
- Huang G, and Elferink CJ (2005) Multiple Mechanisms Are Involved in Ah Receptor-Mediated Cell Cycle Arrest. *Molecular Pharmacology* **67**:88–96.
- Huppi K, Siwarski D, Dosik J, Michieli P, Chedid M, Reed S, Mock B, Givol D, and Mushinski JF (1994) Molecular cloning, sequencing, chromosomal localization and expression of mouse p21 (Waf1). *Oncogene* **9**:3017–3020.

- Hwang H-M, Stanton B, McBride T, and Anderson MJ (2014) Polycyclic aromatic hydrocarbon body residues and lysosomal membrane destabilization in mussels exposed to the Dubai Star bunker fuel oil (intermediate fuel oil 380) spill in San Francisco Bay. *Environmental Toxicology and Chemistry* **33**:1117–1121.
- Ikuta T, Eguchi H, Tachibana T, Yoneda Y, and Kawajiri K (1998) Nuclear localization and export signals of the human aryl hydrocarbon receptor. *Journal of Biological Chemistry* **273**:2895–2904.
- Ikuta T, Tachibana T, Watanabe J, Yoshida M, Yoneda Y, and Kawajiri K (2000) Nucleocytoplasmic shuttling of the aryl hydrocarbon receptor. *Journal of Biochemistry* **127**:503–509.
- Irigoyen JP, Muñoz-Cánoves P, Montero L, Koziczak M, and Nagamine Y (1999) The plasminogen activator system: biology and regulation. *Cellular and Molecular Life Science* **56**:104–132.
- Israel DI, and Whitlock JP (1984) Regulation of cytochrome P1-450 gene transcription by 2,3,7, 8-tetrachlorodibenzo-p-dioxin in wild type and variant mouse hepatoma cells. *Journal of Biological Chemistry* **259**:5400–5402.
- Jackson DP, Joshi AD, and Elferink CJ (2015) Ah receptor pathway intricacies; signaling through diverse protein partners and DNA-motifs. *Toxicology Research* **4**:1143–1158.
- Jackson DP, Li H, Mitchell KA, Joshi AD, and Elferink CJ (2014) Ah Receptor Mediated Suppression of Liver Regeneration through NC-XRE-Driven p21Cip1 Expression. *Molecular Pharmacology* 533–541.

- Jackson LN, Larson SD, Silva SR, Rychahou PG, Chen LA, Qiu S, Rajaraman S, and Evers BM (2008) PI3K/Akt activation is critical for early hepatic regeneration after partial hepatectomy. *American Journal of Liver Physiology* **294**:G1401–G1410
- Jeng Y (2003) KLF6, a putative tumor suppressor gene, is mutated in astrocytic gliomas. *International Journal of Cancer* **105**:625–629.
- Johnston C (2005) *Preliminary Report: Pulp, Paper, and Paperboard Detailed Study*, U.S. Environmental Protection Agency, Washington, D.C.
- Jones P, Galeazzi D, Fisher J, and Whitlock J (1985) Control of cytochrome P1-450 gene expression by dioxin. *Science* **227**:1499–1502.
- Jones PB, Durrin LK, Fisher JM, and Whitlock JP (1986) Control of gene expression by 2,3,7,8-tetrachlorodibenzo-p-dioxin. Multiple dioxin-responsive domains 5'-ward of the cytochrome P1-450 gene. *Journal of Biological Chemistry*
- Jones PB, Durrin LK, Galeazzi DR, and Whitlock JP (1986) Control of cytochrome P1-450 gene expression: analysis of a dioxin-responsive enhancer system. *Proceedings of the National Academy of Sciences* **83**:2802–2806.
- Joshi AD, Carter DE, Tod A Harper J, and Elferink CJ (2015) Aryl Hydrocarbon Receptor–Dependent Stanniocalcin 2 Induction by Cinnabaric Acid Provides Cytoprotection against Endoplasmic Reticulum and Oxidative Stress. *Journal of Pharmacology and Experimental Therapeutics* **353**:201–212.
- Karchner SI, Franks DG, Powell WH, and Hahn ME (2002) Regulatory interactions among three members of the vertebrate aryl hydrocarbon receptor family: AHR repressor, AHR1, and AHR2. *Journal of Biological Chemistry* **277**:6949–6959,

- Kazlauskas A, Poellinger L, and Pongratz I (1999) Evidence That the Co-chaperone p23 Regulates Ligand Responsiveness of the Dioxin (Aryl Hydrocarbon) Receptor. *Journal of Biological Chemistry* **274**:13519–13524.
- Kennedy GD, Nukaya M, Moran SM, Glover E, Weinberg S, Balbo S, Hecht SS, Pitot HC, Drinkwater NR, and Bradfield CA (2014) Liver Tumor Promotion by 2,3,7,8-Tetrachlorodibenzo-p-dioxin Is Dependent on the Aryl Hydrocarbon Receptor and TNF/IL-1 Receptors. *Toxicological Sciences* **140**:135–143.
- Kewley RJ, Whitelaw ML, and Chapman-Smith A (2004) The mammalian basic helix–loop–helix/PAS family of transcriptional regulators. *International Journal of Biochemistry and Cellular Biology* **36**:189–204.
- Kim DW, Gazourian L, Quadri SA, Romieu-Mourez R, Sherr DH, and Sonenshein GE (2000) The RelA NF-kappaB subunit and the aryl hydrocarbon receptor (AhR) cooperate to transactivate the c-myc promoter in mammary cells. *Oncogene* **19**:5498–5506.
- Kimbrough KL, Johnson WE, Lauenstein GG, Christensen JD, and Apeti DA (2008) An Assessment of Two Decades of Contaminant Monitoring in the Nations Coastal Zone. *NOAA Technical Memorandum* 1–118, Silver Spring Maryland.
- Kimbrough RD, Carter CD, Liddle JA, and Cline RE (1977) Epidemiology and pathology of a tetrachlorodibenzodioxin poisoning episode. *Archives of Environmental Health* **32**:77–86.
- Kimmig J, and Schulz KH (1957) Occupational Acne (so-called chloracne) Due to Chlorinated Aromatic Cyclic Ethers. *Dermatologica* **115**:540–546.

- Kinehara M, Fukuda I, Yoshida K-I, and Ashida H (2008) High-throughput evaluation of aryl hydrocarbon receptor-binding sites selected via chromatin immunoprecipitation-based screening in Hepa-1c1c7 cells stimulated with 2,3,7,8-tetrachlorodibenzo-p-dioxin. *Genes and Genetics Systems* **83**:455–468.
- Knudson AG (1971) Mutation and cancer: statistical study of retinoblastoma. *Proceedings of the National Academy of Sciences* **68**:820–823.
- Kolluri S, Weiss C, Koff A, and Gottlicher M (1999) p27Kip1 induction and inhibition of proliferation by the intracellular Ah receptor in developing thymus and hepatoma cells. *Genes & Development* **13**:1742–1753.
- Konda R, Sugimura J, Sohma F, Katagiri T, Nakamura Y, and Fujioka T (2008) Over expression of hypoxia-inducible protein 2, hypoxia-inducible factor-1alpha and nuclear factor kappaB is putatively involved in acquired renal cyst formation and subsequent tumor transformation in patients with end stage renal failure. *The Journal of Urology* **180**:481–485.
- Korashy HM, and El-Kadi AOS (2006) The Role of Aryl Hydrocarbon Receptor in the Pathogenesis of Cardiovascular Diseases. *Drug Metabolism Reviews* **38**:411–450.
- Kren BT, and Steer CJ (1996) Posttranscriptional regulation of gene expression in liver regeneration: role of mRNA stability. *The FASEB Journal* **10**:559–573.
- Kujawinski EB, Kido Soule MC, Valentine DL, Boysen AK, Longnecker K, and Redmond MC (2011) Fate of Dispersants Associated with the Deepwater Horizon Oil Spill. *Environmental Science and Technology* **45**:1298–1306.

- Lakshmanan D, Howell NL, Rifai HS, and Koenig L (2010) Spatial and temporal variation of polychlorinated biphenyls in the Houston Ship Channel. *Chemosphere* **80**:100–112.
- Lalwani A, Stokes RA, Lau SM, and Gunton JE (2014) Deletion of ARNT (Aryl hydrocarbon receptor nuclear translocator) in β -cells causes islet transplant failure with impaired β -cell function. *PLoS ONE* **9**:e98435
- Lang UE, Kocabayoglu P, Cheng GZ, Ghiassi-Nejad Z, Muñoz U, Vetter D, Eckstein DA, Hannivoort RA, Walsh MJ, and Friedman SL (2013) GSK3 β phosphorylation of the KLF6 tumor suppressor promotes its transactivation of p21. *Oncogene* **32**:4557–4564.
- Law RJ, and Hellou J (1999) Contamination of Fish and Shellfish Following Oil Spill Incidents. *Environmental Geosciences* **6**:90–98.
- Law RJ, Kelly C, Baker K, Jones J, McIntosh AD, and Moffat CF (2002) Toxic equivalency factors for PAH and their applicability in shellfish pollution monitoring studies. *Journal of Environmental Monitoring* **4**:383–388.
- Lee K, Prince RC, Greer CW, Doe KG, Wilson JEH, Cobanli SE, Wohlgeschaffen GD, Alroumi D, King T, and Tremblay GH (2003) Composition and Toxicity of Residual Bunker C Fuel Oil in Intertidal Sediments After 30 Years. *Spill Science & Technology Bulletin* **8**:187–199.
- Lee KT, Hong S, Lee JS, Chung KH, Hilscherová K, Giesy JP, and Khim JS (2013) Revised relative potency values for PCDDs, PCDFs, and non-ortho-substituted PCBs for the optimized H4IIE-luc in vitro bioassay. *Environmental Science and Pollution Research International* **20**:8590–8599.

- Legraverend C, Hannah RR, Eisen HJ, Owens IS, Nebert DW, and Hankinson O (1982) Regulatory gene product of the Ah locus. Characterization of receptor mutants among mouse hepatoma clones. *Journal of Biological Chemistry* **257**:6402–6407.
- Leow CC, Wang BE, Ross J, Chan SM, Zha J, Carano RAD, Frantz G, Shen MM, de Sauvage FJ, and Gao WQ (2009) Prostate-specific Klf6 Inactivation Impairs Anterior Prostate Branching Morphogenesis through Increased Activation of the Shh Pathway. *Journal of Biological Chemistry* **284**:21057–21065.
- Levine-Fridman A, Chen L, and Elferink CJ (2004) Cytochrome P4501A1 promotes G1 phase cell cycle progression by controlling aryl hydrocarbon receptor activity. *Molecular Pharmacology* **65**:461–469.
- Li S, Pei X, Zhang W, Xie HQ, and Zhao B (2014) Functional Analysis of the Dioxin Response Elements (DREs) of the Murine CYP1A1 Gene Promoter: Beyond the Core DRE Sequence. *International Journal of Molecular Science* **15**:6475–6487.
- Li X, Florez S, Wang J, Cao H, and Amendt BA (2013) Dact2 Represses PITX2 Transcriptional Activation and Cell Proliferation through Wnt/beta-Catenin Signaling during Odontogenesis. *PLoS ONE* **8**:e54868.
- Lindén J, Lensu S, Tuomisto J, and Pohjanvirta R (2010) Dioxins, the aryl hydrocarbon receptor and the central regulation of energy balance. *Frontiers of Neuroendocrinology* **31**:452–478.
- Liu J, Du T, Yuan Y, He Y, Tan Z, and Liu Z (2010) KLF6 inhibits estrogen receptor-mediated cell growth in breast cancer via a c-Src-mediated pathway. *Molecular and Cellular Biochemistry* **335**:29–35.

- Lo R, and Matthews J (2012) High-resolution genome-wide mapping of AHR and ARNT binding sites by ChIP-Seq. *Toxicological Sciences* **130**:349–361.
- Lo R, Celius T, Forgacs AL, Dere E, MacPherson L, Harper P, Zacharewski T, and Matthews J (2011) Identification of aryl hydrocarbon receptor binding targets in mouse hepatic tissue treated with 2,3,7,8-tetrachlorodibenzo-p-dioxin. *Toxicology and applied Pharmacology* **257**:38–47.
- Lowe MM, Mold JE, Kanwar B, Huang Y, Louie A, Pollastri MP, Wang C, Patel G, Franks DG, Schlezinger J, Sherr DH, Silverstone AE, Hahn ME, and McCune JM (2014) Identification of Cinnabarinic Acid as a Novel Endogenous Aryl Hydrocarbon Receptor Ligand That Drives IL-22 Production. *PLoS ONE* **9**:e87877.
- Loyer P, Glaise D, Cariou S, Baffet G, Meijer L, and Guguen-Guillouzo C (1994) Expression and activation of cdks (1 and 2) and cyclins in the cell cycle progression during liver regeneration. *Journal of Biological Chemistry* **269**:2491–2500.
- Lund AK, Goens MB, Kanagy NL, and Walker MK (2003) Cardiac hypertrophy in Aryl hydrocarbon receptor null mice is correlated with elevated angiotensin II, endothelin-1, and mean arterial blood pressure. *Toxicology and Applied Pharmacology* **193**:177–187.
- Lusska A, Shen E, and Whitlock JP (1993) Protein-DNA interactions at a dioxin-responsive enhancer. Analysis of six bona fide DNA-binding sites for the liganded Ah receptor. *Journal of Biological Chemistry* **268**:6575–6580.

- Ma Q, and Baldwin KT (2000) 2,3,7,8-Tetrachlorodibenzo-p-dioxin-induced Degradation of Aryl Hydrocarbon Receptor (AhR) by the Ubiquitin-Proteasome Pathway. *Journal of Biological Chemistry* **275**:8432–8438.
- Ma Q, and Lu AYH (2007) CYP1A induction and human risk assessment: an evolving tale of in vitro and in vivo studies. *Drug Metabolism and Disposition* **35**:1009–1016.
- Ma Q, and Whitlock JP (1997) A Novel Cytoplasmic Protein That Interacts with the Ah Receptor, Contains Tetratricopeptide Repeat Motifs, and Augments the Transcriptional Response to 2,3,7,8-Tetrachlorodibenzo-p-dioxin. *Journal of Biological Chemistry* **272**:8878–8884.
- Ma Q, and Whitlock JP (1996) The aromatic hydrocarbon receptor modulates the Hepa 1c1c7 cell cycle and differentiated state independently of dioxin. *Molecular and Cellular Biology* **16**:2144–2150.
- Ma Q, Kinneer K, Bi Y, Chan AM, and Kan YW (2004) Induction of murine NAD(P)H:quinone oxidoreductase by 2,3,7,8-tetrachlorodibenzo-p-dioxin requires the CNC (cap “n” collar) basic leucine zipper transcription factor Nrf2 (nuclear factor erythroid 2-related factor 2): cross-interaction between AhR (aryl hydrocarbon receptor) and Nrf2 signal transduction. *Biochemistry Journal* **377**:205
- MacPherson L, Ahmed S, Tamblyn L, Krutmann J, Förster I, Weighardt H, and Matthews J (2014) Aryl hydrocarbon receptor repressor and TiPARP (ARTD14) use similar, but also distinct mechanisms to repress aryl hydrocarbon receptor signaling. *International Journal of Molecular Science* **15**:7939–7957.

- MacPherson L, Tamblyn L, Rajendra S, Bralha F, McPherson JP, and Matthews J (2012) 2,3,7,8-Tetrachlorodibenzo-p-dioxin poly(ADP-ribose) polymerase (TiPARP, ARTD14) is a mono-ADP-ribosyltransferase and repressor of aryl hydrocarbon receptor transactivation. *Nucleic Acids Research* **41**:1604–1621.
- Mahon MJ, and Gasiewicz TA (1995) Ah receptor phosphorylation: localization of phosphorylation sites to the C-terminal half of the protein. *Archives of Biochemistry and Biophysics* **318**:166–174.
- Marlowe JL, and Puga A (2005) Aryl hydrocarbon receptor, cell cycle regulation, toxicity, and tumorigenesis. *Journal of Cellular Biochemistry* **96**:1174–1184.
- Marlowe JL, Knudsen ES, Schwemberger S, and Puga A (2004) The aryl hydrocarbon receptor displaces p300 from E2F-dependent promoters and represses S phase-specific gene expression. *Journal of Biological Chemistry* **279**:29013–29022.
- Martins M, Santos JM, Diniz MS, Ferreira AM, Costa MH, and Costa PM (2015) Effects of carcinogenic versus non-carcinogenic AHR-active PAHs and their mixtures Lessons from ecological relevance. *Environmental Research* **138**:101–111.
- Matikainen T, Perez GI, Jurisicova A, Pru JK, Schlezinger JJ, Ryu HY, Laine J, Sakai T, Korsmeyer SJ, Casper RF, Sherr DH, and Tilly JL (2001) Aromatic hydrocarbon receptor-driven Bax gene expression is required for premature ovarian failure caused by biohazardous environmental chemicals. *Nature Genetics* **28**:355–360.
- Matsumoto N, Kubo A, Liu H, Akita K, Laub F, Ramirez F, Keller G, and Friedman SL (2006) Developmental regulation of yolk sac hematopoiesis by Kruppel-like factor 6. *Blood* **107**:1357–1365.

- McConnell EE, Moore JA, and Dalgard DW (1978) Toxicity of 2,3,7,8-tetrachlorodibenzo-p-dioxin in rhesus monkeys (*Macaca mulatta*) following a single oral dose. *Toxicology and applied Pharmacology* **43**: 175-187
- McGuire J, Whitelaw ML, Pongratz I, Gustafsson JA, and Poellinger L (1994) A cellular factor stimulates ligand-dependent release of hsp90 from the basic helix-loop-helix dioxin receptor. *Molecular and Cellular Biology* **14**:2438–2446.
- McMillan BJ, and Bradfield CA (2007a) The aryl hydrocarbon receptor is activated by modified low-density lipoprotein. *Proceedings of the National Academy of Sciences* **104**:1412–1417.
- McMillan BJ, and Bradfield CA (2007b) The aryl hydrocarbon receptor sans xenobiotics: endogenous function in genetic model systems. *Molecular Pharmacology* **72**:487–498.
- McNutt MK, Camilli R, Crone TJ, Guthrie GD, Hsieh PA, Ryerson TB, Savas O, and Shaffer F (2012) Review of flow rate estimates of the Deepwater Horizon oil spill. *Proceedings of the National Academy of Sciences* **109**:20260–20267.
- Meyer BK, Pray-Grant MG, Heuvel JPV, and Perdew GH (1998) Hepatitis B Virus X-Associated Protein 2 Is a Subunit of the Unliganded Aryl Hydrocarbon Receptor Core Complex and Exhibits Transcriptional Enhancer Activity. *Molecular and Cellular Biology* **18**:978–988.
- Michalopoulos GK, and DeFrances MC (1997) Liver Regeneration. *Science* **276**:60–66.
- Miller AG, Israel D, and Whitlock JP (1983) Biochemical and genetic analysis of variant mouse hepatoma cells defective in the induction of benzo(a)pyrene-metabolizing enzyme activity. *Journal of Biological Chemistry* **258**:3523–3527.

- Mimura J, Ema M, Sogawa K, and Fujii-Kuriyama Y (1999) Identification of a novel mechanism of regulation of Ah (dioxin) receptor function. *Genes & Development* **13**:20–25.
- Mimura J, Yamashita K, Nakamura K, Morita M, Takagi TN, Nakao K, Ema M, Sogawa K, Yasuda M, Katsuki M, and Fujii-Kuriyama Y (1997) Loss of teratogenic response to 2,3,7,8-tetrachlorodibenzo-p-dioxin (TCDD) in mice lacking the Ah (dioxin) receptor. *Genes to Cells* **2**:645–654.
- Mitchell KA, and Elferink CJ (2009) Timing is everything: Consequences of transient and sustained AhR activity. *Biochemical Pharmacology* **77**:947–956.
- Mitchell KA, Lockhart CA, Huang G, and Elferink CJ (2006) Sustained Ah receptor activity attenuates liver regeneration. *Molecular Pharmacology* **70**:163–170.
- Mitchell KA, Wilson SR, and Elferink CJ (2010) The activated aryl hydrocarbon receptor synergizes mitogen-induced murine liver hyperplasia. *Toxicology* **276**:103–109.
- Murk AJ, Legler J, Denison MS, Giesy JP, van de Guchte C, and Brouwer A (1996) Chemical-Activated Luciferase Gene Expression (CALUX): A Novel *in Vitro* Bioassay for Ah Receptor Active Compounds in Sediments and Pore Water. *Fundamental and Applied Toxicology* **33**:149–160.
- Nagy SR, Sanborn JR, D HB, and Denison MS (2002) Development of a Green Fluorescent Protein-Based Cell Bioassay for the Rapid and Inexpensive Detection and Characterization of Ah Receptor Agonists. *Toxicological Sciences* **65**:200–210.
- Nair SC, Toran EJ, Rimerman RA, Hjermsstad S, Smithgall TE, and Smith DF (1996) A pathway of multi-chaperone interactions common to diverse regulatory proteins:

estrogen receptor, Fes tyrosine kinase, heat shock transcription factor Hsf1, and the aryl hydrocarbon receptor. *Cell Stress Chaperones* **1**:237–250.

Nam Y, Kim J-H, Seo M, Kim J-H, Jin M, Jeon S, Seo J-W, Lee W-H, Bing SJ, Jee Y, Lee WK, Park DH, Kook H, and Suk K (2014) Lipocalin-2 Protein Deficiency Ameliorates Experimental Autoimmune Encephalomyelitis: The Pathogenic Role of Lipocalin-2 in the Central Nervous System and Peripheral Lymphoid Tissues. *Journal of Biological Chemistry* **289**:16773–16789.

Narat JK (1925) Experimental Production of Malignant Growths by Simple Chemicals. *The Journal of Cancer Research* **9**:135–147.

Narla G, Difeo A, Reeves HL, Schaid DJ, Hirshfeld J, Hod E, Katz A, Isaacs WB, Hebring S, Komiya A, McDonnell SK, Wiley KE, Jacobsen SJ, Isaacs SD, Walsh PC, Zheng SL, Chang B-L, Friedrichsen DM, Stanford JL, Ostrander EA, Chinnaiyan AM, Rubin MA, Xu J, Thibodeau SN, Friedman SL, and Martignetti JA (2005) A germline DNA polymorphism enhances alternative splicing of the KLF6 tumor suppressor gene and is associated with increased prostate cancer risk. *Cancer Research* **65**:1213–1222.

Narla G, Heath K, Reeves HL, Li D, Giono L, Kimmelman A, Glucksman M, Narla J, Eng F, Chan AM, Ferrari A, Martignetti JA, and Friedman SL (2001) KLF6, a Candidate Tumor Suppressor Gene Mutated in Prostate Cancer. *Science* **294**:2563–2566.

Narla G, Kremer-Tal S, Matsumoto N, Zhao X, Yao S, Kelley K, Tarocchi M, and Friedman SL (2007) In vivo regulation of p21 by the Kruppel-like factor 6 tumor-suppressor gene in mouse liver and human hepatocellular carcinoma. *Oncogene* **26**:4428–4434.

- Nebert DW, and Gelboin HV (1968a) Substrate-inducible Microsomal Aryl Hydroxylase in Mammalian Cell Culture I. *Journal of Biological Chemistry* **243**:6242–6249.
- Nebert DW, and Gelboin HV (1968b) Substrate-inducible Microsomal Aryl Hydroxylase in Mammalian Cell Culture II. *Journal of Biological Chemistry* **243**:6250–6261.
- Nebert DW, Dalton TP, Okey AB, and Gonzalez FJ (2004) Role of Aryl Hydrocarbon Receptor-mediated Induction of the CYP1 Enzymes in Environmental Toxicity and Cancer. *Journal of Biological Chemistry* **279**:23847–23850.
- Nebert DW, Puga A, and Vasiliou V (1993) Role of the Ah receptor and the dioxin-inducible [Ah] gene battery in toxicity, cancer, and signal transduction. *Annals of the New York Academy of Science* **685**:624–640.
- Neeb A, Wallbaum S, Novac N, Dukovic-Schulze S, Scholl I, Schreiber C, Schlag P, Moll J, Stein U, and Sleeman JP (2012) The immediate early gene Ier2 promotes tumor cell motility and metastasis, and predicts poor survival of colorectal cancer patients. *Oncogene* **31**:3796–3806.
- Nguyen LP, and Bradfield CA (2008) The search for endogenous activators of the aryl hydrocarbon receptor. *Chemical Research and Toxicology* **21**:102–116.
- Nisbet ICT, and LaGoy PK (1992) Toxic equivalency factors (TEFs) for polycyclic aromatic hydrocarbons (PAHs). *Regulatory Toxicology and Pharmacology* **16**:290–300.
- NOAA Office of Response and Restoration (2015) No. 6 Fuel oil (Bunker C) Spills.
- NOAA Office of Response and Restoration, Restoration (2015) Kirby Barge Oil Spill, Houston/Texas City Ship Channel, Port Bolivar, Texas.

- North Atlantic Treaty Organization (1988) Pilot Study on Inter-nation Information Exchange on Dioxins and Related Compounds. International Toxicity Equivalency Factor (I-TEF) Method of Risk Assessment for Complex Mixtures of Dioxins and Related Compounds, *Committee on the Challenges of Modern Society*, Report 176, August 1988.
- Nozell S, and Chen X (2002) p21B, a variant of p21Waf1/Cip1, is induced by the p53 family. *Oncogene* **21**:1285–1294.
- Nukaya M, Walisser JA, Moran SM, Kennedy GD, and Bradfield CA (2010) Aryl hydrocarbon receptor nuclear translocator in hepatocytes is required for aryl hydrocarbon receptor-mediated adaptive and toxic responses in liver. *Toxicological Sciences* **118**:554–563.
- Ohtake F, Fujii-Kuriyama Y, and Kato S (2009) AhR acts as an E3 ubiquitin ligase to modulate steroid receptor functions. *Biochemical Pharmacology* **77**:474–484.
- Ohtake F, Takeyama K-I, Matsumoto T, Kitagawa H, Yamamoto Y, Nohara K, Tohyama C, Krust A, Mimura J, Chambon P, Yanagisawa J, Fujii-Kuriyama Y, and Kato S (2003) Modulation of oestrogen receptor signalling by association with the activated dioxin receptor. *Nature* **423**:545–550.
- Okey AB, Bondy GP, Mason ME, Kahl GF, Eisen HJ, Guenther TM, and Nebert DW (1979) Regulatory gene product of the Ah locus. Characterization of the cytosolic inducer-receptor complex and evidence for its nuclear translocation. *Journal of Biological Chemistry* **254**:11636–11648.
- Okey AB, Bondy GP, Mason ME, Nebert DW, Forster-Gibson CJ, Muncan J, and Dufresne MJ (1980) Temperature-dependent cytosol-to-nucleus translocation of

- the Ah receptor for 2,3,7,8-tetrachlorodibenzo-p-dioxin in continuous cell culture lines. *Journal of Biological Chemistry* **255**:11415–11422.
- Overton EB, Ashton BM, and Miles MS (2004) Historical polycyclic aromatic and petrogenic hydrocarbon loading in Northern Central Gulf of Mexico shelf sediments. *Marine Pollution Bulletin* **49**:557–563.
- Palau N, Julià A, Ferrándiz C, Puig L, Fonseca E, Fernández E, López-Lasanta M, Tortosa R, and Marsal S (2013) Genome-wide transcriptional analysis of T cell activation reveals differential gene expression associated with psoriasis. *BMC Genomics* **14**:825.
- Pansoy A, Ahmed S, Valen E, Sandelin A, and Matthews J (2010) 3-Methylcholanthrene Induces Differential Recruitment of Aryl Hydrocarbon Receptor to Human Promoters. *Toxicological Sciences* **117**:90–100.
- Perdew G, and Bradfield C (1996) Mapping the 90 kDa heat shock protein binding region of the Ah receptor. *IUBMB Life* **39**:589–593.
- Perdew GH (1988) Association of the Ah receptor with the 90-kDa heat shock protein. *Journal of Biological Chemistry* **263**:13802–13805.
- Perdew GH (1992) Chemical cross-linking of the cytosolic and nuclear forms of the Ah receptor in hepatoma cell line 1c1c7. *Biochemical and Biophysical Research Communications* **182**:55–62.
- Peters JM, Narotsky MG, Elizondo G, Fernandez-Salguero PM, Gonzalez FJ, and Abbott BD (1999) Amelioration of TCDD-induced teratogenesis in aryl hydrocarbon receptor (AhR)-null mice. *Toxicological Sciences* **47**:86–92.

- Peterson CH, Rice SD, Short JW, Esler D, Bodkin JL, Ballachey BE, and Irons DB (2003) Long-term ecosystem response to the Exxon Valdez oil spill. *Science* **302**:2082–2086.
- Philipsen S, and Suske G (1999) A tale of three fingers: the family of mammalian Sp/XKLF transcription factors. *Nucleic Acids Research* **27**:2991–3000.
- Poland A, and Glover E (1973a) Chlorinated Dibenzo-p-dioxins: Potent Inducers of δ -Aminolevulinic Acid Synthetase and Aryl Hydrocarbon Hydroxylase. *Molecular Pharmacology*.
- Poland A, and Glover E (1973b) Studies on the mechanism of toxicity of the chlorinated dibenzo-p-dioxins. *Environmental Health Perspectives* 245-251.
- Poland A, and Knutson JC (1982) 2,3,7,8-tetrachlorodibenzo-p-dioxin and related halogenated aromatic hydrocarbons: examination of the mechanism of toxicity. *Annual Review of Pharmacology and Toxicology* 517–554.
- Poland A, Glover E, and Kende AS (1976) Stereospecific, high affinity binding of 2,3,7,8-tetrachlorodibenzo-p-dioxin by hepatic cytosol. Evidence that the binding species is receptor for induction of aryl hydrocarbon hydroxylase. *Journal of Biological Chemistry* **251**:4936–4946.
- Poland A, Palen D, and Glover E (1982) Tumour promotion by TCDD in skin of HRS/J hairless mice. *Nature* **300**:271–273.
- Poland AP, Glover E, Robinson JR, and Nebert DW (1974) Genetic Expression of Aryl Hydrocarbon Hydroxylase Activity. *Journal of Biological Chemistry* **249**:5599–5606.

- Pollenz RS, Sattler CA, and Poland A (1994) The aryl hydrocarbon receptor and aryl hydrocarbon receptor nuclear translocator protein show distinct subcellular localizations in Hepa 1c1c7 cells by immunofluorescence microscopy. *Molecular Pharmacology* **45**:428–438.
- Pongratz I, Mason GG, and Poellinger L (1992) Dual roles of the 90-kDa heat shock protein hsp90 in modulating functional activities of the dioxin receptor. Evidence that the dioxin receptor functionally belongs to a subclass of nuclear receptors which require hsp90 both for ligand binding activity and repression of intrinsic DNA binding activity. *Journal of Biological Chemistry* **267**:13728–13734.
- Pongratz I, Strömstedt PE, Mason GG, and Poellinger L (1991) Inhibition of the specific DNA binding activity of the dioxin receptor by phosphatase treatment. *Journal of Biological Chemistry* **266**:16813–16817.
- Porter W, Wang F, Duan R, Qin C, Castro-Rivera E, Kim K, and Safe S (2001) Transcriptional activation of heat shock protein 27 gene expression by 17beta-estradiol and modulation by antiestrogens and aryl hydrocarbon receptor agonists. *Journal of Molecular Endocrinology* **26**:31–42.
- Powell-Coffman JA, Bradfield CA, and Wood WB (1998) Caenorhabditis elegans orthologs of the aryl hydrocarbon receptor and its heterodimerization partner the aryl hydrocarbon receptor nuclear translocator. *Proceedings of the National Academy of Sciences* **95**:2844–2849.
- Prigent L, Robineau M, Jouneau S, Morzadec C, Louarn L, Vernhet L, Fardel O, and Sparfel L (2014) The aryl hydrocarbon receptor is functionally upregulated early in the course of human T-cell activation. *European Journal of Immunology* **44**:1330–1340.

- Probst MR, Reisz-Porszasz S, Agbunag RV, Ong MS, and Hankinson O (1993) Role of the aryl hydrocarbon receptor nuclear translocator protein in aryl hydrocarbon (dioxin) receptor action. *Molecular Pharmacology* **44**:511–518.
- Prokipcak RD, and Okey AB (1988) Physicochemical characterization of the nuclear form of Ah receptor from mouse hepatoma cells exposed in culture to 2,3,7,8-tetrachlorodibenzo-p-dioxin. *Archives of Biochemistry and Biophysics* **267**:811–828.
- Puga A, Barnes SJ, Dalton TP, Chang CY, Knudsen ES, and Maier MA (2000) Aromatic hydrocarbon receptor interaction with the retinoblastoma protein potentiates repression of E2F-dependent transcription and cell cycle arrest. *Journal of Biological Chemistry* **275**:2943–2950.
- Puga A, Maier A, and Medvedovic M (2000) The transcriptional signature of dioxin in human hepatoma HepG2 cells. *Biochemical Pharmacology* **60**:1129–1142.
- Puga A, Nebert DW, and Carrier F (1992) Dioxin induces expression of c-fos and c-jun proto-oncogenes and a large increase in transcription factor AP-1. *DNA Cell Biology* **11**:269–281.
- Ramachandran SD, Hodson PV, Khan CW, and Lee K (2004) Oil dispersant increases PAH uptake by fish exposed to crude oil. *Ecotoxicology and Environmental Safety* **59**:300–308.
- Reddy CM, Arey JS, Seewald JS, Sylva SP, Lemkau KL, Nelson RK, Carmichael CA, McIntyre CP, Fenwick J, Ventura GT, Van Mooy BAS, and Camilli R (2012) Composition and fate of gas and oil released to the water column during the Deepwater Horizon oil spill. *Proceedings of the National Academy of Sciences* **109**:20229–20234.

- Reeves HL, Narla G, Ogunbiyi O, Haq AI, Katz A, Benzeno S, Hod E, Harpaz N, Goldberg S, Tal-Kremer S, Eng FJ, Arthur MJP, Martignetti JA, and Friedman SL (2004) Kruppel-like factor 6 (KLF6) is a tumor-suppressor gene frequently inactivated in colorectal cancer. *Gastroenterology* **126**:1090–1103.
- Reeves WR, Barhoumi R, Burghardt RC, Lemke SL, Mayura K, McDonald TJ, Phillips TD, and Donnelly KC (2001) Evaluation of Methods for Predicting the Toxicity of Polycyclic Aromatic Hydrocarbon Mixtures. *Environmental Science and Technology* **35**:1630–1636.
- Reiners JJ, Jones CL, Hong N, Clift RE, and Elferink C (1997) Downregulation of aryl hydrocarbon receptor function and cytochrome P450 1A1 induction by expression of Ha-ras oncogenes. *Carcinogenesis* **19**:91–100.
- Reisz-Porszasz S, Probst MR, Fukunaga BN, and Hankinson O (1994) Identification of functional domains of the aryl hydrocarbon receptor nuclear translocator protein (ARNT). *Molecular and Cellular Biology* **14**:6075–6086.
- Reyes H, Reisz-Porszasz S, and Hankinson O (1992) Identification of the Ah receptor nuclear translocator protein (Arnt) as a component of the DNA binding form of the Ah receptor. *Science* **256**:1193–1195.
- Rezvani HR, Ali N, Nissen LJ, Harfouche G, de Verneuil H, et al., and Mazurier FEDER (2011) HIF-1alpha in Epidermis: Oxygen Sensing, Cutaneous Angiogenesis, Cancer, and Non-Cancer Disorders. *Journal of Investigative Dermatology* **131**:1793–1805
- Rotkin-Ellman M, Wong KK, and Solomon GM (2011) Seafood Contamination after the BP Gulf Oil Spill and Risks to Vulnerable Populations: A Critique of the FDA Risk Assessment. *Environmental Health Perspectives* **120**:157–161.

- Rubinstein M, Idelman G, Plymate SR, Narla G, Friedman SL, and Werner H (2004) Transcriptional activation of the insulin-like growth factor I receptor gene by the Kruppel-like factor 6 (KLF6) tumor suppressor protein: potential interactions between KLF6 and p53. *Endocrinology* **145**:3769–3777.
- Safe S, and Wormke M (2003) Inhibitory aryl hydrocarbon receptor-estrogen receptor alpha cross-talk and mechanisms of action. *Chemical Research Toxicology* **16**:807–816.
- Safe S, Wang F, Porter W, Duan R, and McDougal A (1998) Ah receptor agonists as endocrine disruptors: antiestrogenic activity and mechanisms. *Toxicology Letters* **102-103**:343–347.
- Safe S, Wormke M, and Samudio I (2000) Mechanisms of Inhibitory Aryl Hydrocarbon Receptor-Estrogen Receptor Crosstalk in Human Breast Cancer Cells. *Journal of Mammary Gland Biology and Neoplasia* **5**:295–306.
- Safe SH (1986) Comparative toxicology and mechanism of action of polychlorinated dibenzo-p-dioxins and dibenzofurans. *Annual Review of Pharmacology and Toxicology* **26**:371–399.
- Saha M, Togo A, Mizukawa K, Murakami M, Takada H, Zakaria MP, Chiem NH, Tuyen BC, Prudente M, Boonyatumanond R, Sarkar SK, Bhattacharya B, Mishra P, and Tana TS (2009) Sources of sedimentary PAHs in tropical Asian waters: Differentiation between pyrogenic and petrogenic sources by alkyl homolog abundance. *Marine Pollution Bulletin* **58**:189–200.
- Sangodkar J, Shi J, Difeo A, Schwartz R, Bromberg R, Choudhri A, McClinch K, Hatami R, Scheer E, Kremer-Tal S, Martignetti JA, Hui A, Leung WK, Friedman SL, and

- Narla G (2009) Functional role of the KLF6 tumour suppressor gene in gastric cancer. *European Journal of Cancer* **45**:666–676.
- Santschi PH, Presley BJ, Wade TL, Garcia-Romero B, and Baskaran M (2001) Historical contamination of PAHs, PCBs, DDTs, and heavy metals in Mississippi River Delta, Galveston Bay and Tampa Bay sediment cores. *Marine Environmental Research* **52**:51–79.
- Satyanarayana A, Klarmann KD, Gavrilova O, and Keller JR (2012) Ablation of the transcriptional regulator Id1 enhances energy expenditure, increases insulin sensitivity, and protects against age and diet induced insulin resistance, and hepatosteatosis. *The FASEB Journal* **26**:309–323.
- Schechter A, Birnbaum L, Ryan JJ, and Constable JD (2006) Dioxins: An overview. *Environmental Research* **101**:419–428.
- Schechter AJ, Sheu SU, Birnbaum LS, DeVito MJ, Denison MS, and Päpke O (1999) A comparison and discussion of two differing methods of measuring dioxin-like compounds: Gas chromatography-mass spectrometry and the CALUX bioassay-implications for health studies. *Organohalogen Compounds* **40**:247–250.
- Schein A, Scott JA, Mos L, and Hodson PV (2009) Oil dispersion increases the apparent bioavailability and toxicity of diesel to rainbow trout (*Oncorhynchus mykiss*). *Environmental Toxicology Chemistry* **28**:595–602.
- Schmidt JV, Su GH, Reddy JK, Simon MC, and Bradfield CA (1996) Characterization of a murine Ahr null allele: involvement of the Ah receptor in hepatic growth and development. *Proceedings of the National Academy of Sciences* **93**:6731–6736.

- Schwetz BA, Norris JM, Sparschu GL, Rowe VK, Gehring PJ, L EJ, and G GC (1973) Toxicology of chlorinated dibenzo-p-dioxins. *Environmental Health Perspectives* **5**:87–99.
- Shen ES, and Whitlock JP (1992) Protein-DNA interactions at a dioxin-responsive enhancer. Mutational analysis of the DNA-binding site for the liganded Ah receptor. *Journal of Biological Chemistry* **267**:6815–6819.
- Sherr CJ, and Roberts JM (2004) Living with or without cyclins and cyclin-dependent kinases. *Genes & Development* 2699–2711.
- Shimada T, and Fujii-Kuriyama Y (2004) Metabolic activation of polycyclic aromatic hydrocarbons to carcinogens by cytochromes P450 1A1 and 1B1. *Cancer Science* **95**:1–6.
- Shimba S, Komiyama K, Moro I, and Tezuka M (2002) Overexpression of the aryl hydrocarbon receptor (AhR) accelerates the cell proliferation of A549 cells. *Journal of Biochemistry* **132**:795–802.
- Shimizu M, Hara A, Okuno M, Matsuno H, Okada K, Ueshima S, Matsuo O, Niwa M, Akita K, Yamada Y, Yoshimi N, Uematsu T, Kojima S, Friedman SL, Moriwaki H, and Mori H (2001) Mechanism of retarded liver regeneration in plasminogen activator-deficient mice: impaired activation of hepatocyte growth factor after Fas-mediated massive hepatic apoptosis. *Hepatology* **33**:569–576.
- Simbolo M, Gottardi M, Corbo V, Fassan M, Mafficini A, Malpeli G, Lawlor RT, and Scarpa A (2013) DNA qualification workflow for next generation sequencing of histopathological samples. *PLoS ONE* **8**:e62692.

- Sirach E, Bureau C, Péron JM, Pradayrol L, Vinel JP, Buscail L, and Cordelier P (2007) KLF6 transcription factor protects hepatocellular carcinoma-derived cells from apoptosis. *Cell Death and Differentiation* **14**:1202–1210.
- Solaimani P, Damoiseaux R, and Hankinson O (2013) Genome-Wide RNAi High-Throughput Screen Identifies Proteins Necessary for the AHR-Dependent Induction of CYP1A1 by 2,3,7,8-Tetrachlorodibenzo-p-dioxin. *Toxicological Sciences* **136**:107–119.
- Son D-S, and Rozman K (2002) 2,3,7,8-Tetrachlorodibenzo- p -dioxin (TCDD) induces plasminogen activator inhibitor-1 through an aryl hydrocarbon receptor-mediated pathway in mouse hepatoma cell lines. *Archives of Toxicology* **76**:404–413.
- Sorg O, Zennegg M, Schmid P, Fedosyuk R, Valikhnovskyi R, Gaide O, Kniazevych V, and Saurat J-H (2009) 2,3,7,8-tetrachlorodibenzo-p-dioxin (TCDD) poisoning in Victor Yushchenko: identification and measurement of TCDD metabolites. *The Lancet* **374**:1179–1185.
- Soshilov A, and Denison MS (2008) Role of the Per/Arnt/Sim domains in ligand-dependent transformation of the aryl hydrocarbon receptor. *Journal of Biological Chemistry* **283**:32995–33005.
- Stachel I, Geismann C, Aden K, Deisinger F, Rosenstiel P, Schreiber S, Sebens S, Arlt A, and Schafer H (2014) Modulation of Nuclear Factor E2-related Factor-2 (Nrf2) Activation by the Stress Response Gene Immediate Early Response-3 (IER3) in Colonic Epithelial Cells. *Journal of Biological Chemistry* **289**:1917–1929.
- Stevens EA, Mezrich JD, and Bradfield CA (2009) The aryl hydrocarbon receptor: a perspective on potential roles in the immune system. *Immunology* **127**:299–311.

- Su Y, Zhang L, Gao X, Meng F, Wen J, Zhou H, Meng A, and Chen Y-G (2007) The evolutionally conserved activity of Dapper2 in antagonizing TGF- β signaling. *The FASEB Journal* **21**:682–690.
- Suske G, Bruford E, and Philipsen S (2005) Mammalian SP/KLF transcription factors: Bring in the family. *Genomics* **85**:551–556.
- Sutter TR, Tang YM, Hayes CL, Wo YY, Jabs EW, Li X, Yin H, Cody CW, and Greenlee WF (1994) Complete cDNA sequence of a human dioxin-inducible mRNA identifies a new gene subfamily of cytochrome P450 that maps to chromosome 2. *Journal of Biological Chemistry* **269**:13092–13099.
- Swanson HI, Chan WK, and Bradfield CA (1995) DNA binding specificities and pairing rules of the Ah receptor, ARNT, and SIM proteins. *Journal of Biological Chemistry* **270**:26292–26302.
- Swedenborg E, Kotka M, Seifert M, Kanno J, Pongratz I, and Rüegg J (2012) The aryl hydrocarbon receptor ligands 2,3,7,8-tetrachlorodibenzo-p-dioxin and 3-methylcholanthrene regulate distinct genetic networks. *Molecular and Cellular Endocrinology* **362**:39–47.
- Tanaka M, Okada K, Ueshima S, Imano M, Ohyanagi H, Carmeliet P, and Matsuo O (2001) Impaired liver regeneration after partial hepatectomy in plasminogen deficient mice. *Fibrinolysis and Proteolysis* **15**:2–8.
- Tarocchi M, Hannivoort R, Hoshida Y, Lee UE, Vetter D, Narla G, Villanueva A, Oren M, Llovet JM, and Friedman SL (2011) Carcinogen-induced hepatic tumors in KLF6 $^{+/-}$ mice recapitulate aggressive human hepatocellular carcinoma associated with p53 pathway deregulation. *Hepatology* **54**:522–531.

- Thomas PE, Kouri RE, and Hutton JJ (1972) The genetics of aryl hydrocarbon hydroxylase induction in mice: A single gene difference between C57BL/6J and DBA/2J. *Biochemistry and Genetics* 157–168.
- Tian Y, Ke S, Denison MS, Rabson AB, and Gallo MA (1999) Ah Receptor and NF- κ B Interactions, a Potential Mechanism for Dioxin Toxicity. *Journal of Biological Chemistry* **274**:510–515.
- Tierney B, Weaver D, Heintz NH, Schaeffer WI, and Bresnick E (1980) The identity and nuclear uptake of a cytosolic binding protein for 3-methylcholanthrene. *Archives of Biochemistry and Biophysics* **200**:513–523.
- Tijet N, Boutros PC, Moffat ID, Okey AB, Tuomisto J, and Pohjanvirta R (2006) Aryl hydrocarbon receptor regulates distinct dioxin-dependent and dioxin-independent gene batteries. *Molecular Pharmacology* **69**:140–153.
- Tohkin M, Fukuhara M, Elizondo G, Tomita S, and Gonzalez FJ (2000) Aryl hydrocarbon receptor is required for p300-mediated induction of DNA synthesis by adenovirus E1A. *Molecular Pharmacology* **58**:845–851.
- Trucco LD, Andreoli V, Nunez NG, Maccioni M, and Bocco JL (2014) Kruppel-like factor 6 interferes with cellular transformation induced by the H-ras oncogene. *The FASEB Journal* **28**:5262–5276.
- Tsuji G, Takahara M, Uchi H, Matsuda T, Chiba T, Takeuchi S, Yasukawa F, Moroi Y, and Furue M (2012) Identification of ketoconazole as an AhR-Nrf2 activator in cultured human keratinocytes: the basis of its anti-inflammatory effect. *Journal of Investigative Dermatology* **132**:59–68.

- Tukey RH, Hannah RR, Negishi M, and Nebert DW (1982) The Ah locus: Correlation of intranuclear appearance of inducer-receptor complex with induction of cytochrome P1-450 mRNA. *Cell* **31**:275–284.
- Tuyen LH, Tue NM, Suzuki G, Misaki K, Viet PH, Takahashi S, and Tanabe S (2014) Aryl hydrocarbon receptor mediated activities in road dust from a metropolitan area, Hanoi-Vietnam: contribution of polycyclic aromatic hydrocarbons (PAHs) and human risk assessment. *Science of the Total Environment* **491-492**:246–254.
- U S Environmental Protection Agency (2012) Exposure and Human Health Reassessment of 2,3,7,8-Tetrachlorodibenzo-p-Dioxin (TCDD) and Related Compounds National Academy Sciences (NAS) Review, *U.S. EPA (U.S. Environmental Protection Agency)*, Research Triangle Park, NC.
- U. S. Environmental Protection Agency (1993) Provisional guidance for quantitative risk assessment of polycyclic aromatic hydrocarbons, *U.S. EPA (U.S. Environmental Protection Agency)*, Research Triangle Park, NC.
- U.S. Food and Drug Administration (2010) Protocol for the Interpretation and use of Sensory Testing and Analytical Chemistry Results for Re-opening Oil-impacted Areas Closed to Seafood Harvesting Due to the Deepwater Horizon Oil Spill.
- United States Coast Guard Public Affairs Detachment Houston (2014) News Release Update: Texas City “Y” Collision.
- Uno S, Dalton TP, Derkenne S, Curran CP, Miller ML, Shertzer HG, and Nebert DW (2004) Oral exposure to benzo[a]pyrene in the mouse: detoxication by inducible cytochrome P450 is more important than metabolic activation. *Molecular Pharmacology* **65**:1225–1237.

- Upton HF (2011) The Deepwater Horizon Oil Spill and the Gulf of Mexico Fishing Industry. *Congressional Research Service* 1–17.
- USCG (United States Coast Guard)., National Response Team (2011) On Scene Coordinator Report: Deepwater Horizon Oil Spill, U.S. EPA (U.S. Environmental Protection Agency), Research Triangle Park, NC.
- Valentine DL, Fisher GB, Bagby SC, Nelson RK, Reddy CM, Sylva SP, and Woo MA (2014) Fallout plume of submerged oil from Deepwater Horizon. *Proceedings of the National Academy of Sciences* **111**:15906–15911.
- Vasquez A, Atallah-Yunes N, Smith FC, You X, Chase SE, Silverstone AE, and Vikstrom KL (2003) A Role for the Aryl Hydrocarbon Receptor in Cardiac Physiology and Function as Demonstrated by AhR Knockout Mice. *Cardiovascular Toxicology* **3**:153–163.
- Veldhoen M, and Duarte JH (2010) The aryl hydrocarbon receptor: fine-tuning the immune-response. *Current Opinions in Immunology* **22**:747–752.
- Vetter D, Cohen-Naftaly M, Villanueva A, Lee YA, Kocabayoglu P, Hannivoort R, Narla G, M Llovet J, Thung SN, and Friedman SL (2012) Enhanced hepatocarcinogenesis in mouse models and human hepatocellular carcinoma by coordinate KLF6 depletion and increased messenger RNA splicing. *Hepatology* **56**:1361–1370.
- Vogel CFA, Khan EM, Leung PSC, Gershwin ME, Chang WLW, Wu D, Haarmann-Stemmann T, Hoffmann A, and Denison MS (2014) Cross-talk between Aryl Hydrocarbon Receptor and the Inflammatory Response: A Role for the Nuclear Factor-KB. *Journal of Biological Chemistry* **289**:1866–1875.

- Vogel CFA, Sciullo E, and Matsumura F (2007) Involvement of RelB in aryl hydrocarbon receptor-mediated induction of chemokines. *Biochemical and Biophysical Research Communications* **363**:722–726.
- Vogel CFA, Sciullo E, Li W, Wong P, Lazennec G, and Matsumura F (2007) RelB, a new partner of aryl hydrocarbon receptor-mediated transcription. *Molecular Endocrinology* **21**:2941–2955.
- Wakayama S, Haque A, Koide N, Kato Y, Odkhuu E, Bilegtsaikhan T, Naiki Y, Komatsu T, Yoshida T, and Yokochi T (2014) Lipopolysaccharide impairs insulin sensitivity via activation of phosphoinositide 3-kinase in adipocytes. *Immunopharmacology and Immunotoxicology* **36**:145–149.
- Wang L, He X, Szklarz GD, Bi Y, Rojanasakul Y, and Ma Q (2013) The aryl hydrocarbon receptor interacts with nuclear factor erythroid 2-related factor 2 to mediate induction of NAD(P)H:quinoneoxidoreductase 1 by 2,3,7,8-tetrachlorodibenzo-p-dioxin. *Archives of Biochemistry and Biophysics* **537**:31–38.
- Wang W, Smith R, and Safe S (1998) Aryl hydrocarbon receptor-Mediated Antiestrogenicity in MCF-7 Cells: Modulation of Hormone-Induced Cell Cycle Enzymes. *Archives of Biochemistry and Biophysics* **356**:239–248.
- Wang Z, Hollebone BP, Fingas M, Fieldhouse B, Sigouin L, Landriault M, Smith P, Noonan J, and Thouin G (2003) Characteristics of spilled oils, fuels, and petroleum products: 1. Composition and properties of selected oils. U.S. EPA (U.S. Environmental Protection Agency), Research Triangle Park, NC.
- Wardlaw GD, Arey JS, Reddy CM, Nelson RK, Ventura GT, and Valentine DL (2008) Disentangling Oil Weathering at a Marine Seep Using GC×GC: Broad Metabolic

- Specificity Accompanies Subsurface Petroleum Biodegradation. *Environmental Science and Technology* **42**:7166–7173.
- Watson AJ, and Hankinson O (1992) Dioxin- and Ah receptor-dependent protein binding to xenobiotic responsive elements and G-rich DNA studied by in vivo footprinting. *Journal of Biological Chemistry* **266**:6874–6878.
- Weglarz TC, and Sandgren EP (2000) Timing of hepatocyte entry into DNA synthesis after partial hepatectomy is cell autonomous. *Proceedings of the National Academy of Sciences* **97**:12595–12600.
- Weintraub SJ, Chow KN, Luo RX, Zhang SH, He S, and Dean DC (1995) Mechanism of active transcriptional repression by the retinoblastoma protein. *Nature* **375**:812–815.
- Weintraub SJ, Prater CA, and Dean DC (1992) Retinoblastoma protein switches the E2F site from positive to negative element. *Nature* **358**:259–261.
- Weiss C, Faust D, Dürk H, Kolluri SK, Pelzer A, Schneider S, Dietrich C, Oesch F, and Göttlicher M (2005) TCDD induces c-jun expression via a novel Ah (dioxin) receptor-mediated p38–MAPK-dependent pathway. *Oncogene* **24**:4975–4983, Nature Publishing Group.
- Weiss C, Kolluri SK, Kiefer F, and Gottlicher M (1996) Complementation of Ah receptor deficiency in hepatoma cells: negative feedback regulation and cell cycle control by the Ah receptor. *Experimental Cell Research* **226**:154–163.
- Wells PG, Lee CJJ, McCallum GP, Perstin J, and Harper PA (2010) Receptor- and reactive intermediate-mediated mechanisms of teratogenesis. *Handbook of Experimental Pharmacology* **196**:131–162.

- White J, and White A (1939) Inhibition of Growth of the Rat by Oral Administration of Methycholanthrene, Benzpyrene, or Pyrene, and the Effects of Various Dietary Supplements. *Journal of Biological Chemistry* **131**:149–161.
- White SS, and Birnbaum LS (2009) An overview of the effects of dioxins and dioxin-like compounds on vertebrates, as documented in human and ecological epidemiology. *J Environ Sci Health C Environ Carcinog Ecotoxicol Rev* **27**:197–211.
- Whitehead A, Dubansky B, Bodinier C, Garcia TI, Miles S, Pilley C, Raghunathan V, Roach JL, Walker N, Walter RB, Rice CD, and Galvez F (2011) Genomic and physiological footprint of the Deepwater Horizon oil spill on resident marsh fishes. *Proceedings of the National Academy of Sciences*, doi: 10.1073/pnas.1109545108.
- Whitlock JP (1999) Induction of cytochrome P4501A1. *Annual Review of Pharmacology and Toxicology* **39**:103–125.
- Wickliffe J, Overton E, Frickel S, Howard J, Wilson M, Simon B, Echsner S, Nguyen D, Gauthe D, Blake D, Miller C, Elferink C, Ansari S, Fernando H, Trapido E, and Kane A (2014) Evaluation of Polycyclic Aromatic Hydrocarbons Using Analytical Methods, Toxicology, and Risk Assessment Research: Seafood Safety after a Petroleum Spill as an Example. *Environmental Health Perspectives* **122**:1–4.
- Wibel FJ, Klose U, and Kiefer F (1991) Toxicity of 2,3,7,8-tetrachlorodibenzo-p-dioxin in vitro: H4IIEC3-derived 5L hepatoma cells as a model system. *Toxicology Letters*.
- Wilson MJ, Frickel S, Nguyen D, Bui T, Echsner S, Simon BR, Howard JL, Miller K, and Wickliffe JK (2015) A Targeted Health Risk Assessment Following the Deep Water Horizon Oil Spill: Polycyclic Aromatic Hydrocarbon Exposure in

Vietnamese-American Shrimp Consumers. *Environmental Health Perspectives* **123**:1–8.

Wilson SR, Joshi AD, and Elferink CJ (2013) The tumor suppressor Kruppel-like factor 6 is a novel aryl hydrocarbon receptor DNA binding partner. *Journal of Pharmacology and Experimental Therapeutics* **345**:419–429.

Windal I, Denison MS, Birnbaum LS, Van Wouwe N, Baeyens W, and Goeyens L (2005) Chemically Activated Luciferase Gene Expression (CALUX) Cell Bioassay Analysis for the Estimation of Dioxin-Like Activity: Critical Parameters of the CALUX Procedure that Impact Assay Results. *Environmental Science and Technology* **39**:7357–7364.

Wu H, Wade M, Krall L, Grisham J, Xiong Y, and Van Dyke T (1996) Targeted in vivo expression of the cyclin-dependent kinase inhibitor p21 halts hepatocyte cell-cycle progression, postnatal liver development and regeneration. *Genes & Development* **10**:245–260.

Wu R, Chang H-C, Khechaduri A, Chawla K, Tran M, Chai X, Wagg C, Ghanefar M, Jiang X, Bayeva M, Gonzalez F, Lopaschuk G, and Ardehali H (2014) Cardiac-specific ablation of ARNT leads to lipotoxicity and cardiomyopathy. *Journal of Clinical Investigation* **124**:4795–4806.

Xia K, Hagood G, Childers C, Atkins J, Rogers B, Ware L, Armbrust K, Jewell J, Diaz D, Gatian N, and Folmer H (2012) Polycyclic Aromatic Hydrocarbons (PAHs) in Mississippi Seafood from Areas Affected by the Deepwater Horizon Oil Spill. *Environmental Science and Technology* **46**:5310–5318.

- Xie G, Peng Z, and Raufman J-P (2012) Src-mediated aryl hydrocarbon and epidermal growth factor receptor cross talk stimulates colon cancer cell proliferation. *American Journal of Liver Physiology* **302**:G1006–G1015.
- Xu G, Li Y, Yoshimoto K, Wu Q, Chen G, and Iwata T (2014) 2,3,7,8-Tetrachlorodibenzo-p-dioxin stimulates proliferation of HAPI microglia by affecting the Akt/GSK-3 β /cyclin D1 signaling pathway. *Toxicology Letters* **224**:362–370.
- Xu MJ, Feng D, Wu H, Wang H, Chan Y, Kolls J, Borregaard N, Porse B, Berger T, Mak TW, Cowland JB, Kong X, and Gao B (2015) Liver is the major source of elevated serum lipocalin-2 levels after bacterial infection or partial hepatectomy: A critical role for IL-6/STAT3. *Hepatology* **61**:692–702.
- Yamagiwa K, and Ichikawa K (1918) Experimental Study of the Pathogenesis of Carcinoma. *The Journal of Cancer Research* **3**:1–29.
- Yamagiwa K, and Murayama K (1924) Summary of the Results of Experiments on the Pathogenesis of Epithelial Growths: I. The Experimental Production of Mammary Carcinoma on Rabbits. *The Journal of Cancer Research* **8**:119–136.
- Yeager KM, Santschi PH, Rifai HS, Suarez MP, Brinkmeyer R, Hung C-C, Schindler KJ, Andres MJ, and Weaver EA (2007) Dioxin Chronology and Fluxes in Sediments of the Houston Ship Channel, Texas: Influences of Non-Steady-State Sediment Transport and Total Organic Carbon. *Environmental Science and Technology* **41**:5291–5298.
- Yeager RL, Reisman SA, Aleksunes LM, and Klaassen CD (2009) Introducing the “TCDD-Inducible AhR-Nrf2 Gene Battery.” *Toxicological Sciences* **111**:238–246.

- Yender R, Michel JM, and Lord C (2002) *Managing seafood safety after an oil spill*. Office of Response and Restoration, NOAA.
- Yin F, Hayworth JS, and Clement TP (2015) A Tale of Two Recent Spills—Comparison of 2014 Galveston Bay and 2010 Deepwater Horizon Oil Spill Residues. *PLoS ONE* **10**:e0118098.
- Ylitalo GM, Krahn MM, Dickhoff WW, Stein JE, Walker CC, Lassitter CL, Garrett ES, Desfosse LL, Mitchell KM, Noble BT, Wilson S, Beck NB, Benner RA, Koufopoulos PN, and Dickey RW (2012) Federal seafood safety response to the Deepwater Horizon oil spill. *Proceedings of the National Academy of Sciences* **109**:20274–20279.
- Zacharewski TR, Bondy KL, McDonell P, and Wu ZF (1994) Antiestrogenic Effect of 2,3,7,8-Tetrachlorodibenzo-p-dioxin on 17 β -Estradiol-induced pS2 Expression. *Cancer Research*.
- Zhang W, Shields JM, Sogawa K, Fujii-Kuriyama Y, and Yang VW (1998) The gut-enriched Krüppel-like factor suppresses the activity of the CYP1A1 promoter in an Sp1-dependent fashion. *Journal of Biological Chemistry* **273**:17917–17925.
- Zhang Y, Guo H, Deis JA, Mashek MG, Zhao M, Ariyakumar D, Armien AG, Bernlohr DA, Mashek DG, and Chen X (2014) Lipocalin 2 Regulates Brown Fat Activation via a Nonadrenergic Activation Mechanism. *Journal of Biological Chemistry* **289**:22063–22077.

Vita

Daniel Patrick Jackson was born April 22nd 1988 to Gregory Scott Jackson and Cathy Louise Jackson in Dayton, Ohio. He has two brothers and a sister and the first in his family to obtain a Doctoral degree. Daniel attended Wittenberg University in Springfield, Ohio for 3 years prior to commencing his graduate studies in cell biology at UTMB. Daniel joined the lab of Dr. Cornelis (Kees) Elferink in 2010 to begin his doctoral research. In his time at UTMB, Dan mentored 3 local high school students in the BENCH tutorials program, 2 SURP students, and several rotating graduate students. Dan also both taught and/or served as student course director (for the UTMB T-32 program's student taught course) for the Fundamentals of Toxicology course at Texas A and M, Galveston. During his studies, Dan was a lecturer and student course director for 2 UTMB GSBS courses, each for two years. Dan has published two first author manuscripts to date (chapters 1 and 2), with an additional two first author manuscripts soon to be submitted (chapters 4 and 5). He also collaborated with another lab during his graduate work, which earned him coauthor status on a manuscript; an additional coauthor publication is further expected (chapter 3).

Permanent address: 106 Whiting Ave, Galveston, Texas 77550.

This dissertation was typed by: Daniel P. Jackson